Contributions to the Chemistry of Higher-Coordinate Silicon: Synthesis, Structure, and Stereodynamics of New Penta- and Hexacoordinate Silicon(IV) Complexes

Dissertation zur Erlangung des
naturwissenschaftlichen Doktorgrades
der Julius-Maximilians-Universität Würzburg

Vorgelegt von
Diplom-Chemikerin
Smaranda Cota
aus Aiud/Rumänien

Würzburg 2010

Eingereicht am: ……
bei der Fakultät für Chemie und Pharmazie

1. Gutachter: ……
2. Gutachter: ……

der Dissertation

1. Prüfer: …….
2. Prüfer: …….
3. Prüfer: …….

des Öffentlichen Promotionskolloquiums

Tag des Öffentlichen Promotionskolloquiums: ……

Doktorurkunde ausgehändigt am: ……

Abbreviations Index

Bn	Benzyl
t-Bu	*tert*-Butyl
i-Pr	Isopropyl
Me	Methyl
Ph	Phenyl
Gly	Glycine
Ala	(*S*)-Alanine
Phe	(*S*)-Phenylalanine
Val	(*S*)-Valine
tert-Leu	(*S*)-*tert*-Leucine
HMDS	Hexamethyldisilazane
dbm	Dibenzoylmethane
BSA	Bis(trimethylsilyl)acetamide
d	Day(s)
h	Hour(s)
min	Minute(s)
CIP	Cahn-Ingold-Prelog
SP	Square Pyramid
TBP	Trigonal Bipyramid
DMSO	Dimethylsulfoxide
THF	Tetrahydrofuran
TMS	Tetramethylsilane
NMR	Nuclear Magnetic Resonance
br.	Broad
s	Singlet
d	Doublet
t	Triplet
m	Multiplet

DEPT	Distortionless Enhancement by Polarisation Transfer
VACP/MAS	Variable Amplitude Cross Polarisation/Magic Angle Spinning

Table of Contents

1 Introduction

Even though silicon is one of the most abundant elements on earth (it makes up about 25.7% of the earth's crust by weight), scientists didn't discover that it is essential for mammals until very recently. The largest concentration of silicon in the body is found in the skin and cartilage, but it also occurs in other tissues and organs. Silicon is found largely as silicon dioxide such as sand (silica), quartz, amethyst, agate, flint, jasper and opal. As an element of the fourth group and the third period of the periodic table, silicon plays an important role not only in medicinal chemistry but also in odorant chemistry. It is also being used as a central atom for the synthesis of complexes in coordination chemistry. With respect to its homologue, the carbon atom, silicon forms easier higher-coordinate complexes. Such complexes are realised when strongly electronegative ligand atoms such as halogen, oxygen, nitrogen and carbon atoms are bound to the silicon atom. In the meantime, also soft ligand atoms such as sulphur, selenium and tellurium have been demonstrated to bind to the silicon atom [1, 2, 3]. Since the first higher-coordinate silicon compound has been reported, the development of the research regarding novel silicon complexes has grown a lot. Higher-coordinate silicon complexes with coordination numbers five, six, seven or even eight have been synthesized in the past decades [4−21]. These complexes can be divided into three main groups: anionic (i.e. **I** [22, 23]), cationic (i.e. **II** [24]), and neutral complexes (i.e. **III** [25]).

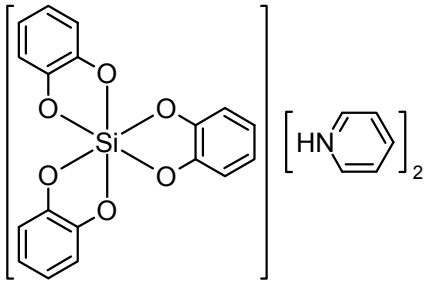

I

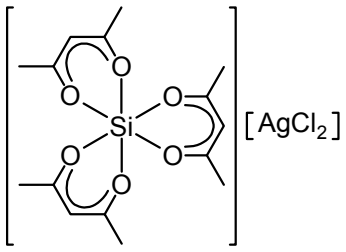

II

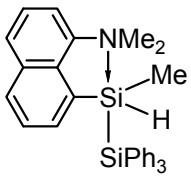

III

Zwitterionic λ^5 *Si*-silicates (i.e. **IV** [16, 26], and **V** [27]) belong also the to the last group.

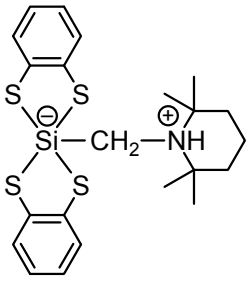

IV

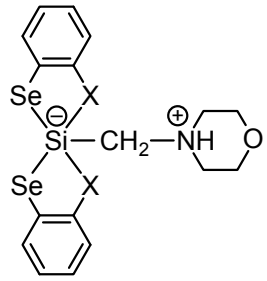

V

X = O, Se

The main interest in the research of higher-coordinate silicon compounds is focused on the dynamic behavior of the silicon coordination polyhedra in solution [28], on the high reactivity of the pentacoordinate silicon species towards nucleophiles [29, 30], and on the analysis of the binding situation at higher-coordinate silicon atoms [31, 32].

2 Aim

One of the main targets of this thesis was to further contribute to the chemistry of higher-coordinate silicon(IV) complexes. Novel chiral higher-coordinate compounds containing cyanato-*N* and thiocyanato-*N* ligands were supposed to be synthesized. Cyanato-*N*- or thiocyanato-*N*-silanes were to be used as the starting materials.

2.1 Syntheses of higher-coordinate silicon(IV) complexes with bidentate ligands derived from *α*-amino acids

In general, the chemistry of higher-coordinate silicon(IV) complexes with bidentate mono- and dianionic ligands is well explored [33]. Very little is known, however, about higher-coordinate silicon compounds that contain bidentate ligands derived from *α*-amino acids. New chiral hexacoordinate silicon(IV) complexes with bidentate ligands derived from the *α*-amino acids: glycine, (*S*)-alanine, (*S*)-phenylalanine, (*S*)-valine, and (*S*)-*tert*-leucine of the formula type **A** and **B**, respectively, were to be synthesized. We were interested to discover if cyanato-*N* ligands could react with disilylated *α*-amino acids, considering the fact that the NCO groups are pseudohalides and can act as bases which can deprotonate the higher-coordinate silicon complexes. We also wished to ascertain which positions could be deprotonated in the higher-coordinate silicon complexes.

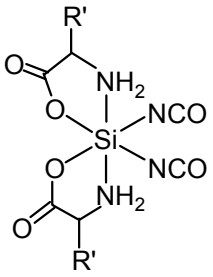

A
R' = H, Me, Bn, *i*-Pr, *t*-Bu

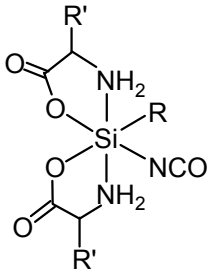

B
R' = H, Me, Bn, *i*-Pr, *t*-Bu
R = Me, Ph

To the best of our knowledge, the hexacoordinate silicon(IV) complex **A** synthesized here was the first neutral hexacoordinate silicon(IV) complexes containing *α*-amino acids as bidentate ligands. In the 80s, B. Fitzsimmons et al. [34] reported the preparation and characterization of some iron complexes with various *α*-amino acids: glycine, alanine, phenylglycine, phenylalanine, serine, tryptophan, histidine, leucine, and P. A. Cusack et al. reported on the synthesis and spectroscopic studies of inorganic tin derivaties of amino acids

and their esters [35]. At the beginning of the 90s, the chemistry of half-sandwich complexes of Co(III), Rh(III), Ru(II), Ir(III) containing α-amino amides had also been explored by W. Beck et al. [36]. A. V. Golovin et al. reported in 2000 about the NMR studies of transformations of amino acid complexes of Pt(II) and Pd(II) in solution [37]. The first hexacoordinate silicon complex containing α-amino acids and two dimethyl fragments was reported in 2002 by M. Nath and S. Goyal [38]. However, the studies from M. Nath and S. Goyal are somewhat unsatisfactory because the identity of these silicon complexes was not established by X-ray analyses. Only a few pentacoordinate silicon complexes, which belong to zwitterionic λ^5 *Si*-silicates [29, 39] are known so far, and these were synthesized using the "zwitterionic trick", i.e., the pentacoordinate (formally negatively charged) silicon atom has been incorporated in a molecular framework that also contains a tetracoordinate (formally positively charged) nitrogen atom. The novel neutral higher-coordinate silicon(IV) complexes should be optically active, and therefore can yield new insights into the properties of such complexes. The dynamic behavior of these complexes in solution should also be investigated.

2.2 Syntheses of higher-coordinate silicon(IV) complexes with acetylacetonato ligands and acetylacetonato derivatives

The syntheses of neutral hexacoordinate silicon(IV) complexes (**C** type) with bidendate ligands of the acetylacetonato type (acac) and acac derivatives were also of great interest, e.g. dbm, leading to novel chiral silicon complexes with *Si*O_4NC skeletons. By the introduction of two different groups at the silicon atom (Ph, NCO), the silicon complexes **C** (R = Me, Ph) could change their properties, which deserves further investigation.

The reactivity of the $(acac)_2Si(NCO)_2$ complex (**71**) should be studied. The substitution of the NCO groups by bidentate dianionic ligands of the glycolato(2−) and oxalato(2−) type should be possible, leading to novel neutral heteroleptic hexacoordinate silicon(IV) complexes with *Si*O_6 skeletons (see formula type **D** and **E**).

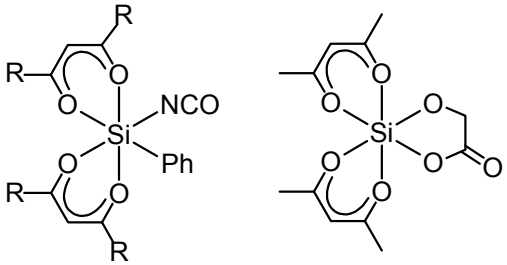

C
R = Me, Ph

D

E

2.3 Syntheses of higher-coordinate silicon(IV) complexes with tridentate ligands

For a further examination of neutral chiral higher-coordinate silicon(IV) compounds, our attention turned to tridentate ligands (*O*,*N*,*O* and *O*,*N*,*N* donors). The mono- and dianionic ligands were supposed to react with the starting materials (cyanato-*N* or thiocyanato-*N* silanes) leading to higher-coordinate silicon(IV) compounds of the formula type **F**, **G**, **H**, and **I**, respectively.

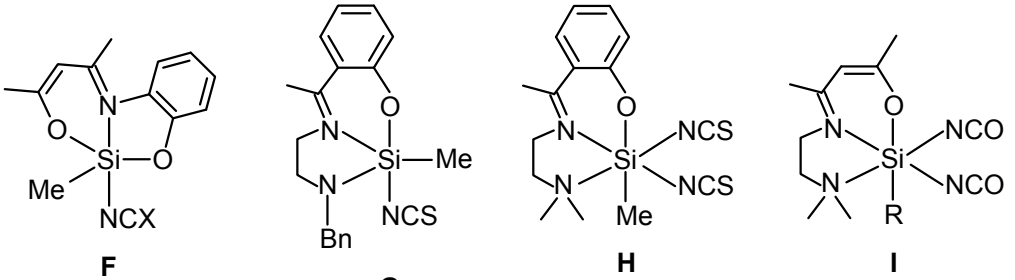

F X = O, S **G** **H** **I** R = Ph, NCO

The stability of these new complexes with SiO$_2$N$_2$C, SiON$_3$C, SiON$_4$C, or SiON$_5$ skeletons should be further investigated by NMR spectroscopy. For a complete characterization of these complexes, their molecular structures were to be determined by X-ray analyses.

2.4 Syntheses of higher-coordinate silicon(IV) complexes with tetradentate ligands

Chiral hexacoordinate silicon(IV) complexes with dianionic tetradentate *O,O,N,N,* donor ligands of the **J** (R = Me, Ph), **K** (R = Me, Ph), and **L** type were to be synthesized. There are very few pentacoordinate binuclear silicon complexes with an oxygen bridge between the silicon atoms known so far [40]. To the best of our knowledge, no binuclear hexacoordinate silicon complexes of a disiloxane type have been reported. Therefore, the synthesis of the neutral binuclear silicon(IV) complex with an SiN$_3$O$_3$ skeleton (of the formula type **M**) was of great interest. The structural characterisation of **M** was to be done in the solid-state (by VACP/MAS studies, elemental analysis, and X-ray analysis) and in solution (by NMR spectroscopy).

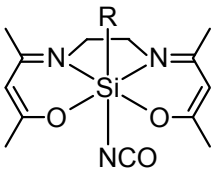

J
R = Me, Ph

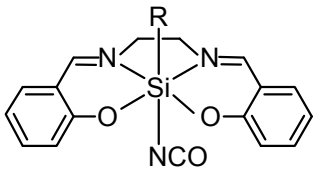

K
R = Me, Ph

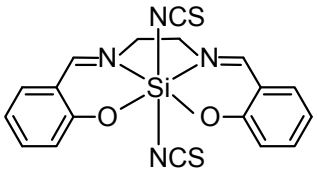

L

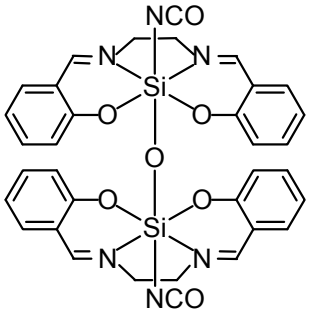

M

In addition to the syntheses of the higher-coordinate silicon(IV) complexes, the focal point of this thesis is the complete characterization of these compounds in the solid-state (by X-ray analyses, NMR spectroscopy (^{13}C, ^{15}N and ^{29}Si VACP/MAS NMR), elemental analyses, and infrared spectroscopy)) and in solution (by NMR spectroscopy (^{1}H, ^{13}C, ^{15}N and ^{29}Si NMR)).

The aims of this thesis are presented in the following chapters.

3 Syntheses

3.1 Silylation of *α*-amino acids

Compounds **16**−**20** were synthesized according to Scheme 1 by treatment of glycine, (*S*)-alanine, (*S*)-phenylalanine, (*S*)-valine, (*S*)-*tert*-leucine (**6**−**10**) with HMDS, *n*-hexane, triethylamine and trimethylsilylchloride. Distillation, under reduced pressure, of the reaction mixtures led to the expected products (yield: **16**, 55%; **17**, 77%; **18**, 96%; **19**, 85%; **20**, 75%).

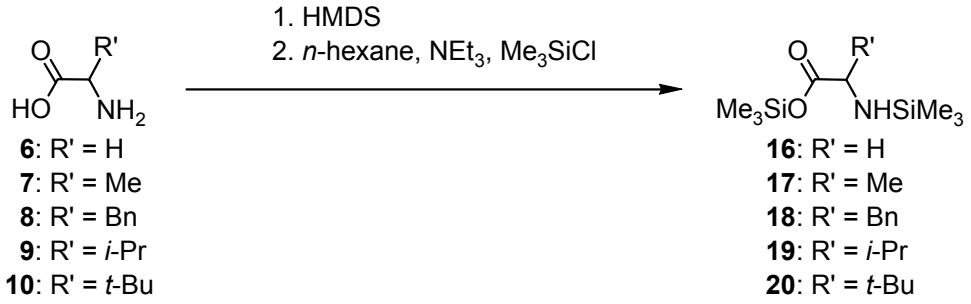

Scheme 1

The identities of **16**−**20** were established by solution NMR spectroscopy and GC/MS.

3.2 Silylation of novel *α*-methyl substituted amino acids

Compound **22** was synthesized according to Scheme 2 by treatment of (*S*)-*α*-[(trimethylsilyl)methyl]alanine (**21**) with one molar equivalent of bis(trimethylsilyl)acetamide (BSA) in acetonitrile, to give **22** in 46% yield.

Scheme 2

Compound **22** was also synthesized by treatment of (*S*)-*α*-[(trimethylsilyl)methyl]alanine with HMDS, *n*-hexane, triethylamine and trimethylsilyl-chloride and BSA. Distillation under reduced pressure of the reaction mixture led to the expected product **22**, but at the cost of the yield (yield 14%). The disadvantage of this method compared to the direct silylation with BSA is the low yield of **22,** and therefore the direct silylation with BSA represents the most effective method. The identity of **22** was established by solution NMR spectroscopy and GC/MS.

3.3 Syntheses of hexacoordinate silicon(IV) complexes with an *Si*O_4NC skeleton

Compound **33** was prepared according to Scheme 3 by treatment of two molar equivalents of acetylacetone (*O*,*O* donor) with one molar equivalent of tri(cyanato-*N*)phenylsilane in tetrahydrofuran (yield: 74%).

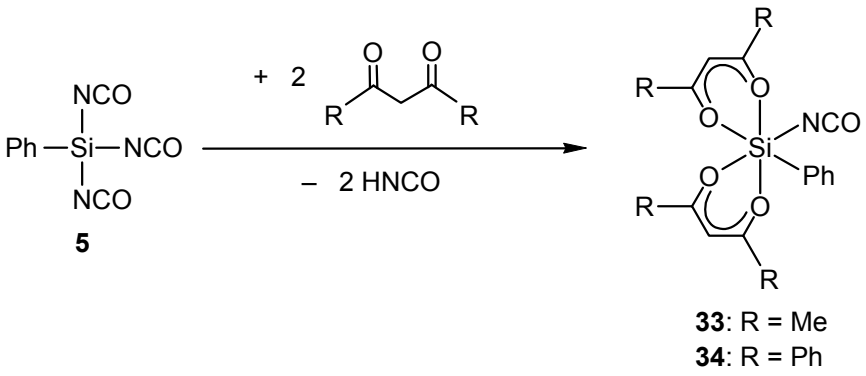

Scheme 3

The identity of **33** was established in solution by NMR studies (^{1}H, ^{13}C, ^{15}N, ^{29}Si). Furthermore, compound **33** was characterized in the solid-state by VACP/MAS NMR spectroscopy (^{13}C, ^{15}N, ^{29}Si), single-crystal X-ray diffraction, and elemental analyses (C, H, N).

Compound **34** was prepared according to Scheme 3 by treatment of two molar equivalents of dibenzoylmethane (*O*,*O* donor) with one molar equivalent of tri(cyanato-*N*)phenylsilane in acetonitrile (yield: 78%). The identity of the chiral complex **34** was established by elemental analyses (C, H, N) and solution NMR studies (^{1}H, ^{13}C, ^{15}N, ^{29}Si). Furthermore, compound **34** was characterized in the solid-state by VACP/MAS NMR spectroscopy (^{13}C, ^{15}N, ^{29}Si) and single-crystal X-ray diffraction.

3.4 Syntheses of hexacoordinate silicon(IV) complexes with an *Si*O_6 skeleton

Compounds **35** and **36** were synthesized according to Scheme 4 by treatment of one molar equivalent of bis[acetylacetonato(2−)]di(cyanato-*N*)silicon(IV) (**71**) with one molar equivalent of bis(trimethylsilyl)glycolate or bis(trimethylsilyl)oxalate, respectively, in THF in good yields (**35**, 88%; **36**, 68%).

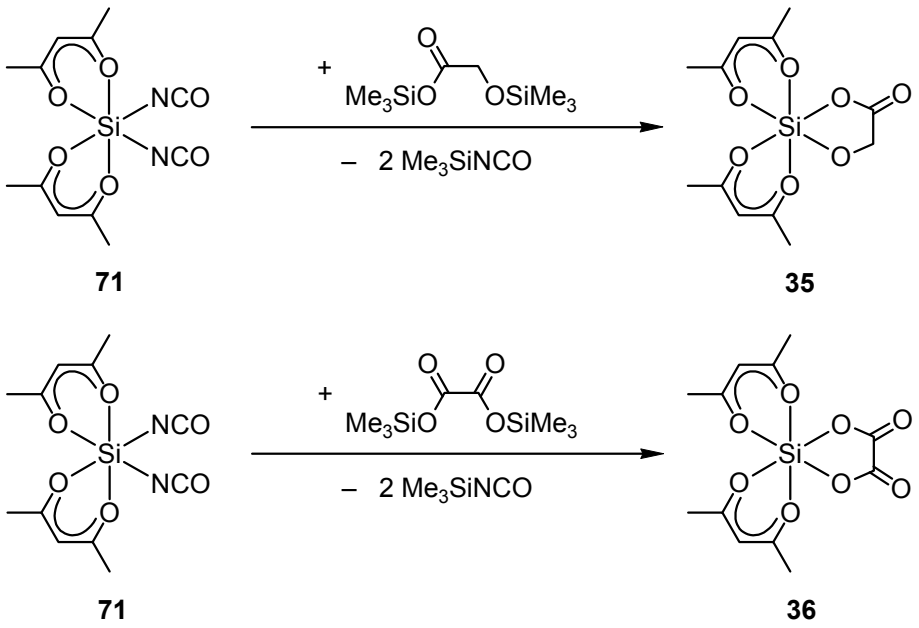

Scheme 4

The hexacoordinate silicon(IV) complexes **35** and **36** were isolated as colorless crystalline solids and their identities were established in the solid-state by single-crystal X-ray diffraction, VACP/MAS studies, elemental analyses (C, H), and in solution by NMR spectroscopy (^{1}H, ^{13}C, and ^{29}Si NMR).

3.5 Syntheses of zwitterionic λ^5 *Si*-silicates

Compounds **38**, **39**, and **43**−**46** were synthesized according to Scheme 5 by treatment of one molar equivalent tri(cyanato-*N*)methylsilane or tri(cyanato-*N*)phenylsilane with two molar equivalents of trimethylsilyl (*S*)-*N*-(trimethylsilyl)alaninate, trimethylsilyl (*S*)-*N*-(trimethylsilyl)phenylalaninate, trimethylsilyl (*S*)-*N*-(trimethylsilyl)valinate, and trimethylsilyl (*S*)-*N*-(trimethylsilyl)-*tert*-leucinate (**17**−**20**) [41]. All syntheses were performed at low temperatures in acetonitrile (from −70 °C to −20 °C).

Trimethylsilyl (*S*)-*N*-(trimethylsilyl)alaninate undergoes a side reaction upon addition of tri(cyanato-*N*)methylsilane or tri(cyanato-*N*)phenylsilane, leading to the formation of an oligopeptide of the formula type $Me_3SiOC(O)CHMe[N(SiMe_3)C(O)CHMe]_nN(SiMe_3)H$ (see Scheme 6, for simplification only the formation of a dipeptide is depicted) and trimethylsilanol (Me_3SiOH), which can undergo a condensation reaction to yield hexamethyldisiloxane ($Me_3SiOSiMe_3$) and water.

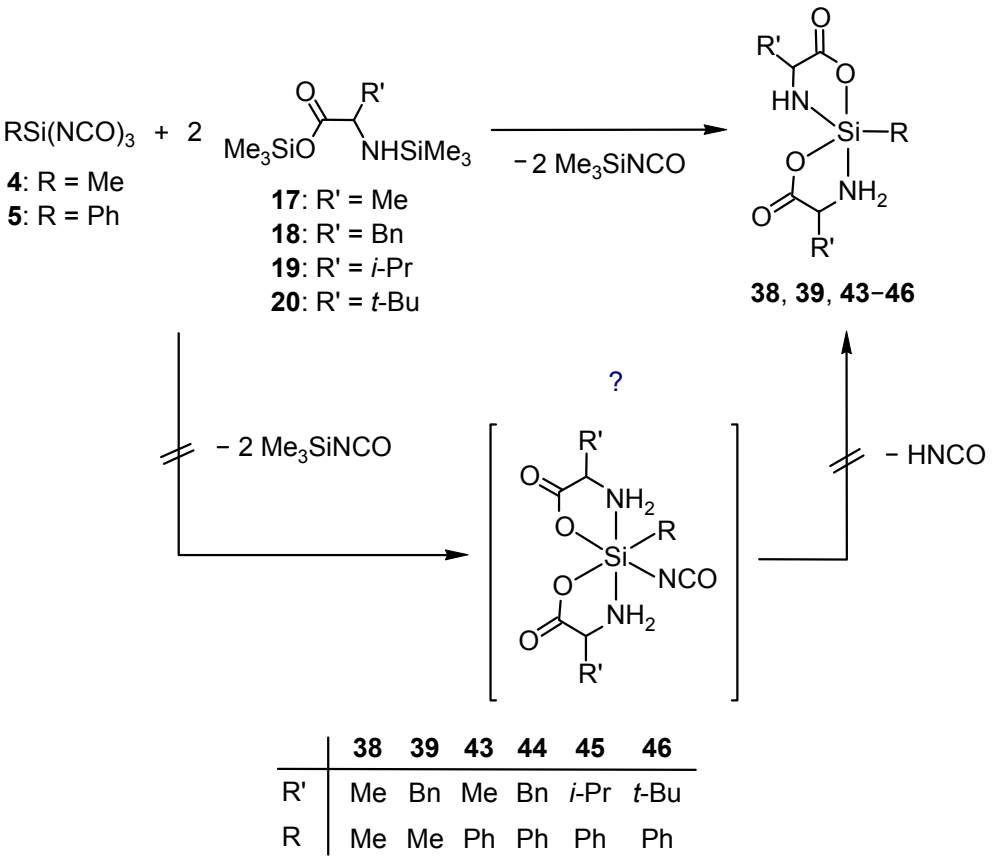

	38	39	43	44	45	46
R'	Me	Bn	Me	Bn	*i*-Pr	*t*-Bu
R	Me	Me	Ph	Ph	Ph	Ph

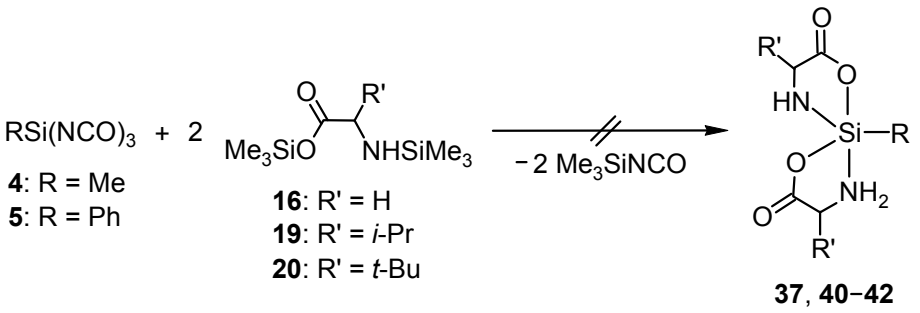

	37	40	41	42
R'	H	*i*-Pr	*t*-Bu	H
R	Me	Me	Me	Ph

Scheme 5

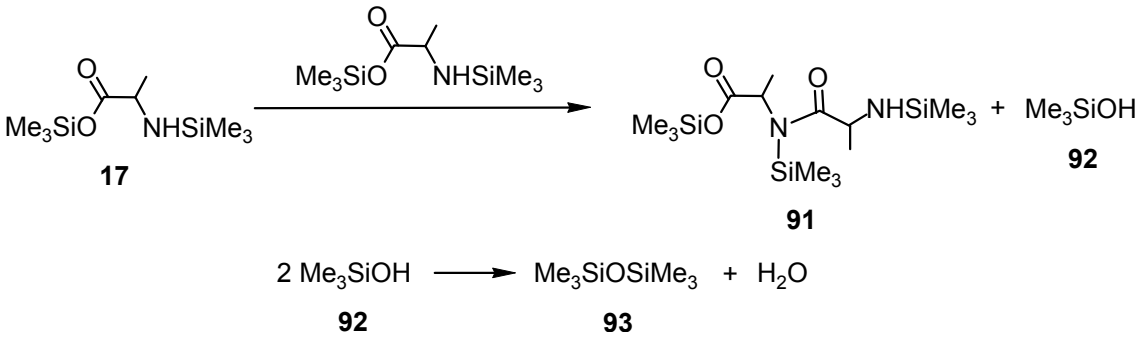

Scheme 6

Both the oligopeptide and the disiloxane could be detected in the reaction mixtures of **38** and **43** (NMR studies, data not given). The water formed in this side reaction might be the proton source that explains the existence of the bidentate monoanionic *O*,*N* ligands (with an NH_2 group) in **38**, **39** and **43**−**46**. The hexacoordinate silicon complexes containing two *α*-amino acids ligands, one alkyl (R = Me, Ph) and one NCO ligand could not be isolated. However, HNCO elimination from the above mentioned hexacoordinate complexes can lead to the formation of the pentacoordinate silicon(IV) complexes **38**, **39** and **43**−**46**.

The products **38**, **39** and **43**−**46** were isolated as colorless solids directly from the reaction mixtures in moderate yields (yield: **38**, 56%; **39**, 48%; **43**, 34%; **44**, 57%; **45**, 81%; **46**, 49%). Due to the moderate yields obtained for **38**, **39**, **43**−**46** and the difficulties encountred in the syntheses of **37,** and **40**−**42**, we searched for other methods to prepare the pentacoordinate silicon(IV) complexes **37**−**46**. Compounds **37**−**46** were supposed to be synthesized according to Scheme 7, by treatment of one molar equivalent tri(cyanato-*N*)methylsilane or tri(cyanato-*N*)phenylsilane with two molar equivalents of the respective *α*-amino acids.

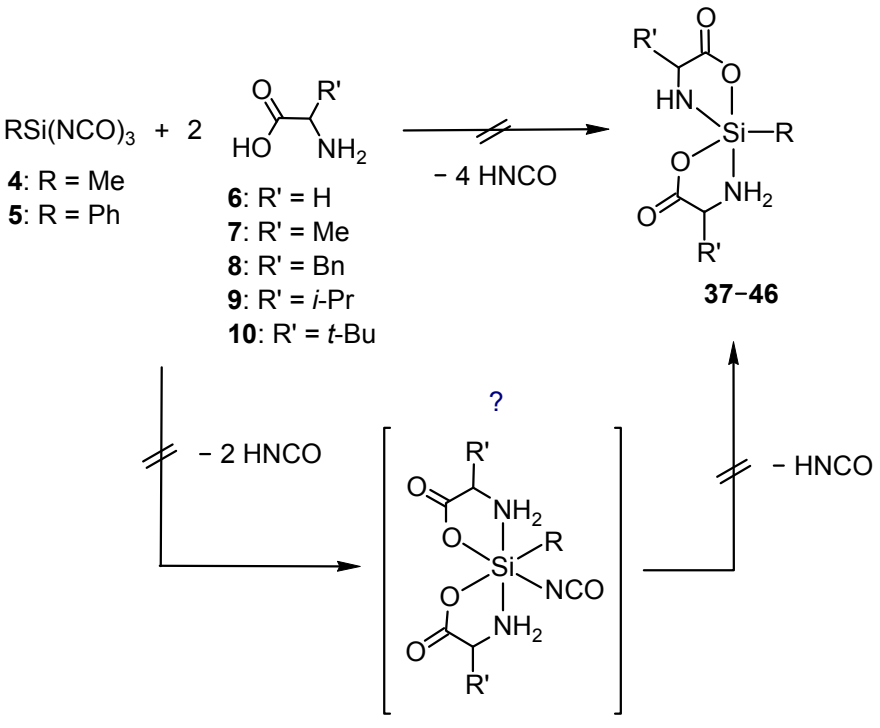

	37	38	39	40	41	42	43	44	45	46
R'	H	Me	Bn	*i*-Pr	*t*-Bu	H	Me	Bn	*i*-Pr	*t*-Bu
R	Me	Me	Me	Me	Me	Ph	Ph	Ph	Ph	Ph

Scheme 7

Different reaction conditions (temperature, amount of reagents and solvent) were used for the preparation of these neutral pentacoordinate silicon(IV) complexes, but unfortunately none of the attempts were successful. Table 1 lists some of the experiments.

Table 1. Attempts in synthesizing the pentacoordinate silicon(IV) complexes **37**−**46**.

compound	molar ratio reagents (silane:amino acid)	temperature	solvent
$(gly)_2SiMe$	1:2	23 °C	CH_3CN
		23 °C	DMF
		−20 °C	CH_3CN
		−70 °C	CH_3CN
		23 °C	CH_2Cl_2
$(ala)_2SiMe$	1:2	23 °C	CH_3CN
		23 °C	DMF
		−20 °C	CH_3CN
		−70 °C	CH_3CN
		reflux	CH_3CN
		23 °C	CH_2Cl_2
		23 °C	DMF
$(phe)_2SiMe$	1:2	23 °C, 15 d	CH_3CN
		23 °C, 5 d	CH_2Cl_2
		23 °C, 5 d	DMF
$(val)_2SiMe$	1:2	23 °C, 5 d	CH_3CN
$(tert\text{-}leu)_2SiMe$	1:2	23 °C, 5 d	CH_3CN
$(gly)_2SiPh$	1:2	23 °C, 5 d	CH_3CN
$(ala)_2SiPh$	1:2	23 °C, 4 d	CH_3CN
	1:2	reflux, 7 h	CH_3CN
$(phe)_2SiPh$	1:2	23 °C, 9 d	CH_3CN
$(val)_2SiPh$	1:2	23 °C, 10 d	CH_3CN
$(tert\text{-}leu)_2SiPh$	1:2	23 °C, 10 d	CH_3CN

According to the NMR studies, the reaction of cyanato-*N* silanes with the non-silylated *α*-amino acids did not lead to pentacoordination. Unknown insoluble colorless products were isolated, which contained, the unreacted *α*-amino acids and urea derivatives (NMR studies, data not given). The formation of the urea derivatives could be due to the nucleophilic attack of the amine function of the *α*-amino acids to the carbon atom of the NCO group (see Scheme 8).

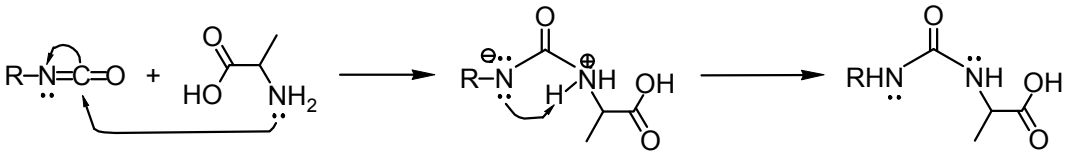

Scheme 8

The identities of the pentacoordinate silicon(IV) complexes **38**, **39**, **43**, **44**, and **46** were established by X-ray analyses, by VACP/MAS and by elemental analyses. Unfortunately, compound **45** could not be obtained as a crystalline solid and therefore it could not be characterized by single-crystal X-ray diffraction. Its identity was established by VACP/MAS studies and by elemental analysis.

3.6 Syntheses of zwitterionic λ^5 *Si*-silicates with novel *α*-methyl substituted amino acids

Compounds **47** and **48** were synthesized according to Scheme 9 by treatment of one molar equivalent of tri(cyanato-*N*)methylsilane and tri(cyanato-*N*)phenylsilane with two molar equivalents of trimethylsilyl (*S*)-*N*-trimethylsilyl-*α*-[(trimethylsilyl)methyl]alaninate in acetonitrile at –60 °C to –20 °C.

Scheme 9

The products were isolated as colorless solids directly from the reaction mixtures in moderate yields (yield: **47**, 49%; **48**, 59%). The identities of the pentacoordinate silicon(IV) complexes **47** and **48** were established by VACP/MAS and by elemental analyses. Unfortunately, suitable single-crystals of compounds **47** and **48** could not be obtained and therefore they could not be characterized by single-crystal X-ray diffraction.

3.7 Syntheses of hexacoordinate silicon(IV) complexes with an SiO_2N_4 skeleton

Compounds **49** and **50** were synthesized according to Scheme 10 by treatment of one molar equivalent of tetra(cyanato-*N*)silane with two molar equivalents of the corresponding

disilylated α-amino acids (**16** and **17**) in acetonitrile at –50 °C to –20 °C (**49**) and –70 °C to –20 °C (**50**), respectively. Compound **52** was synthesized according to Scheme 10 by treatment one molar equivalent of tetra(cyanato-*N*)silane with an excess of the disilylated α-amino acid, compound **19**. The complex **53** was synthesized according to Scheme 10 by treatment of one molar equivalent of tetra(cyanato-*N*)silane with two molar equivalents of the disilylated α-amino acid **20**. The syntheses of **52** and **53** were performed in acetonitrile at 23 °C to –20 °C (**52**) and –30 °C to –20 °C (**53**), respectively.

Compounds **49**, **50**, **52**, and **53** were isolated as colorless solids directly from the reaction mixtures in moderate yields (yield: **49**, 56%; **50**, 51%; **52**, 92%; **53**, 22%). The formation of these complexes was quite a surprise, since the existence of an additional proton at the nitrogen atom was observed (NH_2 group). In order to better understand from where the additional protons came, we studied the behavior of the disilylated amino acids in the solution-state (see Chapter 4, NMR studies) and searched for byproducts of these reactions. We examined this by taking trimethylsilyl (*S*)-*N*-(trimethylsilyl)alaninate as a model system for our studies. We found that trimethylsilyl (*S*)-*N*-(trimethylsilyl)alaninate [$Me_3SiOC(O)CHMeN(SiMe_3)H$] undergoes a side reaction leading to the formation of an oligopeptide of the formula type $Me_3SiOC(O)CHMe[N(SiMe_3)C(O)CHMe]_nN(SiMe_3)H$ (see Scheme 6).

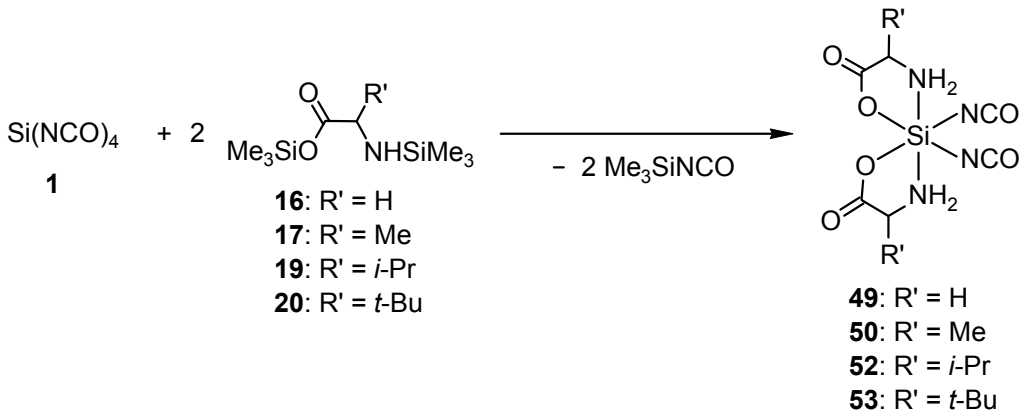

Scheme 10

This oligopeptide formation involves elimination of trimethylsilanol (Me_3SiOH), which can undergo a condensation reaction to yield hexamethyldisiloxane ($Me_3SiOSiMe_3$) and water. Both the oligopeptide and the disiloxane could be detected in the reaction mixtures of **50** (NMR studies, data not given). The water formed in this side reaction might be the proton source that explains the existence of the bidentate monoanionic *O*,*N* ligands (with an NH_2 group) in **49**, **50**, **52**, and **53**. It is interesting to note that the oligopeptide formation from $Me_3SiOC(O)CHMeN(SiMe_3)H$ only occurs upon addition of tetra(cyanato-*N*)silane.

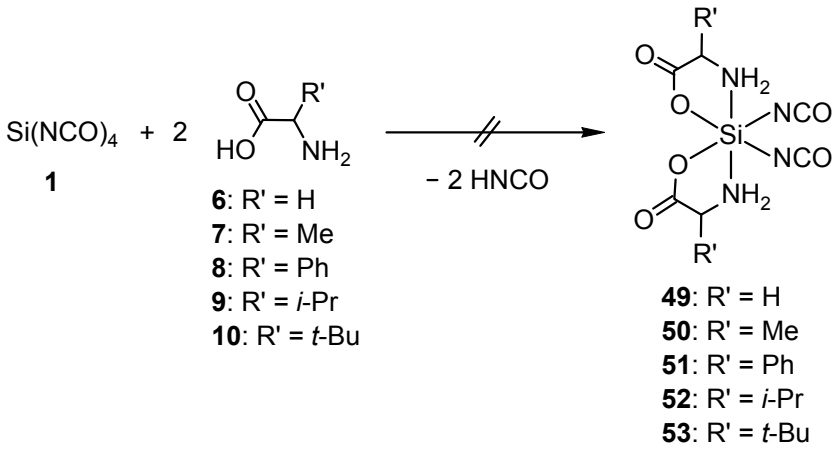

Scheme 11

Table 2. Attempts in synthesizing the hexacoordinate silicon(IV) complexes **49**–**53**.

compound	molar ratio reagents (silane: amino acid)	temperature, time	solvent
$(gly)_2Si(NCO)_2$	1:2	reflux, 7 h	CH_3CN
	1:2	23 °C, 4 d	CH_3CN
	1:2:2 + NEt_3	23 °C, 4 d	CH_3CN
$(ala)_2Si(NCO)_2$	1:2	RT, 30 h	CH_3CN
	1:2	RT, 30 h	CH_2Cl_2/*n*-pentane/THF
	1:2	RT, 6 d −20 °C	toluene/*n*-pentane/THF
	1:2	RT, 6 d −20 °C	DMF/*n*-pentane/THF
	1:2	−20 °C, 5 min −20 °C	CH_3CN
	1:2	reflux 10 min 23 °C, 4 d	DMF/THF
	1:8	reflux, 7 h	CH_3CN
	1:2:2 + NEt_3	23 °C, 4 d −20 °C	CH_3CN
$(phe)_2Si(NCO)_2$	1:2	23 °C, 4 d −20 °C	CH_3CN/*n*-pentane
	1:2 + NEt_3	Reflux, 7 h; 23 °C, 14 d	CH_3CN/*n*-pentane
$(val)_2Si(NCO)_2$	1:2	RT, 8 d	CH_3CN/*n*-pentane
	1:2:2 + NEt_3	RT, 4 d	CH_3CN/*n*-pentane
(*tert*-leu)$_2$Si(NCO)$_2$	1:2	RT, 24 h	CH_3CN/*n*-pentane

	1:2	reflux, 4 h	CH_3CN
	1:2	reflux, 45 min	DMF
	1:2:2 + NEt_3	23 °C, 5 d	CH_3CN/*n*-pentane

Compounds **49**−**53** were to be synthesized according to Scheme 11 by treatment of tetra(cyanato-*N*)silane with two molar equivalents of the corresponding *α*-amino acids at different temperatures and in different organic solvents.

Unfortunately, these syntheses did not result in pure products and most of these reactions showed several inseparable byproducts in the solid-state. Table 2 illustrates some of the attempts in synthesizing the hexacoordinate silicon(IV) complexes **49**−**53**.

The identities of **49**, **50**, **52**, and **53** were established by NMR spectroscopy (VACP/MAS), elemental analyses and IR spectroscopy. Compound **50** was also characterized by single-crystal X-ray diffraction and solution NMR spectroscopy (^{1}H, ^{13}C, ^{15}N, and ^{29}Si NMR). Compound **51** could not be synthesized, either by the method described in Scheme 10 or by the method described in Scheme 11. Steric factors (R = Bn) may be to blame for the failure of this reaction.

3.8 Syntheses of hexacoordinate silicon(IV) complexes containing cyanato-*N* and thiocyanato-*N* ligands

3.8.1 Syntheses of hexacoordinate silicon(IV) complexes containing tridentate ligands

Compound **54** was prepared according to Scheme 12 by treatment of one molar equivalent of the tridentate dianionic ligand (*O*,*N*,*O* donor) with one molar equivalent of tri(cyanato-*N*)methylsilane in acetonitrile (yield: 44%). The identity of **54** was established by solution NMR studies (^{1}H, ^{13}C, ^{15}N, ^{29}Si). Furthermore, compound **54** was characterized in the solid-state by VACP/MAS NMR spectroscopy (^{13}C, ^{15}N, ^{29}Si), single-crystal X-ray diffraction and elemental analyses (C, H, N).

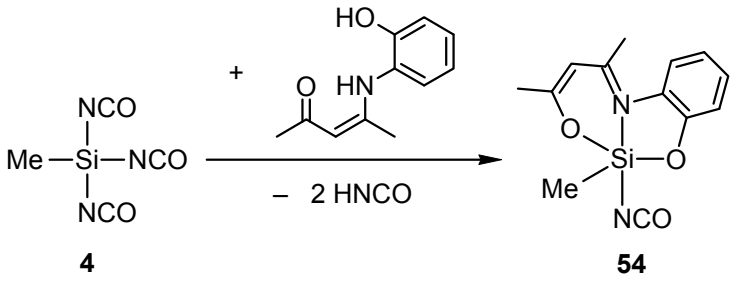

Scheme 12

The starting material methyldi(thiocyanato-*N*)silane (**3**) was synthesized according to Scheme 13 by treatment of dichloro(methyl)silane with two molar equivalents of ammonium thiocyanate in boiling toluene (yield: 61%) [42]. Treatment of **3** with one molar equivalent of 2-{*N*-[2-(benzylamino)ethyl]ethanimidoyl}phenol (**28**) in dichloromethane at 20 °C, in the presence of triethylamine, gave the pentacoordinate silicon(IV) complex **55** (yield: 31%, Scheme 13). Reaction of **3** with one molar equivalent of 2-{*N*-[2-(dimethylamino)ethyl]ethanimidoyl}phenol (**29**) in acetonitrile at 20 °C afforded the hexacoordinate silicon(IV) complex **56** (yield: 17%, Scheme 13). Due to side reactions which could not be suppressed (analysis of the crude products by solid-state NMR spectroscopy), it was very difficult to obtain compounds **55** and **56** as chemically pure solids. However, under the experimental conditions reported, both products could be isolated as crystalline solids, at the cost of the yields (for details, see Experimental Section).

2-{*N*-[2-(Dimethylamino)ethyl]ethanimidoyl}phenol (**29**) was synthesized according to ref. [43], and the hitherto unknown derivative 2-{*N*-[2-(benzylamino)ethyl]ethanimidoyl}phenol (**28**) was obtained from *N*-benzylethane-1,2-diamine and 1-(2-hydroxyphenyl)ethanone (for details, see Experimental Section).

The identities of **3**, **55, 56** and the two *N*,*N*,*O* donor ligands were established by elemental analyses (C, H, N, (S)) and solution NMR studies (^{1}H, ^{13}C, ^{15}N, (^{29}Si)). Furthermore, **55** and **56** were also characterized by VACP/MAS NMR spectroscopy (^{13}C, ^{15}N, ^{29}Si) and single-crystal X-ray diffraction.

Compounds **57** and **58** were prepared according to Scheme 14 by treatment of one molar equivalent of the monoanionic tridentate ligand **30** (*N*,*N*,*O* donors) with one molar equivalent of tetra(cyanato-*N*)silane and tri(cyanato-*N*)phenylsilane, respectively (yields: **57**, 8%; **58**, 39%).

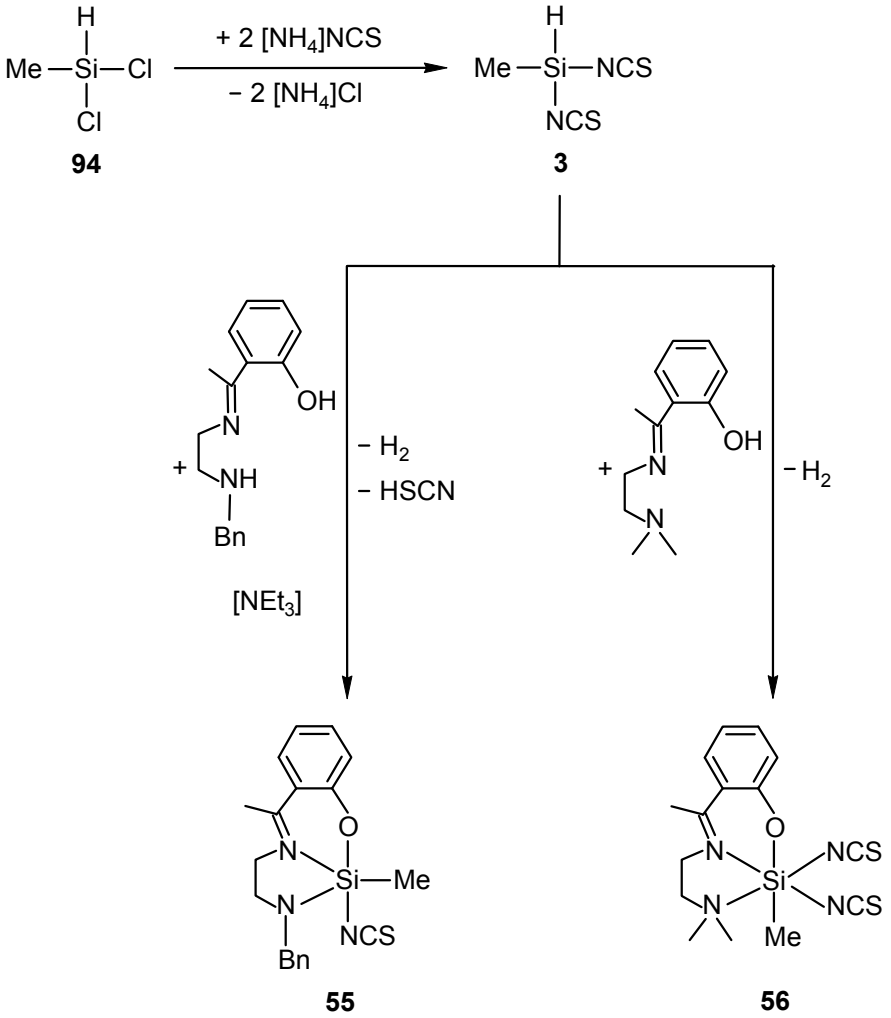

Scheme 13

The identities of **57** and **58** were established by elemental analyses (C, H, N) and solution NMR studies (^{1}H, ^{13}C, ^{15}N, ^{29}Si). Furthermore, compounds **57** and **58** were characterized by VACP/MAS NMR spectroscopy (^{13}C, ^{15}N, ^{29}Si) and single-crystal X-ray diffraction.

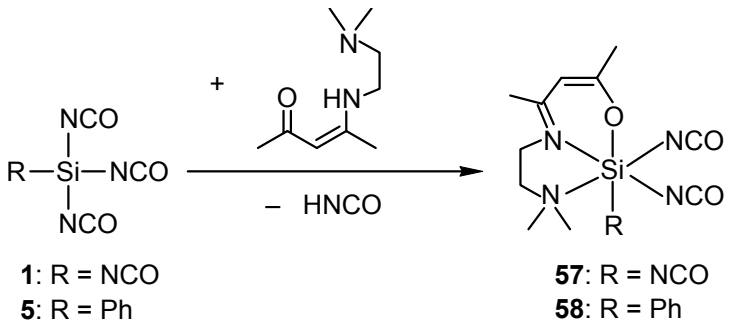

Scheme 14

3.8.2 Syntheses of hexacoordinate silicon(IV) complexes containing tetradentate ligands

Compounds **59** and **60** were prepared according to Scheme 15 by treatment of one molar equivalent of the dianionic tetradentate ligand (*O*,*O*,*N*,*N* donor) with one molar equivalent of **4** and **5**, respectively, in acetonitrile (yield: **59**, 31%; **60**, 66%).

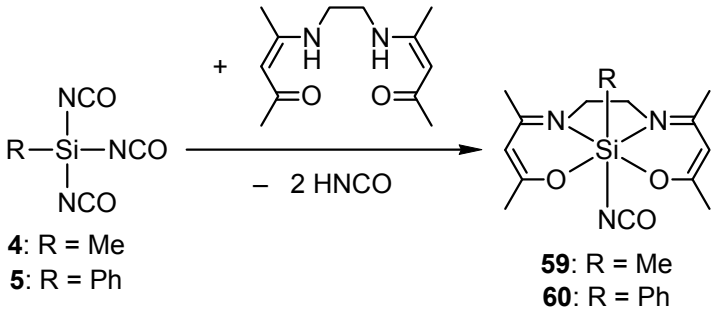

Scheme 15

The identities of **59** and **60** were established by elemental analyses (C, H, N) and solution NMR studies (^{1}H, ^{13}C, ^{15}N, ^{29}Si). Furthermore, these compounds were characterized in the solid-state by VACP/MAS NMR spectroscopy (^{13}C, ^{15}N, ^{29}Si) and single-crystal X-ray diffraction.

Compounds **62** and **63** were prepared according to Scheme 16 by treatment of one molar equivalent of the tetradentate aromatic ligand (*O*,*O*,*N*,*N* donor) with one molar equivalent of tri(cyanato-*N*)methylsilane and tri(cyanato-*N*)phenylsilane, respectively, in acetonitrile (yield: **62**, 28%; **63**, 7%).

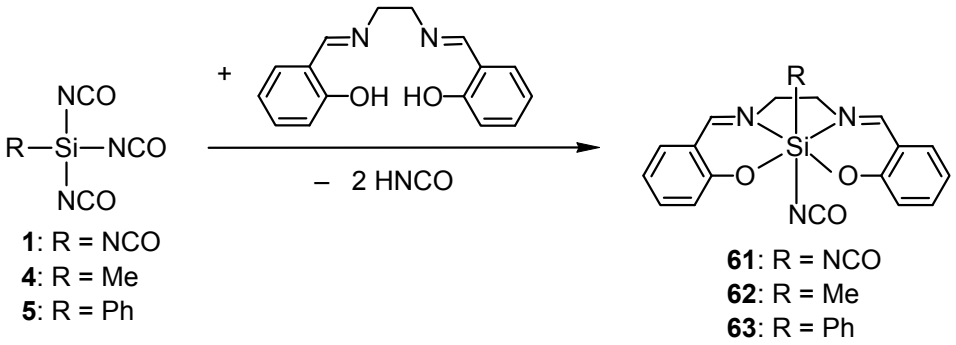

Scheme 16

The identities of **62** and **63** were established by elemental analyses (C, H, N) and solution NMR studies (^{1}H, ^{13}C, ^{15}N, ^{29}Si). Furthermore, compound **62** was characterized in the solid-state by VACP/MAS NMR spectroscopy (^{13}C, ^{15}N, ^{29}Si), and the identities of **62** and **63** were established by single-crystal X-ray diffraction. The synthesis of **61** was unsuccessful. Surprisingly, the reaction of one molar equivalent of the dianionic tetradentate *O*,*O*,*N*,*N*

ligand with one molar equivalent of tetra(cyanato-*N*)silane in acetonitrile afforded instead of **61**, compound **65** (yield 2%, Scheme 18).

Compound **64** was prepared according to Scheme 17 by the reaction of one molar equivalent of tetra(thiocyanato-*N*)silane with one molar equivalent of the tetradentate dianionic *O*,*O*,*N*,*N* ligand in acetonitrile.

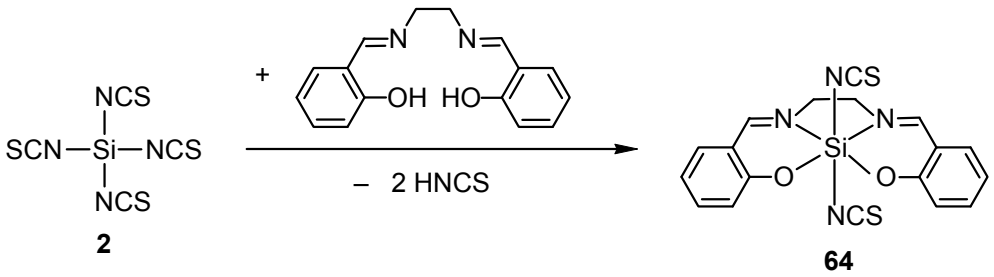

Scheme 17

The neutral thiocyanato-*N* silicon(IV) complex **64** was isolated as a crystalline yellow solid (yield: 47%) directly from the reaction mixture after recrystallization. Its identity was established in solution by NMR studies (^{1}H, ^{13}C, ^{15}N, ^{29}Si) and in the solid-state by elemental analysis (C, H, N, S), VACP/MAS NMR spectroscopy (^{13}C, ^{15}N, ^{29}Si) and single-crystal X-ray diffraction.

The binuclear hexacoordinate silicon(IV) complex **65** was supposed to be synthesized according to Scheme 18 by the hydrolysis of the hexacoordinate silicon(IV) complex **61**. Unfortunately, none of the attempts to prepare **65** led to any success. The hexacoordinate silicon complex **65** could only be obtained as a byproduct of the reaction between **1** and **32**.

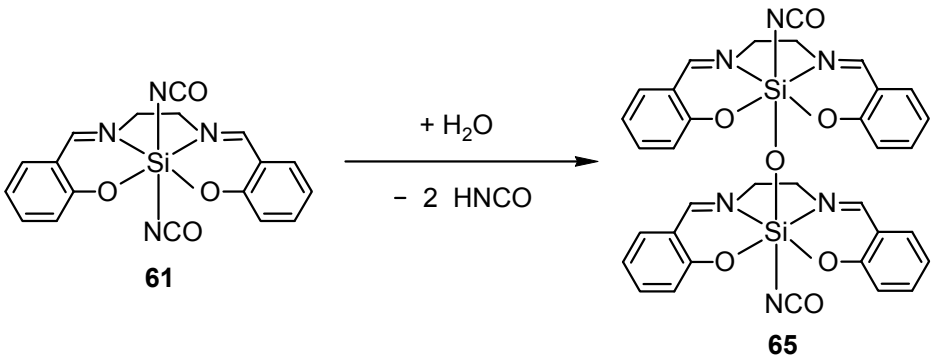

Scheme 18

Due to the low yield, compound **65** could be identified only by single-crystal X-ray diffraction.

4 NMR-Studies

4.1 Behavior of trimethylsilyl *N*-(trimethylsilyl)alaninate in solution

4.1.1 ^{29}Si-NMR studies of trimethylsilyl *N*-(trimethylsilyl)alaninate in solution

The silylation of *α*-amino acids was intensively studied over a large period of time. In the early 60s, L. Birkofer et al. reported on the preparation of trimethylsilyl *N*-(trimethylsilyl)alaninate, trimethylsilyl *N*-(trimethylsilyl)phenylalaninate, trimethylsilyl *N*-(trimethylsilyl)valinate, and trimethylsilyl *N*-(trimethylsilyl)-*tert*-leucinate [41]. However, many groups that tried to synthesize disilylated *α*-amino acids later, reported difficulties when preparing and isolating these compounds [44, 45]. Mixtures of mono- and disilylated *α*-amino acids as products by the protection of the functional groups (NH_2 and COOH) were obtained.

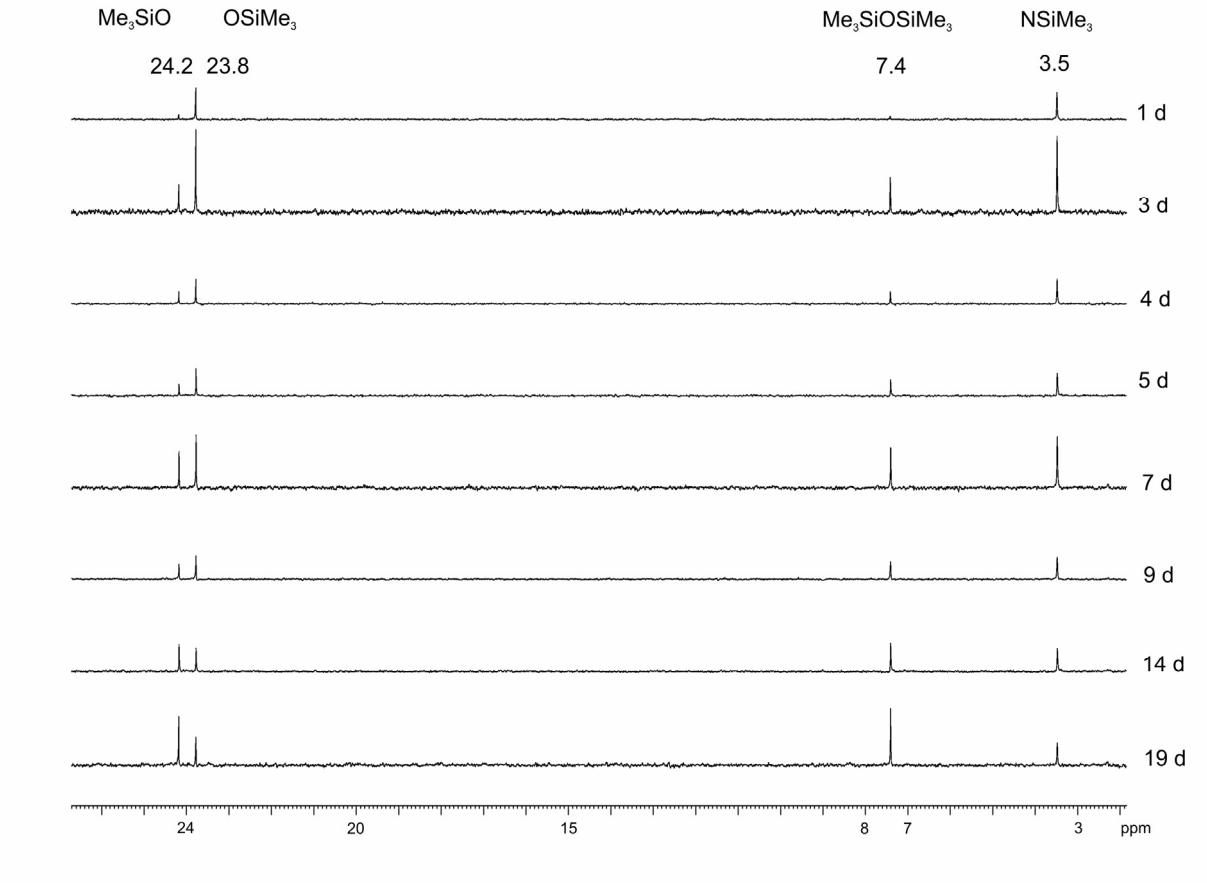

Figure 1. Behavior of trimethylsilyl *N*-(trimethylsilyl)alaninate in solution (CH_2Cl_2 was used as the solvent).

Following the unexpected syntheses of **38**, **39**, **43**−**50**, **52** and **53** (reactions of disilylated *α*-amino acids with cyanato-*N* silanes), our interest was directed towards the

behavior of trimethylsilyl *N*-(trimethylsilyl)alaninate in solution. We supposed that the disilylate *α*-amino acids undergo an isomerisation process in solution. Therefore, we studied the stability of the trimethylsilyl *N*-(trimethylsilyl)alaninate over three weeks by NMR spectroscopy. The ^{29}Si spectra were recorded in CH_2Cl_2 and are depicted in Figure 1. The chemical shifts at 3.5 ppm ($NHSiMe_3$) and 23.8 ppm ($OSiMe_3$) belong to the trimethylsilyl *N*-(trimethylsilyl)alaninate, whereas the peak observed at 7.4 ppm was assigned to $Me_3SiOSiMe_3$. The chemical shift seen at 24.2 ppm ($OSiMe_3$) was assigned to the trimethylsilyl group of the monosilylated alaninate ester. In conclusion, it can be said that the ratio of disilylated *α*-amino acids esters to the monosilylated species changes in time in favor of the monosilylated *α*-amino acids esters. We could clearly observe the formation of hexamethyldisiloxane and an increase of the monosilylated species in solution. Further NMR studies performed with trimethylsilyl (*S*)-*N*-(trimethylsilyl)alaninate that was stored without solvent or as a solution in dichloromethane at room temperature over a period of three weeks did not show any evidence for oligopeptide formation.

4.2 Pentacoordinate silicon(IV) complexes with an *Si*O_2N_2C and *Si*ON_3C skeleton

4.2.1 Comparison of the ^{29}Si NMR shifts of pentacoordinate silicon(IV) complexes with bidentate ligands in the solid-state and solution

The ^{29}Si NMR resonance signals of **38**, **39**, **43**−**46** in the solid-state are split [46, 47, 48] or broad (the singlet is mostly slightly structured) due to the $^1J(^{14}N, ^{29}Si)$ couplings. We were not able to simulate these spectra and ascertain the $^1J(^{14}N, ^{29}Si)$ couplings because these couplings were very poorly resolved.

The isotropic ^{29}Si chemical shifts obtained in the solid-state VACP/MAS measurements for **38**, **39**, **43**−**46** clearly demonstrate the presence of pentacoordinate silicon atoms. The ^{29}Si NMR resonance signals of **44** and **45** found in solution are in good agreement with the chemical shifts found in the solid-state and prove that these complexes also exist in solution. All attempts to characterize compounds **38**, **39**, **43**·CH_3CN, and **46**−**48** by solution NMR spectroscopy failed owing to their poor solubility in common organic solvents. The ^{29}Si NMR resonance shifts obtained in VACP/MAS measurements of **47** and **48** clarly demonstrate the presence of pentacoordinate silicon atoms (**47**, –93.5; **48**, –104.2 ppm).

Table 3: Comparison of the isotropic ^{29}Si-chemical shifts in the solid-state and in solution [ppm].

Compound	δ ^{29}Si (solid-state)	δ ^{29}Si (solution)[a]
38	–84.4[c]	————
39	–87.9 and –85.5[b, d]	————
43·CH_3CN	–96.0[b]	————
44	–98.5[b]	–97.7(**A**)/–99.1(**B**)[e]
45	–93.6[b]	–97.8(**A**)/–98.2(**B**)[f]
46·C_5H_{12}·1/2CH_3CN	–92.3[g]	————
47	–93.5, –1.1, –0.3	————
48	–104.2, –2.2, –1.5	————

[a] All NMR-spectra were recorded in [D_6]DMSO. [b] The ^{29}Si-NMR-Signal is a broad asymmetric doublet, slightly structured due to ^{14}N-coupling. [c] The ^{29}Si-NMR-Signal is split in an asymmetric doublet due to ^{14}N-coupling. [d] Data for two crystallographically independent molecules. [e] The solution-state NMR data refer to two isomers (molar ratio, **A**/**B** = 1:1.3). [f] The solution-state NMR data refer to two isomers (molar ratio, **A**/**B** = 1:0.9). [g] The ^{29}Si-NMR-Signal is a broad singlet, slightly structured due to ^{14}N-coupling.

The chemical shifts at –1.1 and –2.2 ppm and –0.3 and –1.5 ppm were assigned to the "free" trimethylsilyl groups belonging to the mono- and dianionic (methyl)alaninato ligands.

4.2.2 Comparison of the ^{29}Si NMR shifts of pentacoordinate silicon(IV) complexes with tridentate ligands in the solid-state and solution

The isotropic ^{29}Si chemical shifts obtained in the solid-state VACP/MAS measurements for **54** and **55** reflect the presence of pentacoordinate silicon atoms.

Table 4: Comparison of the isotropic ^{29}Si-chemical shifts in the solid-state and in solution [ppm].

Compound	δ ^{29}Si (solid-state)	δ ^{29}Si (solution)
54	–102.0	–105.2[a]
55	–107.1	–105.7[b]

[a] The solution NMR spectrum of **54** was recorded in [D_6]DMSO. [b] The solution NMR spectrum of **55** was recorded in CD_2Cl_2.

The ^{29}Si NMR solution resonance signals of **54** and **55** are in good agreement with the ^{29}Si chemical shifts found in the solid-state and show that these complexes also exist in solution.

4.3 Hexacoordinate silicon(IV) complexes with *Si*O_6, *Si*O_4NC, *Si*O_2N_4, *Si*O_2N_3C, *Si*ON_4C, and *Si*N_5C skeletons

4.3.1 Comparison of the ^{29}Si NMR shifts of hexacoordinate silicon(IV) complexes with an *Si*O_2N_4 skeleton in the solid-state and solution

The ^{29}Si NMR resonance signals of **49**, **50**, **52**, and **53** the solid-state are broad singlets (slightly structured) due to the $^{1}J(^{14}N, ^{29}Si)$ couplings [46, 47, 48]. We were not able to simulate these spectra and ascertain the $^{1}J(^{14}N, ^{29}Si)$ couplings because these couplings were very poorly resolved.

Table 5: Comparison of the isotropic ^{29}Si-chemical shifts in the solid-state and in solution [ppm].

Compound	δ ^{29}Si (solid-state)	δ ^{29}Si (solution)[a]
49	–184.5[b]	–186.6
50	–187.4[b]	–191.8/–191.9[c]
52	–189.5	————
53	–193.4	–193.8/–194.4[d]

[a] All NMR-spectra were recorded in [D_6]DMSO. [b] The ^{29}Si-NMR-signal is a broad singlet, slightly structured due to ^{14}N-coupling. [c] The solution-state NMR data refer to two isomers (molar ratio, **A**/**B** = 1:1). [d] The solution-state NMR data refer to two isomers (molar ratio, **A**/**B** = 1:0.4).

The isotropic ^{29}Si-chemical shifts of **49** and **53** in the solid-state and in solution are very similar and prove that these neutral hexacoordinate silicon(IV) complexes exist in solution as well. For compound **50**, the difference between the ^{29}Si resonance signals found in solution (–191.8/–191.9 ppm) and in the solid-state (–187.4 ppm) is greater, but still clearly shows, in both cases, hexacoordination of the silicon atom. All attempts to characterize compound **52** by solution NMR spectroscopy failed owing to its poor solubility in common organic solvents.

4.3.2 Comparison of the ^{29}Si NMR shifts of hexacoordinate silicon(IV) complexes with *Si*O$_6$, *Si*O$_4$NC, *Si*O$_2$N$_4$, *Si*O$_2$N$_3$C, *Si*ON$_4$C, and *Si*N$_5$C skeletons in the solid-state and solution

The ^{29}Si NMR resonance signals of **33**, **34**, **56**−**61** and **64** in the solid-state are split or broad (the singlet is mostly slightly structured) due to the $^1J(^{14}N, ^{29}Si)$ couplings.

Table 6: Comparison of the isotropic ^{29}Si-chemical shifts in the solid-state and in solution [ppm].

Compound	δ ^{29}Si (solid-state)	δ ^{29}Si (solution)	Skeleton
33	–185.1	–184.4[a]	*Si*O$_4$NC
34	–184.6	–183.6[a]	*Si*O$_4$NC
35	–174.8	–174.3[b]	*Si*O$_6$
36	–187.2	–186.6[c]	*Si*O$_6$
56	–172.9	–172.1[c, d]	*Si*ON$_4$C
57	–199.4[e]	–200.2[a]	*Si*ON$_4$C
58	–180.4	–179.8[a]	*Si*ON$_5$
59	–182.6	–181.5[a]	*Si*O$_2$N$_3$C
60	–190.1	–190.3[c]	*Si*O$_2$N$_3$C
62	–184.0	–184.2[a]	*Si*O$_2$N$_3$C
64	–210.1	–188.5/–189.6/–198.6	*Si*O$_2$N$_4$

[a] The solution NMR-spectra of **33**, **34**, **57**−**59**, **62**, **64** were recorded in [D$_6$]DMSO. [b] The solution NMR-spectra of **35** were recorded in CDCl$_3$. [c] The solution NMR-spectra of **36**, **56**, **60** were recorded in CD$_2$Cl$_2$. [d] The ^{29}Si-NMR-signal is a broad singlet, slightly structured due to ^{14}N-coupling.

The isotropic ^{29}Si-chemical shifts of **33**−**36** and **56**−**60** and **62** in the solid-state and in solution are very similar and prove that these neutral hexacoordinate silicon(IV) complexes exist in solution as well. For compound **64**, the difference between the ^{29}Si resonance signals found in solution (see Experimental Section, –188.5/–189.6/–198.6 ppm) and in the solid-state (–210.1 ppm) is greater, but still clearly shows hexacoordination. In the solution spectra of **64**, the existence of three isomers was noticed, even when this complex was synthesized under different reaction conditions.

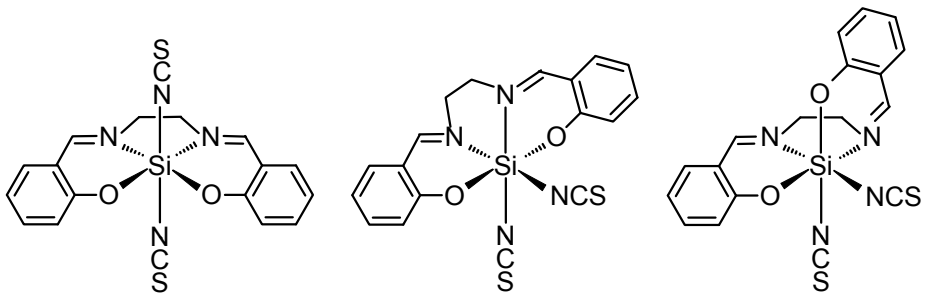

64a **64b** **64c**

Scheme 19

The stereoisomers of **64** might be consistent with the depicted molecular structures presented in Scheme 19, but further studies (NMR, computational calculations) need to be performed to confirm the existence and the stability of these complexes in the solution-state. In addition, the dynamic behavior of **64** needs to be studied.

5 Crystal Structure Analyses

5.1 General Procedures

Suitable single crystals of **33**−**36**, **38**, **39**, **43**·CH_3CN, **44**, **46**·C_5H_{12}·1/2CH_3CN, **50**, **54**, **55**−**62**, **64**, and **65**·2CH_3CN were obtained directly from the respective reaction mixtures (see Syntheses). The crystals were mounted in inert oil (perfluoropolyalkyl ether, ABCR) on a glass fiber and then transferred to the cold nitrogen gas stream of the diffractometer (Stoe IPDS (**33**, **34**, **38**, **39**, **43**·CH_3CN, **54**, **55**, **60**, **62**, and **64**; graphite-monochromated Mo K_α radiation, λ = 0.71073 Å) and Bruker Nonius KAPPA APEX II (**35**, **36**, **44**, **46**·C_5H_{12}·1/2CH_3CN, **50**, **56**, **57**, **58**, **59**, **61** and **65**·2CH_3CN; Montell mirror, Mo K_α radiation, λ = 0.71073 Å)). All structures were solved by direct methods (SHELXS-97 [49]). The non-hydrogen atoms were refined anisotropically (SHELXL-97 [50]). For the CH hydrogen atoms, a riding model was employed. The NH and NH_2 hydrogen atoms of **38**, **39**, **43**·CH_3CN, **44**, **46**·C_5H_{12}·1/2CH_3CN, **50** were resolved directly. For the pentacoordinate systems, two energetical possible arrangements of the silicon coordination polyhedra can be realized, namely: a trigonal bipyramid (TBP) and a square pyramid (SP). For all pentacoordinate silicon(IV) complexes reported in this thesis, a trigonal bipyramidal polyhedron was found in the crystal. The Berry distortion grades (transition TBP to SP) are given in the respective discussions of the crystal structure analyses. A distortion grade of 0% represents an ideal trigonal bipyramid, while a 100% distortion describes a perfect square pyramid. The quantification of the transition TBP to SP was made with the PLATON program [51]. For all hexacoordinate systems, an octahedron silicon polyhedron was found in the crystal.

5.2 Hexacoordinate silicon(IV) complexes with an *Si*O_4NC skeleton

5.2.1 Crystal structure of 33[1]

The hexacoordinate silicon(IV) complex **33** crystallized in the monoclinic space group $P2_1/c$ at −20 °C from acetonitrile. The molecular structure of **33** is depicted in Figure 2.

[1]The crystal structure analysis was performed by Dr. Christian Burschka, Department of Inorganic Chemistry, University of Würzburg: λ, 0.71073 Å; T, 193(2) K; space group, $P2_1/c$; a, 8.4741(12) Å; b, 13.4598(15) Å; c, 15.308(2) Å; α, 90.0°; β, 92.666(18) °; γ, 90.0°; $R1$ [$I>2\sigma(I)$], 0.0411.

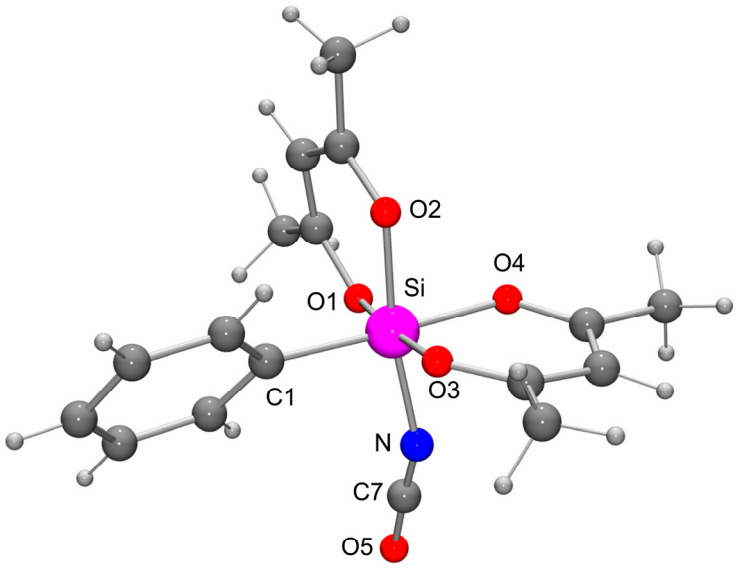

Figure 2. Molecular structure of **33** in the crystal with numbering of the selected atoms. Selected bond lengths [Å] and angles [°]: Si–O1 1.7977(11), Si–O2 1.8079(11), Si–O3 1.7888(10), Si–O4 1.8217(12), Si–N 1.8087(13), Si–C1 1.9130(16); O1–Si–O2 92.76(5), O1–Si–O3 175.61(5), O1–Si–O4 84.56(5), O1–Si–N 89.54(6), O1–Si–C1 93.67(6), O2–Si–O3 85.18(5), O2–Si–O4 85.12(5), O2–Si–N 171.71(6), O2–Si–C1 93.18(6), O3–Si–O4 91.39(5), O3–Si–N 91.97(6), O3–Si–C1 90.32(6), N–Si–C1 94.62(6), Si–N–C7 148.37(14), N–C7–O5 177.5(2).

The Si-coordination polyhedron of **33** represents a distorted octahedron. The silicon atom is surrounded by two bidentate monoanionic acetylacetonato(1−) ligands, one monoanionic pseudohalide ligand (NCO), and one phenyl moiety. The Si−N bond length of **33** (1.8087(13) Å) of the cyanato-*N* ligand is one of the shortest Si−N distance belonging to an NCO group (**62**, 1.9445(12), 1.9584(14); **63**, 1.943(2), 1.928(2); **64**, 1.909(2), 1.9175(19); **65**, 1.9002(9) Å) known in the literature so far. The Si−O bond lengths of **33** (Si–O1 1.7977(11), Si–O2 1.8079(11), Si–O3 1.7888(10), Si–O4 1.8217(12) Å) are similar to those of **62** (1.7409(11), 1.7510(11) Å) and **63** (1.7352(17), 1.7302(17) Å), respectively. The Si−NCO fragment shows again a strong deviation with 148.37(14)° and is still within the range of the Si−NCO angles. Nevertheless, the cyanato-*N* group is almost linear (N−C7−O5, 177.5(2)°). The maximum deviations from the ideal 90° and 180° angles are 5.44° and 8.28°, respectively.

5.2.2 Crystal structure of 34[2]

The hexacoordinate silicon(IV) complex **34** crystallized in the monoclinic space group $P2_1/n$ at 20 °C from acetonitrile. The molecular structure of **34** is depicted in Figure 3.

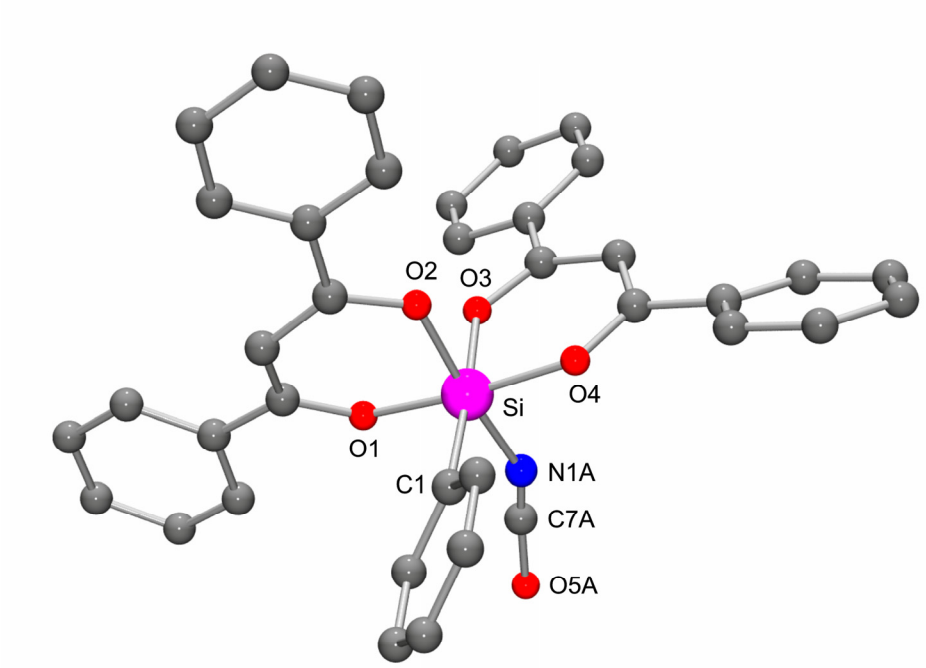

Figure 3. Molecular structure of **34** in the crystal with numbering of the selected atoms. Selected bond lengths [Å] and angles [°]: Si–O1 1.7859(14), Si–O2 1.8017(16), Si–O3 1.8143(15), Si–O4 1.7883(15), Si–N1A 1.838(2), Si–C1 1.9063(19); O1–Si–O2 91.67(6), O1–Si–O3 82.99(6), O1–Si–O4 173.61(7), O1–Si–N1A 88.96(7), O1–Si–C1 94.51(7), O2–Si–O3 85.60(8), O2–Si–O4 86.15(7), O2–Si–N1A 172.71(8), O2–Si–C1 92.71(7), O3–Si–O4 90.85(7), O3–Si–N1A 87.27(9), O3–Si–C1 176.93(8), N1A–Si–C1 94.48(8), Si–N1A–C7A 145.4(2), N1A–C7A–O5A 176.3(6).

The Si-coordination polyhedron of **34** represents a distorted octahedron with a distortion at the nitrogen atom (N1A), as well as at the carbon- (C7A) and oxygen atoms (O5A). The silicon atom is surrounded by two bidentate monoanionic dibezoylmethanato(1−) ligands, one monoanionic pseudohalide ligand (NCO), and one phenyl moiety. The Si−N bond length of **34** (1.838(2) Å) of the cyanato-*N* ligand is one of the shortest Si−N distances known in the literature so far, belonging to an NCO group (**62**, 1.9445(12), 1.9584(14); **63**, 1.943(2), 1.928(2); **64**, 1.909(2), 1.9175(19); **65**, 1.9002(9) Å), and somewhat longer than the Si−N bond length of **33** (1.8087(13) Å). The Si−O bond lengths of **34** (Si–O1 1.7859(14), Si–O2 1.8017(16), Si–O3 1.8143(15), Si–O4 1.7883(15) Å) are very similar to those of **33** (Si–

[2]The crystal structure analysis was performed by Dr. Christian Burschka, Department of Inorganic Chemistry, University of Würzburg: λ, 0.71073 Å; T, 173(2) K; space group, $P2_1/n$; a, 9.3201(19) Å; b, 22.229(4) Å; c, 14.074(3) Å; α, 90.0°; β, 90.58(3) °; γ, 90.0°; $R1$ [$I>2\sigma(I)$], 0.0488.

O1 1.7977(11), Si–O2 1.8079(11), Si–O3 1.7888(10), Si–O4 1.8217(12) Å). The Si−C1 bond length of 1.9063(19) is similar to the corresponding Si−C1 bond length of **33** (1.9130(16) Å). The Si−NCO fragment shows again a strong deviation (145.4(2)°) and is smaller than the Si–N–C angle of **33** (148.37(14)°). This deviation might be explained by the steric influence of the bulkier benzoylato ligands. Nevertheless, the cyanato-*N* group is almost linear (N1A−C7A−O5A, 176.3(6)°). The maximum deviations from the ideal 90° and 180° angles are 7.00° and 7.28°, respectively.

5.3 Hexacoordinate silicon(IV) complexes with an SiO_6 skeleton

5.3.1 Crystal structure of 35[3]

The neutral hexacoordinate silicon(IV) complex **35** with an SiO_6 skeleton crystallized at 20 °C directly from the reaction mixture in the monoclinic space group C_2/c. The molecular structure of **35** is depicted in Figure 4.

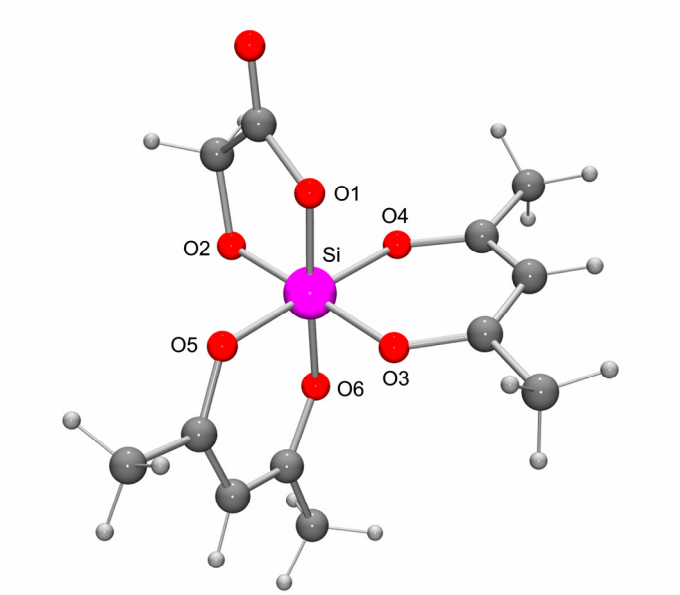

Figure 4. Molecular structure of **35** in the crystal with numbering of the selected atoms. Selected bond lengths [Å] and angles [°]: Si–O1 1.77(9), Si–O2 1.70(9), Si–O3 1.79(11), Si–O4 1.81(10), Si–O5 1.80(12), Si–O6 1.77(9); O1–Si–O2 91.0(6), O1–Si–O3 89.0(6), O1–Si–O4 91.0(6), O1–Si–O5 88.0(6), O1–Si–O6 177.34(14), O2–Si–O3 177.25(9), O2–Si–O4 90.0(6), O2–Si–O5 93.0(6), O2–Si–O6 91.0(6), O3–Si–O4 92.0(6), O3–Si–O5 85.0(7), O3–Si–O6 90.0(6), O4–Si–O5 176.68(7), O4–Si–O6 87.0(6), O5–Si–O6 93.0(6).

[3]The crystal structure analysis was performed by Dr. Christian Burschka, Department of Inorganic Chemistry, University of Würzburg: λ, 0.71073 Å; T, 100(2) K; space group, C_2/c; a, 13(2) Å; b, 11.939 Å; c, 18.620 Å; α, 90.0°; β, 100.53°; γ, 90.0°; $R1$ [$I>2\sigma(I)$], 0.0441.

The Si-coordination polyhedron of **35** is a distorted octahedron with maximal deviations from the ideal 90° and 180° angles of ca. 5° and 3°, respectively. Compound **35** contains two monoanionic acetylacetonato(1−) ligands and one dianionic glycolato(2−) ligand. The acetylacetonato(1−) ligands along with the silicon atom form two six-membered rings, while the glycolato(2−) ligand forms a five-membered ring with the silicon atom. The Si−O bond lengths are, at 1.70(9)−1.81(10) Å, similar to the Si−O bond lengths found in other neutral hexacoordinate silicon complexes with an *Si*O$_6$ skeleton, i.e, to those of **73** (1.7116(14)−1.8010(13) Å) [52] and to those of [benzilato(2−)-O^1,O^2]bis[1,3-diphenylpropan-1,3-dionato(1−)-*O*,*O*′]silicon(IV) (1.6926(10)−1.8208(10) Å) [53]. A short analysis of the C−C bond lengths of the acetylacetonato fragments shows clearly the delocalisation of the π-electrons and shows, as expected, a shortening of the bond lengths from 1.49(10)−1.49(15) Å to 1.38(10)−1.39(14) Å.

5.3.2 Crystal structure of 36[4]

The neutral hexacoordinate silicon(IV) complex **36** with an *Si*O$_6$ skeleton crystallized at 20 °C directly from the reaction mixture. The molecular structure of **36** is depicted in Figure 5.

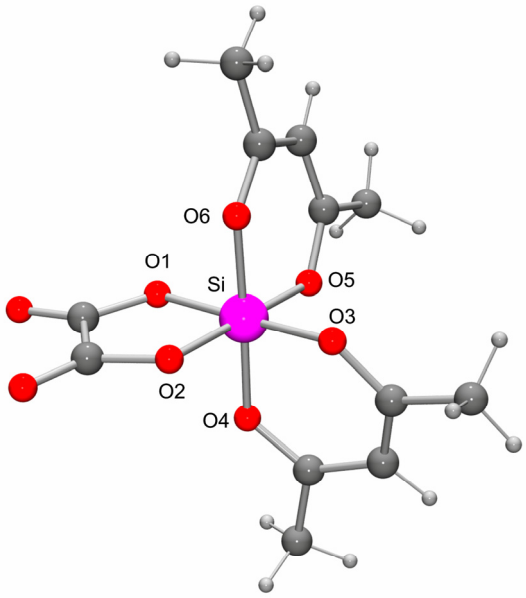

Figure 5. Molecular structure of **36** in the crystal with numbering of the selected atoms. Selected bond lengths [Å] and angles [°]: Si–O1 1.7654(9), Si–O2 1.7728(9), Si–O3 1.7608(10), Si–O4 1.7823(9), Si–O5 1.7577(9), Si–O6 1.7884(9); O1–Si–O2 88.39(4), O1–Si–O3 176.25(4), O1–Si–O4 87.92(4), O1–Si–O5 89.94(4), O1–Si–

[4]The crystal structure analysis was performed by Dr. Christian Burschka, Department of Inorganic Chemistry, University of Würzburg: λ, 0.71073 Å; *T*, 100(2) K; space group, $P2_1/c$; *a*, 12.2975(8) Å; *b*, 8.0588(5) Å; *c*, 14.6828(9) Å; α, 90.0°; β, 106.7270(10)°; γ, 90.0°; *R*1 [$I>2\sigma(I)$], 0.0333.

O6 90.14(4), O2–Si–O3 88.69(5), O2–Si–O4 91.03(4), O2–Si–O5 177.37(5), O2–Si–O6 88.30(4), O3–Si–O4 94.49(4), O3–Si–O5 93.06(4), O3–Si–O6 87.42(4), O4–Si–O5 86.87(4), O4–Si–O6 177.96(4), O5–Si–O6 93.74(4).

The Si-coordination polyhedron of **36** shows a distorted octahedron with maximum deviations from the ideal 90° and 180° angles of ca. 4.49° and 3.75°, respectively. Compound **36** crystallized in the space group $P2_1/c$ and contains two monoanionic acetylacetonato(1−) and one dianionic oxalato(2−) ligand. The acetylacetonato(1−) ligand forms two six-membered rings with the silicon atom, while the oxalato(2−) ligand only forms a five-membered ring with the silicon atom. The Si−O bond lengths of 1.7577(9)−1.7884(9) Å are within the range of Si−O bond lengths known so far for other neutral hexacoordinate silicon complexes with an SiO_6 skeleton, i.e, those of **73** (1.7116(14)−1.8010(13) Å) [52] and to those of the [benzilato(2−)-O^1,O^2]bis[1,3-diphenylpropan-1,3-dionato(1−)-O,O']silicon(IV) complex (1.6926(10)−1.8208(10) Å) [53]. A short analysis of the C−C bond lengths of the acetylacetonato fragments shows clearly the delocalisation of the π-electrons. Compared to the silicon(IV) complex **34**, the hexacoordinate silicon(IV) complex containing [1,3-diphenylpropan-1,3-dionato(1–)-O,O]-ligands and one benzilic acid ligand (Si−O, 1.6926(10)−1.8208(10) Å), where a considerable difference was observed for Si−O bond lengths [56], the Si−O distances of **36** differ very little from each other.

5.4 Zwitterionic λ^5*Si*-silicates

5.4.1 Crystal structure of 38[5]

The pentacoordinate silicon(IV) complex **38** crystallized at –70 °C to –20 °C in acetonitrile and was isolated as the (TB-5-12-Δ)-(*S*,*S*) isomer (Figure 6). The Si-coordination polyhedron of **38** is a distorted trigonal bipyramid, with a Berry distortion (transition trigonal bipyramid → square pyramid; pivot atom C1) of 20.7 % [54].

[5]The crystal structure analysis was performed by Dr. Christian Burschka, Department of Inorganic Chemistry, University of Würzburg: λ, 0.71073 Å; T, 193(2) K; space group, $P2_12_12_1$; a, 7.6563(6) Å; b, 10.9386(9) Å; c, 12.4438(12) Å; α, 90.0°; β, 90.0°; γ, 90.0°; $R1$ [$I>2\sigma(I)$], 0.0301.

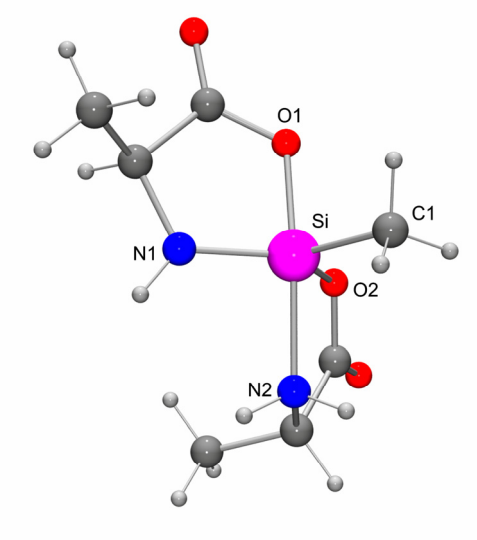

Figure 6. Molecular structure of **38** in the crystal with numbering of the selected atoms. Selected bond lengths [Å] and angles [°]: Si–O1 1.7910(13), Si–O2 1.7118(11), Si–N1 1.6901(14), Si–N2 1.9932(14), Si–C1 1.8401(18); O1–Si–O2 86.63(6), O1–Si–N1 87.69(6), O1–Si–N2 167.64(6), O1–Si–C1 95.29(8), O2–Si–N1 123.85(7), O2–Si–N2 83.57(6), O2–Si–C1 111.63(8), N1–Si–N2 91.52(6), N1–Si–C1 124.52(9), N2–Si–C1 95.31(8).

The axial positions are occupied by the oxygen atom O1 and the nitrogen atom N2, whereas the oxygen atom O2, the nitrogen atom N1, and the carbon atom C1 are found in the equatorial sites. The sum of the equatorial bond angles amounts to 360°, and the axial O1–Si–N2 angle is 167.64(6)°. The Si–O1 (1.7910(13) Å) and Si–N1 bond lengths (1.6901(14) Å) are slightly shorter than the analogous axial Si–O (1.8058(14)–1.8356(19) Å) and equatorial Si–N distances of **66**−**70** (1.7087(17)−1.725(3) Å) [39, 55]. The Si−C1 bond length (1.8401(18) Å) is also shorter than the analogous equatorial Si−C distances of **66**−**70** (1.906(3)−1.9274(18) Å), reflecting the different coordination mode of the monoanionic chelate ligand of **38**. As expected, the equatorial Si–O2 distance of **38** (1.7118(11) Å) is somewhat shorter than the axial Si–O1 bonds, whereas the axial Si–N2 distance of **38** (1.9932(14) Å) is considerably longer than the equatorial Si–N1 distance. Nevertheless, this Si–N2 distance and the bond angles of the SiO_2N_2C skeleton of **38** clearly indicate Si–N2 bonding interactions. As expected, through the amine donor functions (NH, NH_2) and the acceptor functions (O3, O4) of the alaninato ligands, in the crystal of **38**, some intramolecular N−H···O hydrogen bridge bonds were observed. These bonds lead to infinite chains in the crystal (N2−H···O3, N2−H···O4, N1−H···O1). Surprisingly, the alaninato groups act here as monoanionic and as dianionic ligands.

5.4.2 Crystal structure of 39[6]

Compound **39** crystallized at –20 °C directly from the reaction mixture and was isolated as the (TB-5-12-Λ)-(*S*,*S*) isomer showing a non-VSEPR structure. The molecular structures of the two independent molecules found in the crystal of **39** are depicted in Figure 7.

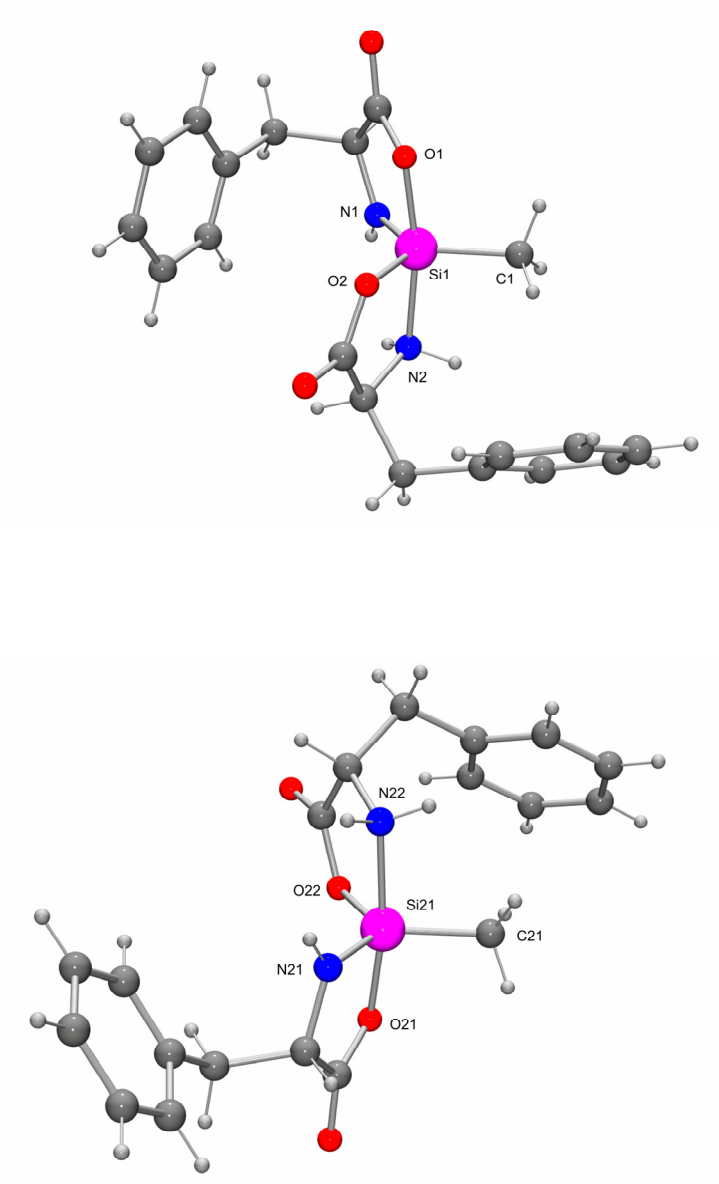

Figure 7: Molecular structures of the two crystallographically independent molecules (top molecule **I**; bottom molecule **II**) of **39** in the crystal with numbering of the selected atoms. Selected bond lengths [Å] and angles

[6]The crystal structure analysis was performed by Dr. Christian Burschka, Department of Inorganic Chemistry, University of Würzburg: λ, 0.71073 Å; *T*, 193(2) K; space group, $P2_12_12_1$; *a*, 6.5828(6) Å; *b*, 23.3334(18) Å; *c*, 24.524(2) Å; α, 90.0°; β, 90.0°; γ, 90.0°; *R*1 [$I>2\sigma(I)$], 0.0328.

[°]of molecule **I**: Si1–O1 1.8038(11), Si1–O2 1.7207(12), Si1–N1 1.7052(15), Si1–N2 1.9731(13), Si1–C1 1.8654(18); O1–Si1–O2 87.85(6), O1–Si1–N1 86.63(6), O1–Si1–N2 169.01(6), O1–Si1–C1 96.42(7), O2–Si1–N1 124.53(7), O2–Si1–N2 85.19(5), O2–Si1–C1 112.11(7), N1–Si1–N2 90.32(6), N1–Si1–C1 123.36(8), N2–Si1–C1 94.07(7). Selected bond lengths [Å] and angles [°] of molecule **II**: Si21–O21 1.7995(10), Si21–O22 1.7220(12), Si21–N21 1.7114(13), Si21–N22 1.9823(12), Si21–C21 1.8581(17); O21–Si21–O22 87.38(5), O21–Si21–N21 87.39(5), O21–Si21–N22 170.55(6), O21–Si21–C21 93.88(7), O22–Si21–N21 120.56(6), O22–Si21–N22 85.21(5), O22–Si21–C21 115.63(7), N21–Si21–N22 91.34(5), N21–Si21–C21 123.80(7), N22–Si21–C21 94.61(7).

Compound **39** crystallized in the space group $P2_12_12_1$, with two crystallographically independent molecules in the asymmetric unit. The bond lengths and bond angles of the two independent molecules of **39** are very similar, except for the equatorial bond angles O−Si−N (124.53(7)°, molecule **I**, and 120.56(6)°, molecule **II**); O−Si−C (112.11(7)°, molecule **I**, and 115.63(7)°, molecule **II**), and the O1−Si1−C1 and O21−Si21−C21 bond angles (96.42(7)° molecule **I**, and 93.88(7)° molecule **II**), which differ by between 3° and 4° from each other (for further details regarding both molecular structures of **39**, see Appendix A). The differences observed here might be due to the orientation of the two independent molecules in the crystal. The Si-coordination polyhedron of **39** represents a distorted trigonal bipyramid (Berry distortion, transition trigonal bipyramid → square pyramid; pivot atom C1: 21.2 % for molecule **I**, and 12.0 % for molecule **II**) [54]. The axial positions are occupied by one oxygen atom (O1, O21), and by one nitrogen atom belonging to the NH_2 group (N2, N21), whereas the other oxygen atom (O2, O22), the nitrogen atom belonging to the NH group (N1, N21) and the carbon atoms C1 and C21 are found in the equatorial sites. The axial Si−O (1.8038(11), 1.7995(10) Å) and the Si−N bond lengths (1.9731(13), 1.9823(12) Å) are slightly longer than the analogous axial Si−O bond lengths of **43**·CH_3CN, and very similar to the analoguos axial Si−O and Si−N bond lengths of **44** (Si–O1, 1.8004(9) Å; Si–N2, 1.9677(11) Å). The equatorial Si−O, Si−N, Si−C distances found in **39** (Si1−O2 1.7207(12) Å, Si21−O22 1.7220(12); Si1–N1, 1.7052(15), Si21–N21, 1.7114(13) Å; Si1−C1, 1.8654(18), Si21−C21, 1.8581(17) Å) are slightly longer than those found in the analogous pentacoordinate silicon(IV) complex **44** (Si−O2 1.7042(10) Å; Si–N1, 1.6989(12) Å; Si−C1, 1.8582(13) Å). An explanation for the shortening of the equatorial Si−O and Si−N distances of **39** and **44** compared with those of **38** and **43**·CH_3CN might be due to the steric arrangement of the mono- and dianionic phenylalaninato-ligands. The sum of the equatorial bond angles of **39** is 360°.

5.4.2 Crystal structure of 43·CH_3CN[7]

Compound **43**·CH_3CN crystallized at –70 °C to –20 °C in acetonitrile. The molecular structure of **43**·CH_3CN is shown in Figure 8 (for clarity the co-crystallized solvent acetonitrile was omitted).

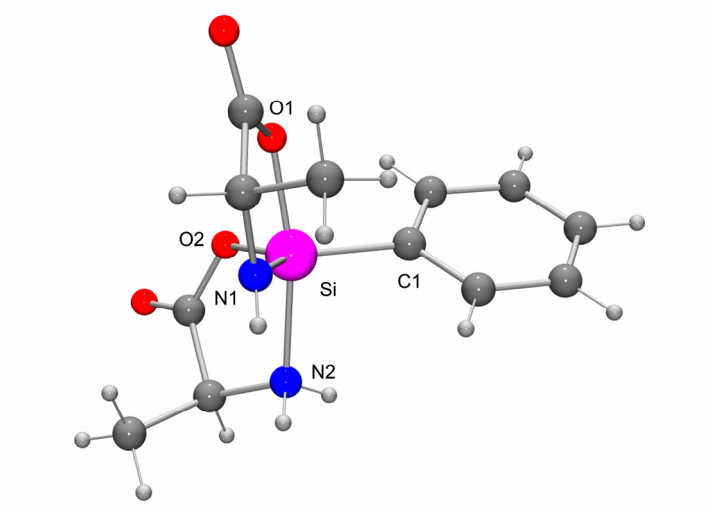

Figure 8. Molecular structure of **43** in the crystal of **43**·CH_3CN with numbering of the selected atoms. Selected bond lengths [Å] and angles [°]: Si–O1 1.7871(14), Si–O2 1.7082(14), Si–N1 1.6885(17), Si–N2 1.9658(17), Si–C1 1.854(2); O1–Si–O2 86.98(7), O1–Si–N1 87.68(7), O1–Si–N2 168.25(7), O1–Si–C1 96.12(8), O2–Si–N1 125.90(9), O2–Si–N2 84.22(7), O2–Si–C1 110.61(9), N1–Si–N2 91.18(8), N1–Si–C1 123.49(10), N2–Si–C1 94.27(8).

The chiral compound **43**·CH_3CN was isolated as the (TB-5-12-Δ)-(*S*,*S*) isomer. The Si-coordination polyhedron of **43**·CH_3CN shows a distorted trigonal bipyramid, with a Berry distortion (transition trigonal bipyramid → square pyramid; pivot atom C1) of 23.8 % [54]. The axial positions are occupied by the oxygen atom O1 and the nitrogen atom N2, whereas the oxygen atom O2, the nitrogen atom N1, and the carbon atom C1 are found in the equatorial sites. The sum of the equatorial bond angles amounts to 360°, and the axial O1–Si–N2 angle is 168.25(7)°. The Si–O1 (1.7871(14) Å) and Si–N1 bond lengths (1.6885(17) Å) are slightly shorter than the analogous axial Si–O (1.8058(14)–1.8356(19) Å) and equatorial Si–N distances of **66**−**70** (1.7087(17)−1.725(3) Å). The Si−C1 bond length (1.854(2) Å) is also shorter than the analogous equatorial Si−C distances of **66**−**70** (1.906(3)−1.9274(18) Å),

[7]The crystal structure analysis was performed by Dr. Christian Burschka, Department of Inorganic Chemistry, University of Würzburg: λ, 0.71073 Å; *T*, 193(2) K; space group, $P2_12_12_1$; *a*, 8.5016(7) Å; *b*, 11.1129(13) Å; *c*, 17.5068(16) Å; α, 90.0°; β, 90.0°; γ, 90.0°; *R*1 [$I>2\sigma(I)$], 0.0445.

reflecting the different coordination mode of the monoanionic chelate ligand of **43**·CH_3CN. As expected, the equatorial Si–O2 distance of **43**·CH_3CN (1.7082(14) Å) is somewhat shorter than the axial Si–O1 bond, whereas the axial Si–N2 distance of **43**·CH_3CN (1.9658(17) Å) is considerably longer than the equatorial Si–N1 distance. Nevertheless, the Si–N2 distance and the bond angles of the SiO_2N_2C skeleton of **43**·CH_3CN clearly indicate Si–N2 bonding interactions.

5.4.4 Crystal structure of 44[8]

Compound **44** crystallized in the monoclinic space group $P2_1$ at –20 °C from acetonitrile and was isolated as the (TB-5-12-Λ)-(*S*,*S*) isomer showing a non-VSEPR structure. The molecular structure of **44** is depicted in Figure 9.

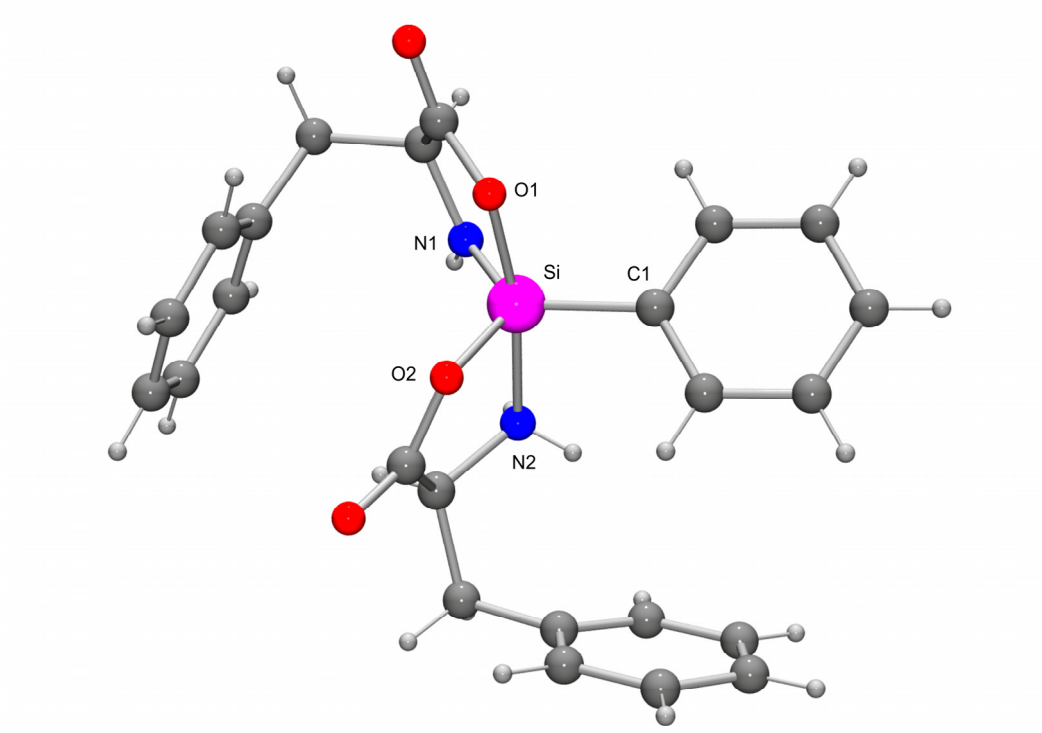

Figure 9. Molecular structure of **44** in the crystal with numbering of the selected atoms. Selected bond lengths [Å] and angles [°]: Si–O1 1.8004(9), Si–O2 1.7042(10), Si–N1 1.6991(12), Si–N2 1.9677(11), Si–C1 1.8582(13); O1–Si–O2 88.35(5), O1–Si–N1 87.11(5), O1–Si–N2 169.43(5), O1–Si–C1 95.04(5), O2–Si–N1 123.98(5), O2–Si–N2 84.66(5), O2–Si–C1 111.65(5), N1–Si–N2 90.24(5), N1–Si–C1 124.37(6), N2–Si–C1 94.90(5).

[8]The crystal structure analysis was performed by Dr. Christian Burschka, Department of Inorganic Chemistry, University of Würzburg: λ, 0.71073 Å; T, 100(2) K; space group, $P2_1$; a, 6.6931(4) Å; b, 13.5206(9) Å; c, 11.9450(8) Å; α, 90.0°; β, 103.534(2)°; γ, 90.0°; $R1$ [$I>2\sigma(I)$], 0.0269.

The Si-coordination polyedron of **44** represents a distorted trigonal bipyramid with a Berry distortion (transition trigonal bipyramid → square pyramid; pivot atom C1) of 19.6 % [54]. The axial positions of the Si-coordination polyhedron of **44** are occupied by one oxygen atom O1 and by one nitrogen atom belonging to the NH_2 group (N2), whereas the other oxygen atom O2, the nitrogen atom belonging to the NH group (N1) and the carbon atom C1 are found in the equatorial sites. The axial Si−N distance of **44** (Si–N2, 1.9677(11) Å) is slightly shorter than the Si−N bond lengths of **39** (1.9731(13), 1.9823(12) Å) and very similar to the analoguos axial Si−N bond lengths of **43**·CH_3CN (Si–N2, 1.9658(17) Å). The equatorial Si−O, Si−N, Si−C distances found in **44** (Si−O2 1.7042(10) Å; Si–N1, 1.6991(12) Å; Si−C1, 1.8582(13) Å) are slightly shorter than those found in the analogous pentacoordinate silicon(IV) complex **39** and might be due to the steric arrangement of the mono- and dianionic phenylalaninato-ligands and by the replacement of the new phenyl rest (**44**) instead of the methyl fragment (**39**). The sum of the equatorial bond angles of **44** amounts to 360°.

5.4.5 Crystal structure of 46·C_5H_{12}·1/2CH_3CN [9]

The pentacoordinate silicon(IV) complex **46** crystallized in the tetragonal space group $I4_1$, and was found as the solvate **46**·C_5H_{12}·1/2CH_3CN (for clarity the co-crystallized solvents *n*-pentane and acetonitrile were omitted in Figure 10). The molecular structure of **46** is shown in Figure 10.

Compound **46** was isolated as the (TB-5-11-Δ)-(*S*,*S*) isomer. The Si-coordination polyhedron of **46** is a distorted trigonal bipyramid, with a Berry distortion (transition trigonal bipyramid → square pyramid; pivot atom C1) of 26.8 % [54]. The nitrogen atoms N1 and N2 of the mono- and dianionic ligands and the carbon atom C1 occupy equatorial positions, according to the VSEPR concept. The axial sites are occupied by the oxygen atoms O1 and O2. Surprisingly, the arrangement of the oxygen and nitrogen atoms found in the crystal of **46** fits no longer to the expected model of **38**, **39**, **43**·CH_3CN, and **44**, and is similar to the one found in the hitherto λ^5 *Si*-silicates, which contains (*S*)-leucinate groups [54]. The axial Si−O distances of **46** (Si–O1 1.8199(8), Si–O2 1.7876(8) Å) are similar to the analogous axial Si–O distances of **38**, **39**, **43**·CH_3CN and **44** (1.7871(14)−1.8038(11) Å). The Si–N1 distance of **46** (1.7040(9) Å) is fairly typical, whereas the equatorial Si–N2 bond length (1.8842(9) Å) is

[9]The crystal structure analysis was performed by Dr. Christian Burschka, Department of Inorganic Chemistry, University of Würzburg: λ, 0.71073 Å; *T*, 100(2) K; space group, $I4_1$; *a*, 17.9928(2) Å; *b*, 17.9928(2) Å; *c*, 16.1878(4) Å; α, 90.0°; β, 90.0°; γ, 90.0°; *R*1 [$I>2\sigma(I)$], 0.0373.

significantly shorter than the observed Si–N distances in **38**, **39**, **43**·CH_3CN and **44**, respectively (1.9677(11)−1.9932(14) Å). The decrease in length might be explained by the new arrangement of the bidentate ligands in the Si-coordination polyhedron. The axial O1−Si−O2 angle amounts to 164.88(4)°.

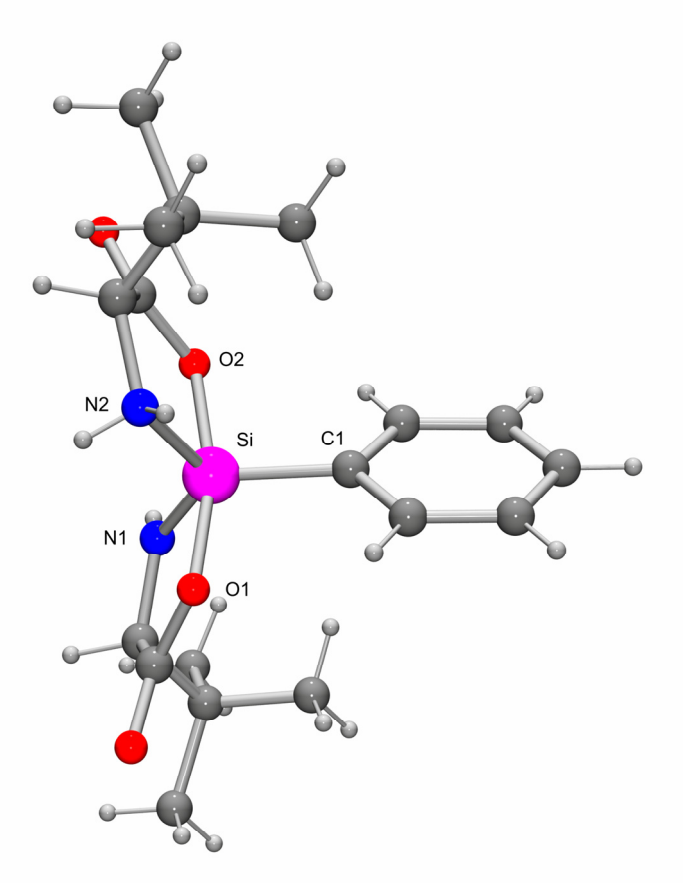

Figure 10. Molecular structure of **46** in the crystal of **46**·C_5H_{12}·1/2CH_3CN with numbering of the selected atoms. Selected bond lengths [Å] and angles [°]: Si–O1 1.8199(8), Si–O2 1.7876(8), Si–N1 1.7040(9), Si–N2 1.8842(9), Si–C1 1.8659(11); O1–Si–O2 164.88(4), O1–Si–N1 86.48(4), O1–Si–N2 84.91(4), O1–Si–C1 96.70(4), O2–Si–N1 90.28(4), O2–Si–N2 84.86(4), O2–Si–C1 97.59(4), N1–Si–N2 124.96(4), N1–Si–C1 121.45(5), N2–Si–C1 113.53(4).

The maximum deviations from the ideal 90° and 180° angles of **46** are 7.59° and 15.12°, respectively. The sum of the bond angles of the equatorial plane is 359.95(3)°.

5.5 Hexacoordinate silicon(IV) complexes with an SiO_2N_4 skeleton

5.5.1 Crystal structure of 50[10]

The chiral hexacoordinate silicon(IV) complex **50** was isolated as the (OC-6-22-Λ)-(*S*,*S*) isomer. The Si-coordination polyhedron of **50** represents a distorted octahedron and is shown in Figure 11.

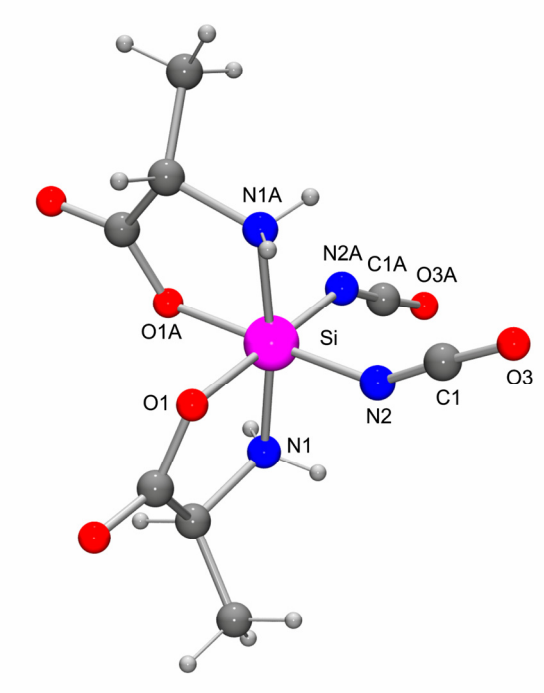

Figure 11. Molecular structure of **50** in the crystal with numbering of the selected atoms. Selected bond lengths [Å] and angles [°]: Si–O1 1.7995(10), Si–N1 1.8857(11), Si–N2 1.8026(12); O1-Si-O1A 88.27(7), O1-Si-N1 86.51(5), O1-Si-N1A 87.80(5), O1-Si-N2 89.77(5), O1-Si-N2A 176.83(5), N1-Si-N1A 172.08(8), N1-Si-N2 94.57(5), N1-Si-N2A 90.92(5), N2-Si-N2A 92.29(8), Si-N2-C1 146.33(13), N2-C1-O3 176.99(19).

The two monodentate cyanato-*N* ligands and the two oxygen ligand atoms O1 and O1A occupy *cis* positions, whereas the two nitrogen ligand atoms N1 and N1A are found in *trans* positions. The maximum deviations from the ideal 90° and 180° angles amount to 4.57° (N1−Si−N2, 94.57(5)°) and 7.92° (N1−Si−N1A, 172.08(8)°), respectively. The Si–O distances (1.7995(10) Å) are somewhat shorter than the axial Si–O bond lengths of the trigonal-bipyramidal Si-coordination polyhedra of **66**–**70** (1.8058(14)–1.8356(19) Å) and similar to the axial Si–O distances of **38** (1.7910(13) Å) and **43**·CH_3CN (1.7871(14) Å).

[10]The crystal structure analysis was performed by Dr. Christian Burschka, Department of Inorganic Chemistry, University of Würzburg: λ, 0.71073 Å; *T*, 100(2) K; space group, $P4_12_12$; *a*, 7.69110(10) Å; *b*, 7.69110(10) Å; *c*, 20.1180(4) Å; α, 90.0°; β, 90.0°; γ, 90.0°; *R*1 [$I>2\sigma(I)$], 0.0299.

Surprisingly, the Si–N1 and Si–N1A bond lengths of **50** (1.8857(11) Å) are significantly shorter than the axial Si−N2 distances of **38** (1.9932(14) Å) and **43**·CH_3CN (1.9658(17) Å) (same coordination mode). An explanation for this finding might be the relatively high Lewis acidity of **50** with its two strongly electronegative cyanato-*N* ligands (in this context, compare the isotropic ^{29}Si chemical shifts of **50** (δ = −187.4 ppm), **38** (δ = −85.4 to −82.8 ppm), and **43**·CH_3CN (δ = −95.7 ppm)). The Si−N distances of the Si−NCO moieties of **50** are similar to those of other hexacoordinate silicon(IV) complexes with cyanato-*N* ligands [56, 57]. The same holds true for the N−C−O angles of the Si−NCO groups, whereas the Si−N2−C1 and Si−N2A−C1A angles (146.33(13)°) of **50** are significantly smaller than the N−C−O angles of the Si−NCO groups of other hexacoordinate silicon(IV) complexes (151.62(12)−169.77(12)°) [55, 56].

5.6 Penta- and hexacoordinate silicon(IV) complexes with cyanato-*N* and thiocyanato-*N*-ligands

5.6.1 Crystal structure of 54[11]

The neutral pentacoordinate silicon(IV) complex **54** crystallized at −20 °C in acetonitrile in the monoclinic space group $P2_1/n$. The molecular structure is depicted in Figure 12.

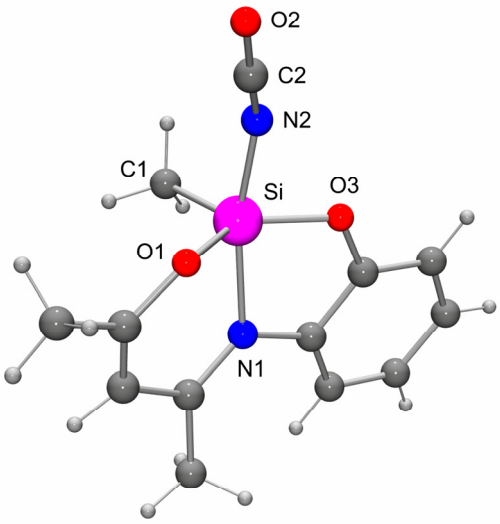

Figure 12. Molecular structure of **54** in the crystal with numbering of the selected atoms. Selected bond lengths [Å] and angles [°]: Si–O1 1.6875 (12), Si–O3 1.6839(12), Si–N1 1.9947(14), Si–N2 1.8033(15), Si–C1

[11]The crystal structure analysis was performed by Dr. Christian Burschka, Department of Inorganic Chemistry, University of Würzburg: λ, 0.71073 Å; T, 173(2) K; space group, $P2_1/n$; a, 7.2636(15) Å; b, 8.5367(17) Å; c, 20.867(4) Å; α, 90.0°; β, 99.82(3) °; γ, 90.0°; $R1$ [$I>2\sigma(I)$], 0.0389.

1.8466(17), C2–O2 1.175(2), C2–N2 1.170(2); O1–Si–O3 131.69(6), O1–Si–N1 88.77(6), O1–Si–N2 88.42(6), O1–Si–C1 113.19(7), O3–Si–N1 83.65(6), O3–Si–N2 87.54(6), O3–Si–C1 114.85(7), N1–Si–N2 165.40(7), N1–Si–C1 93.47(7), N2–Si–C1 100.80(7), Si–N2–C2 149.40(14), N2–C2–O2 176.15(19).

The Si-coordination polyhedron of **54** represents a distorted trigonal bipyramid with a Berry distortion (transition trigonal bipyramid → square pyramid; pivot atom C1) of 38.5 %. The axial positions of the trigonal bipyramid are occupied by the nitrogen atoms N1 and N2, wheras the equatorial positions of the Si-coordination polyhedron are occupied by the oxygen atoms O1 and O3, and by the carbon atom C1. Both Si−O bond lengths of **54** show almost the same values Si−O1 (1.6875 (12) Å) and Si−O3 (1.6839(12) Å), and are similar to those found in the well-known pentacoordinate silicon(IV) complexes containing the same tridentate ligand and two cyanato-*N* fragments (**77**, 1.6779(14), 1.6891(14) Å) [53]. The Si−N1 bond length of 1.9947(14) Å is somewhat longer than the Si−N distances found in similar pentacoordinate silicon(IV) complexes (**77**, 1.9668(16), **78**, 1.9218(12) Å) [53], and as expected longer than the Si−N bond length of the NCO group (1.8033(15) Å). This elongation might be due to the replacement of the linear NCO or NCS groups by the methyl fragment, which is more sterically demanding. The Si−C distance is 1.8466(17) Å. The Si−N−C angle of the Si–NCO fragment is 149.40(14)°, and the N−C−O angle is, at 176.15(19)°, almost linear. The sum of the equatorial angles (359.75(0)°) is very close to the ideal 360° angle.

5.6.2 Crystal structure of methyl 55[12]

The pentacoordinate silicon(IV) complex **55** crystallized in the orthorhombic space group *Pbca*. The Si-coordination polyhedron is a distorted trigonal bipyramid (Berry distortion, 15.8 % [58]; Figure 13).

The oxygen atom O and the nitrogen atom N2 of the tridentate ligand and the carbon atom C1 of the methyl group occupy the equatorial sites. The nitrogen atoms N1 (NCS group) and N3 (tridentate ligand) are found in the axial positions. The Si–O (1.6908(13) Å) and the Si−N3 (1.9601(15) Å) distances of **55** are slightly longer than the comparable bond lengths in the crystal of **78** (Si−O, 1.6657(11) and 1.6716(11) Å; Si−N, 1.9218(12) Å) [59]; however, any further discussion of these differences would only be speculative.

[12]The crystal structure analysis was performed by Dr. Christian Burschka, Department of Inorganic Chemistry, University of Würzburg: λ, 0.71073 Å; *T*, 193(2) K; space group, *Pbca*; *a*, 9.7847(14) Å; *b*, 10.5451(10) Å; *c*, 36.065(4) Å; α, 90.0°; β, 90.0°; γ, 90.0°; *R*1 [$I>2\sigma(I)$], 0.0364.

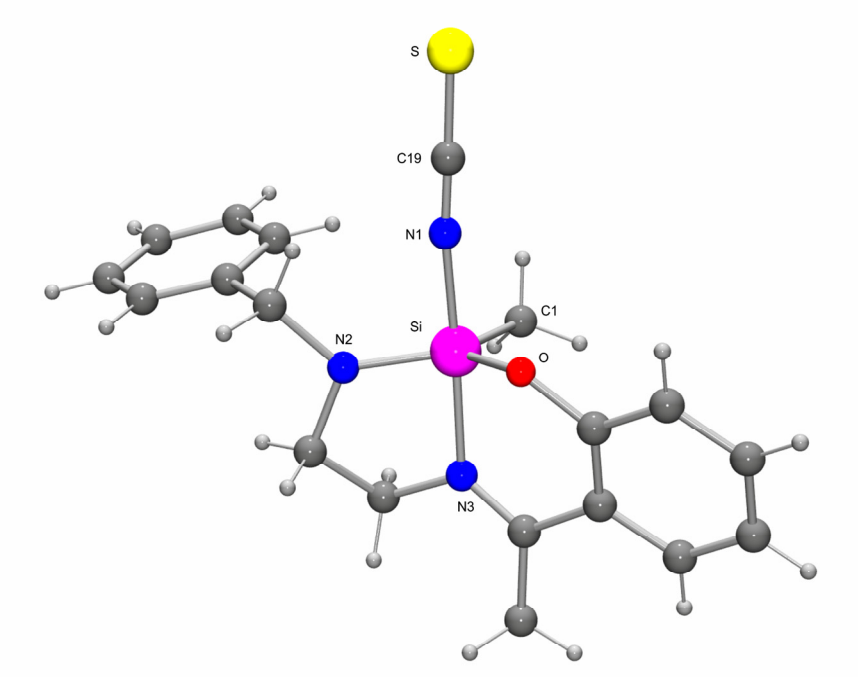

Figure 13. Molecular structure of **55** in the crystal with numbering of the selected atoms. Selected bond lengths [Å] and angles [°]: Si−O 1.6908(13), Si−N1 1.8735(16), Si−N2 1.7199(15), Si−N3 1.9601(15), Si−C1 1.867(2); O−Si−N1 87.10(7), O−Si−N2 123.55(7), O−Si−N3 88.90(6), O−Si−C1 112.44(9), N1−Si−N2 93.31(7), N1−Si−N3 173.32(8), N1−Si−C1 94.19(8), N2−Si−N3 84.44(7), N2−Si−C1 123.77(9), N3−Si−C1 92.29(8), Si−N1−C19 172.29(16), N1−C19−S 178.40(19).

The Si–N1 bond distance of **55** (1.8735(16) Å) is significantly longer than those observed for the Si−NCS bonds of compounds **72** (1.8093(17) and 1.8145(16) Å), **76** (1.8135(16) and 1.8153(16) Å), and **78** (1.7375(13) and 1.7985(13) Å) and similar to the Si−NCS bond lengths of **74** (1.8401(12) Å), **75** (1.8619(11) Å), and **82** (1.857(2) Å) [56]. A satisfactory explanation for this variability of the Si–N(CS) bond distance cannot be given. The Si−N2 bond length of **55** is 1.7199(15) Å. The Si−N1−C19 angle of the Si–NCS group is 172.29(16)° and is within the range observed for compounds **72**, **74**−**76**, **78**, and **82** (156.68(12)−176.99(16)°) [56, 59, 60], and the N1−C19−S angle (178.40(19)°) is very similar to the N−C−S angles reported for **72**, **74**−**76**, **78**, and **82** (178.34(18)−179.88(14)°) [56, 59, 60]. The NCH_2CH_2N group of **55** adopts a *gauche* conformation.

5.6.3 Crystal structure of 56[13]

The hexacoordinate silicon(IV) complex **56** crystallized in the monoclinic space group $P2_1/n$, some of the atoms surrounding the ligand atom N3 were disordered (Figure 14) [61].

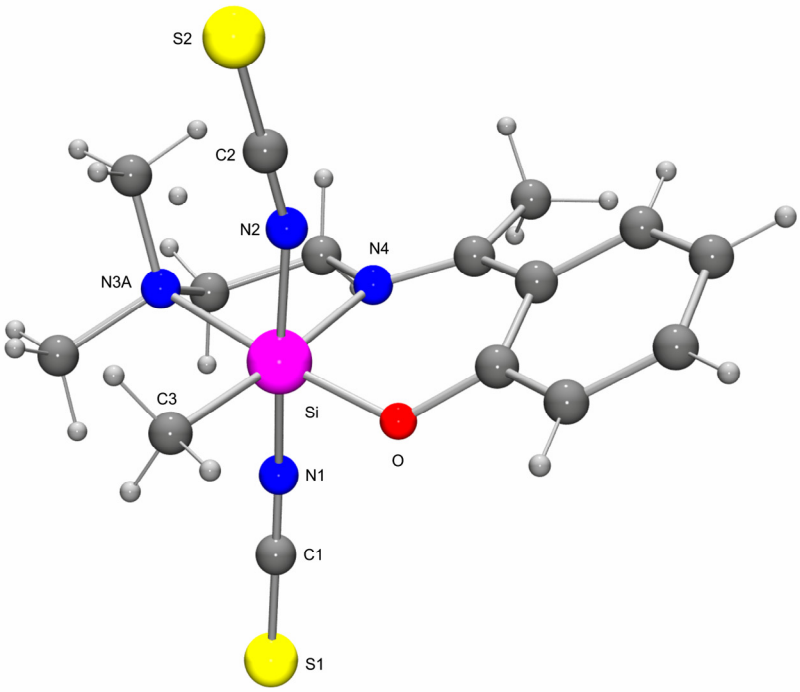

Figure 14. Molecular structure of **56** in the crystal with numbering of the selected atoms. Selected bond lengths [Å] and angles [°]: Si−O 1.7238(10), Si−N1 1.8666(11), Si−N2 1.8761(12), Si−N3A 2.0899(13), Si−N4 1.9460(11), Si−C3 1.8933(15); O−Si−N1 89.36(5), O−Si−N2 92.46(5), O−Si−N3A 170.04(5), O−Si−N4 90.04(4), O−Si−C3 94.98(6), N1−Si−N2 173.39(6), N1−Si−N3A 86.60(5), N1−Si−N4 86.83(5), N1−Si−C3 94.02(6), N2−Si−N3A 90.57(5), N2−Si−N4 86.81(5), N2−Si−C3 92.15(6), N3A−Si−N4 80.65(5), N3A−Si−C3 94.38(7), N4−Si−C3 174.91(7), Si−N1−C1 168.08(12), Si−N2−C2 163.58(12), N1−C1−S1 179.18(13), N2−C2−S2 178.95(14).

The Si-coordination polyhedron of **56** is a distorted octahedron. The nitrogen atoms N1 and N2 of the two thiocyanato-N ligands occupy *trans* positions. The Si−NCS distances of **56** (1.8666(11) and 1.8761(12) Å) are significantly longer than those of **72**, **76**, and **78** and similar to those of **74**, **75**, **82**, [56] and **55**. The Si−N1−C1 (168.08(12)°) and Si−N2−C2 (163.58(12)°) angles of the Si−NCS groups are within the range observed for **72**, **74**−**76**, **78**, and **82** and **55**, and the angles N1−C1−S1 (179.18(13)°) and N2−C2−S2 (178.95(14)°) are very similar to the N−C−S angles of **72**, **74**−**76**, **78**, and **82** [56] and **55**. The Si–N4 bond

[13]The crystal structure analysis was performed by Dr. Christian Burschka, Department of Inorganic Chemistry, University of Würzburg: λ, 0.71073 Å; T, 100(2) K; space group, $P2_1/n$; a, 8.5416(3) Å; b, 12.1365(4) Å; c, 17.3355(6) Å; α, 90.0°; β, 100.7490(10) °; γ, 90.0°; $R1$ [$I>2\sigma(I)$], 0.0308.

length of **56** (1.9460(11) Å) is similar to the corresponding Si–N distances of **78** (1.9218(12) Å) and **55** (1.9601(15) Å). The Si–N3A distance of **56** (2.0899(13) Å) is significantly longer than the corresponding Si−N distance of **55** (1.7199(15) Å) and follows the trend for a Si–N bond elongation when comparing a tricoordinate to a tetracoordinate nitrogen atom. As expected, an elongation of the Si–O and Si−C distances is observed when going from pentacoordination (**55**) to hexacoordination (**56**) (Si−O: **55**, 1.6908(13) Å → **56**, 1.7238(10) Å; Si−C: **55**, 1.867(2) Å → **56**, 1.8933(15) Å). The maximum deviations from the ideal 90° and 180° angles of **56** are 9.35° and 9.96°, respectively. The sums of bond angles of the three planes spanned by the coordination atoms are 359.0° (O, N1, N2, N3A), 360.1° (O, N3A, N4, C3), and 359.8° (N1, N2, N4, C3).

5.6.4 Crystal structure of 57[14]

The hexacoordinate silicon(IV) complex **57** crystallized in the trigonal space group $R\bar{3}$ directly from the reaction mixture at −20 °C in acetonitrile. The molecular structure of **57** is depicted in Figure 15.

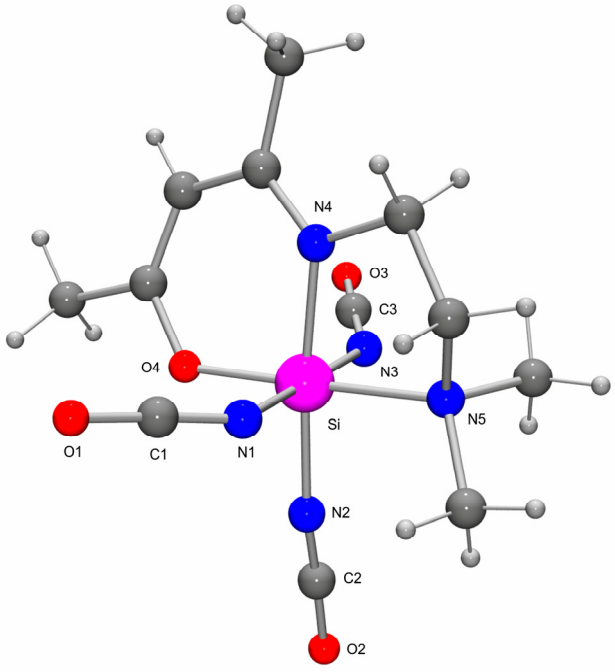

Figure 15. Molecular structure of **57** in the crystal with numbering of the selected atoms. Selected bond lengths [Å] and angles [°]: Si−O4 1.7560(9), Si−N1 1.8252(11), Si−N2 1.8001(11), Si−N3 1.8324(11), Si−N4 1.8969(10), Si−N5 2.0199(11); O4−Si−N1 90.05(5), O4−Si−N2 91.30(5), O4−Si−N3 91.19(4), O4−Si−N4

[14]The crystal structure analysis was performed by Dr. Christian Burschka, Department of Inorganic Chemistry, University of Würzburg: λ, 0.71073 Å; T, 100(2) K; space group, $R\bar{3}$; a, 32.966(2) Å; b, 32.966(2) Å; c, 8.1473(5) Å; α, 90.0°; β, 90.0°; γ, 120.0°; $R1$ [$I>2\sigma(I)$], 0.0396.

94.11(4), O4−Si−N5 176.22(4), N1−Si−N2 90.80(5), N1−Si−N3 178.43(5), N1−Si−N4 90.02(5), N1−Si−N5 86.95(5), N2−Si−N3 90.14(5), N2−Si−N4 174.52(5), N2−Si−N5 91.04(5), N3−Si−N4 88.93(5), N3−Si−N5 91.77(4), N4−Si−N5 83.60(4), Si−N1−C1 143.62(10), Si−N2−C2 159.32(11), Si−N3−C3 145.93(9), N1−C1−O1 177.41(15), N2−C2−O2 177.49(16), N3−C3−O3 176.92(13).

The Si-coordination polyhedron of **57** is a distorted octahedron. The nitrogen atoms N1 and N3 of the two cyanato-*N* ligands occupy *trans* positions. The Si−N bond distances of the Si−NCO fragments of **57** (1.8252(11), 1.8001(11) and 1.8324(11) Å) are shorter than those observed of the hexacoordinate silicon complex **58** (1.8364(12) and 1.8516(12) Å). The Si−N1−C1 (143.62(10)°), Si−N2−C2 (159.32(11)°) and Si−N3−C3 (145.93(9)°) angles of the Si−NCO groups are within the range of the Si−N−C angles observed for **58** (Si−N1−C1, 152.26(13)°; Si−N2−C2, 157.02(12)°). The angles N1−C1−O1 (177.41(15)°), N2−C2−O2 (177.49(16)°) and N3−C3−O3 (176.92(13)°) are very similar to the N−C−O angles of **58** (N1−C1−O1, 177.06(19)°; N2−C2−O2, 177.85(19)°). The Si–N4 bond length of **57** (1.8969(10) Å) is significantly shorter than the corresponding Si–N bond distance of **58** (1.9537(11) Å). The Si–N5 bond distance of **57** (2.0199(11) Å) is also significantly shorter than the corresponding Si−N bond distance of **58** (2.0883(12) Å) and follows the trend for a Si–N bond elongation when going from a tricoordinate to a tetracoordinate nitrogen atom. The maximum deviations from the ideal 90° and 180° angles of **57** are ca. 6.40° and 36.38°, respectively. The sums of bond angles of the three planes spanned by the coordination atoms are 360.05° (O4, N2, N5, N4), 359.96° (O4, N1, N5, N3), and 359.89° (N1, N2, N3, N4).

5.6.5 Crystal structure of 58[15]

The hexacoordinate silicon(IV) complex **58** crystallized in the monoclinic space group $P2_1/c$ directly from the reaction mixture at −20 °C. The molecular structure of **58** is depicted in Figure 16.

[15]The crystal structure analysis was performed by Dr. Christian Burschka, Department of Inorganic Chemistry, University of Würzburg: λ, 0.71073 Å; T, 123(2) K; space group, $P2_1/c$; a, 14.841(2) Å; b, 8.3712(11) Å; c, 14.6084(18) Å; α, 90.0°; β, 94.990(3) °; γ, 90.0°; $R1$ [$I>2\sigma(I)$], 0.0495.

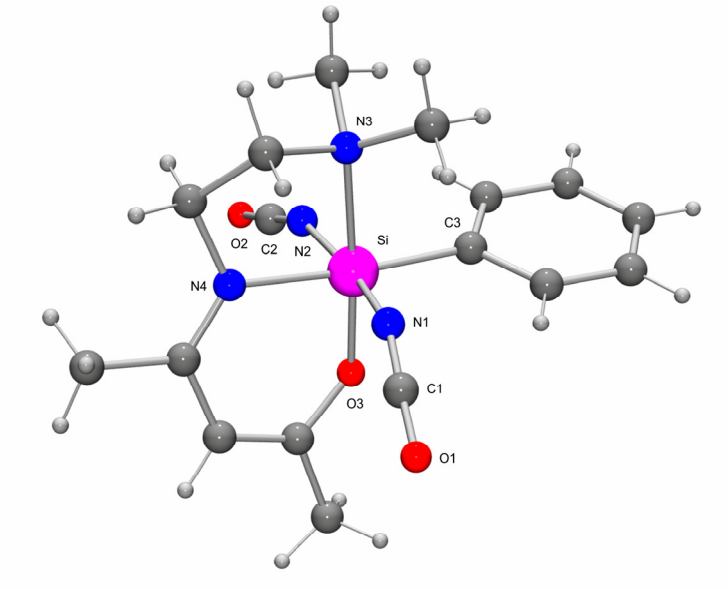

Figure 16. Molecular structure of **58** in the crystal with numbering of the selected atoms. Selected bond lengths [Å] and angles [°]: Si−O3 1.7689(10), Si−N1 1.8364(12), Si−N2 1.8516(12), Si−N3 2.0883(12), Si−N4 1.9537(11), Si−C3 1.9281(13); O3−Si−N1 92.14(5), O3−Si−N2 90.14(5), O3−Si−N3 175.99(5), O3−Si−N4 92.67(5), O3−Si−C3 92.40(5), N1−Si−N2 170.32(6), N1−Si−N3 87.30(5), N1−Si−N4 85.61(5), N1−Si−C3 95.07(6), N2−Si−N3 89.77(5), N2−Si−N4 84.89(5), N2−Si−C3 94.23(5), N3−Si−N4 83.33(5), N3−Si−C3 91.61(5), N4−Si−C3 174.86(5), Si−N1−C1 152.26(13), Si−N2−C2 157.02(12), N1−C1−O1 177.06(19), N2−C2−O2 177.85(19).

The Si-coordination polyhedron of **58** is a distorted octahedron. The nitrogen atoms N1 and N2 of the two cyanato-*N* ligands occupy *trans* positions. The Si−N distances of the Si−NCO fragments of **58** (1.8364(12) and 1.8516(12) Å) are significantly longer than that of **71** (1.8024(12) Å), and those of the similar hexacoordinate silicon complex **74** but containing two NCS ligands instead of two NCO groups (1.8199(11) Å), **77** (1.7847(11) and 1.7330(18) Å) and similar to those of **81** and **55** [42]. The Si−N1−C1 (152.26(13)°) and Si−N2−C2 (157.02(12)°) angles of the Si−NCO groups are within the range observed for **71** (153.35(11)°), for the similar complex **74** with NCS fragments (151.62(12)°) and for **77** (149.47(18)°−167.97(17)°), and the angles N1−C1−O1 (177.06(19)°) and N2−C2−O2 (177.85(19)°) are very similar to the N−C−O angles of **71** (177.09(16)°), of the similar complex **74** with NCS fragments (177.96(18)°) and of **77** (177.3(3)°, 177.4(2)°). The Si–N4 bond length of **58** (*N,N,O* donor, 1.9537(11) Å) is similar to the corresponding Si–N distances of **55** (1.9601(15) Å) [42]. The Si–N3 distance of **58** (2.0883(12) Å) is significantly longer than the corresponding Si−N distance of **55** (1.7199(15) Å) and follows the trend for a Si–N bond elongation when comparing a tricoordinate to a tetracoordinate nitrogen atom. As expected, an increase in the Si–O and Si−C distances is observed when going from

pentacoordination (**55**) to hexacoordination (**58**) (Si–O: **55**, 1.6908(13) Å → **58**, 1.7689(10) Å; Si–C: **55**, 1.867(2) Å → **58**, 1.9281(13) Å). The maximum deviations from the ideal 90° and 180° angles of **58** are 6.67 and 9.97°, respectively. The sums of bond angles of the three planes spanned by the coordination atoms are 359.35° (O3, N1, N2, N3), 360.01° (O3, N3, N4, C3), and 359.8° (N1, N2, N4, C3).

5.6.6 Crystal structure of 59[16]

The hexacoordinate silicon(IV) complex **59** crystallized in the space group *C*2/*c* at –20 °C from acetonitrile. The molecular structure of **59** is depicted in Figure 17.

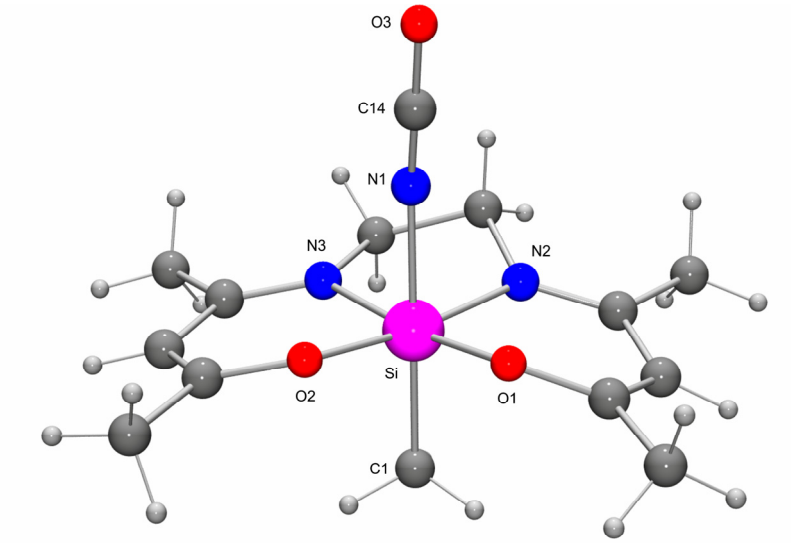

Figure 17. Molecular structure of **59** in the crystal with numbering of the selected atoms. Selected bond lengths [Å] and angles [°]: Si–O1 1.7819(13), Si–O2 1.7681(13), Si–N1 1.8912(17), Si–N2 1.9084(16), Si–N3 1.9209(15), Si–C1 1.921(2); O1–Si–O2 87.94(6), O1–Si–N1 87.55(7), O1–Si–N2 92.99(6), O1–Si–N3 173.34(7), O1–Si–C1 94.24(7), O2–Si–N1 87.04(7), O2–Si–N2 172.68(7), O2–Si–N3 94.16(6), O2–Si–C1 94.14(7), N1–Si–N2 85.74(7), N1–Si–N3 86.26(7), N1–Si–C1 177.89(8), N2–Si–N3 84.13(7), N2–Si–C1 93.04(8), N3–Si–C1 91.91(7), Si–N1–C14 160.26(15).

The Si-coordination polyhedron of **59** represents a distorted octahedron. The oxygen atoms O1 und O2, as well as the nitrogen atoms N2 und N3 are situated *cis* to each other. The carbon atom C1 and the nitrogen atom N1 occupy *trans* positions. In comparison to the corresponding Si–O and Si–N bond lengths of similar hexacoordinate silicon(IV) complex **82** (Si–O, 1.759(2) Å; Si–N, 1.871(3) Å) [56], the Si–O and Si–N bonds of the chelate ligand of

[16]The crystal structure analysis was performed by Dr. Christian Burschka, Department of Inorganic Chemistry, University of Würzburg: λ, 0.71073 Å; *T*, −173(2) K; space group, *C*2/*c*; *a*, 11.9820(9) Å; *b*, 9.3295(6) Å; *c*, 27.1744(18) Å; α, 90.0°; β, 96.631(3) °; γ, 90.0°; *R*1 [$I>2\sigma(I)$], 0.0486.

59 are significantly longer (Si–O, 1.7819(13), 1.7681(13) Å; Si–N, 1.9084(16), 1.9209(15) Å). The Si–N bond distance (1.8912(17) Å) of the Si−NCO ligand is also longer than the Si–N bond length found in the similar hexacoordinate silicon(IV) complex **82** (1.857(2) Å) [56]. The Si–C1 bond length is 1.921(2) Å. The Si−N1−C14 angle is with 160.26(15)° smaller as the Si−N−C angle found in the compound **82** (170.41(19)°). The maximum deviations from the ideal 90° and 180° angles of **59** are 5.86° and 7.31°, respectively.

5.6.7 Crystal structure of 60[17]

The hexacoordinate silicon(IV) complex **60** crystallized in the space group $P2_1/c$ at –20 °C from acetonitrile. The molecular structure of **60** is depicted in Figure 18.

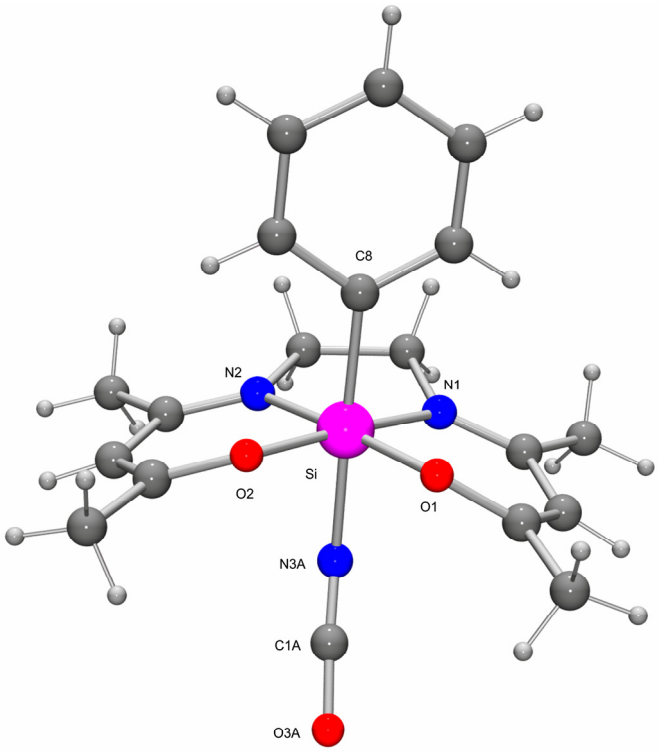

Figure 18. Molecular structure of **60** in the crystal with numbering of the selected atoms. Selected bond lengths [Å] and angles [°]: Si–O1 1.7674(10), Si–O2 1.7647(10), Si–N1 1.8856(12), Si–N2 1.8992(12), Si–N3A 1.887(5), Si–C8 1.9291(14); O1–Si–O2 89.07(5), O1–Si–N1 93.18(5), O1–Si–N2 174.86(5), O1–Si–N3A 86.4(3), O1–Si–C8 91.92(5), O2–Si–N1 174.93(5), O2–Si–N2 93.38(5), O2–Si–N3A 88.2(4), O2–Si–C8 92.10(5), N1–Si–N2 84.02(6), N1–Si–N3A 87.5(4), N1–Si–C8 92.37(6), N2–Si–N3A 89.1(3), N2–Si–C8 92.50(6), N3A–Si–C8 178.3(3), Si–N3A–C1A 145.3(9), N3A–C1A–O3A 176.9(8).

[17] The crystal structure analysis was performed by Dr. Christian Burschka, Department of Inorganic Chemistry, University of Würzburg: λ, 0.71073 Å; T, 173(2) K; space group, $P2_1/c$; a, 12.003(2) Å; b, 12.789(3) Å; c, 12.922(3) Å; α, 90.0°; β, 107.98(3) °; γ, 90.0°; $R1$ [$I>2\sigma(I)$], 0.0405.

The Si-coordination polyhedron of **60** represents a distorted octahedron, some of the atoms belonging to the monoanionic NCO ligand are disordered. The oxygen atoms O1 and O2, as well as the nitrogen atoms N1 and N2 occupy *cis* positions. The carbon atom C8 and the nitrogen atom N3A occupy *trans* positions. Compared with the corresponding Si–O and Si–N bond lengths of similar hexacoordinate silicon(IV) complexes of **82** (Si–O, 1.759(2) Å; Si–N, 1.871(3) Å) [56], the Si–O and Si–N bond lengths of the chelate ligand of **60** are significantly longer (Si–O, 1.7674(10), 1.7647(10) Å; Si–N, 1.8856(12), 1.8992(12) Å). The Si–N bond length (1.887(5) Å) of the Si−NCO ligand is also longer than the Si–N found in the similar hexacoordinate silicon(IV) complex (1.857(2) Å) of **82** [56]. The Si–C8 bond length of 1.9291(14) Å is somewhat longer than the corresponding Si–C bond distance of **59** (1.921(2) Å). The Si−N3A−C1A angle is at 145.3(9)°, significantly smaller than the Si–N–C angle of **59** (160.26(15)°). The maximum deviations from the ideal 90° and 180° angles of **60** are 5.97° and 5.13°, respectively.

5.6.8 Crystal structure of 62[18]

The hexacoordinate silicon(IV) complex **62** crystallized in the space group $Pca2_1$ at –20 °C from acetonitrile. The molecular structure of **62** is depicted in Figure 19.

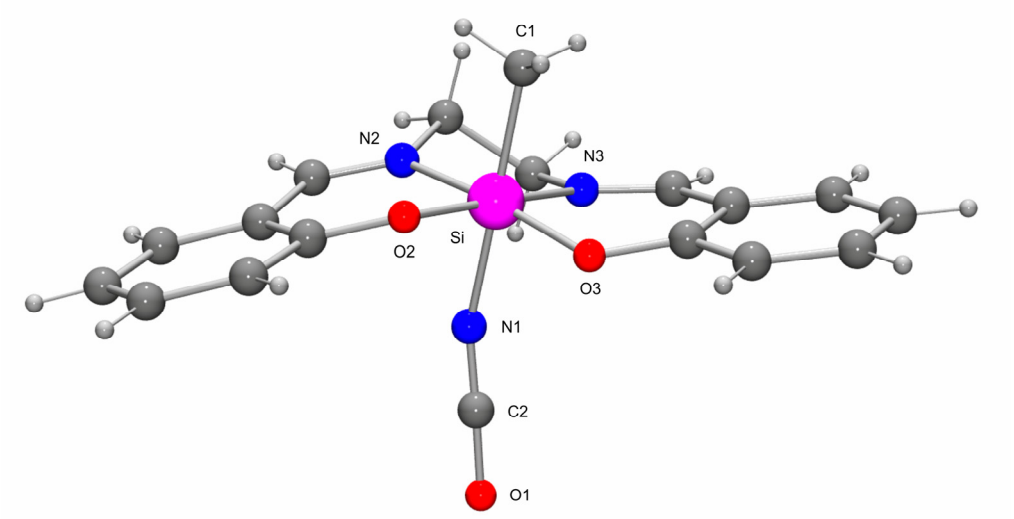

Figure 19. Molecular structure of **62** in the crystal with numbering of the selected atoms. Selected bond lengths [Å] and angles [°]: Si−O2 1.7409(11), Si−O3 1.7510(11), Si−N1 1.8791(14), Si−N2 1.9445(12), Si−N3 1.9584(14), Si−C1 1.9107(16); O2−Si−O3 92.51(5), O2−Si−N1 90.22(6), O2−Si−N2 92.63(5), O2−Si−N3 173.07(5), O2−Si−C1 92.43(6), O3−Si−N1 88.07(6), O3−Si−N2 170.59(6), O3−Si−N3 92.53(5), O3−Si−C1

[18]The crystal structure analysis was performed by Dr. Christian Burschka, Department of Inorganic Chemistry, University of Würzburg: λ, 0.71073 Å; T, 100(2) K; space group, $Pca2_1$; a, 18.2956(5) Å; b, 6.7270(2) Å; c, 13.1328(3) Å; α, 90.0°; β, 90.0°; γ, 90.0°; $R1$ [$I>2\sigma(I)$], 0.0298.

95.17(6), N1−Si−N2 84.04(6), N1−Si−N3 85.20(6), N1−Si−C1 175.72(7), N2−Si−N3 81.73(5), N2−Si−C1 92.48(6), N3−Si−C1 91.85(6), Si−N1−C2 156.45(12), N1−C2−O1 178.53(18).

The neutral silicon complex **62** crystallized in the orthorhombic space group $Pca2_1$. The Si-coordination polyhedron is a distorted octahedron. The nitrogen atom N1 and the carbon atom C1 are *trans* to one another, whereas the salen ligand with the atoms O1, O2, N2, N3 expands quite linear a plane. Two oxygen atoms of the salen ligand occupy *cis* positions, as well as the nitrogen atoms, belonging to the same ligand. The maximum deviations from the ideal 90° and 180° angles are 8.26° and 9.40°, respectively. The Si−N bond lengths (1.9445(12), 1.9584(14) Å) of the salen ligand are longer than the Si−N bond length of the (cyanato-*N*) group (1.8791(14) Å) and somewhat longer than the Si−N bond lengths of **84** and **85** (**84**, 1.932(2), 1.928(2) Å; **85**, 1.925(2), 1.919(2) Å) [62]. The Si−O bond lengths (1.7409(11), 1.7510(11) Å) are longer than the Si−O bond lengths of other hexacoordinate silicon species containing analogues salen ligands and monoanionic halide ligands, e.g. compounds **83** (Si−O 1.721(1), 1.724(1) Å) [63, 64] and **88** (1.758(2) and 1.763(2) Å) [65]. The Si−NCO fragment shows a strong deviation with an Si−N1−C2 angle of 156.45(12)°. Nevertheless, the cyanato-*N* group is almost linear (N1−C2−O1 178.53(18)°).

5.6.9 Crystal structure of 63[19]

The hexacoordinate silicon(IV) complex **63** crystallized in the space group $P2_1/n$ at – 20 °C from acetonitrile. The molecular structure of **63** is depicted in Figure 20.

[19]The crystal structure analysis was performed by Dr. Christian Burschka, Department of Inorganic Chemistry, University of Würzburg: λ, 0.71073 Å; *T*, 193(2) K; space group, $P2_1/n$; *a*, 7.2540(15) Å; *b*, 18.572(4) Å; *c*, 14.313(3) Å; α, 90.0°; β, 101.03(3) °; γ, 90.0°; *R*1 [$I>2\sigma(I)$], 0.0617.

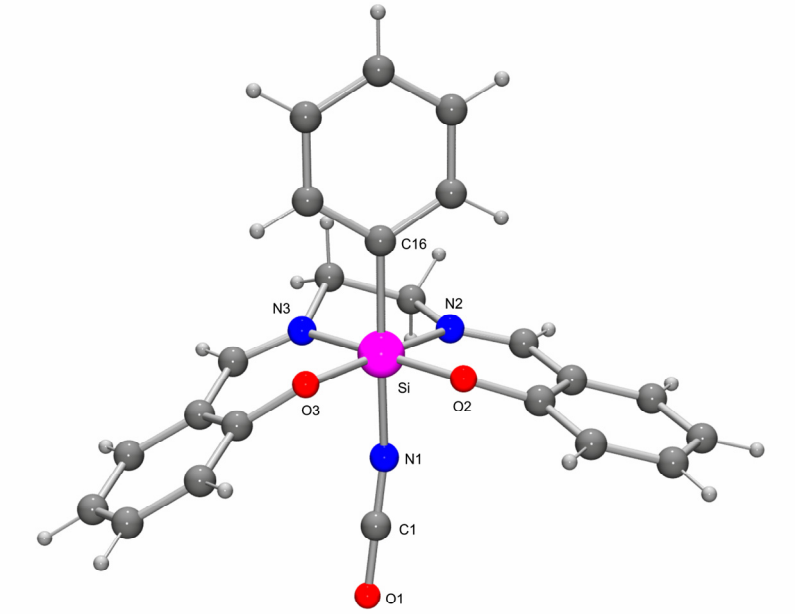

Figure 20. Molecular structure of **63** in the crystal with numbering of the selected atoms. Selected bond lengths [Å] and angles [°]: Si–O2 1.7352(17), Si–O3 1.7302(17), Si–N1 1.867(2), Si–N2 1.943(2), Si–N3 1.928(2), Si–C16 1.918(2); O2–Si–O3 93.84(8), O2–Si–N1 89.32(9), O2–Si–N2 93.48(8), O2–Si–N3 173.68(9), O2–Si–C16 92.79(10), O3–Si–N1 89.86(9), O3–Si–N2 170.84(9), O3–Si–N3 91.62(9), O3–Si–C16 94.24(9), N1–Si–N2 84.71(9), N1–Si–N3 87.51(9), N1–Si–C16 175.25(10), N2–Si–N3 80.79(9), N2–Si–C16 90.91(9), N3–Si–C16 89.98(9), Si–N1–C1 159.4(2), N1–C1–O1 177.4(3).

The neutral silicon complex **63** crystallized in the monoclinic space group $P2_1/n$. The Si-coordination polyhedron of **63** is a distorted octahedron. The nitrogen atom N1 and the carbon atom C16 are located *trans* to each other, and the O2, O3, N2, and N3 atoms form a plane in the equatorial positions. Two oxygen atoms of the salen ligand occupy *cis* positions, as well as the nitrogen atoms, belonging to the same ligand. The maximum deviations from the ideal 90° and 180° angles are 9.21° and 9.16°, respectively. The Si−N bond lengths (1.943(2), 1.928(2) Å) of the salen ligand are longer than the Si−N bond length of the (cyanato-*N*) group (1.867(2) Å) and are similar to the bond lengths found in **61** (1.9445(12), 1.9584(14) Å). The Si−O bond lengths of **63** (1.7352(17) and 1.7302(17) Å) are somewhat shorter than the Si−O bond lengths of **62** (1.7409(11) and 1.7510(11) Å) but longer than the Si−O bond lengths of **83** (1.721(1) and 1.724(1) Å) [63]. Similar Si−O bond lengths were found for hexacoordinate silicon(IV) complexes containing similar tetradentate ligands, one phenyl fragment and one monoanionic benzoate or picrate fragment (**84**, 1.733(1), 1.735(1); **85**, 1.729(2), 1.792(2) Å) [62]. Due to the orientation of the phenyl ligand, the tetradentate dianionic salen ligand is much more folded as in compound **62**. This behavior might be due to steric reasons (phenyl moiety instead of methyl) and to an electronic repulsion of the

delocalized π-electrons, between the phenyl moiety and the phenyl rings of the tetradentate ligand. The Si−NCO fragment shows a strong deviation with an Si−N1−C1 angle of 159.4(2)°. Nevertheless, the cyanato-*N* group is almost linear (N1−C1−O1 177.4(3)°).

5.6.10 Crystal structure of 64[20]

The hexacoordinate silicon(IV) complex **64** crystallized in the rhombohedral space group $R\bar{3}$ at 20 °C from acetonitrile. The molecular structure of **64** is depicted in Figure 21.

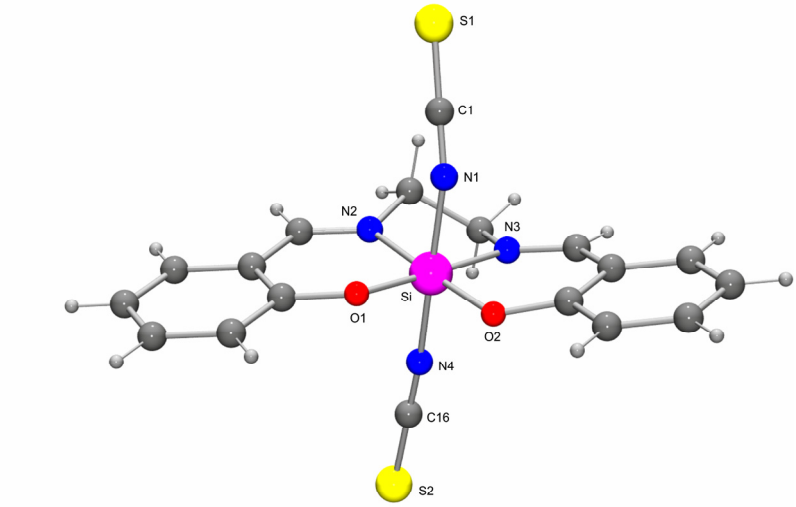

Figure 21. Molecular structure of **64** in the crystal with numbering of the selected atoms. Selected bond lengths [Å] and angles [°]: Si–O1 1.7055(17), Si–O2 1.7078(17), Si–N1 1.857(2), Si–N2 1.909(2), Si–N3 1.9175(19), Si–N4 1.863(2); O1–Si–O2 89.44(8), O1–Si–N1 92.80(10), O1–Si–N2 94.31(8), O1–Si–N3 177.18(9), O1–Si–N4 92.29(9), O2–Si–N1 92.87(10), O2–Si–N2 176.24(9), O2–Si–N3 93.35(8), O2–Si–N4 91.86(9), N1–Si–N2 87.25(9), N1–Si–N3 87.43(9), N1–Si–N4 173.08(10), N2–Si–N3 82.90(8), N2–Si–N4 87.70(9), N3–Si–N4 87.26(8), Si–N1–C1 148.7(2), Si–N4–C16 175.8(2), N1–C1–S1 179.2(3), N4–C16–S2 179.9(2).

The Si-coordination polyhedron of **64** is a distorted octahedron. The NCS nitrogen atoms N1 and N4 are orientated *trans* to each other. The O1, O2, N2, and N3 atoms of the salen fragment form a plane. Two oxygen atoms of the salen ligand occupy *cis* positions, as well as the nitrogen atoms, belonging to the same ligand. The maximum deviations from the ideal 90° and 180° angles are 7.09° and 3.75°, respectively. The Si−N bond lengths of the salen ligand (1.909(2) and 1.9175(19) Å) are longer than the Si−N bond length of the (thiocyanato-*N*) group (1.857(2) and 1.863(2) Å) and are shorter than the corresponding bond lengths of **62** (1.9445(12), 1.9584(14) Å), **63** (1.943(2), 1.928(2) Å), **89** (1.989(2), 1.964(2) Å) and **90** (1.949(2), 1.972(2) Å) [66]. Surprisingly, the Si−O bond lengths of **64** (1.7055(17),

[20]The crystal structure analysis was performed by Dr. Christian Burschka, Department of Inorganic Chemistry, University of Würzburg: λ, 0.71073 Å; T, 193(2) K; space group, $R\bar{3}$; a, 33.761(4) Å; b, 33.761(4) Å; c, 8.5880(8) Å; α, 90.0°; β, 90.0 °; γ, 120.0°; $R1$ [$I>2\sigma(I)$], 0.0521.

1.7078(17) Å) are also shorter than the Si−O bond lengths of **62** (1.7409(11), 1.7510(11) Å) and **63** (1.7352(17), 1.7302(17) Å), respectively. One Si−NCS fragment shows a strong deviation from the ideal 180° angle for the Si−N1−C1 angle with 148.7(2)°. The other Si−NCS fragment is almost linear (Si–N4–C16, 175.8(2)°). Nevertheless, the thiocyanato-*N* groups are almost linear (N1−C1−S1, 179.2(3)°; N4–C16–S2, 179.9(2)°).

5.6.11 Crystal structure of 65·2CH$_3$CN [21]

The hexacoordinate dinuclear silicon(IV) complex **65**·2CH$_3$CN crystallized in the monoclinic space group $P2_1/c$ at −20 °C from acetonitrile. The molecular structure of **65**·2CH$_3$CN is depicted in Figure 22 (co-crystallized acetonitrile was omitted for clarity).

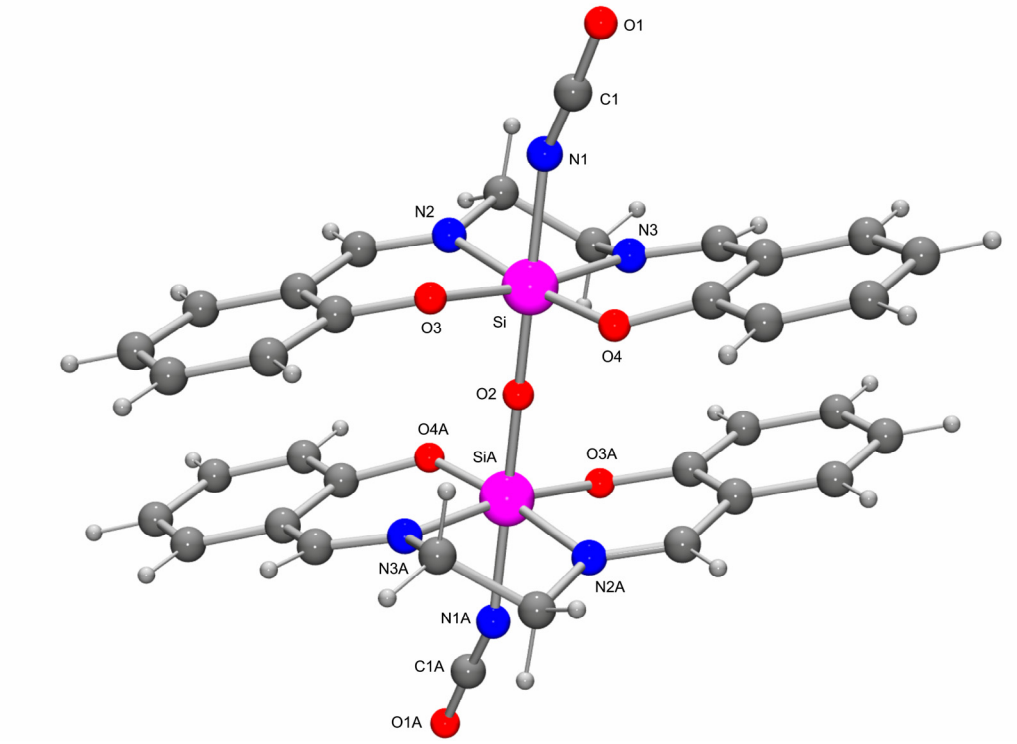

Figure 22. Molecular structure of **65** in the crystal of **65**·2CH$_3$CN with numbering of the selected atoms. Selected bond lengths [Å] and angles [°]: Si–O2 1.6475(3), Si–O3 1.7449(8), Si–O4 1.7395(8), Si–N1 1.9002(9), Si–N2 1.9340(9), Si–N3 1.9228(9); O2–Si–O3 96.43(3), O2–Si–O4 94.82(3), O2–Si–N1 173.83(3), O2–Si–N2 89.26(3), O2–Si–N3 90.64(3), O3–Si–O4 90.68(4), O3–Si–N1 87.74(4), O3–Si–N2 92.87(4), O3–Si–N3 171.53(4), O4–Si–N1 89.66(4), O4–Si–N2 174.27(4), O4–Si–N3 93.37(4), N1–Si–N2 85.99(4), N1–Si–N3 84.85(4), N2–Si–N3 82.54(4), Si–N1–C1 151.35(9), N1–C1–O1 176.71(13), Si–O2–SiA 180.0.

[21]The crystal structure analysis was performed by Dr. Christian Burschka, Department of Inorganic Chemistry, University of Würzburg: λ, 0.71073 Å; T, 98(2) K; space group, $P2_1/c$; a, 10.3363(2) Å; b, 16.1359(4) Å; c, 11.2908(3) Å; α, 90.0°; β, 103.3650(10) °; γ, 90.0°; $R1$ [$I>2\sigma(I)$], 0.0312.

The Si-coordination polyhedron of **65** is a distorted octahedron. The nitrogen atom N1 and the oxygen atom O2, as well as the oxygen atom O2 and the nitrogen N1A are orientated *trans* to each other. The salen ligand atoms O3, O4, N2, N3 and O3A, O4A, N2A, N3A form a plane. Two oxygen atoms of the salen ligand occupy *cis* positions, as well as the nitrogen atoms, belonging to the same ligand. The maximum deviations from the ideal 90° and 180° angles are 7.45° and 8.46°, respectively. The Si−N bond lengths (1.9340(9), 1.9228(9) Å) of the salen ligand are longer than the Si−N bond length of the (cyanato-*N*) group (1.9002(9) Å) and shorter than the corresponding bond lengths of **62** (1.9445(12), 1.9584(14) Å) and **63** (1.943(2), 1.928(2) Å). However, the Si−N bond lengths (1.9340(9), 1.9228(9) Å) of **65** are longer than those of **64** (1.909(2), 1.9175(19) Å). The Si−O bond lengths of **65** (1.7449(8), 1.7395(8) Å) are similar to those of **62** (1.7409(11), 1.7510(11) Å) and **63** (1.7352(17), 1.7302(17) Å), respectively. The Si−NCO fragments show a strong deviation from the ideal angle with 151.35(9)°. Nevertheless, the cyanato-*N* groups are almost linear (N1−C1−O1, 176.71(13)°).

5.7 Comparison of selected bond lengths and angles of 38, 39, 43·CH_3CN, 44 and 46·C_5H_{12}·1/2CH_3CN

All pentacoordinate silicon(IV) complexes (SiO_2N_2C skeletons) discussed here (**38**, **39**, **43**·CH_3CN, **44** and **46**·C_5H_{12}·1/2CH_3CN) contain bidentate ligands, which derived from an *α*-amino acid ((*S*)-alanine, (*S*)-phenylalanine, or (*S*)-*tert*-leucine). Only one of these complexes displays a VSEPR structure in the crystal, while the other neutral pentacoordinate silicon(IV) species show non-VSEPR structures. The influence of the *α*-amino acid ligands on the structure properties of the pentacoordinate silicon(IV) complexes is shown in Table 7 by a comparison of some relevant bond lengths and angles the higher-coordinate silicon complexes **38**, **39**, **43**·CH_3CN, **44** and **46**·C_5H_{12}·1/2CH_3CN.

Table 7: Selected bond lengths [Å] and angles [°] of **38**, **39**, **43**·CH_3CN, **44** and **46**·C_5H_{12}·1/2CH_3CN.

	38	**39**	**43**·CH_3CN	**44**	**46**·C_5H_{12}·1/2CH_3CN
Si−O_{ax}	1.7910(13)	1.8038(11)[a] 1.7995(10)[b]	1.7871(14)	1.8004(9)	1.8199(8)[c] 1.7876(8)[c]
Si−N_{ax}	1.9932(14)	1.9731(13)[a] 1.9823(12)[b]	1.9658(17)	1.9677(11)	————

O_{ax}−Si−N_{ax}	167.64(6)	169.01(6)[a] 170.55(6)[b]	168.25(7)	169.43(5)	————

[a] Compound **39** shows two independent molecules (**I** and **II**) in the crystal. The axial bond length of **39** belongs to molecule **I**. [b] Compound **39** shows in the crystal two independent molecules (**I** and **II**). The axial bond length of **39** belongs to molecule **II**. [c] Compound **46**·C_5H_{12}·1/2CH_3CN showed in the crystal a VSEPR structure with both oxygen atoms occupying the axial sites of the trigonal bipyramid.

The molecular structures of **38**, **39**, **43**·CH_3CN and **44** show similar atom arrangements of the bidentate ligands, with an oxygen and a nitrogen atom occupying the equatorial positions. The axial O–Si–N-angles of **38**, **39**, **43**·CH_3CN and **44** are within the range of 167.64(6)–170.55(6)°. The axial O–Si–O angle of **46**·C_5H_{12}·1/2CH_3CN amounts to 164.88(4)° and deviates from the values of the axial O–Si–N angles of **38**, **39**, **43**·CH_3CN and **44** by ca. 2−5°. Interestingly, the equatorial O–Si–N angles of **38**, **39**, **43**·CH_3CN, **44** show a larger deviation from the ideal 120° angle (120.56(6)–125.90(9)°). The N_{eq}–Si–N_{eq} angle of **46**·C_5H_{12}·1/2CH_3CN amounts to 124.96(4)° and is within the range observed for the equatorial angles of **38**, **39**, **43**·CH_3CN and **44**. The deviation of the angles found here might be due to steric effects. However, all compounds studied form intermolecular N−H···O hydrogen bonds that lead to the formation of infinite three-dimensional (**38**, **43**·CH_3CN) or two-dimensional (**39**) networks or infinite one-dimensional chains (**44**, **46**·C_5H_{12}·1/2CH_3CN). The equatorial Si–N bond lengths (1.6885(17)–1.8842(9) Å) are, as expected, shorter than the axial Si–N bond distances (1.8658(17)–1.9932(14) Å). The equatorial Si–O bond lengths (1.7042(10)–1.7220(12) Å) are, as expected, shorter than the axial Si–O bond distances (1.7871(14)–1.8199(8) Å).

Table 8: Selected bond lengths [Å] and angles [°] of **38**, **39**, **43**·CH_3CN, **44** and **46**·C_5H_{12}·1/2CH_3CN.

	38	**39**	**43**·CH_3CN	**44**	**46**·C_5H_{12}·1/2CH_3CN
Si−O_{eq}	1.7118(11)	1.7207(12)[a] 1.7220(12)[b]	1.7082(14)	1.7042(10)	————
Si−N_{eq}	1.6901(14)	1.7052(15)[a] 1.7114(13)[b]	1.6885(17)	1.6991(12)	1.7040(9)[c] 1.8842(9)[c]
Si−C_{eq}	1.8401(18)	1.8654(18)[a] 1.8581(17)[b]	1.854(2)	1.8582(13)	1.8659(11)
O_{eq}−Si−N_{eq}	123.85(7)	124.53(7)[a] 120.56(6)[b]	125.90(9)	123.98(5)	————

[a] Compound **39** shows two independent molecules (**I** and **II**) in the crystal. The equatorial bond length of **39** belongs to molecule **I**. [b] Compound **39** showed in the crystal two independent molecules (**I** and **II**). The equatorial bond length of **39** belongs to molecule **II**. [c] Compound **46**·C_5H_{12}·1/2CH_3CN showed in the crystal a VSEPR structure with both nitrogen atoms occupying the equatorial sites of the trigonal bipyramid.

The axial Si–O bond distances (1.7871(14)–1.8199(8) Å) are very close to the sum of the covalent radii of silicon and oxygen (1.77 Å), whereas the equatorial Si–O bond lengths are significantly shorter (1.7042(10)–1.7220(12) Å). The equatorial Si–N bond lengths (1.6885(17)–1.8842(9) Å) are close to the the sum of the covalent radii of silicon and nitrogen (1.82 Å), whereas the axial Si–N bonds are significantly longer (1.8658(17)–1.9932(14) Å).

5.8 Comparison of selected bond lengths and angles of 54 and 55

The pentacoordinate silicon(IV) complexes **54** and **55** (SiO_2N_2C and $SiON_3C$ skeletons) contain both one tridentate ligand. The difference between the two tridentate ligands is that different atoms bind to the silicon center. Compound **54** contains an *O*,*N*,*O* donor, while compound **55** contains an *O*,*N*,*N* donor. It is interesting to compare the bond lengths and angles in the two trigonal bipyramid polyhedra. Table 9 shows some relevant bond lengths and angles of the higher-coordinate silicon complexes **54** and **55**.

Table 9: Selected bond lengths [Å] and angles [°] of **54** and **55.**

	54	**55**
$Si–O_{eq}$	1.6875(12) 1.6839(12)	1.6908(13)
$Si–N_{ax}$	1.8033(15) 1.9947(14)	1.8735(16) 1.9601(15)
$Si–N_{eq}$	————	1.7199(15)
$Si–C_{eq}$	1.8466(17)	1.867(2)
$N_{ax}–Si–N_{ax}$	165.40(7)	173.32(8)
$O_{eq}–Si–C_{eq}$	113.19(7) 114.85(7)	112.44(9)
Si–N–C	149.40(14)	172.29(16)

The molecular structures of **54** and **55** show similar arrangements of the tridentate ligands. Two oxygen atoms and a carbon atom occupy the equatorial positions of **54**, while an oxygen atom, a nitrogen and a carbon atom occupy the equatorial sites of **55**. The axial positions are occupied in both cases by two nitrogen atoms. The axial N–Si–N angles of **54** and **55** amount to 165.40(7)° and 173.32(8)°, respectively, and therefore a large difference is

observed. This could be explained by a stronger tension in the complex containing an *O*,*N*,*O* donor regarding to the complex **55**, which contains an *O*,*N*,*N* ligand. The equatorial O–Si–C angles of **54** and **55** are very similar and range from 112.44(9)° to 113.19(7)° and 114.85(7)°, respectively. Interestingly, the equatorial O–Si–O angle of **54** deviates strongly from the ideal 120° angle (131.69(6)°). The axial Si–N–C angles of **54** and **55** are very different and range from 149.40(14)° (Si-NCO group; strong deviation from linearity) to 172.29(16)° (Si-NCS group; almost linear). The equatorial Si–O bond distances (**54**, 1.6839(12), 1.6875(12); **55**, 1.6908(13) Å) are shorter than the sum of the covalent radii of silicon and oxygen (1.77 Å). The same behavior is noticed for the equatorial Si–N bond length of **55** (1.7199(15) Å) compared to the the sum of the covalent radii of silicon and nitrogen (1.82 Å). The axial Si–N bond lengths vary from 1.8033(15) and 1.9947(14) to 1.8735(16) and 1.9601(15) and are closer to the sum of the covalent radii of silicon and nitrogen (1.82 Å).

5.9 Comparison of selected bond lengths and angles of 56, 57 and 58

The hexacoordinate silicon(IV) complexes **56**, **57** and **58** (*Si*ON_4C and *Si*ON_5 skeletons) contain one *O*,*N*,*N* tridentate ligand, two or three NCX (X = O, S) ligands and one alkyl or aryl group. All complexes show in the crystal distorted octahedrons. It is interesting to compare the bond lengths and angles of these hexacoordinate silicon(IV) complexes. Table 10 shows some relevant bond lengths and angles of the higher-coordinate silicon complexes **56**, **57** and **58**.

Table 10: Selected bond lengths [Å] and angles [°] of **56**, **57** and **58**.

	56	**57**	**58**
Si−O	1.7238(10)	1.7560(9)	1.7689(10)
Si−N (NCX group)	1.8666(11) 1.8761(12)	1.8252(11) 1.8001(11) 1.8324(11)	1.8364(12) 1.8516(12)
Si−N (*O*,*N*,*N* donor)	2.0899(13) 1.9460(11)	2.0199(11) 1.8969(10)	2.0883(12) 1.9537(11)
Si−C	1.8933(15)	————	1.9281(13)
N_{trans}–Si–N_{trans} (NCX group)	173.39(6)	178.43(5)	170.32(6)
Si–N–C (NCX group)	168.08(12) 163.58(12)	143.62(10) 159.32(11) 145.93(9)	152.26(13) 157.02(12)

The molecular structures of **56**, **57** and **58** show similar arrangements of the tridentate ligands. One oxygen atom and a nitrogen atom from the tridentate ligands occupy *trans* positions, as well as the nitrogen atoms belonging to the NCX (X = S, O) groups. The N–Si–N angles, with nitrogen atoms occupying *trans* positions, of **56**, **57** and **58** range from 170.32(6)° to 173.39(6)° and 178.43(5)°, and are near to the ideal 180° angle. The Si–N–C angles of **56**, **57** and **58** show larger differences and range from 143.62(10)° to 168.08(12)°, respectively. Surprisingly, the Si–N–C angles of **57** (143.62(10)° and 145.93(9)°) are more distorted than the corresponding angles of **58**. At present, this finding is unexplained. The Si–O bond distances (**56**, 1.7238(10); **57**, 1.7560(9); **58**, 1.7689(10) Å) are close to the sum of the covalent radii of silicon and oxygen (1.77 Å). The Si–N bonds of **56**, **57** and **58** (*O*,*N*,*N* donor; 1.8969(10)−2.0899(13) Å) are very long compared with the the sum of the covalent radii of silicon and nitrogen (1.82 Å). The Si–N bond lenghts (NCX groups; 1.8001(11)−1.8761(12) Å) are closer to the sum of the covalent radii of silicon and nitrogen.

5.10 Comparison of selected bond lengths and angles of 59 and 60

The hexacoordinate silicon(IV) complexes **59** and **60** ($Si O_2N_3C$ skeleton) contain one *O*,*O*,*N*,*N* tetradentate ligand, one NCO ligand and one alkyl or aryl group. These complexes show, in the crystal, distorted octahedral configurations. It is interesting to compare the bond lengths and angles of these hexacoordinate silicon(IV) complexes. Table 11 shows some relevant bond lengths and angles of the higher-coordinate silicon complexes **59** and **60**.

Table 11: Selected bond lengths [Å] and angles [°] of **59** and **60**.

	59	**60**
Si−O	1.7819(13) 1.7681(13)	1.7674(10) 1.7647(10)
Si−N (NCO group)	1.8912(17)	1.887(5)
Si−N (*O*,*O*,*N*,*N* donor)	1.9084(16) 1.9209(15)	1.8856(12) 1.8992(12)
Si−C	1.921(2)	1.9291(14)
N–Si–C	177.89(8)	178.3(3)
Si–N–C (NCX group)	160.26(15)	145.3(9)

The molecular structures of **59** and **60** show similar arrangements of the tetradentate ligands. The nitrogen atoms belonging to the NCO groups and the carbon atom which belongs to the alkyl or aryl group occupy *trans* positions. The *O*,*O*,*N*,*N* donors form a plane and the oxygen atoms, as well as the nitrogen atoms, occupy *cis* positions. The N–Si–C angles of **59** and **60** are almost linear. The Si–N–C angles of **59** and **60** show bigger distortions from the ideal 180° angle and range from 145.3(9)° to 160.26(15)°, respectively. This finding could be due to steric effects (exchange of the methyl group for an aryl fragment). The Si–O bond distances (1.7647(10)−1.7819(13) Å) are close to the sum of the covalent radii of silicon and oxygen (1.77 Å). The Si–N distances of **59** and **60** (*O*,*O*,*N*,*N* donor; 1.8856(12)−1.9209(15) Å) approach the sum of the covalent radii of silicon and nitrogen (1.82 Å). The Si–N bond lenghts (NCO groups; 1.887(5)−1.8912(17) Å) are longer than the sum of the covalent radii of silicon and nitrogen.

5.11 Comparison of selected bond lengths and angles of 62, 63 and 64

The hexacoordinate silicon(IV) complexes **62**, **63** and **64** (SiO_2N_3C and SiO_2N_4 skeletons) contain one tetradentate *O*,*O*,*N*,*N* ligand, one or two NCX (X = O, S) ligand(s) and one alkyl or aryl group. These complexes show distorted octahedrons in the crystal. Table 12 shows some relevant bond lengths and angles of the higher-coordinate silicon complexes **62**, **63** and **64**.

Table 12: Selected bond lengths [Å] and angles [°] of **62**, **63** and **64**.

	62	**63**	**64**
Si−O	1.7409(11) 1.7510(11)	1.7352(17) 1.7302(17)	1.7055(17) 1.7078(17)
Si−N (NCX group)	1.8791(14)	1.867(2)	1.857(2) 1.863(2)
Si−N (*O*,*O*,*N*,*N* donor)	1.9445(12) 1.9584(14)	1.943(2) 1.928(2)	1.909(2) 1.9175(19)
Si−C	1.9107(16)	1.918(2)	————
N–Si–C	175.72(7)	175.25(10)	————
N_{trans}–Si–N_{trans}	————	————	173.08(10)
Si–N–C (NCX group)	156.45(12)	159.4(2)	148.7(2) 175.8(2)

The molecular structures of **62**, **63** and **64** show similar arrangements of the tetradentate *O*,*O*,*N*,*N* ligands. The nitrogen atom belonging to the NCO group and the carbon atom which belongs to the alkyl or aryl group occupy *trans* positions (**62** and **63**). The two nitrogen atoms belonging to the NCS fragments occupy *trans* positions as well (**64**). The *O*,*O*,*N*,*N* donors form a plane. The oxygen and the nitrogen atoms follow the trend observed for **59** and **60**, occupying *cis* positions. The N–Si–C angles of **62** and **63** are almost linear (175.72(7)°, 175.25(10)°). The Si–N–C angles of **62**, **63** and **64** show greater deviations from the ideal 180° angle and range from 148.7(2)° to 175.8(2)°. This distortion is probably caused by steric interactions (exchange of the methyl group for an aryl fragment in **62** and **63**). Interestingly, the Si–N–C angles of **64** are very different from each other. As yet the large distortion observed for one of the Si–N–C angles is unexplained. The Si–O bond distances (1.7055(17)−1.7510(11) Å) are significantly shorter than the sum of the covalent radii of silicon and oxygen (1.77 Å). The Si–N bonds of **62**, **63** and **64** (*O*,*O*,*N*,*N* donor; 1.909(2)−1.9584(14) Å) are significantly longer than the sum of the covalent radii of silicon and nitrogen (1.82 Å). The Si–N bond lenghts (NCO groups; 1.857(2)−1.8791(14) Å) are close to the sum of the covalent radii of silicon and nitrogen.

6 Computational Studies

6.1 Computational studies of the neutral hexacoordinate silicon(IV) complex 50[22]

To further our understanding of the stereochemistry of **50**, structure optimizations and frequency calculations for the eight possible stereoisomers of the hexacoordinate silicon(IV) complex **50** were performed. The computational studies were performed with the TURBOMOLE 5.10 [67, 68, 69] program package at the BP86 [70]/SVP [71] level of theory.

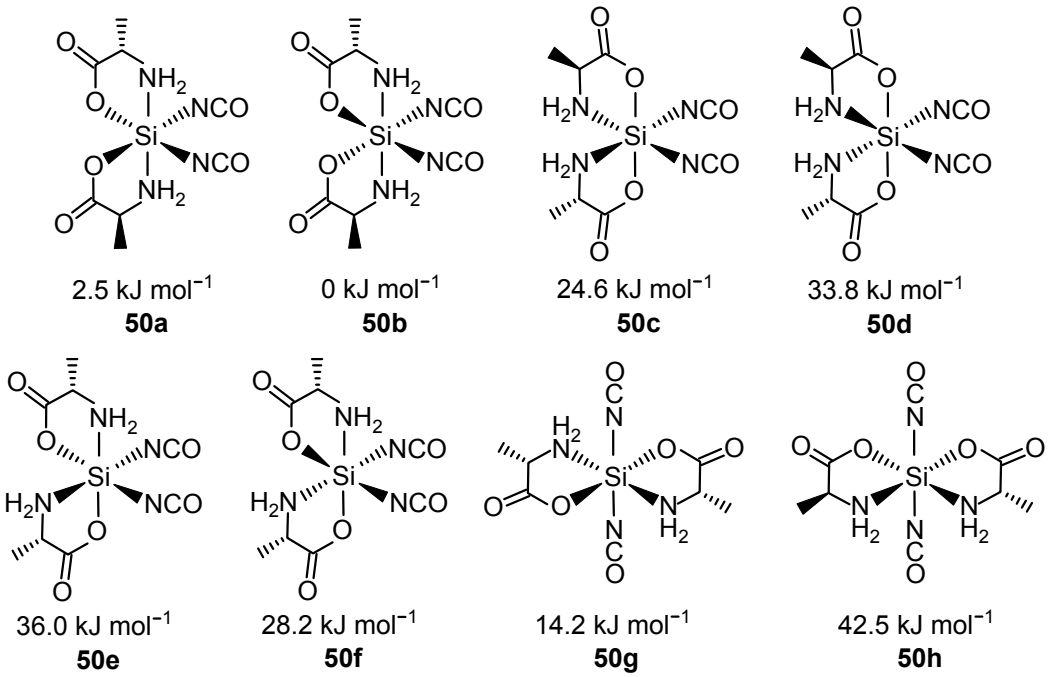

Scheme 20. Configurations and calculated relative energies for the eight possible stereoisomers of **50**, the diastereoisomers **50a**–**50h**.

The configurations of the eight possible stereoisomers of **50**, the diastereoisomers **50a**–**50h**, and their calculated relative energies are shown in Scheme 20. The maximum energy difference amounts to 42.5 kJ mol^{-1}. The three isomers with both NH_2 groups in *trans*-positions (**50a**, 2.5 kJ mol^{-1}; **50b**, 0 kJ mol^{-1}; **50g**, 14.2 kJ mol^{-1}) are the most stable species, and the configuration of **50a** corresponds to the experimentally established structure of **50** in the crystal (see Figure 11). Based on these results, it is likely to assume that the two most stable isomers **50a** and **50b** represent the two species (molar ratio, ca. 1:1) detected NMR spectroscopically in solution (solvent, [D_6]DMSO; see experimental section).

[22]The computational studies were performed by Dr. K. Götz, Department of Inorganic Chemistry, University of Würzburg.

6.2 Computational studies of the neutral pentacoordinate silicon(IV) complex 38[23]

To obtain more information about the stereochemistry of **38**, **39**, **43**·CH_3CN, and **44**−**46**, structure optimizations and frequency calculations for the six possible stereoisomers of the pentacoordinate silicon(IV) complex **38** were performed. In these studies, compound **38** served as a model system for the related pentacoordinate silicon compounds **38**, **39**, **43**·CH_3CN, and **44**−**46**. The studies were performed with the TURBOMOLE5.10 [67, 68, 69] program package and at the BP86 [70]/SVP[71] level of theory.

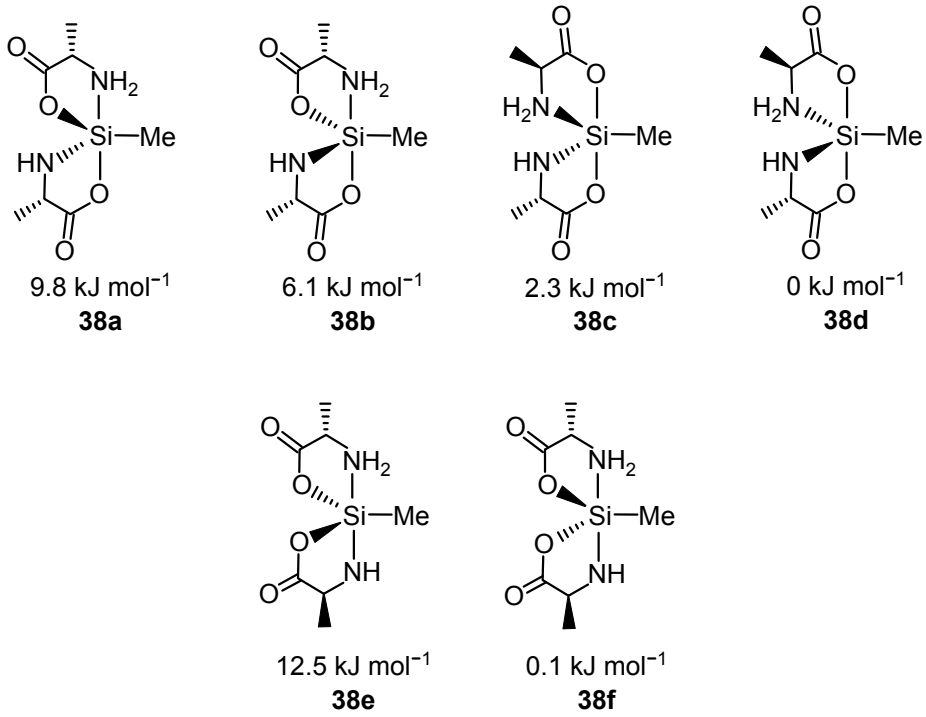

Scheme 21. Configurations and calculated relative energies for six possible stereoisomers of **38**, the diastereoisomers **38a**−**38f**.

Our interest was focused on the two different coordination modes of the pentacoordinate silicon complexes found in the crystal of **38** and **46**. In the molecular structure of **38**, one oxygen and one nitrogen atom occupy the axial position of the trigonal bipyramid, while in the molecular structure of **46** both axial positions of the trigonal bipyramid are occupied by oxygen atoms.

The configurations of the six possible stereoisomers of **38**, the diastereoisomers **38a**−**38f**, and their calculated relative energies are shown in Scheme 21. The maximum

[23]The computational studies were performed by Dr. K. Götz, Department of Inorganic Chemistry, University of Würzburg.

energy difference amounts to 12.5 kJ mol^{-1}. The configuration of **38a** corresponds to the experimentally established structure of **38** and **43** (studied as **43**·CH_3CN) in the crystal, whereas **38c** corresponds to the structure of **46** in the crystal of **46**·C_5H_{12}·1/2CH_3CN (see Figure 10). The configuration of **38b** corresponds to the crystal structures of **39** and **44** (see Figures 8 and 9). As the maximum energy difference observed for **38a**−**38f** is rather small, it is not surprising that the three different configurations, namely, **38a**, **38b**, and **38c** are realized in the crystal structures of the pentacoordinate silicon(IV) complexes studied. Due to this small energy difference, a configurational assignment for the two species of **44** (molar ratio; ca. 1:1.3) detected NMR-spectroscopically in solution (solvent, [D_6]DMSO) is not possible (see experimental section).

7 Zusammenfassung

Im Vordergrund dieser Arbeit stand die Synthese und strukturelle Charakterisierung penta- und hexakoordinierter Silicium(IV)-Komplexe. Im Verlauf dieser Untersuchungen wurden die neutralen pentakoordinierten Silicium(IV)-Komplexe **38**, **39**, **43**−**48**, **54** und **55** dargestellt. Weiterhin konnten die neutralen hexakoordinierten Silicium(IV)-Komplexe **33**−**36**, **49**, **50**, **52**, **53**, **56**−**62**, **63**, **64** und **65** synthetisiert werden. Die Charakterisierung aller Verbindungen erfolgte durch Elementaranalyse, NMR-Spektroskopie in Lösung (^{1}H, ^{13}C, ^{15}N, ^{29}Si) und im Festkörper (^{13}C, ^{15}N, ^{29}Si VACP/MAS NMR), sowie durch Kristallstrukturanalyse (außer **45**, **47**−**49**, **52**, **53** und **63**).

Die Synthesen von **33** und **34** erfolgten durch Reaktion von Tri(cyanato-*N*)phenylsilan mit Acetylaceton bzw. mit Dibenzoylmethan. Beide Verbindungen eignen sich als Vorstufen zur Synthese von weiteren hexakoordinierten Silicium-Verbindungen, zum Beispiel durch Substitution der NCO-Gruppe durch andere monoanionische Liganden (Cl, Br, NCS usw.).

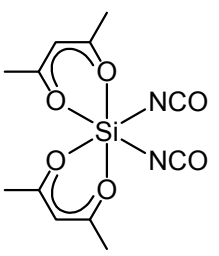

71

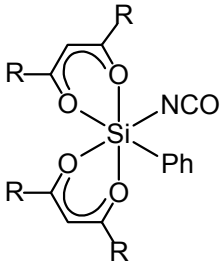

33: R = Me
34: R = Ph

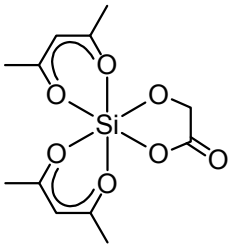

35

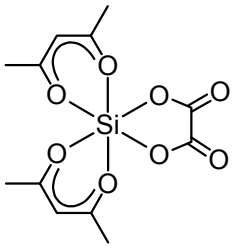

36

Die Reaktivität des hexakoordinierten Silicium-Komplexes **71** ($(acac)_2Si(NCO)_2$) wurde untersucht, indem die zwei NCO-Fragmente durch *O,O*-Liganden ersetzt wurden. Dies geschah durch Umsetzung von **71** mit einem Moläquivalent disilylierter Glycolsäure bzw. disilylierter Oxalsäure. Die Verbindungen **35** und **36** eignen sich als potentielle Edukte zur Synthese von weiteren hexakoordinierten Silicium-Verbindungen.

Die pentakoordinierten Verbindungen **38**, **39**, **43**−**48** konnten durch Umsetzung von disilylierten α-Aminosäuren ((*S*)-Alanin, (*S*)-Phenylalanin, (*S*)-Valin, (*S*)-*tert*-Leucin und **21**) mit $RSi(NCO)_3$ (R = Me, Ph) dargestellt werden. Erstmalig konnten damit pentakoordinierte Silicium-Verbindungen mit einem neuen Koordinationsmodus der Aminosäure-Liganden an Silicium (gleichzeitig mono- und dianionische zweizähnige Liganden) synthetisiert und charakterisiert werden.

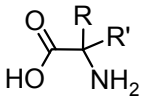

21: R = Me, R' = CH_2SiMe_3

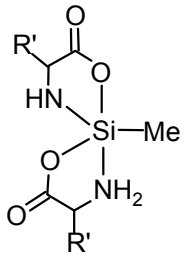

38: R = Me
39: R = Bn

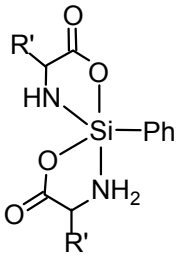

43: R = Me
44: R = Bn
45: R = *i*-Pr
46: R = *t*-Bu

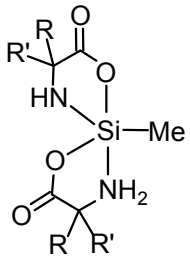

47: R = Me, R' = CH_2SiMe_3

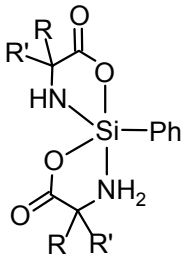

48: R = Me, R' = CH_2SiMe_3

Die hexakoordinierten Verbindungen **49**, **50**, **52** und **53** konnten durch Umsetzung der entsprechenden disilylierten *α*-Aminosäuren (Glycin, (*S*)-Alanin, (*S*)-Valin, *(S)*-*tert*-Leucin) mit $Si(NCO)_4$ dargestellt werden. Erstmalig konnten damit hexakoordinierte Silicium-Verbindungen mit monoanionischen Liganden, die sich aus *α*-Aminosäure-Liganden herleiten, synthetisiert und charakterisiert werden.

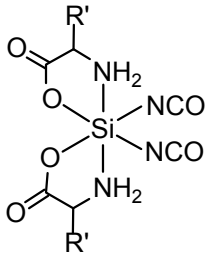

49: R = H
50: R = Me
52: R = *i*-Pr
53: R = *t*-Bu

Die pentakoordinierte Verbindung **54** konnte durch Reaktion von **4** mit **27** dargestellt werden. Mit dieser konnte gezeigt werden, dass Tri(cyanato-*N*)methylsilan eine geeignete Vorstufe für die Synthese neuer pentakoordinierten Silicium(IV)-Komplexen ist. Verbindung **54** könnte sich zudem als Vorstufe zur Synthese von weiteren pentakoordinierten Silicum-Verbindungen eignen, z. B. durch Substitution der NCO-Liganden durch andere Substituenten (z. B.: N_3, NCS).

$RSi(NCO)_3$

4: R = Me

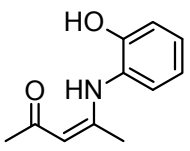

27

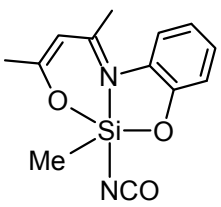

54

Die Synthesen der Verbindungen **55** (*Si*ON_3C Gerüst) und **56** (*Si*ON_4C Gerüst) ausgehend von $MeSi(NCS)_2H$ (**3**) ermöglichten den Zugang zu Vertretern zweier neuer Klassen höherkoordinierter Silicium(IV)-Komplexe. Methyldi(thiocyanato-*N*)silan (**3**) erwies sich damit als geeignete Vorstufe für die Synthese von neuen höherkoordinierten Silicium-Komplexen dieser Formeltypen. Mit ihren reaktiven Si-NCS-Funktionen könnten die Komplexe **55** und **56** ebenso als Vorstufen zur Synthese weiterer höherkoordinierter Silicium-Verbindungen dienen.

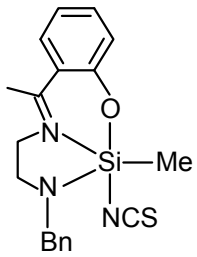

55

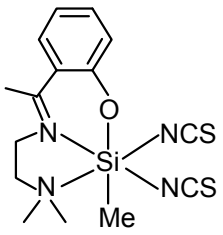

56

Die pentakoordinierten Verbindungen **57** und **58** konnten durch Reaktion von Tetra(cyanato-*N*)silan bzw. Tri(cyanato-*N*)phenylsilan mit **30** dargestellt werden. Hexakoordinierte Silicium-Komplexe mit drei Si–NCO-Einheiten (**57**) wurden bisher nicht synthetisiert.

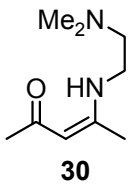

30

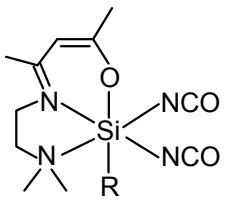

57: R = NCO
58: R = Ph

Die hexakoordinierten Verbindungen **59**, **60**, **62** und **63** konnten durch Umsetzung von $RSi(NCO)_3$ (R = Me, Ph) mit **31** bzw. **32** dargestellt werden. Diese Silicium-Komplexe mit ihren reaktiven Si-NCO-Funktionen könnten als Vorstufen zur Darstellung neuer höherkoordinierter Silicium-Verbindungen dienen.

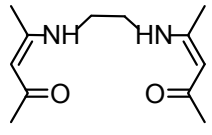

31

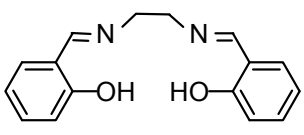

32

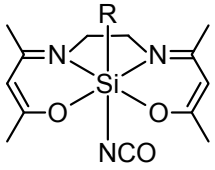

59: R = Me
60: R = Ph

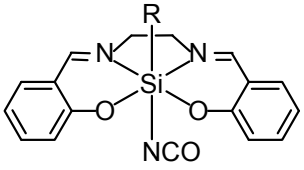

62: R = Me
63: R = Ph

Die hexakoordinierte Verbindung **64** konnte durch Umsetzung von $Si(NCS)_4$ mit **32** dargestellt werden. NMR-Untersuchungen von **64** zeigten die Existenz mehrerer Isomere in Lösung.

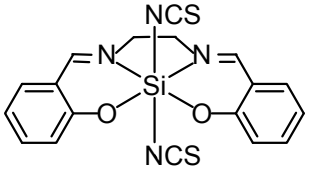

64

Die hexakoordinierte Verbindung **65** konnte als Nebenprodukt bei der Umsetzung von $Si(NCO)_4$ mit **32** dargestellt werden. Die Charakterisierung des Komplexes **65** erfolgte durch Röntgenstrukturanalyse.

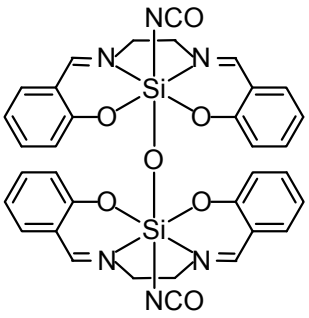

65

Verbindung **65** ist der erste binucleare hexakoordinierte Silicium-Komplex mit NCO-Liganden und einer Sauerstoff-Brücke zwischen den Silicium-Atomen.

8 Summary

The main aim of this thesis was the synthesis and structural characterization of penta- and hexacoordinate silicon(IV) complexes. In the course of these studies, the neutral pentacoordinate silicon(IV) complexes **38**, **39**, **43**−**48**, **54** and **55** were prepared. Furthermore, the neutral hexacoordinate silicon(IV) complexes **33**−**36**, **49**, **50**, **52**, **53**, **56**−**62**, **63**, **64** and **65** were synthesized. All compounds were characterized by elemental analyses, NMR spectroscopy in solution (^{1}H, ^{13}C, ^{15}N, ^{29}Si) and in the solid-state (^{13}C, ^{15}N, ^{29}Si VACP/MAS NMR), as well as single-crystal X-ray diffraction (except **45**, **47**−**49**, **52**, **53** and **63**).

The synthesis of **33** and **34** was carried out by the reaction of tri(cyanato-*N*)phenylsilane with acetylacetone or dibenzoylmethane. Both compounds are suitable as precursors for the synthesis of further hexacoordinate silicon compounds as well, for instance, by substitution of the NCO group with other monoanionic ligands (Cl, Br, NCS).

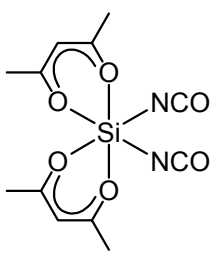

71

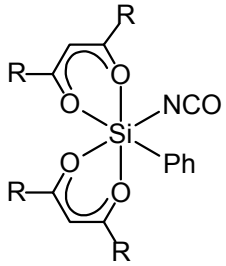

33: R = Me
34: R = Ph

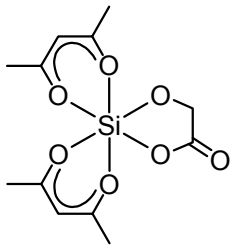

35

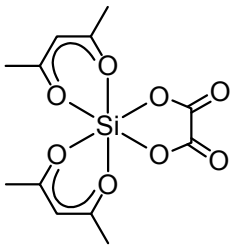

36

The reactivity of the hexacoordinate silicon complex **71** ($(acac)_2Si(NCO)_2$) was tested by the substitution of the two NCO-fragments by *O,O*-ligands. This was done by treatment of **71** with disilylated glycolic acid or with disilylated oxalic acid. Compunds **35** and **36** are also suitable as precursors for the synthesis of further hexacoordinate silicon compounds.

The pentacoordinate compounds **38**, **39**, **43**−**48** could be obtained by treatment of the disilylated *α*-amino acids ((*S*)-alanine, (*S*)-phenylalanine, (*S*)-valine, (*S*)-*tert*-leucine and **21**, respectively) with $RSi(NCO)_3$ (R = Me, Ph). For the first time, pentacoordinate silicon(IV) complexes with a novel coordination modus of the *α*-amino acids ligands (which act simultaneously as mono- und dianionic bidentate ligands) were synthesized and characterized.

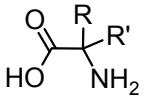

21: R = Me, R' = CH_2SiMe_3

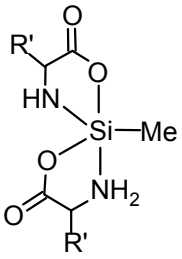

38: R = Me
39: R = Bn

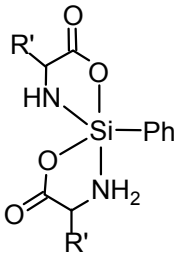

43: R = Me
44: R = Bn
45: R = *i*-Pr
46: R = *t*-Bu

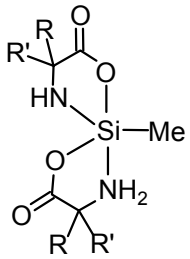

47: R = Me, R' = CH_2SiMe_3

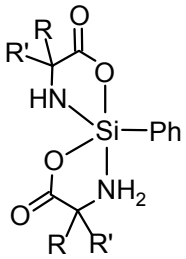

48: R = Me, R' = CH_2SiMe_3

The hexacoordinate compounds **49**, **50**, **52** and **53** were synthesized by treatment of the corresponding disilylated *α*-amino acids (glycine, (*S*)-alanine, (*S*)-valine, (*S*)-*tert*-leucine) with $Si(NCO)_4$. For the first time, hexacoordinate silicon(IV) complexes with a novel coordination modus of the *α*-amino acids ligands (monoanionic bidentate ligands) could be synthesized and characterized.

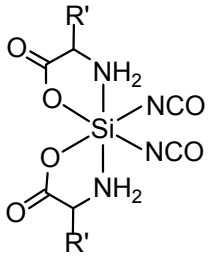

49: R = H
50: R = Me
52: R = *i*-Pr
53: R = *t*-Bu

The pentacoordinate compound **54** was synthesized by the reaction of **4** and **27**. With the synthesis of **54** could be demonstrated that tri(cyanato-*N*)methylsilane is a suitable precursor for the synthesis of new pentacoordinate silicon(IV) complexes. Compound **54** should also be suitable as precursor for the synthesis of further pentacoordinate silicon(IV) compounds, for instance by substitution of the NCO ligands with other moieties (e. g. N_3, NCS).

$RSi(NCO)_3$

4: R = Me

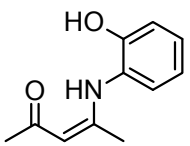

27

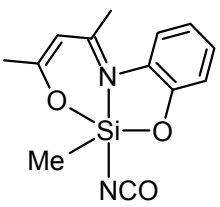

54

With the synthesis of compounds **55** (*Si*ON_3C skeleton) and **56** (*Si*ON_4C skeleton), which started from $MeSi(NCS)_2H$ (**3**), members of two new classes of higher-coordinate silicon(IV) complexes have been made accessible. Methyldi(thiocyanato-*N*)silane (**3**) has been demonstrated to be a suitable precursor for the synthesis of higher-coordinate silicon compounds of these particular formula types. Due to their reactive Si−NCS groups, compounds **55** and **56** themselves may serve as precursors for the synthesis of other novel higher-coordinate silicon compounds.

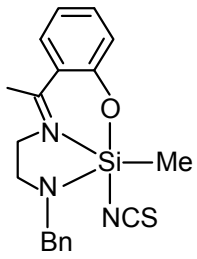

55

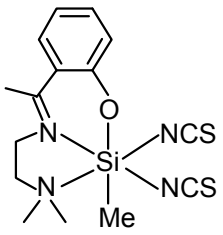

56

The pentacoordinate compounds **57** und **58** were synthesized by reaction of tri(cyanato-*N*)phenylsilane or tetra(cyanato-*N*)silane with one molar equivalent of **30**. Hexacoordinate silicon complexes with three Si–NCO-moieties had not previously been synthesized.

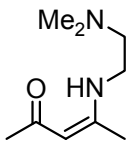

30

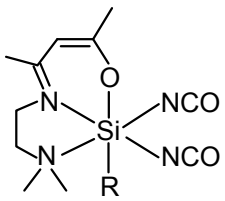

57: R = NCO
58: R = Ph

The hexacoordinate compounds **59**, **60**, **62** and **63** were synthesized by treatment of $RSi(NCO)_3$ (R = Me, Ph) with **31** or **32**. These hexacoordinate silicon(IV) complexes, with their reactive Si-NCO-moieties, could serve as precursors for the synthesis of novel higher-coordinate silicon complexes.

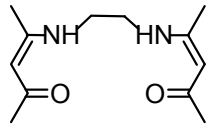

31

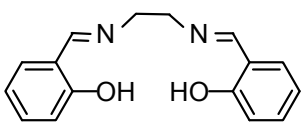

32

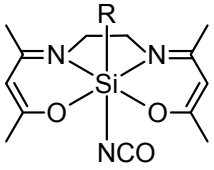

59: R = Me
60: R = Ph

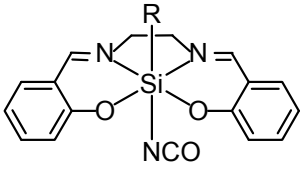

62: R = Me
63: R = Ph

Compound **64** was synthesized by treatment of $Si(NCS)_4$ with **32**. NMR studies of the hexacoordinate complex **64** in solution showed the existence of more than one species.

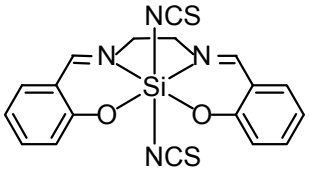

64

The hexacoordinate compound **65** was obtained as byproduct of the reaction of $Si(NCO)_4$ with **32**. The characterization of **65** was carried out by single-crystal X-ray diffraction.

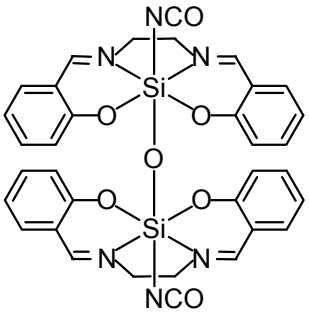

65

Compound **65** is the first binuclear silicon complex containing NCO ligands and an oxygen-bridge between the silicon atoms and might serve as precursor for the synthesis of novel higher-coordinate silicon complexes.

9 Experimental Section

9.1 General Procedures

Syntheses. All syntheses were carried out under dry argon or dry nitrogen. The organic solvents used were dried and purified according to standard procedures and stored under dry argon/nitrogen. The melting points were determined using a Büchi Melting Point B-540 apparatus with samples in sealed glass capillaries. The elemental analyses were determined with a Vario Cube apparatus of Elementar Analysensysteme.

IR spectroscopy. The IR spectra were recorded using a Bruker Equinox IFS 55 spectrometer (wavelength region, 4000−400 cm^{-1}). The samples were prepared as KBr-pellets under atmospheric conditions.

NMR spectroscopy. The ^{1}H, ^{13}C, and ^{29}Si solution NMR spectra were recorded at 23 °C on a Bruker Avance 500- NMR spectrometer (^{1}H, 500.1 MHz; ^{13}C, 125.8 MHz; ^{29}Si, 99.4 MHz), on a Bruker DRX-300 NMR spectrometer (^{1}H, 300.1 MHz; ^{13}C, 75.5 MHz; ^{29}Si, 59.6 MHz) or on a Bruker Avance- 400 NMR spectrometer (^{1}H, 400.1 MHz; ^{13}C, 100.6 MHz; ^{29}Si, 79.5 MHz) using [D_6]DMSO, $CDCl_3$ and CD_2Cl_2 as the solvents. The ^{15}N HMBC solution NMR spectra were recorded at 23 °C on a Bruker DRX-300 NMR spectrometer (^{15}N, 30.4 MHz) or on a Bruker Avance 500- NMR spectrometer (^{15}N, 50.7 MHz). Chemical shifts (ppm) were determined relative to internal [D_5]DMSO (^{1}H, δ = 2.49; [D_6]DMSO), internal $CHDCl_2$ (^{1}H, δ = 5.32; CD_2Cl_2), internal $CDCl_3$ (^{1}H, δ = 7.24; $CDCl_3$), internal [D_6]DMSO (^{13}C, δ = 39.5; [D_6]DMSO), CD_2Cl_2 (^{13}C, δ = 53.8; CD_2Cl_2), internal $CDCl_3$ (^{13}C, δ = 77.0; $CDCl_3$), external formamide (^{15}N, δ = –268.0; [D_6]DMSO, CD_2Cl_2, $CDCl_3$), or external TMS (^{29}Si, δ = 0; [D_6]DMSO, CD_2Cl_2, $CDCl_3$). Analysis and assignment of the ^{1}H NMR data was supported by 2D ^{1}H,^{1}H, ^{13}C,^{1}H, ^{15}N,^{1}H, and ^{29}Si,^{1}H correlation experiments. Assignment of the ^{13}C NMR data was supported by DEPT 135 experiments and the above mentioned ^{13}C,^{1}H correlation experiments. Solid-state ^{13}C, ^{15}N, and ^{29}Si VACP/MAS NMR spectra were recorded at 22 °C on a Bruker DSX-400 NMR spectrometer with bottom layer rotors of ZrO_2 (diameter, 7 mm) containing ca. 300 mg of sample (^{13}C, 100.6 MHz; ^{15}N, 40.6 MHz; ^{29}Si, 79.5 MHz; external standard, TMS (^{13}C, ^{29}Si; δ = 0) or glycine (^{15}N, δ = –342.0); spinning rate, 6–7 kHz; contact time, 2 ms (^{13}C), 1−3 ms (^{15}N), or 3−5 ms (^{29}Si); 90° ^{1}H transmitter pulse length, 3.6 μs; repetition time, 4 s).

Mass spectrometry. The GC/EI MS studies were peformed with a ThermoQuest gas chromatograph MS-8060 (phenomenex Zebron ZB-1 capillary column, 15 m, i.d. 0.32 mm,

flow rate: 0.73 mL/min, injector, split (1:25), 220 °C; carrier gas: helium) and a ThermoQuest mass spectrometer TRIO-1000 (EI-MS, 70 eV).

All commercially available chemicals were used without further purification. The solvents used for NMR experiments were taken from sealed ampoules without further purification.

9.2 Syntheses

Tetra(cyanato-*N*)silane (**1**) was prepared according to ref. [72] using toluene as the solvent.

Tetra(thiocyanato-*N*)silane (**2**) was prepared according to ref. [73] using toluene as the solvent and ammonium thiocyanate instead of ammoniacal silver.

Methyldi(thiocyanato-*N*)silane (**3**)

Dichloro(methyl)silane (22.1 g, 192 mmol) was added at 22 °C to a stirred suspension of ammonium thiocyanate (28.9 g, 380 mmol) in toluene (100 mL), and the reaction mixture was then stirred under reflux for 4 h. After the mixture was cooled to 22 °C, the resulting precipitate was filtered off and discarded. The solvent of the filtrate was removed by distillation at normal pressure, and the residue was distilled in vacuo to give a colorless liquid (b.p.: 75 °C/11 mbar). Yield: 18.8 g (117 mmol, 61%). — ^{1}H NMR (500.1 MHz, $CDCl_3$): δ = 0.59 (d, $^{3}J(^{1}H,^{1}H)$ = 2.5 Hz, 3 H, CH_3), 4.87 (br. s and satellites (d, $^{1}J(^{1}H,^{29}Si)$ = 272 Hz, 4.7% abundance), 1 H, Si*H*). — ^{13}C NMR (125.8 MHz, $CDCl_3$): δ = –0.7 (*C*H_3), 144.3 (t, $^{1}J(^{13}C,^{14}N)$ = 24 Hz, N*C*S). ^{15}N NMR (30.4 MHz, $CDCl_3$): δ = –275.0. — ^{29}Si NMR (99.4 MHz, $CDCl_3$): δ = –45.0 (m).

$C_3H_4N_2S_2Si$ (160.30)	Calcd.:	C 22.48	H 2.52	N 17.48	S 40.01
	Found:	C 22.3	H 2.6	N 17.9	S 39.8

Tri(cyanato-*N*)methylsilane (**4**) was prepared according to ref. [72] using toluene as the solvent and sodium cyanate instead of silver cyanate.

Tri(cyanato-*N*)phenylsilane (**5**) was prepared according to ref. [74] using toluene as the solvent.

Compounds **16**–**20** were prepared according to ref. [41].

(*S*)-*α*-[(trimethylsilyl)methyl]alanine (**21**) was prepared according to ref. [75].

Trimethylsilyl 2-methyl 3-(trimethylsilyl)-*N*-(trimethylsilyl)alanine (**22**)

Method A. *N,O*-bis(trimethylsilyl)acetamide (2.98 g, 14.7 mmol) was added to a stirred solution of (*S*)-2-amino-2-methyl-3-(trimethylsilyl)propanoic acid (2.57 g, 14.7 mmol) in acetonitrile (30 mL). The reaction mixture was heated under reflux for 7 h, and then stirred for further 12 h at 22 °C. The resulting precipitate was filtered off and discarded. The solvent was removed by distillation at normal pressure, and the residue was distilled in vacuo to give a viscous colorless liquid (b.p.: 90–93 °C/10 mbar). Yield: 2.14 g (6.69 mmol, 46%). — ^{1}H NMR (500.1 MHz, CD_2Cl_2): δ = 0.03 (s, 9 H, Si(CH_3)$_3$), 0.20 (s, 9 H, NSi(CH_3)$_3$), 0.27 (s, 9 H, OSi(CH_3)$_3$), 1.10 (s, 2 H, CH_2), 1.17 (s, 1 H, N*H*), 1.38 (s, 3 H, CH_3). — ^{13}C NMR (125.8 MHz, CD_2Cl_2): δ = –0.2 (Si(*C*H$_3$)$_3$), 0.5 (OSi(*C*H$_3$)$_3$), 2.1 (NSi(*C*H$_3$)$_3$), 28.1 (*C*H$_3$), 33.2 (*C*H$_2$), 59.4 (*C*CH$_3$), 178.9 (*C*O). — ^{29}Si NMR (99.4 MHz, CD_2Cl_2): δ = –1.1 (*Si*(CH$_3$)$_3$), 5.1 (N*Si*(CH$_3$)$_3$), 23.3 (O*Si*(CH$_3$)$_3$). — GC/EI-MS (pos.): t_R = 6.004 min (80/20); *m*/*z* (%) 318 (1) [M$^+$], 202 (100) [M$^+$ – COOSi(CH$_3$)$_3$], 114 (33) [COOSi(CH$_3$)$_3$], 73 (95) [$^+$Si(CH$_3$)$_3$].

Method B. (*S*)-2-Amino-2-methyl-3-(trimethylsilyl)propanoic acid (3.10 g, 17.7 mmol) was added to hexamethyldisilazane (20 mL) and the reaction mixture was heated under reflux for 6 h. After the mixture was cooled to 22 °C, *n*-hexane (15 mL), triethylamine (940 mg, 9.29 mmol) and trimethylsilyl chloride (870 mg, 8.01 mmol) were added sequentially in single portions to the reaction mixture. The mixture was stirred at 22 °C for 1 h. The resulting precipitate was filtered off and discarded. The solvent was removed by distillation at normal pressure, and the residue was distilled in vacuo to give 1.00 g of a colorless liquid. The NMR spectra showed a mixture of mono and disilylated amino acid. *N,O*-bis(trimethylsilyl)acetamide (832 mg, 4.09 mmol) was added to the mixture in 10 mL acetonitrile and the mixture was stirred at 30 °C for further 20 h. The reaction mixture was distilled in vacuo to give a viscous colorless liquid (b.p.: 90–93 °C/10 mbar). Yield: 765 mg (2.39 mmol, 14%). — ^{1}H NMR (500.1 MHz, CD_2Cl_2): δ = 0.03 (s, 9 H, Si(CH_3)$_3$), 0.20 (s, 9 H, NSi(CH_3)$_3$), 0.27 (s, 9 H, OSi(CH_3)$_3$), 1.10 (s, 2 H, CH_2), 1.17 (s, 1 H, N*H*), 1.38 (s, 3 H, CH_3). — ^{13}C NMR (125.8 MHz, CD_2Cl_2): δ = –0.2 (Si(*C*H$_3$)$_3$), 0.5 (OSi(*C*H$_3$)$_3$), 2.1 (NSi(*C*H$_3$)$_3$), 28.1 (*C*H$_3$), 33.2 (*C*H$_2$), 59.4 (*C*CH$_3$), 178.9 (*C*O). — ^{29}Si NMR (99.4 MHz, CD_2Cl_2): δ = –1.1 (*Si*(CH$_3$)$_3$), 5.1 (N*Si*(CH$_3$)$_3$), 23.3 (O*Si*(CH$_3$)$_3$). — GC/EI-MS (pos.): t_R = 6.004 min (80/20); *m*/*z* (%) 318 (1) [M$^+$], 202 (100) [M$^+$ – COOSi(CH$_3$)$_3$], 114 (33) [COOSi(CH$_3$)$_3$], 73 (95) [$^+$Si(CH$_3$)$_3$].

Glycolic acid bis(trimethylsilyl) ester (**23**)

Glycolic acid (5.00 g, 65.7 mmol) was added in a single portion to HMDS (20 mL), and the mixture was heated under reflux for 3 h. The solvent was removed by distillation and the residue was distilled in vacuo to give a colorless liquid (b.p.: 80 °C/12 mbar). Yield: 14.1 g (63.8 mmol, 97%). — ^{1}H NMR (300.1 MHz, [D$_6$]DMSO): δ = –0.14 (s, 9 H, OSi(CH_3)$_3$), 0.18 (s, 9 H, OSi(CH_3)$_3$), 4.07 (s, 2 H, CH_2). — ^{13}C NMR (75.5 MHz, [D$_6$]DMSO): δ = –0.3 (OSi(*C*H$_3$)$_3$), 0.4 (OSi(*C*H$_3$)$_3$), 61.7 (*C*H$_2$), 172.0 (*C*O). — ^{29}Si NMR (59.6 MHz, [D$_6$]DMSO): δ = 20.1 (O*Si*(CH$_3$)$_3$), 24.4 (O*Si*(CH$_3$)$_3$).

Oxalic acid bis(trimethylsilyl) ester (**24**)

Oxalic acid (4.24 g, 47.1 mmol) was added in a single portion to HMDS (20 mL) and the mixture was heated under reflux for 3 h. After cooling at 22 °C, the resulting solid was isolated by filtration, washed with *n*-pentane (20 mL) and dried in vacuo (0.01 mbar, 22 °C, 5 h). Yield: 8.69 g (37.1 mmol, 79%); m.p.: 65 °C. — ^{1}H NMR (300.1 MHz, CD$_2$Cl$_2$): δ = 0.36 (s, 18 H, OSi(CH_3)$_3$). — ^{13}C NMR (75.5 MHz, CD$_2$Cl$_2$): δ = –0.5 (OSi(*C*H$_3$)$_3$), 158.6 (*C*O). ^{29}Si NMR (59.6 MHz, CD$_2$Cl$_2$): δ = 29.8 (O*Si*(CH$_3$)$_3$) [76].

Acetylacetone (**25**) was commercially available from Aldrich and was used without further purification.

Dibenzoylmethane (**26**) was commercially available from Aldrich and was used without further purification.

4-[(2-Hydroxyphenyl)amino]pent-3-en-2-one (**27**) was prepared according to ref. [77].

2-{*N*-[2-(Benzylamino)ethyl]ethanimidoyl}phenol (**28**)

N-Benzylethane-1,2-diamine (3.00 g, 20.0 mmol) was added at 22 °C to a stirred solution of 2-hydroxyphenylethanone (2.72 g, 20.0 mmol) in ethanol (20 mL), and the reaction mixture was heated under reflux for 4 h. After the mixture was cooled to 22 °C, it was concentrated to 10 mL and then kept undisturbed at –20 °C for 24 h. The resulting yellow solid was isolated by filtration, washed successively with *n*-pentane (2 × 10 mL) and diethyl ether (10 mL), and dried in vacuo (1.0 mbar, 22 °C, 5 h). Yield: 4.21 g (15.7 mmol, 79%); m.p.: 52 °C. — ^{1}H NMR (500 MHz, CD$_2$Cl$_2$): δ = 1.62 (br. s, 1 H, N*H*), 2.34 (t, ^{5}J(^{1}H,^{1}H) = 0.7 Hz, 3 H, CH_3),

3.01 (t, $^{3}J(^{1}H,^{1}H)$ = 6.2 Hz, 2 H, CH_2NCH_2C$_6$H$_5$), 3.68 (tq, $^{3}J(^{1}H,^{1}H)$ = 6.2 Hz, $^{5}J(^{1}H,^{1}H)$ = 0.7 Hz, 2 H, CH_2N=CCH$_3$), 3.86 (s, 2 H, CH$_2$NCH_2C$_6$H$_5$), 6.78 (1 H, *H*-4 (H_A), C$_6$H$_4$), 6.87 (1 H, *H*-6 (H_B), C$_6$H$_4$), 7.27 (1 H, *H*-5 (H_C), C$_6$H$_4$), and 7.55 (1 H, *H*-3 (H_D), C$_6$H$_4$) (ABCD system, ^{4}J(A,B) = 1.3 Hz, ^{3}J(A,C) = 7.0 Hz, ^{3}J(A,D) = 8.0 Hz, ^{3}J(B,C) = 8.3 Hz, ^{5}J(B,D) = 0.4 Hz, ^{4}J(C,D) = 1.7 Hz), 7.22–7.27 (m, 1 H, *H*-4, C$_6$H$_5$), 7.30–7.38 (m, 4 H, *H*-2/*H*-3/*H*-5/*H*-6, C$_6$H$_5$), 16.2 (br. s, 1 H, O*H*). — ^{13}C NMR (125.8 MHz, CD$_2$Cl$_2$): δ = 14.8 (*C*H$_3$), 49.7 (*C*H$_2$NCH$_2$C$_6$H$_5$), 50.1 (*C*H$_2$N=CCH$_3$), 54.1 (CH$_2$N*C*H$_2$C$_6$H$_5$), 117.2 (*C*-4, C$_6$H$_4$), 118.7 (*C*-6, C$_6$H$_4$), 119.9 (*C*-2, C$_6$H$_4$), 127.2 (*C*-4, C$_6$H$_5$), 128.4 (*C*-2/*C*-6, C$_6$H$_5$), 128.5 (*C*-3, C$_6$H$_4$), 128.7 (*C*-3/*C*-5, C$_6$H$_5$), 132.6 (*C*-5, C$_6$H$_4$), 141.1 (*C*-1, C$_6$H$_5$), 164.2 (*C*-1, C$_6$H$_4$), 172.7 (CH$_2$N=*C*CH$_3$). — ^{15}N NMR (30.4 MHz, CD$_2$Cl$_2$): δ = –343.3 (CH$_2$*N*CH$_2$C$_6$H$_5$), –109.8 (CH$_2$*N*=CCH$_3$). — ^{13}C VACP/MAS NMR: δ = 15.3 (*C*H$_3$), 49.3 (*C*H$_2$NCH$_2$C$_6$H$_5$), 50.2 (*C*H$_2$N=CCH$_3$), 52.4 (CH$_2$N*C*H$_2$C$_6$H$_5$), 116.6 (*C*-4, C$_6$H$_4$), 118.3 (*C*-6, C$_6$H$_4$), 119.0 (*C*-2, C$_6$H$_4$), 125.6, 127.0, 128.8, and 130.2 (*C*-2/*C*-6, C$_6$H$_5$; *C*-3/*C*-5, C$_6$H$_5$; *C*-4, C$_6$H$_5$; *C*-3, C$_6$H$_4$), 132.6 (*C*-5, C$_6$H$_4$), 142.3 (*C*-1, C$_6$H$_5$), 164.8 (*C*-1, C$_6$H$_4$), 172.1 (CH$_2$N=*C*CH$_3$). — ^{15}N VACP/MAS NMR: δ = –350.9 (CH$_2$*N*CH$_2$C$_6$H$_5$), –116.9 (CH$_2$*N*=CCH$_3$).

C$_{17}$H$_{20}$N$_2$O (268.36)	Calcd.:	C 76.09	H 7.51	N 10.44
	Found:	C 76.0	H 7.5	N 10.4

2-{*N*-[2-(Dimethylamino)ethyl]ethanimidoyl}phenol (29)

N,N-Dimethylethane-1,2-diamine (4.41 g, 50.0 mmol) was added at 22 °C to 2-hydroxyphenylethanone (6.81 g, 50.0 mmol), and the reaction mixture was then stirred at 22 °C for 1 h. The resulting yellow solid was isolated by filtration, washed successively with *n*-pentane (2 × 10 mL) and diethyl ether (2 × 10 mL), and dried in vacuo (1.0 mbar, 22 °C, 5 h). Yield: 8.33 g (40.4 mmol, 81%); m.p.: 36 °C. — ^{1}H NMR (500.1 MHz, CDCl$_3$): δ = 2.29 (s, 6 H, N(CH_3)$_2$), 2.32 (t, $^{5}J(^{1}H,^{1}H)$ = 0.7 Hz, 3 H, CH$_2$N=CCH_3), 2.67 (t, $^{3}J(^{1}H,^{1}H)$ = 7.0 Hz, 2 H, CH_2N(CH$_3$)$_2$), 3.63 (t, $^{3}J(^{1}H,^{1}H)$ = 7.0 Hz, 2 H, CH_2N=CCH$_3$), 6.72 (1 H, *H*-4 (H_A), C$_6$H$_4$), 6.89 (1 H, *H*-6 (H_B), C$_6$H$_4$), 7.24 (1 H, *H*-5 (H_C), C$_6$H$_4$), and 7.47 (1 H, *H*-3 (H_D), C$_6$H$_4$) (ABCD system, ^{4}J(A,B) = 1.3 Hz, ^{3}J(A,C) = 7.0 Hz, ^{3}J(A,D) = 8.1 Hz, ^{3}J(B,C) = 8.3 Hz, ^{5}J(B,D) not resolved, ^{4}J(C,D) = 1.7 Hz), 16.4 (br. s, 1 H, O*H*). — ^{13}C NMR (125.8 MHz, CDCl$_3$): δ = 14.4 (CH$_2$N=C*C*H$_3$), 45.8 (N(*C*H$_3$)$_2$), 47.8 (*C*H$_2$N=CCH$_3$), 59.6 (*C*H$_2$N(CH$_3$)$_2$), 116.8 (*C*-4, C$_6$H$_4$), 118.9 (*C*-6, C$_6$H$_4$), 119.1 (*C*-2, C$_6$H$_4$), 127.9 (*C*-3, C$_6$H$_4$), 132.4 (*C*-5, C$_6$H$_4$), 164.3 (*C*-1, C$_6$H$_4$), 171.8 (CH$_2$N=*C*CH$_3$). — ^{15}N NMR (30.4 MHz, CDCl$_3$): δ = –356.8 (*N*(CH$_3$)$_2$), –114.4 (CH$_2$*N*=CCH$_3$). — ^{13}C VACP/MAS NMR: δ = 11.5 (CH$_2$N=C*C*H$_3$), 46.0 (*C*H$_2$N=CCH$_3$), 47.4 (N(*C*H$_3$)$_2$), 60.6 (*C*H$_2$N(CH$_3$)$_2$), 114.8 (*C*-4, C$_6$H$_4$), 118.2 (*C*-2, C$_6$H$_4$),

120.2 (*C*-6, C_6H_4), 127.6 (*C*-3, C_6H_4), 132.1 (*C*-5, C_6H_4), 166.6 (*C*-1, C_6H_4), 170.9 (CH_2N=*C*CH_3). — ^{15}N VACP/MAS NMR: δ = –352.8 ($N(CH_3)_2$), (CH_2N=CCH_3) not detected (the sample became liquid under the MAS conditions, before the ^{15}N resonace signal of the CH_2N=CCH_3 moiety could be detected).

$C_{12}H_{18}N_2O$ (206.29)	Calcd.:	C 69.87	H 8.79	N 13.58
	Found:	C 69.7	H 9.0	N 13.6

4-{[2-(Dimethylamino)ethyl]amino}pent-3-en-2-one (**30**)

N,N-Dimethylethane-1,2-diamine (4.00 g, 45.4 mmol) was added dropwise at 0 °C to acetylacetone (4.54 g, 45.5 mmol), and the reaction mixture was then stirred at 0 °C for 10 min. After the solution was warmed to 22 °C, the reaction mixture was stirred at this temperature for further 2 d. The resulting brownish solution was distilled in vacuo (b.p.: 153 °C/24 mbar). Yield: 5.88 g (34.6 mmol, 76%). — ^{1}H NMR (400.1 MHz, [D$_6$]DMSO): δ = 1.94 (s, 3 H, CH_3), 2.10 (s, 3 H, CH_3), 2.17 (t, 1 H, N*H*), 2.65 (s, 6 H, N(CH_3)$_2$), 3.08 (t, ^3J(^{1}H,^{1}H) = 6.4 Hz, 2 H, CH_2N(CH$_3$)$_2$), 3.67 (t, ^3J(^{1}H,^{1}H) = 6.3 Hz, 2 H, CH_2N=CCH$_3$), 5.40 (br. s, 1 H, C*H*). — ^{13}C NMR (100.6 MHz, [D$_6$]DMSO): δ = 18.5 (*C*H$_3$), 28.4 (*C*H$_3$), 40.1 (*C*H$_2$N=CCH$_3$), 44.9 (N(*C*H$_3$)$_2$), 58.2 (*C*H$_2$N(CH$_3$)$_2$), 94.4 (*C*H), 162.4 (CH$_2$N=*C*CH$_3$), 192.4 (*C*O). — ^{15}N NMR (30.4 MHz, [D$_6$]DMSO): δ = –354.8 (*N*(CH$_3$)$_2$), –187.2 (CH$_2$*N*=CCH$_3$).

$C_9H_{18}N_2O$ (170.14)	Calcd.:	C 63.49	H 10.66	N 16.45
	Found:	C 63.6	H 10.4	N 16.2

4,4′-(Ethane-1,2-diyldiimino)bis(pent-3-en-2-one) (**31**) was prepared according to ref. [62].

2-[({2-[(2-Hydroxybenzylidene)amino]ethyl}imino)methyl]phenol (**32**) was prepared according to ref. [81].

Bis[acetylacetonato(1–)-*O*,*O*′](cyanato-*N*)phenylsilicon(IV) (**33**)

Acetylacetone (1.12 g, 11.2 mmol) was added at 22 °C to a stirred solution of tri(cyanato-*N*)phenylsilane (1.30 g, 5.62 mmol) in THF (20 mL), the mixture was stirred at 22 °C for 1 h and *n*-pentane (20 mL) was carefully added. The reaction mixture was kept then undisturbed at –20 °C for 3 d. The resulting solid was isolated by filtration, washed with *n*-pentane (3 × 10 mL), and dried in vacuo (0.6 mbar, 22 °C, 6 h). Yield: 1.43 g (4.13 mmol, 74%); m.p.: 174 °C. — ^{1}H NMR (500.1 MHz, [D$_6$]DMSO): δ = 1.94 (s, 3 H, CH_3), 2.08 (s, 3 H, CH_3), 2.09 (s, 3 H, CH_3), 2.13 (s, 3 H, CH_3), 5.81 (s, 1 H, C*H*), 6.04 (s, 1 H, C*H*), 7.05–7.08 (m, *H*-4, C_6H_5),

7.11−7.15 (m, *H*-3/*H*-5, C_6H_5), 7.43−7.45 (m, *H*-2/*H*-6, C_6H_5). — ^{13}C NMR (125.8 MHz, [D$_6$]DMSO): δ = 25.2 (*C*H$_3$), 25.4 (*C*H$_3$), 25.5 (*C*H$_3$), 25.6 (*C*H$_3$), 101.7 (*C*H), 102.1 (*C*H), 120.6 (N*C*O), 125.8 (*C*-4, C_6H_5), 126.2 (*C*-3/*C*-5, C_6H_5), 133.0 (*C*-2/*C*-6, C_6H_5), 152.7 (*C*-1, C_6H_5), 191.1 (*C*O), 191.4 (*C*O), 191.5 (*C*O), 191.6 (*C*O). — ^{29}Si NMR (99.4 MHz, [D$_6$]DMSO): δ = –184.5. — ^{13}C VACP/MAS NMR: δ = 24.9 (*C*H$_3$), 25.7 (*C*H$_3$), 26.5 (*C*H$_3$), 27.3 (*C*H$_3$), 101.0 (*C*H), 102.4 (*C*H), 122.2 (N*C*O), 127.5 (*C*-4, *C*-3/*C*-5, C_6H_5), 134.6 (*C*-2, C_6H_5), 135.3 (*C*-6, C_6H_5), 155.6 (*C*-1, C_6H_5), 191.6 (*C*O), 192.9 (*C*O). — ^{15}N VACP/MAS NMR: δ = –319.1 (*N*CO). — ^{29}Si VACP/MAS NMR: δ = –185.1.

$C_{17}H_{19}NO_5Si$ (345.40)	Calcd.:	C 59.12	H 5.54	N 4.05
	Found:	C 58.9	H 5.4	N 4.0

(Cyanato-*N*)bis[1,3-diphenylpropan-1,3-dionato(1–)-*O*,*O′*]phenylsilicon(IV) (34)

Tri(cyanato-*N*)phenylsilane (578 mg, 2.50 mmol) was added at 22 °C to a stirred solution of dibenzoylmethane (1.12 g, 5.00 mmol) in acetonitrile (15 mL), and the mixture was stirred at 22 °C for 1 h. After that, *n*-pentane (15 mL) was carefully added, and the mixture was kept undisturbed at 22 °C for 10 d. The resulting yellowish solid was filtered off, washed with diethyl ether (30 mL) and dried in vacuo (1.3 mbar, 22 °C, 5 h). Yield: 1.16 g (1.95 mmol, 78%); m.p.: 261°C (decomp.). — ^{1}H NMR (500.1 MHz, [D$_6$]DMSO): δ = 7.35 (s, 2 H, C*H*), 6.87−8.46 (m, 25 H, C*H*, C_6H_5). — ^{13}C NMR (125.8 MHz, [D$_6$]DMSO): δ = 93.3 (2 *C*H), 127.4, 128.8, and 133.0 (3 *C*H, C_6H_5), 134.6 (*C*-1, C_6H_5), 185.3 (*C*O), N*C*O could not be detected. — ^{29}Si NMR (99.4 MHz, [D$_6$]DMSO): δ = –178.4. — ^{13}C VACP/MAS NMR: δ = 92.7 (*C*H), 94.2 (*C*H), 122.5 (N*C*O), 124.9−136.8 (15 *C*H, C_6H_5), 154.2 (*C*-1, C_6H_5), 181.2 (*C*O), 182.9 (*C*O). — ^{15}N VACP/MAS NMR: δ = –312.3 (*N*CO). — ^{29}Si VACP/MAS NMR: δ = –184.6.

$C_{37}H_{27}NO_5Si$ (593.71)	Calcd.:	C 74.85	H 4.58	N 2.36
	Found:	C 74.6	H 4.6	N 2.6

Bis[acetylacetonato(1–)-*O*,*O′*][glycolato(2–)-*O*^{1},*O*^{2}]silicon(IV) (35)

Compound **23** (551 mg, 2.50 mmol) was added in a single portion to a stirred solution of *cis*-bis[acetylacetonato(1–)-*O*,*O′*]di(cyanato-*N*)silicon(IV) (776 mg, 2.50 mmol) in THF (20 mL) at 22 °C, and the mixture was stirred at 22 °C for 2 d. *n*-Pentane (15 mL) was carefully added and the mixture was kept undisturbed at 22 °C for 3 d. The resulting colorless solid was filtered off, washed with *n*-pentane (20 mL) and dried in vacuo (1.3 mbar, 22 °C, 6 h). Yield: 658 mg (2.19 mmol, 88%); m.p.: 201 °C (decomp.). — ^{1}H NMR (500.1 MHz, $CDCl_3$): δ =

2.04 (s, 3 H, CH_3), 2.06 (s, 3 H, CH_3), 2.12 (s, 3 H, CH_3), 2.13 (s, 3 H, CH_3), 4.08−4.18 (dd, 2 H, C$H_A H_B$), 5.73 (s, 1 H, C*H*), 5.74 (s, 1 H, C*H*). — ^{13}C NMR (125.8 MHz, $CDCl_3$): δ = 25.4 (*C*H_3), 25.5 (*C*H_3), 25.9 (*C*H_3), 26.0 (*C*H_3), 63.3 (*C*H_2), 102.2 (*C*H), 102.4 (*C*H), 175.9 (CH_2*C*(O)O), 189.5 (*C*O), 190.7 (*C*O), 193.6 (*C*O), 193.7 (*C*O). — ^{29}Si NMR (99.4 MHz, $CDCl_3$): δ = –174.3. — ^{13}C VACP/MAS NMR: δ = 25.6 (*C*H_3), 26.7 (*C*H_3), 27.4 (*C*H_3), 27.8 (*C*H_3), 64.2 (*C*H_2), 102.8 (2 *C*H), 175.9 (CH_2*C*(O)O), 191.4 (2 *C*O), 193.7 (*C*O), 194.8 (*C*O). — ^{29}Si VACP/MAS NMR: δ = –174.8.

$C_{12}H_{16}O_7Si$ (300.34)	Calcd.:	C 47.99	H 5.37
	Found:	C 47.7	H 5.2

Bis[acetylacetonato(1–)-*O*,*O*′][oxalato(2–)-O^1,O^2]silicon(IV) (36)

Compound **24** (586 mg, 2.50 mmol) was added at 22 °C to a stirred solution of *cis*-bis[acetylacetonato(1–)-*O*,*O*′]di(cyanato-*N*)silicon(IV) (776 mg, 2.50 mmol) in THF (20 mL). The resulting mixture was stirred at 22 °C for 1 h, and then kept undisturbed at 22 °C for 3 d. The resulting solid was washed with *n*-pentane (3 × 10 mL) and dried in vacuo (0.6 mbar, 22 °C, 5 h). Yield: 531 mg (1.69 mmol, 68%); m.p.: 255 °C. — ^{1}H NMR (500.1 MHz, CD_2Cl_2): δ = 2.16 (s, 6 H, CH_3), 2.19 (s, 6 H, CH_3), 5.93 (s, 2 H, C*H*). — ^{13}C NMR (125.8 MHz, CD_2Cl_2): δ = 25.8 (*C*H_3), 26.2 (*C*H_3), 103.4 (*C*H), 159.2 (O*C*O), 192.2 (*C*O), 195.3 (*C*O). — ^{29}Si NMR (99.4 MHz, CD_2Cl_2): δ = –186.6. — ^{13}C VACP/MAS NMR: δ = 25.5 (*C*H_3), 25.9 (*C*H_3), 26.2 (*C*H_3), 26.6 (*C*H_3), 102.5 (*C*H), 104.7 (*C*H), 159.5 (O*C*O), 192.8 (*C*O), 194.6 (*C*O), 195.1 (*C*O), 195.2 (*C*O). — ^{29}Si VACP/MAS NMR: δ = –187.2.

$C_{12}H_{14}O_8Si$ (314.32)	Calcd.:	C 45.85	H 4.49
	Found:	C 45.3	H 4.4

[Alaninato(1–)-*N*,*O*][alaninato(2–)-*N*,*O*]methylsilicon(IV) (38)

Trimethylsilyl (*S*)-*N*-(trimethylsilyl)alaninate (1.17 g, 5.01 mmol) was added in a single portion at −70 °C to a stirred solution of tri(cyanato-*N*)methylsilane (423 mg, 2.50 mmol) in acetonitrile (10 mL), and the mixture was then kept undisturbed at −20 °C for 3 d. The resulting colorless crystalline solid was isolated by filtration, washed with cold *n*-pentane (3 × 10 mL), and dried in vacuo (0.8 mbar, 22 °C, 24 h). Yield: 306 mg (1.40 mmol, 56%); m.p. >288 °C (decomp.). — ^{13}C VACP/MAS NMR: δ = 4.6 (Si*C*H_3), 16.9 (C*C*H_3), 22.7 (C*C*H_3), 50.1 (asymmetric “d”, *C*H) [45, 46, 47], 52.3 (asymmetric “d”, *C*H) [45, 46, 47], 176.1 (*C*O), 180.0 (*C*O). — ^{15}N VACP/MAS NMR: δ = –325.8 (*N*H or *N*H_2), –324.1 (*N*H or *N*H_2). — ^{29}Si VACP/MAS NMR: δ = –84.4 ppm (asymmetric “d”) [46, 47, 48].

$C_7H_{14}N_2O_4Si$ (218.29)	Calcd.:	C 38.52	H 6.46	N 12.83
	Found:	C 38.5	H 6.4	N 12.8

[Phenylalaninato(1–)-*N*,*O*][phenylalaninato(2–)-*N*,*O*]methylsilicon(IV) (39)

Trimethylsilyl (*S*)-*N*-(trimethylsilyl)phenylalaninate (1.51 g, 4.88 mmol) was added in a single portion at −30 °C to a solution of tri(cyanato-*N*)methylsilane (413 mg, 2.44 mmol) in acetonitrile (10 mL), and the mixture was then kept undisturbed at −20 °C for 10 d. The resulting colorless crystalline solid was isolated by filtration, washed with cold *n*-pentane (2 × 10 mL), and dried in vacuo (0.1 mbar, 60 °C, 8 h). Yield: 429 mg (1.16 mmol, 48%); m.p. >368°C (decomp.). The following NMR data refer to two crystallographically independent molecules: — ^{13}C VACP/MAS NMR: δ = 1.8 (Si*C*H$_3$), 34.7 (*C*H$_2$), 38.2 (*C*H$_2$), 43.1 (*C*H$_2$), 45.7 (*C*H$_2$), 54.6 (br. asymmetric "d", *C*H) [45, 46, 47], 56.0 (br. asymmetric "d", *C*H) [45, 46, 47], 57.1 (br. asymmetric "d", *C*H) [45, 46, 47], 59.5 (br. asymmetric "d", *C*H) [45, 46, 47], 126.1, 126.5, 127.3, 127.6, 128.8, 129.5, 130.4, 131.4, 135.3, 135.7, 136.6, and 139.1 (C_6H_5), 172.4 (*C*O), 173.3 (*C*O), 179.0 (2 *C*O). — ^{15}N VACP/MAS NMR: δ = –332.2 (2 N, *N*H or *N*H$_2$), –323.1 (*N*H or *N*H$_2$), –321.2 (*N*H or *N*H$_2$). — ^{29}Si VACP/MAS NMR: δ = –87.9 (br. asymmetric "d") [45, 46, 47], –85.5 (br. asymmetric "d") [46, 47, 48].

$C_{19}H_{22}N_2O_4Si$ (370.48)	Calcd.:	C 61.60	H 5.99	N 7.56
	Found:	C 61.3	H 6.0	N 7.7

[Alaninato(1–)-*N*,*O*][alaninato(2–)-*N*,*O*]phenylsilicon(IV)−acetonitrile (43·CH$_3$CN)

Trimethylsilyl (*S*)-*N*-(trimethylsilyl)alaninate (1.17 g, 5.01 mmol) was added in a single portion at −70 °C to a solution of tri(cyanato-*N*)phenylsilane (578 mg, 2.50 mmol) in acetonitrile (10 mL), and the mixture was then kept undisturbed at −20 °C for 3 d. The resulting colorless crystalline solid was isolated by filtration, washed with cold *n*-pentane (2 × 10 mL), and dried in vacuo (0.1 mbar, 60 °C, 8 h). Yield: 240 mg (856 µmol, 34%); m.p. >360°C (decomp.). — ^{13}C VACP/MAS NMR: δ = 15.5 (*C*H$_3$), 22.1 (*C*H$_3$), 50.3 (br. asymmetric "d", *C*H) [[45, 46, 47], 52.7 (asymmetric "d", *C*H [45, 46, 47]), 128.2, 130.6, and 138.5 (C_6H_5), 173.9 (*C*O), 177.4 (*C*O). — ^{15}N VACP/MAS NMR: δ = –323.2 (*N*H or *N*H$_2$), –320.3 (*N*H or *N*H$_2$). — ^{29}Si VACP/MAS NMR: δ = –96.0 (br. asymmetric "d") [46, 47, 48].

$C_{12}H_{16}N_2O_4Si$ (280.36)	Calcd.:	C 51.41	H 5.75	N 9.99
	Found:	C 50.7	H 5.7	N 9.7 [82]

[Phenylalaninato(1–)-*N*,*O*][phenylalaninato(2–)-*N*,*O*]phenylsilicon(IV) (44)

Trimethylsilyl (*S*)-*N*-(trimethylsilyl)phenylalaninate (1.58 g, 5.10 mmol) was added in a single portion at −70 °C to a stirred solution of tri(cyanato-*N*)phenylsilane (590 mg, 2.55 mmol) in acetonitrile (11 mL), and the mixture was then kept undisturbed at −20 °C for 3 d. The resulting colorless crystalline solid was isolated by filtration, washed with cold *n*-pentane (3 × 10 mL), and dried in vacuo (0.8 mbar, 22 °C, 24 h). Yield: 628 mg (1.45 mmol, 57%); m. p.: >320 °C (decomp.). The following solution-state NMR data refer to two isomers (**A** and **B**; molar ratio **A**:**B**, ca. 1:1.3): — ^{1}H NMR (500.1 MHz, [D$_6$]DMSO; *c*, 72 mM): δ = 2.51−3.24 (m, $\sum$ = 4 H; C*H*$_2$), 2.89 (**A**) and 2.95 (**B**) (d, $^{3}J \approx$ 1.7 Hz, $\sum$ = 1 H; N*H*), 3.53−3.94 (m, $\sum$ = 2 H; C*H*), 5.11 (t, *J* = 11.0 Hz, *J* = 11.0 Hz, **B**) and 5.50 (dd, *J* = 12.0 Hz, *J* = 9.2 Hz, **A**) and 6.05−6.11 (m, **A**/**B**) ($\sum$ = 2 H; N*H*$_2$), 7.14−7.43 (m, $\sum$ = 15 H; C$_6$*H*$_5$). — ^{13}C NMR (125.8 MHz, [D$_6$]DMSO; *c*, 72 mM): δ = 34.9/41.54 (*C*H$_2$, **B**), 36.1/41.48 (*C*H$_2$, **A**), 54.4/57.2 (*C*H, **A**), 55.4/56.7 (CH, **B**), 126.2, 126.3, 126.6, 126.7, 126.8, 127.5, 127.6, 128.07, 128.09, 128.26, 128.33, 128.36, 128.44, 128.6, 128.7, 129.1, 129.15, 129.18, 129.4, 129.5, 131.8, 132.6, 136.6, 138.4, 137.3, 138.3, 138.6, and 139.6 (**A**/**B**, *C*$_6$H$_5$), 170.5/174.4 (*C*O, **B**), 171.2/174.5 (*C*O, **A**). — ^{15}N NMR (50.7 MHz, [D$_6$]DMSO; *c*, 72 mM): δ = –340.5 (*N*H, **B**), –337.4 (*N*H, **A**), –327.9 (*N*H$_2$, **B**), –326.8 (*N*H$_2$, **A**). — ^{29}Si NMR (99.4 MHz, [D$_6$]DMSO; *c*, 72 mM): δ = –99.1 (**B**), –97.7 (**A**). — ^{13}C VACP/MAS NMR: δ = 32.9 (*C*H$_2$), 40.1 (*C*H$_2$), 54.2 (br. asymmetric "d", *C*H) [45, 46, 47], 57.9 (asymmetric "d", *C*H) [45, 46, 47], 127.3, 127.6, 127.8, 128.4, 129.2, 130.2, 130.6, 133.0, 134.7, and 137.7 (*C*$_6$H$_5$), 168.9 (*C*O), 181.2 (*C*O). — ^{15}N VACP/MAS NMR: δ = –334.0 (*N*H), –324.4 (*N*H$_2$). — ^{29}Si VACP/MAS NMR: δ = –98.5 (br. asymmetric "d") [46, 47, 48].

$C_{24}H_{24}N_2O_4Si$ (432.54)	Calcd.:	C 66.64	H 5.59	N 6.48
	Found:	C 66.3	H 5.5	N 6.6

[Valinato(1–)-*N*,*O*][valinato(2–)-*N*,*O*]phenylsilicon(IV) (45)

Trimethylsilyl *N*-(trimethylsilyl)valinate (1.34 mg, 5.10 mmol) was added at 22 °C to a stirred solution of tri(cyanato-*N*)phenylsilane (590 mg, 2.55 mmol) in acetonitrile (5 mL). The reaction mixture was kept for 20 min. at –30 °C and then kept undisturbed at –20 °C for 3 d. The resulting colorless solid was isolated by filtration, washed twice with *n*-pentane (10 mL), and dried in vacuo (0.2 mbar, 22 °C, 2 h). Yield: 694 mg (2.06 mmol, 81%); m.p.: 208 °C (decomp.). The following ^{29}Si NMR solution-state data refer to two isomers (**A** and **B**; molar ratio **A**:**B**, ca. 1:0.9). The following ^{1}H NMR and ^{13}C NMR solution-state data refer to the major isomer **45A**: — ^{1}H NMR (300.1 MHz, [D$_6$]DMSO): δ = 0.37–1.05 (m, 12 H, C*H*$_3$),

1.88–2.03 (m, 2 H, C*H*(CH_3)$_2$), 3.27–3.65 (m, 2 H, C*H*), 4.57–5.31 (m, 1 H, N*H*), 5.47–7.03 (m, 2 H, NH_2), 7.24–7.83 (m, 5 H, C_6H_5). — ^{13}C NMR (75.5 MHz, [D_6]DMSO): δ = 15.6 (*C*H_3), 16.8 (*C*H_3), 18.5 (*C*H_3), 19.6 (*C*H_3), 28.4 (*C*H(CH_3)$_2$), 31.4 (*C*H(CH_3)$_2$), 58.4 (*C*H), 61.1 (*C*H), 126.4−135.0 (*C*H, C_6H_5), 136.5 (*C*-1, C_6H_5), 171.1 (*C*O), 174.7 (*C*O). — ^{29}Si NMR (59.6 MHz, [D_6]DMSO): δ = –98.2 (**B**), –97.8 (**A**). — ^{13}C VACP/MAS NMR: δ = 14.8 (*C*H_3), 16.8 (*C*H_3), 19.2 (*C*H_3), 22.6 (*C*H_3), 28.9 (*C*H(CH_3)$_2$), 31.8 (*C*H(CH_3)$_2$), 59.2 (*C*H), 61.9 (*C*H), 125.0–135.0 (*C*H, C_6H_5), 137.6 (*C*-1), 175.9 (*C*O), 176.9 (*C*O). — ^{15}N VACP/MAS NMR: δ = –342.2 (*N*H or *N*H_2), –330.1 (*N*H or *N*H_2). — ^{29}Si VACP/MAS NMR: δ = –93.6.

$C_{16}H_{24}N_2O_4Si$ (336.46)	Calcd.:	C 57.12	H 7.19	N 8.33
	Found:	C 57.0	H 6.9	N 8.6

[*tert*-Leucinato(1–)-*N*,*O*][*tert*-leucinato(2–)-*N*,*O*]phenylsilicon(IV)−*n*-pentane hemiacetonitrile (46·C_5H_{12}·1/2CH_3CN)

Trimethylsilyl (*S*)-*N*-trimethylsilyl)leucinate (1.50 g, 5.44 mmol) was added in a single portion at –45 °C to a stirred solution of tri(cyanato-*N*)phenylsilane (610 mg, 2.64 mmol) in acetonitrile (20 mL). The reaction mixture was kept for 5 min. at –45 °C, then layered with *n*-pentane (15 mL), and kept undisturbed at –20 °C for 20 d. The resulting colorless solid was isolated by filtration, washed with *n*-pentane (2 × 10 mL), and dried in vacuo (0.8 mbar, 60 °C, 14 h). Yield: 468 mg (1.28 mmol, 49%); m.p.: 241 °C (subl.). — ^{13}C VACP/MAS NMR: δ = 28.2 (C(*C*H_3)$_3$), 34.8 (*C*(CH_3)$_3$), 37.4 (*C*(CH_3)$_3$), 65.8 (br. asymmetric "d", *C*H) [45, 46, 47], 128.4, 129.0, 130.8, 137.3, and 138.7 (C_6H_5), 171.6 (*C*O), 179.4 (*C*O), resonance signals for *n*-pentane and acetonitrile not detected. — ^{15}N VACP/MAS NMR: δ = –339.2 (*N*H or *N*H_2), –328.8 (*N*H or *N*H_2). — ^{29}Si VACP/MAS NMR: δ = –92.3 (br. "s") [46, 47, 48].

$C_{18}H_{28}N_2O_4Si$ (364.52)	Calcd.:	C 59.31	H 7.74	N 7.69
	Found:	C 58.7	H 7.8	N 7.7 [82]

{*α*-[(trimethylsilyl)methyl]alaninato(1−)-*N*,*O*}{*α*-[(trimethylsilyl)methyl]alaninato(2−)-*N*,*O* }methylsilicon(IV) (47)

Compound **22** (363 mg, 1.13 mmol) was added at –60 °C to a solution of tri(cyanato-*N*)methylsilane (95.0 mg, 0.56 mmol) in acetonitrile (20 mL). The reaction mixture was kept 10 min at –60 °C, and then kept undisturbed at –20 °C for 3 d. The resulting colorless solid was isolated by filtration, washed with *n*-pentane (10 mL), and dried in vacuo (0.8 mbar, 22 °C, 5 h). Yield: 106 mg (0.27 mmol, 49%); m.p.: 245 °C (decomp.). — ^{13}C VACP/MAS

NMR: δ = 0.7, 1.1 (Si(*C*H$_3$)$_3$), 6.5 (Si*C*H$_3$), 28.1 (2 C*C*H$_3$), 36.6 (2 *C*H$_2$), 59.2 (*C*CH$_3$), 61.5 (*C*CH$_3$), 172.6 (*C*O), 182.5 (*C*O). — ^{15}N VACP/MAS NMR: δ = –293.1 (*N*H or *N*H$_2$), –312.3 (*N*H or *N*H$_2$). — ^{29}Si VACP/MAS NMR: δ = –93.5 (*Si*CH$_3$), –1.1 (*Si*(CH$_3$)$_3$), –0.3 (*Si*(CH$_3$)$_3$).

$C_{15}H_{34}N_2O_4Si_3$ (390.70)	Calcd.:	C 46.11	H 8.77	N 7.17
	Found:	C 45.6	H 8.4	N 6.9

{*α*-[(trimethylsilyl)methyl]alaninato(1−)-*N*,*O*}{*α*-[(trimethylsilyl)methyl]alaninato(2−)-*N*,*O* }phenylsilicon(IV) (48)

Compound **22** (267 mg, 0.84 mmol) was added at –60 °C to a solution of tri(cyanato-*N*)phenylsilane (96.0 mg, 0.41 mmol) in acetonitrile (5 mL). The reaction mixture was kept 10 min at –40 °C, and then kept undisturbed at –20 °C for 24 h. The resulting colorless solid was isolated by filtration, washed with *n*-pentane (10 mL), and dried in vacuo (0.8 mbar, 22 °C, 5 h). Yield: 109 mg (0.24 mmol, 59%); m.p.: 265 °C (decomp.). — ^{13}C VACP/MAS NMR: δ = –0.6, –0.2 (Si(*C*H$_3$)$_3$), 25.7 (*C*H$_3$), 28.6 (C*C*H$_3$), 36.7 (2 *C*H$_2$), 59.2, 61.2 (*C*CH$_3$), 127.5, 130.2, 134.2, 137.8, 138.5, 140.2 (C$_6$H$_5$), 173.6 (*C*O), 182.5 (*C*O). — ^{15}N VACP/MAS NMR: δ = –314.2 (*N*H or *N*H$_2$), –312.1 (*N*H or *N*H$_2$). — ^{29}Si VACP/MAS NMR: δ = –104.2 (*Si*C$_6$H$_5$), –2.2 (*Si*(CH$_3$)$_3$), –1.5 (*Si*(CH$_3$)$_3$).

$C_{20}H_{36}N_2O_4Si_3$ (452.77)	Calcd.:	C 53.05	H 8.01	N 6.19
	Found:	C 52.8	H 8.4	N 5.9

Bis(cyanato-*N*)bis[glycinato(1–)-*N*,*O*]silicon(IV) (49)

Trimethylsilyl (*S*)-*N*-(trimethylsilyl)glycinate (1.09 g, 5.00 mmol) was added in a single portion at −50 °C to a stirred solution of tetra(cyanato-*N*)silane (490 mg, 2.50 mmol) in acetonitrile (40 mL), and the mixture was kept undisturbed at −20 °C for 4 d. The resulting colorless solid was isolated by filtration, washed with cold *n*-pentane (3 × 10 mL), and dried in vacuo (0.8 mbar, 22 °C, 10 h). Yield: 361 mg (1.40 mmol, 56%); m.p.: >220 °C (decomp.). — ^{1}H NMR (300.1 MHz, [D$_6$]DMSO): δ = 3.21−3.41 (m, 4 H, C*H*$_2$), 6.79−7.15 (m, 4 H, N*H*$_2$). — ^{13}C NMR (75.5 MHz, [D$_6$]DMSO): δ = 42.1 (*C*H$_2$), 118.8 (d, 2 N*C*O), 168.3 (*C*O). — ^{29}Si NMR (59.6 MHz, [D$_6$]DMSO): δ = –186.9. — ^{13}C VACP/MAS NMR: δ = 42.2 (*C*H$_2$), 120.4 (br. “d”, slightly structured, (due to due to ^{14}N coupling), N*C*O), 175.4 (*C*O). — ^{15}N VACP/MAS NMR: δ = –330.6 (*N*H$_2$), –321.0 (*N*CO). — ^{29}Si VACP/MAS NMR: δ = –184.5 (br. “s”, slightly structured, (due to ^{14}N coupling)) [46, 47, 48].

$C_6H_8N_4O_6Si$ (260.24)	Calcd.:	C 27.69	H 3.09	N 21.53
	Found:	C 27.4	H 3.4	N 20.9

Bis[alaninato(1–)-*N,O*]bis(cyanato-*N*)silicon(IV) (50)

Trimethylsilyl (*S*)-*N*-(trimethylsilyl)alaninate (1.17 g, 5.01 mmol) was added in a single portion at −70 °C to a stirred solution of tetra(cyanato-*N*)silane (490 mg, 2.50 mmol) in acetonitrile (15 mL), and the mixture was then kept undisturbed at −20 °C for 3 d. The resulting colorless crystalline solid was isolated by filtration, washed with cold *n*-pentane (3 × 10 mL), and dried in vacuo (0.8 mbar, 20 °C, 6 h). Yield: 365 mg (1.27 mmol, 51%); m.p. >230 °C (decomp.). The following solution-state NMR data refer to two isomers (**A** and **B**; molar ratio **A**:**B**, ca. 1:1): — ^{1}H NMR (500.1 MHz, [D$_6$]DMSO; *c*, 20 mM): δ = 1.32/1.33 (d, 6 H, ^{3}J(H,H) = 7.3 Hz; C*H*$_3$), 3.48−3.57/3.57−3.66 (m, 2 H, C*H*), 6.58−6.69 and 7.10−7.28 (m, 4 H, N*H*$_2$). — ^{13}C NMR (125.8 MHz, [D$_6$]DMSO; *c*, 20 mM): δ = 16.4/16.8 (*C*H$_3$), 49.81/49.83 (*C*H), 118.7 (br. "s", N*C*O), 171.2/171.4 (*C*O). — ^{15}N NMR (30.4 MHz, [D$_6$]DMSO; *c*, 20 mM)): δ = –322.0 (*N*H$_2$, ^{15}N signals for the two isomers not resolved), ^{15}N signals for the NCO moieties not detected. — ^{29}Si NMR (99.4 MHz, [D$_6$]DMSO; *c*, 20 mM): δ = –191.9/–191.8. — ^{13}C VACP/MAS NMR: δ = 18.7 (*C*H$_3$), 51.0 (asymmetric "d", *C*H) [45, 46, 47], 122.8 (br. "d", N*C*O) [45, 46, 47], 177.0 (*C*O). — ^{15}N VACP/MAS NMR: δ = –315.9 (*N*CO), –314.2 (*N*H$_2$). — ^{29}Si VACP/MAS NMR: δ = –187.4 (br. "s") [46, 47, 48].

$C_8H_{12}N_4O_6Si$ (288.29)	Calcd.:	C 33.33	H 4.20	N 19.43
	Found:	C 33.5	H 4.3	N 19.3

Bis(cyanato-*N*)bis[valinato(1–)-*N,O*]silicon(IV) (52)

Trimethylsilyl (*S*)-*N*-(trimethylsilyl)valinate (1.51 g, 5.77 mmol) was added at 22 °C in a single portion to a stirred solution of tetra(cyanato-*N*)silane (490 mg, 2.50 mmol) in acetonitrile (20 mL), and the mixture was kept undisturbed at –20 °C for 6 d. The reaction mixture was allowed to warm to 22 °C, and then layered with *n*-pentane (20 mL). After 4 d at –20 °C, another portion of trimethylsilyl (*S*)-*N*-(trimethylsilyl)valinate (1.30 g, 4.97 mmol) was added to the reaction mixture. After further 14 d at –20 °C, the resulting colorless solid was isolated by filtration, washed twice with *n*-pentane (10 mL), and dried in vacuo (0.2 mbar, 22 °C, 14 h). Yield: 794 mg (2.31 mmol, 92%); m.p.: 368–400 °C (decomp.). — ^{13}C VACP/MAS NMR: δ = 15.9 (*C*H$_3$), 17.5 (*C*H$_3$), 19.2 (*C*H$_3$), 19.9 (*C*H$_3$), 29.4 (*C*H(CH$_3$)$_2$), 31.8 (*C*H(CH$_3$)$_2$), 61.1 (br "s", 2 *C*H), 121.6 (N*C*O), 124.0 (N*C*O), 170.6 (*C*O), 176.1 (*C*O). — ^{15}N VACP/MAS NMR: δ = –338.2 (*N*H$_2$ or *N*H or *N*CO), –334.5 (*N*H$_2$ or *N*H or *N*CO), –327.5 (2 N, *N*H$_2$ or *N*H or *N*CO). — ^{29}Si VACP/MAS NMR: δ = –189.5 (br "s", slightly structured, (due to the ^{14}N coupling)) [46, 47, 48].

$C_{12}H_{20}N_4O_6Si$ (344.40)	Calcd.:	C 41.85	H 5.85	N 16.27
	Found:	C 41.2	H 5.3	N 15.8

Bis(cyanato-*N*)bis[*tert*-leucinato(1–)-*N,O*]silicon(IV) (53)

Trimethylsilyl (*S*)-*N*-(trimethylsilyl)leucinate (658 mg, 5.00 mmol) was added at –30 °C to a stirred solution of tetra(cyanato-*N*)silane (490 mg, 2.50 mmol) in acetonitrile (10 mL). The reaction mixture was kept 20 min at –30 °C and then at –20 °C for a further 6 d. The resulting colorless solid was isolated by filtration, washed twice with *n*-pentane (10 mL), and dried in vacuo (0.7 mbar, 22 °C, 2 h). Yield: 208 mg (0.56 mmol, 22%); m.p.: 301 °C (subl.). The following ^{29}Si solution-state NMR data refer to two isomers (**A** and **B**; molar ratio **A**:**B**, ca. 1:0.4). The following ^{1}H and ^{13}C solution-state NMR data refer to the major isomer **A**: — ^{1}H NMR (300.1 MHz, [D$_6$]DMSO; *c*, 37.5 mM): δ = 1.06 (s, 18 H, C(C*H*$_3$)$_3$), 3.18–3.29 (m, 2 H, C*H*), 5.54–5.90 and 7.13–7.40 (m, 4 H, N*H*$_2$). — ^{13}C NMR (75.5 MHz, [D$_6$]DMSO; *c*, 37.5 mM): δ = 26.3 (3 *C*H$_3$, C(*C*H$_3$)$_3$), 26.4 (2 *C*H$_3$, C(*C*H$_3$)$_3$), 26.5 (C(*C*H$_3$)$_3$), 33.6 (*C*(CH$_3$)$_3$), 33.7 (*C*(CH$_3$)$_3$), 63.1 (*C*H), 63.4 (*C*H), 118.4 (d, due to ^{14}N coupling, N*C*O), 168.8 (*C*O), 169.3 (*C*O). — ^{29}Si NMR (59.6 MHz, [D$_6$]DMSO; *c*, 37.5 mM): δ = –194.4 (**A**), –193.8 (**B**). — ^{13}C VACP/MAS NMR: δ = 27.9 (asymmetric d, 6 *C*H$_3$, C(*C*H$_3$)$_3$), 33.6 (2 C, *C*(CH$_3$)$_3$), 64.7 (br "d", 2 *C*H), 120.2 (N*C*O), 122.6 (N*C*O), 169.6 (*C*O), 170.3 (*C*O). — ^{15}N VACP/MAS NMR: δ = –335.8 (*N*H$_2$ or *N*H or *N*CO), –322.8 (*N*H$_2$ or *N*H or *N*CO), –321.3 (*N*H$_2$ or *N*H or *N*CO), –318.4 (*N*H$_2$ or *N*H or *N*CO). — ^{29}Si VACP/MAS NMR: δ = –193.4 (br "s", slightly structured, (due to the ^{14}N coupling)) [46, 47, 48].

$C_{14}H_{24}N_4O_6Si$ (372.45)	Calcd.:	C 45.15	H 6.49	N 15.04
	Found:	C 45.2	H 6.5	N 16.6

(Cyanato-*N*)[4-((2-hydroxyphenyl)imino)pent-3-en-2-olato(2−)-*N,O,O′*]methylsilicon(IV) (54)

Tri(cyanato-*N*)methylsilane (1.77 g, 10.5 mmol) was added at 22 °C in a single portion to a solution of **27** (2.00 g, 10.5 mmol) in acetonitrile (10 mL). The reaction mixture was heated under reflux for 4 h, and then stirred at 22 °C for further 6 h. The resulting solid was isolated by filtration and discarded, and the filtrate was kept undisturbed at −20 °C for 6 weeks. The resulting green-yellowish crystals were isolated by filtration, washed with cold *n*-pentane (10 mL, 0 °C), and dried in vacuo (0.8 mbar, 22 °C, 12 h). Yield: 1.25 g (4.56 mmol; 44%); m.p: 94 °C. — ^{1}H NMR (300.1 MHz, [D$_6$]DMSO): δ = 0.06 (s, 3 H, C*H*$_3$), 2.11 (s, 3 H, C*H*$_3$), 2.51 (s, 3 H, C*H*$_3$), 5.97 (s, 1 H, C*H*), 6.94 (m, 1 H, C*H*, C$_6$H$_4$), 7.04 (m, 1 H, C*H*, C$_6$H$_4$), 7.21 (m,

1 H, C*H*, C_6H_4), 7.57 (m, 1 H, C*H*, C_6H_4). — ^{13}C NMR (75.5 MHz, [D$_6$]DMSO): δ = 2.0 (Si*C*H$_3$), 23.7 (*C*H$_3$), 23.9 (*C*H$_3$), 105.8 (*C*H), 114.8 (*C*H, C_6H_4), 120.3 (*C*H, C_6H_4), 120.7 (N*C*O), 121.0 (*C*H, C_6H_4), 128.2 (*C*H, C_6H_4), 131.4 (*C*-2, C_6H_4), 150.4 (*C*-1, C_6H_4), 168.4 (*C*O or *C*N), 170.5 (*C*O or *C*N). — ^{15}N NMR (30.4 MHz, [D$_6$]DMSO): δ = –174.4 (C*N*), *N*CO could not be detected. — ^{29}Si NMR (59.6 MHz, [D$_6$]DMSO): δ = –105.2. — ^{13}C VACP/MAS NMR: δ = −0.8 (Si*C*H$_3$), 24.0 (2 *C*H$_3$), 106.5 (*C*H), 114.4 (*C*H, C_6H_4), 120.3 (*C*H, C_6H_4), 121.6 (*C*H, C_6H_4; N*C*O), 128.4 (*C*H, C_6H_4), 133.1 (*C*-2, C_6H_4), 150.9 (*C*-1, C_6H_4), 169.1 (*C*O or *C*N), 172.0 (*C*O or *C*N). — ^{15}N VACP/MAS NMR: δ = –319.4 (*N*CO), –168.5 (C*N*). — ^{29}Si VACP/MAS NMR: δ = –102.0.

$C_{13}H_{14}N_2O_3Si$ (274.35)	Calcd.:	C 56.91	H 5.14	N 10.21
	Found:	C 56.8	H 5.1	N 10.1

[2-{*N*-[2-(Benzylamino)ethyl]ethanimidoyl}phenolato(2–)-*O,N,N*]methyl(thiocyanato-*N*)silicon(IV) (55)

Compound **28** (1.80 g, 6.70 mmol) was added to a stirred solution of **3** (1.10 g, 6.70 mmol) and triethylamine (1.50 g, 14.8 mmol) in dichloromethane (10 mL). The reaction mixture was stirred at 22 °C for 48 h. *n*-Pentane (15 mL) was carefully added and the mixture was stored undisturbed at –20 °C for 7 d. The resulting yellowish solid was filtered off, washed with *n*-pentane (3 × 5 mL) and THF (15 mL), and dried in vacuo (1.3 mbar, 22 °C, 15 h). The yellowish solid was recrystallized from CH_3CN (10 mL). The crystalline product was isolated by filtration, washed with diethyl ether (15 mL), and dried in vacuo (1.3 mbar, 22 °C, 10 h). Yield: 765 mg (2.08 mmol, 31%); m.p.: 153 °C (decomp.). — ^{1}H NMR (500.1 MHz, CD_2Cl_2): δ = 0.23 (s, 3 H, SiC*H*$_3$), 2.46 (s, 3 H, CH_2N=CC*H*$_3$), 2.91–3.02 (m, 2 H, C*H*$_2$NCH$_2$C$_6$H$_5$), 3.67–3.78 and 3.87–3.95 (m, 2 H, C*H*$_2$N=CCH$_3$), 4.33 (H_A) and 4.49 (H_B) (2 H, AB system, ^2J(A,B) = 15.8 Hz, $CH_2NCH_AH_BC_6H_5$), 7.08 (1 H, *H*-4 (H_A), C_6H_4), 7.15 (1 H, *H*-6 (H_B), C_6H_4), 7.52 (1 H, *H*-5 (H_C), C_6H_4), and 7.64 (1 H, *H*-3 (H_D), C_6H_4) (ABCD system, ^4J(A,B) = 1.2 Hz, ^3J(A,C) = 7.3 Hz, ^3J(A,D) = 8.1 Hz, ^3J(B,C) = 8.3 Hz, ^5J(B,D) not resolved, ^4J(C,D) = 1.7 Hz), 7.21–7.26 (m, 1 H, *H*-4, C_6H_5), 7.31–7.39 (m, 4 H, *H*-2/*H*-3/*H*-5/*H*-6, C_6H_5). — ^{13}C NMR (125.8 MHz, CD_2Cl_2): δ = 5.4 (Si*C*H$_3$), 17.6 (CH_2N=C*C*H$_3$), 46.4 (*C*H$_2$NCH$_2$C$_6$H$_5$), 46.9 (*C*H$_2$N=CCH$_3$), 54.0 ($CH_2NCH_2C_6H_5$), 120.7 (*C*-2, C_6H_4), 121.3 (*C*-4, C_6H_4), 122.6 (*C*-6, C_6H_4), 126.8 (*C*-4, C_6H_5), 127.6 (*C*-2/*C*-6, C_6H_5), 128.6 (*C*-3/*C*-5, C_6H_5), 129.2 (*C*-3, C_6H_4), 134.7 (t, ^1J(^{13}C,^{14}N) = 20 Hz, N*C*S), 135.6 (*C*-5, C_6H_4), 141.9 (*C*-1, C_6H_5), 157.7 (*C*-1, C_6H_4), 169.1 (CH_2N=*C*CH$_3$). — ^{15}N NMR (50.7 MHz, CD_2Cl_2): δ = –138.4 (CH_2*N*=CCH$_3$), *N*CS and CH_2*N*$CH_2C_6H_5$ not detected. — ^{29}Si NMR (99.4 MHz, CD_2Cl_2): δ =

–105.7. — ^{13}C VACP/MAS NMR: δ = 4.0 (Si*C*H$_3$), 19.2 (CH$_2$N=C*C*H$_3$), 44.3 (*C*H$_2$NCH$_2$C$_6$H$_5$), 47.8 (*C*H$_2$N=CCH$_3$), 52.1 (CH$_2$N*C*H$_2$C$_6$H$_5$), 120.1 (*C*-2, C$_6$H$_4$), 122.0 (*C*-4/*C*-6, C$_6$H$_4$), 127.2, 128.0, 128.7, 129.4, and 130.2 (*C*-3, C$_6$H$_4$, and *C*-2/*C*-3/*C*-4/*C*-5/*C*-6, C$_6$H$_5$), 132.8 (N*C*S), 135.1 (*C*-5, C$_6$H$_4$), 141.4 (*C*-1, C$_6$H$_5$), 157.1 (*C*-1, C$_6$H$_4$), 168.9 (CH$_2$N=*C*CH$_3$). — ^{15}N VACP/MAS NMR: δ = –323.9 (CH$_2$*N*CH$_2$C$_6$H$_5$), –224.6 (*N*CS), –132.1 (CH$_2$*N*=CCH$_3$). — ^{29}Si VACP/MAS NMR: δ = –107.1 (br. s, slight shoulder).

C$_{19}$H$_{21}$N$_3$OSSi (367.55)	Calcd.:	C 62.09	H 5.76	N 11.43	S 8.72
	Found:	C 61.5	H 5.8	N 11.4	S 8.6

[2-{*N*-[2-(Dimethylamino)ethyl]ethanimidoyl}phenolato(2–)-*O*,*N*,*N*]methyl[di(thiocyanato-*N*)]silicon(IV) (56)

Compound **29** (1.53 g, 7.42 mmol) was added at 22 °C to a stirred solution of **3** (1.23 g, 7.67 mmol) in acetonitrile (10 mL), and the reaction mixture was then stirred at 22 °C for 24 h. The resulting precipitate was filtered off and discarded. *n*-Pentane (7 mL) was added carefully to the filtrate, and the mixture was then kept undisturbed at –20 °C for 7 d. The resulting yellowish solid was filtered off, washed with *n*-pentane (3 × 5 mL), and dried in vacuo (1.0 mbar, 22 °C, 15 h). Yield: 460 mg (1.29 mmol, 17%); m.p.: 143 °C (decomp.). — ^{1}H NMR (500.1 MHz, CD$_2$Cl$_2$): δ = 0.46 (s, 3 H, SiC*H*$_3$), 2.60 (s, 3 H, CH$_2$N=CC*H*$_3$), 2.74 (s, 6 H, N(C*H*$_3$)$_2$), 3.15 (t, ^{3}J(^{1}H,^{1}H) = 6.4 Hz, 2 H, C*H*$_2$N(CH$_3$)$_2$), 3.88 (t, ^{3}J(^{1}H,^{1}H) = 6.4 Hz, 2 H, C*H*$_2$N=CCH$_3$), 6.93 (1 H, *H*-6 (*H*$_A$), C$_6$H$_4$), 6.96 (1 H, *H*-4 (*H*$_B$), C$_6$H$_4$), 7.50 (1 H, *H*-5 (*H*$_C$), C$_6$H$_4$), and 7.64 (1 H, *H*-3 (*H*$_D$), C$_6$H$_4$) (ABCD system, ^{4}J(A,B) = 1.2 Hz, ^{3}J(A,C) = 8.3 Hz, ^{5}J(A,D) not resolved, ^{3}J(B,C) = 7.2 Hz, ^{3}J(B,D) = 8.2 Hz, ^{4}J(C,D) = 1.6 Hz). — ^{13}C NMR (125.8 MHz, CD$_2$Cl$_2$): δ = 12.0 (Si*C*H$_3$), 20.2 (CH$_2$N=C*C*H$_3$), 45.3 (*C*H$_2$N=CCH$_3$), 49.2 (N(*C*H$_3$)$_2$), 57.5 (*C*H$_2$N(CH$_3$)$_2$), 119.4 (*C*-2, C$_6$H$_4$), 119.7 (*C*-4, C$_6$H$_4$), 121.9 (*C*-6, C$_6$H$_4$), 129.9 (*C*-3, C$_6$H$_4$), 135.5 (2 C, N*C*S), 136.9 (*C*-5, C$_6$H$_4$), 160.1 (*C*-1, C$_6$H$_4$), 173.8 (CH$_2$N=*C*CH$_3$) [83]. — ^{29}Si NMR (99.4 MHz, CD$_2$Cl$_2$): δ = –172.1 (br. s, slight shoulder). — ^{13}C VACP/MAS NMR: δ = 15.1 (Si*C*H$_3$), 20.0 (CH$_2$N=C*C*H$_3$), 45.5 (*C*H$_2$N=CCH$_3$), 49.4 and 50.5 (N(*C*H$_3$)$_2$), 57.5 (*C*H$_2$N(CH$_3$)$_2$), 118.9 and 119.4 (*C*-2/*C*-4, C$_6$H$_4$), 122.0 (*C*-6, C$_6$H$_4$), 132.1 (2 C, N*C*S), 132.5 (*C*-3, C$_6$H$_4$), 138.9 (*C*-5, C$_6$H$_4$), 159.4 (*C*-1, C$_6$H$_4$), 174.6 (CH$_2$N=*C*CH$_3$). — ^{15}N VACP/MAS NMR: δ = −328.9 (*N*(CH$_3$)$_2$), −222.8 and −220.0 (*N*CS), −147.0 (CH$_2$*N*=CCH$_3$). — ^{29}Si VACP/MAS NMR: δ = −172.9.

C$_{15}$H$_{20}$N$_4$OS$_2$Si (364.57)	Calcd.:	C 49.42	H 5.53	N 15.37	S 17.59
	Found:	C 48.8	H 5.7	N 14.9	S 17.2

Tri(cyanato-*N*){4-[2-(dimethylamino)ethyl]imino}[pent-3-en-2-olato(1−)-*N*,*N*′,*O*]silicon(IV) (57)

Tetra(cyanato-*N*)silane (490 mg, 2.50 mmol) was added in a single portion at 22 °C to a solution of **30** (425 mg, 2.50 mmol) in dichloromethane (20 mL). The reaction mixture was stirred at 22 °C for 1 h, the resulting solid was removed by filtration and discarded. The filtrate was carefully layered with *n*-pentane (15 mL) and stored at −20 °C for 7 d. The resulting pale yellowish solid was isolated by filtration, washed with *n*-pentane (15 mL), and dried in vacuo (1.7 mbar, 22 °C, 15 h). Yield: 60.0 mg (0.19 mmol, 8%); m.p.: 131 °C (decomp.). — ^{1}H NMR (500.1 MHz, [D$_6$]DMSO): δ = 1.94 (s, 3 H, CH_3), 2.10 (s, 3 H, CH_3), 2.65 (s, 6 H, N(CH_3)$_2$), 3.08 (t, ^{3}J(^{1}H,^{1}H) = 6.4 Hz, 2 H, CH_2N=CCH$_3$), 3.67 (t, ^{3}J(^{1}H,^{1}H) = 6.4 Hz, 2 H, CH_2N(CH$_3$)$_3$), 5.74 (s, 1 H, C*H*, CH$_3$CC*H*CCH$_3$). — ^{13}C NMR (125.8 MHz, [D$_6$]DMSO): δ = 22.1 (*C*H$_3$), 23.8 (CH$_2$N=C*C*H$_3$), 41.7 (*C*H$_2$N=CCH$_3$), 48.6 (N(*C*H$_3$)$_2$), 55.8 (*C*H$_2$N(CH$_3$)$_2$), 98.9 (*C*H, CH$_3$C*C*HCCH$_3$), 120.5 (N*C*O), 122.4 (2 C, N*C*O), 170.5 (*C*O), 174.1 (CH$_2$N=*C*CH$_3$). — ^{15}N NMR (30.4 MHz, [D$_6$]DMSO): δ = −334.8 (*N*(CH$_3$)$_3$), −187.1 (CH$_3$*N*=C). — ^{29}Si NMR (99.4 MHz, [D$_6$]DMSO): δ = –200.2. — ^{13}C VACP/MAS NMR: δ = 23.0 (*C*H$_3$), 24.6 (*C*H$_3$), 42.8 (*C*H$_2$N=CCH$_3$), 46.6 and 48.8 (N(*C*H$_3$)$_2$), 56.7 (*C*H$_2$N(CH$_3$)$_2$), 99.4 (*C*H), 119.6 (m, N*C*O), 124.8 (m, 2 C, N*C*O), 172.2 (*C*O), 175.5 (CH$_2$N=*C*CH$_3$). — ^{15}N VACP/MAS NMR: δ = −329.0 (*N*(CH$_3$)$_2$), −318.1 and −310.1 (*N*CO), −179.6 (CH$_2$*N*=CCH$_3$). — ^{29}Si VACP/MAS NMR: δ = −199.4.

$C_{12}H_{17}N_5O_4Si$ (323.38)	Calcd.:	C 44.57	H 5.30	N 21.66
	Found:	C 44.1	H 5.1	N 21.1

Di(cyanato-*N*){4-[2-(dimethylamino)ethyl]imino}[pent-3-en-2-olato(1−)-*N*,*N*′,*O*]phenyl-silicon(IV) (58)

Tri(cyanato-*N*)phenylsilane (578 mg, 2.50 mmol) was added in a single portion at 22 °C to a solution of **30** (425 mg, 2.50 mmol) in acetonitrile (10 mL). The reaction mixture was stirred at 22 °C for 1 h. The resulting pale yellowish solid was isolated by filtration, washed with *n*-pentane (15 mL), and dried in vacuo (1.0 mbar, 22 °C, 15 h). The filtrate was carefully layered with *n*-pentane (15 mL), and stored at −20 °C for 7 d. The resulting pale yellow solid was isolated by filtration, washed with *n*-pentane (3 × 5 mL), and dried in vacuo (1.0 mbar, 22 °C, 15 h). Yield: 346 mg (0.97 mmol, 39%); m.p.: 116 °C (decomp.). — ^{1}H NMR (500.1 MHz, [D$_6$]DMSO): δ = 1.77 (s, 3 H, CH_3), 2.12 (s, 3 H, CH_3), 2.30 (s, 6 H, N(CH_3)$_2$), 3.06 (t, ^{3}J(^{1}H,^{1}H) = 6.3 Hz, 2 H, CH_2N(CH$_3$)$_2$), 3.73 (t, ^{3}J(^{1}H,^{1}H) = 6.3 Hz, 2 H, CH_2N=CCH$_3$), 5.34 (s, 1 H, C*H*, CH$_3$CC*H*CCH$_3$), 7.16 (m, 1 H, C$_6H_5$), 7.22 (m, 2 H, C$_6H_5$), 7.76 (m, 2 H, C$_6H_5$).

— ^{13}C NMR (125.8 MHz, [D$_6$]DMSO): δ = 21.3 (*C*H$_3$), 22.8 (CH$_2$N=C*C*H$_3$), 41.1 (*C*H$_2$N=CCH$_3$), 47.2 (N(*C*H$_3$)$_2$), 55.7 (*C*H$_2$N(CH$_3$)$_2$), 97.7 (*C*H, CH$_3$C*C*HCCH$_3$), 122.5 (2 C, N*C*O), 125.4 (*C*-4, C$_6$H$_5$), 125.7 (*C*-3/*C*-5, C$_6$H$_5$), 133.3 (*C*-2/*C*-6, C$_6$H$_5$), 149.8 (*C*-1, C$_6$H$_5$), 167.5 (*C*O), 172.8 (CH$_2$N=*C*CH$_3$). — ^{29}Si NMR (99.4 MHz, [D$_6$]DMSO): δ = –179.8. — ^{13}C VACP/MAS NMR: δ = 22.0 (*C*H$_3$), 25.4 (*C*H$_3$), 42.7 (*C*H$_2$N=CCH$_3$), 48.8 and 49.1 (N(*C*H$_3$)$_2$), 56.3 (*C*H$_2$N(CH$_3$)$_2$), 98.7 (*C*H), 122.7 (N*C*O), 123.3 (N*C*O), 125.8, 128.3, 129.6, 133.6, 137.4 (5 *C*H, C$_6$H$_5$), 148.3 (*C*-1, C$_6$H$_5$), 165.6 (*C*O), 172.4 (CH$_2$N=*C*CH$_3$). — ^{15}N VACP/MAS NMR: δ = −332.0 (*N*(CH$_3$)$_2$), −321.3 and −312.7 (*N*CO), −165.0 (CH$_2$*N*=CCH$_3$). — ^{29}Si VACP/MAS NMR: δ = −180.4.

$C_{17}H_{22}N_4O_3Si$ (358.47)	Calcd.:	C 56.96	H 6.19	N 15.63
	Found:	C 56.6	H 6.3	N 15.7

(Cyanato-*N*){4,4′-(Ethane-1,2-diyldinitrilo)bis[pent-2-en-2-olato(1−)]-*N*,*N*′,*O*,*O*′}methylsilicon(IV) (59)

Tri(cyanato-*N*)methylsilane (490 mg, 2.90 mmol) was added at 22 °C to a stirred solution of **31** (677 mg, 3.02 mmol) in acetonitrile (10 mL), and the mixture was stirred at 22 °C for 3 h. The resulting solid was removed by filtration and discarded, *n*-pentane (20 mL) was carefully added, and the filtrate was kept undisturbed at −20 °C for 14 d. The resulting solid was washed with *n*-pentane (3 × 10 mL) and dried in vacuo (0.7 mbar, 22 °C, 9 h). Yield: 275 mg (0.89 mmol, 31%); m.p: >150 °C (decomp.). — ^{1}H NMR (300.1 MHz, [D$_6$]DMSO): δ = –0.17 (s, 3 H, SiC*H*$_3$), 1.82 (s, 6 H, NCC*H*$_3$), 2.00 (s, 6 H, OCC*H*$_3$), 3.53–3.68 (m, 4 H, NC*H*$_2$), 5.10 (s, 2 H, C*H*). — ^{13}C NMR (75.5 MHz, [D$_6$]DMSO): δ = 11.6 (Si*C*H$_3$), 21.4 (NC*C*H$_3$), 24.2 (OC*C*H$_3$), 43.8 (*C*H$_2$), 97.8 (*C*H), 121.6 (N*C*O), 167.8 (*C*O or *C*N), 174.1 (*C*O or *C*N). — ^{29}Si NMR (59.6 MHz, [D$_6$]DMSO): δ = –181.5. ^{13}C VACP/MAS NMR: δ = 7.9 (Si*C*H$_3$), 21.4 (*C*H$_3$), 22.6 (*C*H$_3$), 24.1 (*C*H$_3$), 26.5 (*C*H$_3$), 44.2 (*C*H$_2$), 98.6 (*C*H), 99.6 (*C*H), 121.0 (N*C*O), 168.5 (*C*O or *C*N), 170.3 (*C*O or *C*N), 176.0 (*C*O or *C*N), 176.5 (*C*O or *C*N). — ^{15}N VACP/MAS NMR: δ = –300.5 (*N*CO), –182.1 (*N*CH$_2$), 178.0 (*N*CH$_2$). — ^{29}Si VACP/MAS NMR: δ = –182.6.

$C_{14}H_{21}O_3N_3Si$ (307.42)	Calcd.:	C 54.70	H 6.89	N 13.67
	Found:	C 54.3	H 6.7	N 13.4

(Cyanato-*N*)[4,4′-(Ethane-1,2-diyldinitrilo)bis[pent-2-en-2-olato(1−)]-*N*,*N*′,*O*,*O*′]phenylsilicon(IV) (60)

Tri(cyanato-*N*)phenylsilane (870 mg, 3.76 mmol) was added at 22 °C to a stirred solution of **31** (844 mg, 3.76 mmol) in acetonitrile (20 mL), and the mixture was stirred at 22 °C for 5 h. The resulting solid was separated by filtration and discarded, *n*-pentane (15 mL) was carefully added, and the filtrate was kept undisturbed at 22 °C for 10 d. The resulting solid was washed with *n*-pentane (3 × 10 mL), and dried in vacuo (0.1 mbar, 22 °C, 5 h). Yield: 916 mg (2.48 mmol, 66%); m.p: 208 °C (decomp.). — ^{1}H NMR (500.1 MHz, CD_2Cl_2): δ = 1.98 (s, 6 H, CH_3), 2.04 (s, 6 H, CH_3), 3.31–3.35 (m, 2 H, NCH_2C), 3.58–3.62 (m, 2 H, CCH_2N), 5.22 (s, 2 H, C*H*), 7.05–7.08 (m, *H*-4, C_6H_5), 7.09–7.13 (m, *H*-3/*H*-5, C_6H_5), 7.26–7.28 (m, *H*-2/*H*-6, C_6H_5). — ^{13}C NMR (125.8 MHz, CD_2Cl_2): δ = 21.8 (*C*H$_3$), 24.8 (*C*H$_3$), 43.8 (*C*H$_2$), 99.4 (*C*H), 121.9 (N*C*O), 126.2 (*C*-4, C_6H_5), 127.0 (*C*-3/*C*-5, C_6H_5), 132.6 (*C*-2/*C*-6, C_6H_5), 159.6 (*C*-1, C_6H_5), 170.0 (*C*O or *C*N), 177.4 (*C*O or *C*N). — ^{29}Si NMR (99.4 MHz, CD_2Cl_2): δ = –190.3. — ^{13}C VACP/MAS NMR: δ = 21.6 (*C*H$_3$), 22.8 (*C*H$_3$), 24.5 (*C*H$_3$), 25.2 (*C*H$_3$), 43.3 (*C*H$_2$), 44.2 (*C*H$_2$), 100.5 (*C*H), 101.4 (*C*H), 122.1 (N*C*O), 128.1 (*C*-4, *C*-3/*C*-5, C_6H_5), 133.4 (*C*-2, C_6H_5), 134.5 (*C*-6, C_6H_5), 160.3 (*C*-1, C_6H_5), 170.9 (*C*O or *C*N), 173.5 (*C*O or *C*N), 176.0 (*C*O or *C*N), 178.8 (*C*O or *C*N). — ^{15}N VACP/MAS NMR: δ = –316.5 (Si*N*CH$_2$), –183.8 (C*N*). — ^{29}Si VACP/MAS NMR: δ = –190.1.

$C_{19}H_{23}N_3O_3Si$ (369.49)	Calcd.:	C 61.76	H 6.27	N 11.37
	Found:	C 60.9	H 6.4	N 11.7

(Cyanato-*N*){2-[({2-[(2-Hydroxybenzylidene)amino]ethyl}imino)methyl]phenolato(2–)-*N*,*N*′,*O*,*O*′}methylsilicon(IV) (62)

Tri(cyanato-*N*)methylsilane (421 mg, 2.49 mmol) was added at 22 °C to a stirred solution of **32** (616 mg, 2.30 mmol) in acetonitrile (20 mL). The reaction mixture was heated under reflux for 4 h. The resulting solid was separated by filtration and discarded. The filtrate was kept at –20 °C for 12 d. The resulting yellow solid was isolated by filtration, washed with *n*-pentane (10 mL), and dried in vacuo (0.01 mbar, 22 °C, 3 h). Yield: 245 mg (0.70 mmol, 28%); m.p.: 197 °C (decomp.). — ^{1}H NMR (300.1 MHz, [D$_6$]DMSO): δ = –0.10 (s, 3 H, SiCH_3), 4.04 (s, 4 H, CH_2), 6.79–6.86 (m, 4 H, C*H*, C_6H_4), 7.40–7.47 (m, 4 H, C*H*, C_6H_4), 8.45 (s, 2 H, N=C*H*). — ^{13}C NMR (75.5 MHz, [D$_6$]DMSO): δ = 12.7 (Si*C*H$_3$), 51.7 (*C*H$_2$), 117.5 (*C*-2, C_6H_4), 117.9, 120.3, 133.5, 136.4 (*C*H, C_6H_4), 160.7 (*C*-1, C_6H_4), 163.8 (H*C*N), N*C*O could not be detected. — ^{15}N NMR (30.4 MHz, [D$_6$]DMSO): δ = –144.0 (C*N*), –143.8 (C*N*=CH). — ^{29}Si NMR (59.6 MHz, [D$_6$]DMSO): δ = –184.2. — ^{13}C VACP/MAS NMR: δ =

11.9 (Si*C*H$_3$), 53.5 (*C*H$_2$), 54.5 (*C*H$_2$), 117.7 (2 *C*-2 and *C*H, C$_6$H$_4$), 119.9, 120.1, 121.8, 122.7 (*C*H, C$_6$H$_4$), 133.6 (2 *C*H, C$_6$H$_4$), 136.8 (*C*H, C$_6$H$_4$), 161.8 (2 *C*-1, C$_6$H$_4$), 162.8 (*C*N). — ^{15}N VACP/MAS NMR: δ = –311.7 (*N*CO), –134.9 and –133.3 (HC-*N*). — ^{29}Si VACP/MAS NMR: δ = –184.0.

$C_{18}H_{17}N_3O_3Si$ (351.44)	Calcd.:	C 61.52	H 4.88	N 11.96
	Found:	C 61.2	H 4.9	N 11.9

(Cyanato-*N*){2-[({2-[(2-Hydroxybenzylidene)amino]ethyl}imino)methyl]phenolato(2–)-*N,N′,O,O′*}phenylsilicon(IV) (63)

Tri(cyanato-*N*)phenylsilane (610 mg, 2.64 mmol) was added to a stirred solution of **32** (670 mg, 2.50 mmol) in acetonitrile (20 mL), and the reaction mixture was stirred at 22 °C for 24 h. The resulting solid was isolated by filtration and discarded. The filtrate was kept at –20 °C for 7 d. The resulting colorless solid was isolated by filtration, washed with *n*-pentane (10 mL), and dried in vacuo (0.2 mbar, 23 °C, 6 h). Yield: 78.6 mg (0.19 mmol, 7.0%); m.p.: 234 °C (decomp.). — ^{1}H NMR (500.1 MHz, [D$_6$]DMSO): δ = 3.91 (s, 4 H, C*H*$_2$), 6.84–7.61 (m, 13 H, C$_6$*H*$_4$, C$_6$*H*$_5$) 8.67 (br s, 2 H, NC*H*). — ^{13}C NMR (125.8 MHz, [D$_6$]DMSO): δ = 58.7 (*C*H$_2$), 116.4, 118.5, 131.6, 132.3, 134.0, (*C*$_6$H$_4$), 127.1, 127.2, 128.9 (*C*$_6$H$_5$), 134.1 (*C*-1, *C*$_6$H$_5$), 160.5 (*C*-1, *C*$_6$H$_4$), 166.9 (N*C*H). — ^{29}Si NMR (59.6 MHz, [D$_6$]DMSO): δ = –254.8.

{2-[({2-[(2-Hydroxybenzylidene)amino]ethyl}imino)methyl]phenolato(2–)-*N,N′,O,O′*}di(thiocyanato-*N*)silicon(IV) (64)

Compound **32** (6.84 mg, 2.55 mmol) was added at 22 °C to a stirred solution of tetra(thiocyanato-*N*)silane (664 mg, 2.55 mmol) in acetonitrile (10 mL), and the mixture was then stirred for 24 h at 22 °C. *n*-Pentane (15 mL) was added and the mixture was kept undisturbed at 22 °C for 3 d. The resulting yellow-orange solid was isolated by filtration, washed with *n*-pentane (10 mL), and dried in vacuo (0.4 mbar, 22 °C, 8 h). Yield: 490 mg (1.19 mmol, 47%); m.p.: >327 °C (decomp.). Upon disolution of **64** in [D$_6$]DMSO the existence of three isomers was observed, with molar ratio, ca. **A**:**B**:**C** = 1.00:0.48:0.96 [84]. NMR data for **64A**: — ^{1}H NMR (500.1 MHz, [D$_6$]DMSO): δ = 4.16 (s, 4 H, C*H*$_2$), 7.17 (m, 4 H, C$_6$H$_4$), 7.74 (m, 4 H, C$_6$H$_4$), 8.99 (s, 2 H, C*H*). — ^{13}C NMR (125.8 MHz, [D$_6$]DMSO): δ = 51.8 (2 *C*H$_2$), 116.9 (*C*-2, C$_6$H$_4$), 120.2 (*C*H, C$_6$H$_4$), 120.6 (*C*H, C$_6$H$_4$), 134.0 (*C*H, C$_6$H$_4$), 137.9 (*C*H, C$_6$H$_4$; N*C*S), 158.8 (*C*-1, C$_6$H$_4$), 168.2 (N*C*H). ^{15}N NMR (30.4 MHz, [D$_6$]DMSO): δ = –163.7 (*N*CH), –162.0 (*N*CH$_2$). — ^{29}Si NMR (99.4 MHz, [D$_6$]DMSO): δ = –188.5. NMR data for **64B**: — ^{1}H NMR (500.1 MHz, [D$_6$]DMSO): δ = 3.97 (m, 4 H, C*H*$_2$),

6.77 (m, 1 H, C_6H_4), 6.85 (m, 1 H, C_6H_4), 6.93 (m, 1 H, C_6H_4), 7.00 (m, 1 H, C_6H_4), 7.05 (m, 1 H, C_6H_4), 7.44 (m, 1 H, C_6H_4), 7.62 (m, 1 H, C_6H_4), 7.95 (s, 1 H, C_6H_4), 8.88 (s, 2 H, C*H*). — ^{13}C NMR (125.8 MHz, [D_6]DMSO): δ = 51.7 (*C*H_2), 51.9 (*C*H_2), 116.6 (*C*-2, C_6H_4), 117.0 (*C*-2, C_6H_4), 118.7 (*C*H, C_6H_4), 119.3 (*C*H, C_6H_4), 120.1 (*C*H, C_6H_4), 120.3 (*C*H, C_6H_4), 133.4 (*C*H, C_6H_4), 134.0 (2 *C*H, C_6H_4), 136.1 (*C*H and N*C*S, C_6H_4), 159.0 (*C*-1, C_6H_4), 159.6 (*C*-1, C_6H_4), 167.5 (N*C*H). — ^{15}N NMR (30.4 MHz, [D_6]DMSO): δ = –160.4 (*N*CH), –162.0 (*N*CH_2). — ^{29}Si NMR (99.4 MHz, [D_6]DMSO): δ = –189.7. NMR data for **64C**: — ^{1}H NMR (500.1 MHz, [D_6]DMSO): δ = 4.10−4.22 (m, 4 H, C*H*$_2$), 7.10 (m, 4 H, C_6H_4), 7.68 (m, 4 H, C_6H_4), 8.93 (s, 2 H, C*H*). — ^{13}C NMR (125.8 MHz, [D_6]DMSO): δ = 51.9 (2 *C*H_2), 117.2 (*C*-2, C_6H_4), 119.9 (*C*H, C_6H_4), 121.1 (*C*H, C_6H_4), 134.1 (*C*H, C_6H_4), 137.9 (*C*H, C_6H_4; N*C*S), 158.6 (*C*-1, C_6H_4), 168.7 (N*C*H). — ^{15}N NMR (30.4 MHz, [D_6]DMSO): δ = –160.3 (*N*CH), –162.0 (*N*CH_2). — ^{29}Si NMR (99.4 MHz, [D_6]DMSO): δ = –198.6. — ^{13}C VACP/MAS NMR: δ = 55.0 (*C*H_2), 55.1 (*C*H_2), 117.1 (2 *C*H, C_6H_4), 119.2 (*C*H, C_6H_4), 120.6 (2 *C*H, C_6H_4), 121.9 (*C*H, C_6H_4), 135.3 (2 N*C*S and 2 *C*-2), 140.8 (2 *C*H, C_6H_4), 160.07 (*C*O or *C*N), 160.09 (*C*O or *C*N), 165.8 (*C*O or *C*N), 167.1 (*C*O or *C*N). — ^{29}Si VACP/MAS NMR: δ = –210.1.

$C_{18}H_{14}N_4O_2S_2Si$ (410.55)	Calcd.:	C 52.66	H 3.44	N 13.65	S 15.62
	Found:	C 52.6	H 3.6	N 13.8	S 15.4

10 References and notes

[1] S. Metz, *Dissertation,* Universität Würzburg, **2008**.

[2] B. Theis, *Dissertation,* Universität Würzburg, **2009**.

[3] S. Metz, C. Burschka, D. Platte, R. Tacke, *Angew. Chem.* **2007**, *119*, 7136−7139; *Angew. Chem. Int. Ed.* **2007**, *46*, 7006−7009.

[4] A. R. Bassindale, P. G. Taylor, in: *The Chemistry of Organic Silicon Compounds, Part 1* (Eds.: S. Patai, Z. Rappoport), Wiley, Chichester, **1989**, pp. 839−892.

[5] W. S. Sheldrick, in: *The Chemistry of Organic Silicon Compounds, Part 1* (Eds.: S. Patai, Z. Rappoport), Wiley, Chichester, **1989**, pp. 227−303.

[6] R. J. P. Corriu, J. C. Young, in: *The Chemistry of Organic Silicon Compounds, Part 2* (Eds.: S. Patai, Z. Rappoport), Wiley, Chichester, **1989**, pp. 1241−1288.

[7] S. N. Tandura, M. G. Voronov, N. V. Alekseev, *Top. Curr. Chem.* **1986**, *131*, 99−189.

[8] R. R. Holmes, *Chem Rev.* **1990**, *90*, 17−31.

[9] R. R. Holmes, *Chem Rev.* **1996**, *96*, 927−950.

[10] J. G. Verkade, *Coord. Chem. Rev.* **1994**, *137*, 233−295.

[11] D. Kost, I. Kalikhman, in: *The Chemistry of Organic Silicon Compounds*, *Vol. 2*, *Part 2* (Eds.: Z. Rappoport, Y. Apeloig), Wiley, Chichester, **1998**, pp. 1339–1445.

[12] V. Pestunovich, S. Kirpichenko, M. Voronkov, in: *The Chemistry of Organic Silicon Compounds*, *Vol. 2*, *Part 2* (Eds.: Z. Rappoport, Y. Apeloig), Wiley, Chichester, **1998**, pp. 1447–1537.

[13] C. Chiut, R. J. P. Corriu, C. Reyé, in: *Chemistry of Hypervalent Compounds* (Ed.: K. Akiba), Wiley−VCH, New York, **1999**, pp. 81–146.

[14] M. A. Brook, *Silicon in Organic, Organometallic, and Polymer Chemistry*, Wiley, New York, **2000**, pp. 97–114.

[15] R. Tacke, O. Seiler, in: *Silicon Chemistry: From the Atom to Extended Systems* (Eds.: P. Jutzi, U. Schubert), Wiley−VCH, Weinheim, **2003**, pp. 324–337.

[16] R. Tacke, M. Pülm, B. Wagner, *Adv. Organomet. Chem*. **1999**, *44*, 221–273.

[17] R. Tacke, O. Dannappel, in: *Tailor-made Silicon-Oxygen Compounds − From Molecules to Materials* (Eds.: R. Corriu, P. Jutzi), Vieweg, Braunschweig-Wiesbaden, **1996**, pp. 75−86.

[18] E. Lukevics, O. A. Pudova, *Chem. Heterocycl. Compd (Engl. Transl.)* **1996**, *32*, 1381−1418.

[19] C. W. Wong, J. D. Woollins, *Coord. Chem. Rev.* **1994**, *130*, 175−241.

[20] R. Tacke, J. Becht, A. Lopez-Mras, J. Sperlich, *J. Organomet. Chem*. **1993**, *446*, 1–8.

[21] C. Chiut, R. J. P. Corriu, C. Reyé, J. C. Young, *Chem. Rev.* **1993**, *93*, 1371−1448.

[22] R. Rosenheim, O. Sorge, *Ber. Dtsch. Chem. Ges.* **1920**, *53*, 932−939.

[23] J. J. Flynn, F. P. Boer, *J. Am. Chem. Soc.* **1969**, 9*1*, 5756–5761.

[24] D. Högerle, U. Link, U. Thewalt, *Z. Naturforsch.* **1993**, *48b*, 691–693.

[25] K. Tamao, M. Asahara, A. Kawachi, *J. Organomet. Chem.* **1996**, *521*, 325−334.

[26] R. Tacke, M. Mallack, R. Willeke, *Angew. Chem.* **2001**, *113*, 2401−2403; *Angew. Chem. Int. Ed.* **2001**, *40*, 2339−2341.

[27] B. Theis, S. Metz, C. Burschka, R. Bertermann, S. Maisch, R. Tacke, *Chem. Eur. J.* **2009**, *15*, 7329−7338.

[28] R. Tacke, R. Bertermann, C. Burschka, S. Dragota, M. Penka, I. Richter, *J. Am. Chem. Soc.* **2004**, *16*, 14493–14505.

[29] R. J. P. Corriu, C. Guerin, B. J. L. Henner, W. W. C. Wong Chi Man, *Organometallics* **1988**, *7*, 237−238.

[30] J.-L. Brefort, R. J. P. Corriu, C. Guerin, B. J. L. Henner, W. W. C. Wong Chi Man, *Organometallics* **1990**, *9*, 2080−2085.

[31] A. A. Korlyukov, K. A. Lyssenko, M. Y. Antipin, *Russ. Chem. Bull., Int. Ed.* **2002**, *51*, 1423–1432.

[32] N. Kocher, J. Henn, B. Gostevskii, D. Kost, I. Kalikhman, B. Engels, D. Stalke, *J. Am. Chem. Soc.* **2004**, *126*, 5563–5568.

[33] Selected reviews dealing with higher-coordinate silicon compounds: a) D. Kost, I. Kalikhman, *Adv. Organomet. Chem*. **2004**, *50*, 1–106; b) D. Kost, I. Kalikhman, *Acc. Chem. Res*. **2009**, *42,* 303–314.

[34] B. Fitzsimmons, A. Hume, L. F. Larkworthy, M. H. Turnbull, A. Yavari, *Inorg. Chim. Acta* **1985**, *106*, 109–114.

[35] P. A. Cusack, P. J. Smith, J. D. Donaldson, *J. Chem. Soc., Dalton Trans.* **1982**, *2*, 439–444.

[36] R. Krämer, M. Maurus, R. Bergs, K. Polborn, K. Sünkel, B. Wagner, W. Beck, *Chem. Ber.* **1993**, *126*, 1969–1980.

[37] L. F. Krylova, A. V. Golovin, *J. Structural Chem.* **2000**, *41*, 254−262.

[38] M. Nath, S. Goyal, *Phosphorus, Sulfur and Silicon* **2002**, *177*, 841–851.

[39] S. Dragota, R. Bertermann, C. Burschka, M. Penka, R. Tacke, *Organometallics* **2005**, *24*, 5560–5568.

[40] I. Richter, *Dissertation*, Universität Würzburg, **2000**.

[41] L. Birkofer, A. Ritter, *Chem. Ber.* **1960**, *93*, 424−427.

[42] G. González-Garcia, J. A. Gutiérrez, S. Cota, S. Metz, R. Bertermann, C. Burschka, R. Tacke, *Z. Anorg. Allg. Chem.* **2008**, *634*, 1281−1286.

[43] N. Mondal, D. K. Dey, S. Mitra, K. M. Abdul Malik, *Polyhedron* **2000**, *19*, 2707−2711.

[44] K. Rühlmann, J. Hills, *Liebigs Ann. Chem.* **1965**, *683*, 211−215.

[45] J. Schrami, M. Kvičalová, J. Schwarzová, J. Velišek, *Magnetic Resonance in Chemistry* **1994**, *32*, 591−595.

[46] S. J. Opella, M. H. Frey, T. A. Cross, *J. Am. Chem. Soc*. **1979**, *101*, 5856−5857.

[47] A. Olivieri, L. Frydman, M. Grasselli, L. Diaz, *Magnetic Resonance in Chemistry* **1988**, *26*, 615−618.

[48] a) J. G. Hexem, M. H. Frey, S. J. Opella, *J. Am. Chem. Soc*. **1981**, *103*, 224−226; b) J. Böhm, D. Fenzke, H. Pfeifer, *J. Magn. Res.* **1983**, *55*, 197−204.

[49] G. M. Sheldrick, SHELXS-97 Program for crystal structure solution, University of Göttingen, Göttingen, Germany, **1997**.

[50] G. M. Sheldrick, SHELXL-97 Program for crystal structure refinement, University of Göttingen, Göttingen, Germany, **1997**.

[51] R. R. Holmes, *Progr. Inorg. Chem.* **1984**, *32*, 119−235.

[52] O. Seiler, C. Burschka, T. Fenske, D. Troegel, R. Tacke, *Inorg. Chem.* **2007**, *46*, 5419−5424.

[53] O. Seiler, *Dissertation*, Universität Würzburg, **2005**.

[54] The hydrogen bonding systems were analysed by using the program system PLATON: a) A. L. Spek, PLATON; University of Utrecht: Utrecht, The Netherlands, **1998**; b) A. L. Spek, Acta Crystallogr., Sect. A **1990**, *46*, C34.

[55] S. Dragota, *Dissertation*, Universität Würzburg, **2005**.

[56] O. Seiler, C. Burschka, M. Fischer, M. Penka, R. Tacke, *Inorg. Chem*. **2005**, *44*, 2337−2346.

[57] O. Seiler, C. Burschka, K. Götz, M. Kaupp, S. Metz, R. Tacke, *Z. Anorg. Allg. Chem.* **2007**, *633*, 2667–2670.

[58] a) E. L. Muetterties, L. J. Guggenberger, *J. Am. Chem. Soc.* **1974**, *96*, 1748−1756; b) R. R. Holmes, J. A. Deiters, *J. Am. Chem. Soc.* **1977**, *99*, 3318−3326; c) The degree of distortion was calculated by using the dihedral angle method described in refs.

[57a] and [57b]. All nine dihedral angles and the values for the reference geometry of the ideal square pyramid given in ref. 57a] were considered for this calculation.

[59] O. Seiler, C. Burschka, S. Metz, M. Penka, R. Tacke, *Chem. Eur. J.* **2005**, *11*, 7379−7386.

[60] O. Seiler, R. Bertermann, N. Buggisch, C. Burschka, M. Penka, D. Tebbe, R. Tacke, *Z. Anorg. Allg. Chem.* **2003**, *639*, 1403–1411.

[61] The disorder originates from two different conformations of the envelope shaped five-membered ring Si–N3–C6–C7–N4, which cause a split position of the atom C6, so that C6A (80% occupied) approaches N1 while C6B (20% occupied) approaches N2. The split positions C6A and C6B lead to a similar splitting of the atoms C4 and C5 which are bonded to the common atom N3.

[62] J. Wagler, U. Böhme, E. Brendler, B. Thomas, S. Goutal, H. Mayr, B. Kempf, G. Ya. Remennikov, G. Roewer, *Inorg. Chim. Acta* **2005**, *358*, 4270−4286.

[63] F. Mucha, J. Haberecht, U. Böhme, G. Roewer, *Monatsh. Chem.* **1999**, *130*, 117–132.

[64] J. Wagler, *Dissertation*, Universität Freiburg, **2004**.

[65] K. Lippe, D. Gerlach, E. Kroke, J. Wagler, *Organometallics* **2009**, *28*, 621−629.

[66] J. Wagler, G. Roewer, *Inorg. Chim. Acta* **2007**, *360*, 1717−1724.

[67] M. v. Arnim, R. Ahlrichs, *J. Comput. Chem.* **1998**, *19*, 1746−1757.

[68] O. Treutler, R. Ahlrichs, *J. Chem. Phys.* **1995**, *102*, 346−354.

[69] R. Ahlrichs, M. Bär, M. Häser, H. Horn, C. Kölmel, *Chem. Phys. Let.* **1989**, *162*, 165−169.

[70] a) J. P. Perdew, *Phys. Rev. B* **1986**, *33*, 8822−8824; b) A. D. Becke, *Phys. Rev. A* **1988**, *38*, 3098−3100.

[71] A. Schäfer, H. Horn, R. Ahlrichs, *J. Chem. Phys.* **1992**, *97*, 2571−2577.

[72] R. G. Neville, J. J. McGee, *Inorganic Syntheses*, *Vol. VIII* (Ed.: H. F. Holtzclaw, Jr.), McGraw-Hill, New York, **1966**, pp. 23−27.

[73] R. G. Neville, J. J. McGee, *Inorganic Syntheses*, *Vol. VIII* (Ed.: H. F. Holtzclaw, Jr.), McGraw-Hill, New York, **1966**, pp. 27−31.

[74] G. S. Forbes, H. H. Anderson, *J. Am. Chem. Soc.* **1948**, *70,* 1043–1044.

[75] S. Falgner, C. Burschka, S. Wagner, A. Böhm, J. O. Daiß, R. Tacke, *Organometallics* **2009**, *28*, 6059−6066.

[76] R. Tacke, M. Pülm, I. Richter, B. Wagner, R. Willeke, *Z. Anorg. Allg. Chem.* **1999**, *625*, 2169–2177.

[77] M. Kabak, A. Elmali, Y. Elerman, *J. Mol. Struct.* **1998**, *470,* 295–300.

[78] F. Mucha, U. Böhme, G. Roewer, *Chem. Commun.* **1998**, *130*, 1289–1230.

[79] J. Wagler, U. Böhme, G. Roewer, *Angew. Chem.* **2002**, *114*, 1825–1827; *Angew. Chem. Int. Ed.* **2002**, *41*, 1732−1734.

[80] J. Wagler, T. Doert, G. Roewer, *Angew. Chem.* **2004**, *116*, 2495–2498; *Angew. Chem. Int. Ed.* **2004**, *43*, 2441−2444.

[81] U. Dinjus, H. Stahl, E. Uhlig, *Z. Anorg. Allg. Chem.* **1980**, *464*, 37–44.

[82] The accuracy of the elemental analysis is affected by partial loss of acetonitrile even at storage under standard conditions of temperature and pressure.

[83] The accuracy of the elemental analysis is affected by partial loss of acetonitrile and *n*-pentane even at storage under standard conditions of temperature and pressure.

[84] The ^{1}H and ^{13}C spectra of **56** showed small amounts of impurities that may indicate a slow decomposition of the hexacoordinate silicon(IV) complex. Due to the poor solubility of **56** in CD_2Cl_2, no ^{15}N NMR signals could be detected in solution.

[85] The NMR spectra of **64** showed in solution more than one set of resonance signals indicating the existence of three isomers.

Appendix A: Crystal Structure Data

Table A1. Crystal data and experimental parameters for the crystal structure analyses of **33**–**35**.

	33	**34**	**35**
empirical formula	$C_{17}H_{19}NO_5Si$	$C_{37}H_{27}NO_5Si$	$C_{12}H_{16}O_7Si$
formula mass [g·mol^{-1}]	345.42	593.69	300.34
temperature [K]	193(2)	173(2)	100(2)
λ (Mo Kα) [Å]	0.71073	0.71073	0.71073
crystal system	monoclinic	monoclinic	monoclinic
space group (No.)	$P2_1/c$ (14)	$P2_1/n$ (14)	C_2/c (15)
a [Å]	8.4741(12)	9.3201(19)	13(2)
b [Å]	13.4598(15)	22.229(4)	11.939
c [Å]	15.308(2)	14.074(3)	18.620
β [°]	92.666(18)	90.58(3)	100.53
V [Å^3]	1744.1(4)	2915.6(10)	2787(437)
Z	4	4	8
D_{calcd} [g·cm^{-3}]	1.315	1.353	1.432
μ [mm^{-1}]	0.160	0.128	0.197
F(000)	728	1240	1264
crystal size [mm]	0.5 × 0.3 × 0.3	0.5 × 0.25 × 0.15	0.25 × 0.2 × 0.06
2θ range [°]	4.82–56.14	4.74–56.26	4.44–61.44
index ranges	$-11 \le h \le 11$, $-17 \le k \le 17$, $-20 \le l \le 20$	$-12 \le h \le 11$, $-29 \le k \le 29$, $-17 \le l \le 18$	$-18 \le h \le 17$, $0 \le k \le 17$, $0 \le l \le 26$
no. of collected reflections	16068	24867	6216
no. of independent reflections	4044	6931	6301
R_{int}	0.0520	0.0430	0.0000
no. of reflections used	4044	6931	6301
restraints	0	30	0
no. of parameters	221	406	186
S[a)]	1.052	1.028	1.143
weight parameters a/b[b)]	0.0716/0.2843	0.0603/0.5634	0.0664/1.8977
$R1$[c)] [$I > 2\sigma(I)$]	0.0411	0.0488	0.0441
$wR2$[d)] (all data)	0.1199	0.1235	0.1300
max./min. residual electron density [e·Å^{-3}]	+0.342/–0.300	+0.285/–0.290	+0.383/–0.350

[a)] $S = \{\Sigma[w(F_o^2 - F_c^2)^2]/(n-p)\}^{0.5}$; n = no. of reflections; p = no. of parameters.
[b)] $w^{-1} = \sigma^2(F_o^2) + (aP)^2 + bP$, with $P = [\max(F_o^2,0) + 2F_c^2]/3$.
[c)] $R1 = \Sigma||F_o| - |F_c||/\Sigma|F_o|$.
[d)] $wR2 = \{\Sigma[w(F_o^2 - F_c^2)^2]/\Sigma[w(F_o^2)^2]\}^{0.5}$.

Table A2. Crystal data and experimental parameters for the crystal structure analyses of **36**, **38**, and **39**.

	36	**38**	**39**
empirical formula	$C_{12}H_{14}O_8Si$	$C_7H_{14}N_2O_4Si$	$C_{19}H_{22}N_2O_4Si$
formula mass [g·mol^{-1}]	314.32	218.29	370.48
temperature [K]	100(2)	193(2)	193(2)
λ (Mo Kα) [Å]	0.71073	0.71073	0.71073
crystal system	monoclinic	orthorhombic	orthorhombic
space group (No.)	$P2_1/c$ (14)	$P2_12_12_1$ (19)	$P2_12_12_1$ (19)
a [Å]	12.2975(8)	7.6563(6)	6.5828(6)
b [Å]	8.0588(5)	10.9386(9)	23.3334(18)
c [Å]	14.6828(9)	12.4438(12)	24.524(2)
β [°]	106.7270(10)	90.0	90.0
V [Å^3]	1393.54(15)	1042.16(16)	3766.9(6)
Z	4	4	8
D_{calcd} [g·cm^{-3}]	1.498	1.391	1.307
μ [mm^{-1}]	0.206	0.218	0.151
F(000)	656	464	1568
crystal size [mm]	0.33 × 0.16 × 0.14	0.5 × 0.5 × 0.5	0.5 × 0.4 × 0.3
2θ range [°]	3.46–56.58	7.28–56.16	4.82–55.96
index ranges	$-16 \le h \le 16$, $-10 \le k \le 10$, $-19 \le l \le 19$	$-10 \le h \le 9$, $-11 \le k \le 14$, $-16 \le l \le 16$	$-8 \le h \le 8$, $-29 \le k \le 30$, $-26 \le l \le 32$
no. of collected reflections	33679	6283	27644
no. of independent reflections	3468	2512	8931
R_{int}	0.0416	0.0220	0.0414
no. of reflections used	3468	2512	8931
restraints	0	0	0
no. of parameters	194	139	489
S[a)]	1.045	1.061	0.977
weight parameters a/b[b)]	0.0516/0.6792	0.0530/0.0676	0.0455/0.0000
$R1$[c)] [$I > 2\sigma(I)$]	0.0333	0.0301	0.0328
$wR2$[d)] (all data)	0.0965	0.0801	0.0755
max./min. residual electron density [e·Å^{-3}]	+0.403/–0.341	+0.235/–0.151	+0.276/–0.178

[a)] $S = \{\Sigma[w(F_o^2 - F_c^2)^2]/(n-p)\}^{0.5}$; n = no. of reflections; p = no. of parameters.
[b)] $w^{-1} = \sigma^2(F_o^2) + (aP)^2 + bP$, with $P = [\max(F_o^2,0) + 2F_c^2]/3$.
[c)] $R1 = \Sigma||F_o| - |F_c||/\Sigma|F_o|$.
[d)] $wR2 = \{\Sigma[w(F_o^2 - F_c^2)^2]/\Sigma[w(F_o^2)^2]\}^{0.5}$.

Table A3. Crystal data and experimental parameters for the crystal structure analyses of **43**·CH_3CN, **44**, and **46**·C_5H_{12}·1/2CH_3CN.

	43·CH_3CN	**44**	**46**·C_5H_{12}·1/2CH_3CN
empirical formula	$C_{14}H_{19}N_3O_4Si$	$C_{24}H_{24}N_2O_4Si$	$C_{24}H_{41.50}N_{2.50}O_4Si$
formula mass [g·mol^{-1}]	321.41	432.54	457.19
temperature [K]	193(2)	100(2)	100(2)
λ (Mo Kα) [Å]	0.71073	0.71073	0.71073
crystal system	orthorhombic	monoclinic	tetragonal
space group (No.)	$P2_12_12_1$ (19)	$P2_1$ (4)	$I4_1$ (80)
a [Å]	8.5016(7)	6.6931(4)	17.9928(2)
b [Å]	11.1129(13)	13.5206(9)	17.9928(2)
c [Å]	17.5068(16)	11.9450(8)	16.1878(4)
β [°]	90.0	103.534(2)	90
V [Å^3]	1654.0(3)	1050.94(12)	5240.65(15)
Z	4	2	8
D_{calcd} [g·cm^{-3}]	1.291	1.367	1.159
μ [mm^{-1}]	0.162	0.147	0.121
F(000)	680	456	1992
crystal size [mm]	0.5 × 0.5 × 0.5	0.36 × 0.1 × 0.1	0.3 × 0.1 × 0.03
2θ range [°]	5.92–56.08	3.50–57.04	3.20–66.30
index ranges	$-11 \le h \le 10$, $-14 \le k \le 13$, $-23 \le l \le 18$	$-8 \le h \le 8$, $-18 \le k \le 16$, $-16 \le l \le 15$	$-27 \le h \le 27$, $-27 \le k \le 27$, $-24 \le l \le 24$
no. of collected reflections	8202	30894	102915
no. of independent reflections	3983	5062	10016
R_{int}	0.0349	0.0520	0.0475
no. of reflections used	3983	5062	10016
restraints	0	1	41
no. of parameters	211	289	304
S[a)]	1.072	1.028	1.077
weight parameters a/b[b)]	0.0630/0.0000	0.0264/0.3140	0.0604/1.9965
$R1$[c)] [$I > 2\sigma(I)$]	0.0445	0.0268	0.0373
$wR2$[d)] (all data)	0.1028	0.0666	0.1032
max./min. residual electron density [e·Å^{-3}]	+0.345/–0.209	+0.263/–0.192	+0.494/–0.438

[a)] $S = \{\Sigma[w(F_o^2 - F_c^2)^2]/(n-p)\}^{0.5}$; n = no. of reflections; p = no. of parameters.
[b)] $w^{-1} = \sigma^2(F_o^2) + (aP)^2 + bP$, with $P = [\max(F_o^2,0) + 2F_c^2]/3$.
[c)] $R1 = \Sigma||F_o| - |F_c||/\Sigma|F_o|$.
[d)] $wR2 = \{\Sigma[w(F_o^2 - F_c^2)^2]/\Sigma[w(F_o^2)^2]\}^{0.5}$.

Table A4. Crystal data and experimental parameters for the crystal structure analyses of **50**, **54**, and **55**.

	50	**54**	**55**
empirical formula	$C_8H_{12}N_4O_6Si$	$C_{13}H_{14}N_2O_3Si$	$C_{19}H_{21}N_3OSSi$
formula mass [g·mol^{-1}]	288.31	274.35	367.54
temperature [K]	100(2)	173(2)	193(2)
λ (Mo Kα) [Å]	0.71073	0.71073	0.71073
crystal system	tetragonal	monoclinic	orthorhombic
space group (No.)	$P4_12_12$ (92)	$P2_1/n$ (14)	*Pbca* (61)
a [Å]	7.69110(10)	7.2636(15)	9.7847(14)
b [Å]	7.69110(10)	8.5367(17)	10.5451(10)
c [Å]	20.1180(4)	20.867(4)	36.065(4)
β [°]	90.0	99.82(3)	90.0
V [Å^3]	1190.04(3)	1275.0(4)	3721.2(8)
Z	4	4	8
D_{calcd} [g·cm^{-3}]	1.609	1.429	1.312
μ [mm^{-1}]	0.230	0.190	0.250
F(000)	600	576	1552
crystal size [mm]	0.2 × 0.1 × 0.1	0.5 × 0.4 × 0.3	0.5 × 0.4 × 0.3
2θ range [°]	5.68–61.00	6.20–56.00	4.52–51.74
index ranges	$-10 \le h \le 10$, $-7 \le k \le 10$, $-25 \le l \le 28$	$-9 \le h \le 9$, $-11 \le k \le 10$, $-27 \le l \le 27$	$-12 \le h \le 12$, $-11 \le k \le 12$, $-44 \le l \le 44$
no. of collected reflections	9842	12855	27775
no. of independent reflections	1812	3035	3500
R_{int}	0.0357	0.0492	0.0496
no. of reflections used	1812	3035	3500
restraints	0	0	0
no. of parameters	97	175	228
S[a)]	1.146	1.035	1.065
weight parameters a/b[b)]	0.0405/0.3333	0.0666/0.1240	0.0512/0.8682
$R1$[c)] $[I > 2\sigma(I)]$	0.0307	0.0389	0.0364
$wR2$[d)] (all data)	0.0816	0.1064	0.0961
max./min. residual electron density [e·Å^{-3}]	+0.358/–0.214	+0.472/–0.254	+0.217/–0.195

[a)] $S = \{\Sigma[w(F_o^2 - F_c^2)^2]/(n-p)\}^{0.5}$; n = no. of reflections; p = no. of parameters.
[b)] $w^{-1} = \sigma^2(F_o^2) + (aP)^2 + bP$, with $P = [\max(F_o^2,0) + 2F_c^2]/3$.
[c)] $R1 = \Sigma||F_o| - |F_c||/\Sigma|F_o|$.
[d)] $wR2 = \{\Sigma[w(F_o^2 - F_c^2)^2]/\Sigma[w(F_o^2)^2]\}^{0.5}$.

Table A5. Crystal data and experimental parameters for the crystal structure analyses of **56**–**58**.

	56	**57**	**58**
empirical formula	$C_{15}H_{20}N_4OS_2Si$	$C_{12}H_{17}N_5O_4Si$	$C_{17}H_{22}N_4O_3Si$
formula mass [g·mol^{-1}]	364.56	323.40	358.48
temperature [K]	100(2)	100(2)	123(2)
λ (Mo Kα) [Å]	0.71073	0.71073	0.71073
crystal system	monoclinic	trigonal	monoclinic
space group (No.)	$P2_1/n$ (14)	$R\bar{3}$ (148)	$P2_1/c$ (14)
a [Å]	8.5416(3)	32.966(2)	14.841(2)
b [Å]	12.1365(4)	32.966(2)	8.3712(11)
c [Å]	17.3355(6)	8.1473(5)	14.6084(18)
β [°]	100.7490(10)	90.0	94.990(3)
V [Å^3]	1765.55(10)	7668.0(8)	1808.0(4)
Z	4	18	4
D_{calcd} [g·cm^{-3}]	1.372	1.261	1.317
μ [mm^{-1}]	0.378	0.161	0.154
F(000)	768	3060	760
crystal size [mm]	0.26 × 0.19 × 0.08	0.4 × 0.1 × 0.1	0.27 × 0.18 × 0.05
2θ range [°]	4.12–56.74	4.28–59.54	2.76–66.26
index ranges	$-10 \le h \le 11$, $-15 \le k \le 16$, $-23 \le l \le 23$	$-45 \le h \le 22$, $0 \le k \le 46$, $0 \le l \le 11$	$-22 \le h \le 22$, $-12 \le k \le 12$, $-21 \le l \le 16$
no. of collected reflections	48065	4873	31330
no. of independent reflections	4364	4873	6756
R_{int}	0.0456	0.0000	0.0740
no. of reflections used	4364	4873	6756
restraints	0	0	0
no. of parameters	242	203	230
S[a)]	1.044	1.101	1.036
weight parameters a/b[b)]	0.0334/0.9517	0.0743/5.39650	0.066600/0.266600
$R1$[c)] [$I > 2\sigma(I)$]	0.0308	0.0396	0.0495
$wR2$[d)] (all data)	0.0821	0.1246	0.1506
max./min. residual electron density [e·Å^{-3}]	+0.607/–0.556	+ 0.509/– 0.414	+0.360/–0.384

[a)] $S = \{\Sigma[w(F_o^2 - F_c^2)^2]/(n-p)\}^{0.5}$; n = no. of reflections; p = no. of parameters.
[b)] $w^{-1} = \sigma^2(F_o^2) + (aP)^2 + bP$, with $P = [\max(F_o^2,0) + 2F_c^2]/3$.
[c)] $R1 = \Sigma||F_o| - |F_c||/\Sigma|F_o|$.
[d)] $wR2 = \{\Sigma[w(F_o^2 - F_c^2)^2]/\Sigma[w(F_o^2)^2]\}^{0.5}$.

Table A6. Crystal data and experimental parameters for the crystal structure analyses of **59**, **60**, and **62**.

	59	**60**	**62**
empirical formula	$C_{14}H_{21}N_3O_3Si$	$C_{19}H_{23}N_3O_3Si$	$C_{18}H_{17}N_3O_3Si$
formula mass [g·mol^{-1}]	307.43	369.49	351.44
temperature [K]	173(2)	173(2)	100(2)
λ (Mo Kα) [Å]	0.71073	0.71073	0.71073
crystal system	monoclinic	monoclinic	orthorhombic
space group (No.)	*C*2/*c* (15)	$P2_1/c$ (14)	$Pca2_1/n$ (29)
a [Å]	11.9820(9)	12.003(2)	18.2956(5)
b [Å]	9.3295(6)	12.789(3)	6.7270(2)
c [Å]	27.1744(18)	12.922(3)	13.1328(3)
β [°]	96.631(3)	107.98(3)	90.0
V [Å^3]	3017.4(4)	1886.7(7)	1616.31(7)
Z	8	4	4
D_{calcd} [g·cm^{-3}]	1.353	1.301	1.444
μ [mm^{-1}]	0.170	0.148	0.169
F(000)	1312	784	736
crystal size [mm]	0.4 × 0.3 × 0.2	0.5 × 0.3 × 0.2	0.30 × 0.13 × 0.05
2θ range [°]	3.02–56.68	4.60–56.46	4.46–56.70
index ranges	$-15 \le h \le 15$, $-12 \le k \le 11$, $-36 \le l \le 35$	$-15 \le h \le 15$, $-16 \le k \le 16$, $-17 \le l \le 17$	$-24 \le h \le 24$, $-8 \le k \le 8$, $-15 \le l \le 17$
no. of collected reflections	39429	32525	24880
no. of independent reflections	3741	4592	3884
R_{int}	0.0730	0.0788	0.0461
no. of reflections used	3741	4592	3884
restraints	0	64	1
no. of parameters	195	267	227
S[a]	1.141	1.047	1.062
weight parameters *a*/*b*[b]	0.0401/6.7273	0.0539/0.4893	0.0471/0.3192
*R*1[c] [$I > 2\sigma(I)$]	0.0486	0.0405	0.0298
*wR*2[d] (all data)	0.1259	0.1110	0.0790
max./min. residual electron density [e·Å^{-3}]	+0.495/–0.361	+0.299/–0.260	+0.333/–0.196

[a] $S = \{\Sigma[w(F_o^2 - F_c^2)^2]/(n-p)\}^{0.5}$; *n* = no. of reflections; *p* = no. of parameters.
[b] $w^{-1} = \sigma^2(F_o^2) + (aP)^2 + bP$, with $P = [\max(F_o^2,0) + 2F_c^2]/3$.
[c] $R1 = \Sigma||F_o| - |F_c||/\Sigma|F_o|$.
[d] $wR2 = \{\Sigma[w(F_o^2 - F_c^2)^2]/\Sigma[w(F_o^2)^2]\}^{0.5}$.

Table A7. Crystal data and experimental parameters for the crystal structure analyses of **63**, **64**, and **65**·2CH_3CN.

	63	**64**	**65**·2CH_3CN
empirical formula	$C_{23}H_{19}N_3O_3Si$	$C_{18}H_{14}N_4O_2S_2Si$	$C_{38}H_{34}N_8O_7Si_2$
formula mass [g·mol^{-1}]	413.50	410.54	770.91
temperature [K]	193(2)	193(2)	98(2)
λ (Mo Kα) [Å]	0.71073	0.71073	0.71073
crystal system	monoclinic	rhombohedral	monoclinic
space group (No.)	$P2_1/n$ (14)	$R\bar{3}$ (148)	$P2_1/c$ (14)
a [Å]	7.2540(15)	33.761(4)	10.3363(2)
b [Å]	18.572(4)	33.761(4)	16.1359(4)
c [Å]	14.313(3)	8.5880(8)	11.2908(3)
β [°]	101.03(3)	90.0	103.3650(10)
V [Å^3]	1892.6(7)	8477.2(15)	1832.14(8)
Z	4	18	2
D_{calcd} [g·cm^{-3}]	1.451	1.448	1.397
μ [mm^{-1}]	0.157	0.368	0.160
F(000)	864	3816	804
crystal size [mm]	0.5 × 0.4 × 0.3	0.5 × 0.3 × 0.2	0.34 × 0.19 × 0.10
2θ range [°]	4.38–56.10	4.82–55.90	4.06–56.68
index ranges	$-9 \le h \le 9$, $-24 \le k \le 24$, $-18 \le l \le 18$	$-44 \le h \le 44$, $-44 \le k \le 44$, $-11 \le l \le 11$	$-13 \le h \le 13$, $-21 \le k \le 21$, $-13 \le l \le 15$
no. of collected reflections	19861	27221	70557
no. of independent reflections	4553	4486	4549
R_{int}	0.1306	0.0463	0.0475
no. of reflections used	4553	4486	4549
restraints	0	0	0
no. of parameters	271	244	251
S[a)]	1.036	1.033	1.048
weight parameters a/b[b)]	0.0851/0.3499	0.0696/17.6925	0.0470/0.7655
$R1$[c)] [$I > 2\sigma(I)$]	0.0617	0.0521	0.0312
$wR2$[d)] (all data)	0.1571	0.1387	0.0900
max./min. residual electron density [e·Å^{-3}]	+0.594/–0.397	+1.180/–0.916	+0.409/–0.333

[a)] $S = \{\Sigma[w(F_o^2 - F_c^2)^2]/(n-p)\}^{0.5}$; n = no. of reflections; p = no. of parameters.
[b)] $w^{-1} = \sigma^2(F_o^2) + (aP)^2 + bP$, with $P = [\max(F_o^2,0) + 2F_c^2]/3$.
[c)] $R1 = \Sigma||F_o| - |F_c||/\Sigma|F_o|$.
[d)] $wR2 = \{\Sigma[w(F_o^2 - F_c^2)^2]/\Sigma[w(F_o^2)^2]\}^{0.5}$.

Silicon(IV) complex **33**

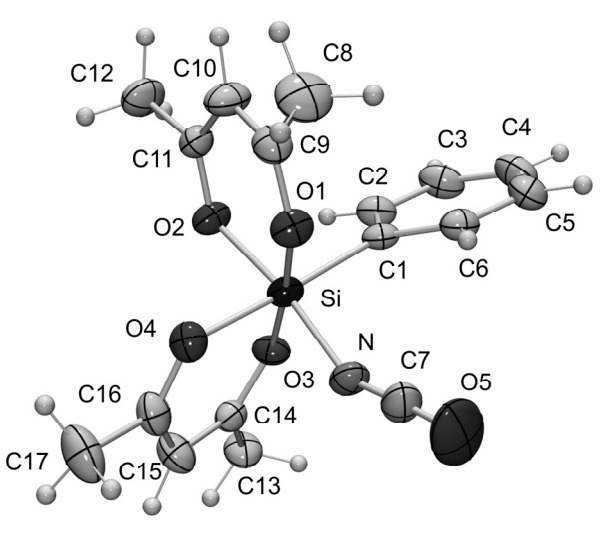

Figure A1: Molecular structure of the silicon (IV) complex **33** in the crystal showing the atomic numbering scheme (probability level of displacement ellipsoids 50%).

Table A8. Atomic coordinates ($\times 10^4$) and equivalent isotropic displacement parameters ($Å^2 \times 10^3$) for **33**. U_{eq} is defined as one third of the trace of the orthogonalized U_{ij} tensor.

	x	y	z	U_{eq}
Si	2754(1)	2666(1)	9830(1)	27(1)
N	1921(2)	3564(1)	9060(1)	36(1)
O1	1631(1)	1703(1)	9275(1)	34(1)
O2	3399(1)	1847(1)	10712(1)	33(1)
O3	3774(1)	3613(1)	10451(1)	31(1)
O4	987(1)	2834(1)	10448(1)	36(1)
O5	719(3)	3918(2)	7704(1)	101(1)
C1	4600(2)	2429(1)	9188(1)	28(1)
C2	6098(2)	2394(1)	9600(1)	34(1)
C3	7465(2)	2306(1)	9140(1)	43(1)
C4	7356(2)	2241(1)	8241(1)	47(1)
C5	5891(2)	2246(1)	7811(1)	42(1)
C6	4535(2)	2334(1)	8281(1)	34(1)
C7	1336(2)	3722(1)	8386(1)	46(1)
C8	960(3)	157(2)	8689(1)	55(1)
C9	1820(2)	767(1)	9367(1)	35(1)
C10	2722(2)	345(1)	10038(1)	44(1)
Cl1	3407(2)	902(1)	10707(1)	33(1)
C12	4184(3)	427(1)	11488(1)	49(1)
C13	4361(2)	5067(1)	11235(1)	40(1)
C14	3199(2)	4312(1)	10902(1)	30(1)
C15	1628(2)	4363(1)	11095(1)	41(1)
C16	600(2)	3601(1)	10880(1)	38(1)
C17	-1075(2)	3628(2)	11145(1)	57(1)

Table A9. Bond lengths [Å] and angles [°] for **33**.

Si–O1	1.7977(11)	O4–C16	1.2769(19)	C10–C11	1.376(2)
Si–O2	1.8079(11)	O5–C7	1.176(2)	C11–C12	1.483(2)
Si–O3	1.7888(10)	C1–C2	1.391(2)	C13–C14	1.489(2)
Si–O4	1.8217(12)	C1–C6	1.394(2)	C14–C15	1.379(2)
Si–N	1.8087(13)	C2–C3	1.388(2)	C15–C16	1.375(2)
Si–Cl	1.9130(16)	C3–C4	1.378(3)	C16–C17	1.495(2)
N-C7	1.144(2)	C4–C5	1.378(3)		
O1–C9	1.2768(18)	C5–C6	1.389(2)		
O2–C11	1.2719(17)	C8–C9	1.488(2)		
O3–C14	1.2763(17)	C9–C10	1.374(2)		
O1–Si–O2	92.76(5)	C7–N–Si	148.37(14)	O1–C9–C8	114.42(15)
O1–Si–O3	175.61(5)	C9–O1–Si	126.76(10)	C10–C9–C8	122.03(16)
O1–Si–O4	84.56(5)	C11–O2–Si	127.36(10)	C9–C10–C11	122.16(15)
O1–Si–N	89.54(6)	C14–O3–Si	128.69(10)	O2–C11–C10	123.16(14)
O2–Si–O3	85.18(5)	C16–O4–Si	127.30(10)	O2–C11–C12	115.41(14)
O2–Si-O4	85.12(5)	C2–C1–C6	116.19(14)	C10–C11–C12	121.42(14)
O2–Si–N	171.71(6)	C2–C1–Si	121.60(11)	O3–C14–C15	123.32(14)
O3–Si–N	91.97(6)	C6–C1–Si	122.12(12)	O3–C14–C13	115.15(14)
O3–Si–O4	91.39(5)	C3–C2–C1	122.59(16)	C15–C14–C13	121.50(14)
N–Si–O4	87.18(6)	C4–C3–C2	119.56(17)	C16–C15–C14	121.22(15)
O3–Si–C1	90.32(6)	C5–C4–C3	119.57(16)	O4–C16–C15	123.50(15)
O1–Si–C1	93.67(6)	C4–C5–C6	120.13(16)	O4–C16–C17	115.48(15)
O2–Si–C1	93.18(6)	C5–C6–C1	121.91(16)	C15–C16–C17	121.02(15)
N–Si–C1	94.62(6)	N–C7–O5	177.5(2)		
O4–Si–C1	177.48(6)	O1–C9–C10	123.54(14)		

Silicon(IV) complex **34**

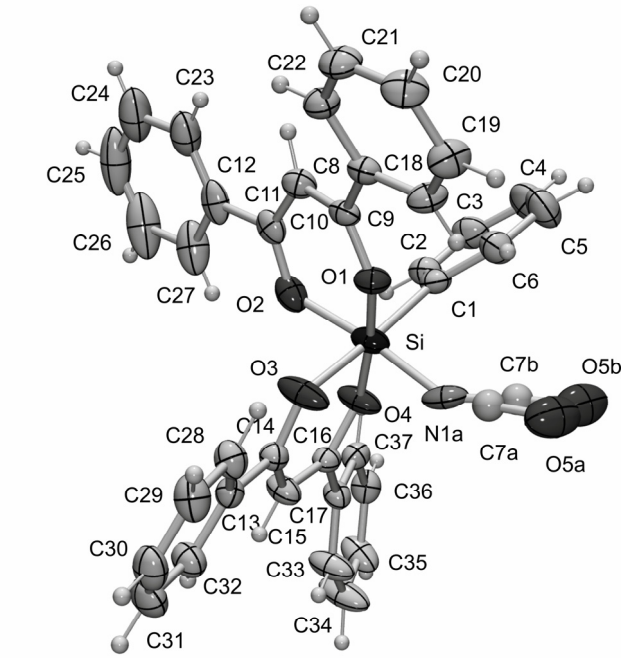

Figure A2: Molecular structure of the silicon(IV) complex **34** in the crystal showing the atomic numbering scheme (probability level of displacement ellipsoids 50%).

Table A10. Atomic coordinates ($\times 10^4$) and equivalent isotropic displacement parameters ($Å^2 \times 10^3$) for **34**. U_{eq} is defined as one third of the trace of the orthogonalized U_{ij} tensor.

	x	y	z	U_{eq}
C1	794(2)	9216(1)	2779(1)	33(1)
C2	1162(2)	9720(1)	3318(1)	38(1)
C3	146(3)	10097(1)	3704(2)	49(1)
C4	–1282(3)	9981(1)	3562(2)	62(1)
C5	–1695(3)	9490(1)	3026(2)	62(1)
C6	–668(2)	9116(1)	2641(2)	45(1)
C7B	613(6)	7716(2)	2767(3)	35(1)
C8	38(2)	8743(1)	–249(1)	31(1)
C9	1022(2)	8954(1)	504(1)	30(1)
C10	1694(2)	9506(1)	472(1)	35(1)
C11	2834(2)	9643(1)	1071(1)	35(1)
C12	3746(2)	10177(1)	939(2)	45(1)
C13	5290(2)	7496(1)	1444(1)	31(1)
C14	4630(2)	7956(1)	2051(1)	30(1)
C15	5165(2)	8102(1)	2939(1)	38(1)
C16	4475(2)	8497(1)	3528(1)	29(1)
C17	5024(2)	8635(1)	4489(1)	31(1)
C18	–827(2)	8245(1)	–73(1)	38(1)
C19	–1722(2)	8020(1)	–770(1)	44(1)
C20	–1759(2)	8286(1)	–1653(1)	46(1)
C21	–914(2)	8776(1)	–1838(1)	45(1)
C22	–20(2)	9009(1)	–1145(1)	38(1)
C23	3527(3)	10577(1)	198(2)	56(1)
C24	4417(3)	11069(1)	97(2)	74(1)
C25	5521(4)	11164(1)	726(3)	89(1)
C26	5752(3)	10773(2)	1459(2)	85(1)
C27	4874(3)	10275(1)	1571(2)	62(1)
C28	4564(2)	7310(1)	628(1)	38(1)
C29	5094(2)	6845(1)	89(2)	46(1)
C30	6362(2)	6576(1)	333(2)	47(1)
C31	7115(2)	6767(1)	1121(2)	51(1)
C32	6580(2)	7222(1)	1681(1)	41(1)
C33	5861(3)	8224(1)	4990(2)	55(1)
C34	6310(3)	8351(1)	5907(2)	68(1)
C35	5963(2)	8893(1)	6323(1)	52(1)
C36	5118(2)	9298(1)	5837(1)	39(1)
C37	4635(2)	9168(1)	4930(1)	32(1)
O1	1244(1)	8570(1)	1173(1)	34(1)
O2	3210(1)	9297(1)	1764(1)	41(1)
O3	3510(2)	8199(1)	1715(1)	55(1)
O4	3321(2)	8770(1)	3294(1)	46(1)
Si	2196(1)	8686(1)	2266(1)	36(1)
N1A	1355(2)	8002(1)	2737(1)	44(1)
C7A	139(6)	7746(2)	2980(4)	34(1)
O5A	-885(8)	7493(3)	3203(7)	75(2)
N1B	1355(2)	8002(1)	2737(1)	44(1)
C7B	613(6)	7716(2)	2767(3)	35(1)
O5B	–417(8)	7361(3)	2900(7)	78(2)

Table A11. Bond lengths [Å] and angles [°] for **34**.

C1–C2	1.393(3)	C12–C27	1.387(3)	C26–C27	1.387(4)
C1–C6	1.392(3)	C13–C32	1.386(3)	C28–C29	1.376(3)
C1–Si	1.9063(19)	C13–C28	1.389(3)	C29–C30	1.366(3)
C2–C3	1.382(3)	C13–C14	1.471(2)	C30–C31	1.374(3)
C3–C4	1.369(3)	C14–O3	1.264(2)	C31–C32	1.378(3)
C4–C5	1.378(4)	C14–C15	1.379(2)	C33–C34	1.382(3)
C5–C6	1.382(3)	C15–C16	1.373(2)	C34–C35	1.379(3)
C7A–O5A	1.154(7)	C16–O4	1.275(2)	C35–C36	1.374(3)
C7B–O5B	1.258(6)	C16–C17	1.474(2)	C36–C37	1.380(3)
C8–C18	1.393(3)	C17–C37	1.386(2)	O1–Si	1.7859(14)
C8–C9	1.471(2)	C17–C33	1.389(3)	O2–Si	1.8017(16)
C8–C22	1.393(2)	C18–C19	1.375(3)	O3–Si	1.8143(15)
C9–O1	1.286(2)	C19–C20	1.377(3)	O4–Si	1.7883(15)
C9–C10	1.377(3)	C20–C21	1.371(3)	Si–N1A	1.838(2)
C10–C11	1.383(3)	C21–C22	1.378(3)	N1A–C7A	1.317(6)
C11–O2	1.289(2)	C23–C24	1.381(3)		
C11–C12	1.472(3)	C24–C25	1.367(5)		
C12–C23	1.385(3)	C25–C26	1.365(5)		
C2–C1–C6	116.06(18)	C15–C14–C13	122.74(16)	C35–C36–C37	120.16(18)
C2–C1–Si	122.42(15)	C16–C15–C14	122.05(17)	C36–C37–C17	120.55(17)
C6–C1–Si	121.52(14)	O4–C16–C15	123.23(16)	C9–O1–Si	127.57(12)
C3–C2–C1	122.4(2)	O4–C16–C17	114.95(15)	C11–O2–Si	127.37(13)
C4–C3–C2	119.8(2)	C15–C16–C17	121.81(16)	C14–O3–Si	130.91(12)
C3–C4–C5	119.7(2)	C37–C17–C33	118.95(17)	C16–O4–Si	130.18(11)
C4–C5–C6	120.0(2)	C37–C17–C16	119.87(16)	O1–Si–O4	173.61(7)
C5–C6–C1	122.0(2)	C33–C17–C16	121.06(16)	O1–Si–O2	91.67(6)
C18–C8–C22	118.81(17)	C19–C18–C8	120.64(17)	O4–Si–O2	86.15(7)
C18–C8–C9	118.88(15)	C18–C19–C20	119.84(19)	O1–Si–O3	82.99(6)
C22–C8–C9	122.27(17)	C21–C20–C19	120.21(19)	O4–Si–O3	90.85(7)
O1–C9–C10	122.97(17)	C20–C21–C22	120.58(18)	O2–Si–O3	85.60(8)
O1–C9–C8	114.21(15)	C21–C22–C8	119.91(18)	O1–Si–N1A	88.96(7)
C10–C9–C8	122.76(16)	C24–C23–C12	120.1(3)	O4–Si–N1A	92.44(8)
C9–C10–C11	121.56(17)	C25–C24–C23	120.4(3)	O2–Si–N1A	172.71(8)
O2–C11–C10	122.03(17)	C26–C25–C24	120.1(3)	O3–Si–N1A	87.27(9)
O2–C11–C12	115.08(18)	C25–C26–C27	120.4(3)	O1–Si–C1	94.51(7)
C10–C11–C12	122.83(18)	C26–C27–C12	119.8(3)	O4–Si–C1	91.60(7)
C23–C12–C27	119.2(2)	C29–C28–C13	120.35(19)	O2–Si–C1	92.71(7)
C23–C12–C11	122.1(2)	C30–C29–C28	120.3(2)	O3–Si–C1	176.93(8)
C27–C12–C11	118.7(2)	C29–C30–C31	120.09(18)	N1A–Si–C1	94.48(8)
C32–C13–C28	118.79(17)	C30–C31–C32	120.2(2)	C7A–N1A–Si	145.4(2)
C32–C13–C14	122.17(17)	C31–C32–C13	120.2(2)	O5A–C7A–N1A	176.3(6)
C28–C13–C14	118.97(16)	C34–C33–C17	120.1(2)		
O3–C14–C15	121.85(16)	C35–C34–C33	120.3(2)		
O3–C14–C13	115.39(15)	C36–C35–C34	119.84(19)		

Silicon(IV) complex **35**

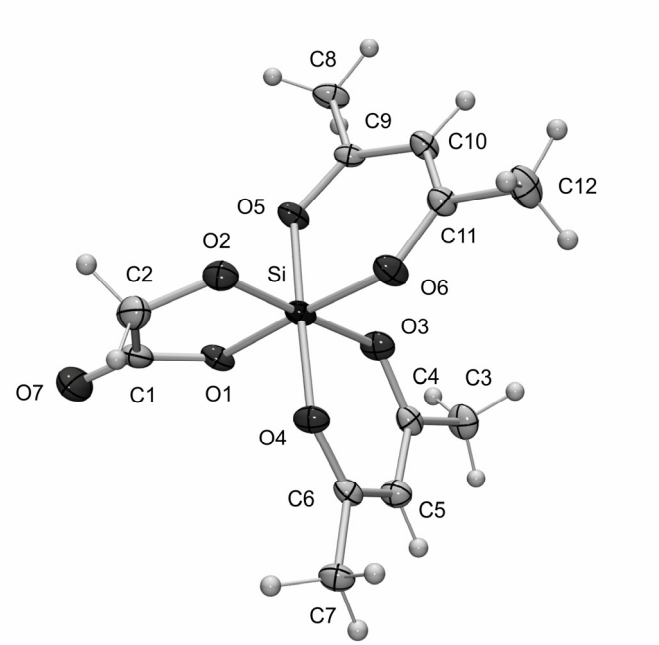

Figure A3: Molecular structure of the silicon(IV) complex **35** in the crystal showing the atomic numbering scheme (probability level of displacement ellipsoids 50%).

Table A12. Atomic coordinates ($\times 10^4$) and equivalent isotropic displacement parameters ($Å^2 \times 10^3$) for **35**. U_{eq} is defined as one third of the trace of the orthogonalized U_{ij} tensor.

	x	y	z	U_{eq}
C1	2500(2)	10404(2)	625(1)	26(1)
C2	1527(2)	10783(2)	924(1)	29(1)
C3	4044(1)	6157(2)	1658(1)	27(1)
C4	3130(1)	6932(2)	1407(1)	20(1)
C5	2329(1)	6676(2)	823(1)	22(1)
C6	1433(1)	7351(1)	638(1)	18(1)
C7	538(1)	7028(2)	39(1)	22(1)
C8	4439(1)	10065(2)	3414(1)	24(1)
C9	3461(1)	9501(1)	3018(1)	18(1)
C10	2829(1)	8836(1)	3381(1)	20(1)
C11	1887(1)	8369(2)	3018(1)	20(1)
C12	1164(1)	7734(2)	3415(1)	30(1)
O1	2930(1)	9499(1)	970(1)	22(1)
O2	1452(1)	10158(1)	1549(1)	23(1)
O3	3139(1)	7837(1)	1788(1)	24(1)
O4	1301(1)	8263(1)	977(1)	21(1)
O5	3245(1)	9685(1)	2325(1)	21(1)
O6	1558(1)	8456(1)	2320(1)	23(1)
O7	2845(1)	10854(1)	132(1)	42(1)
Si	2248(1)	9008(1)	1655(1)	18(1)

Table A13. Bond lengths [Å] and angles [°] for **35**.

C1–C2	1.52(17)	C6–O4	1.284(6)	O1–Si	1.77(9)
C1–O1	1.32(3)	C6–C7	1.49(11)	O2–Si	1.70(9)
C1–O7	1.21(3)	C8–C9	1.49(15)	O3–Si	1.79(11)
C2–O2	1.401(4)	C9–O5	1.288(2)	O4–Si	1.81(10)
C3–C4	1.49(13)	C9–C10	1.39(8)	O5–Si	1.80(12)
C4–C5	1.38(10)	C10–C11	1.38(15)	O6–Si	1.77(9)
C4–O3	1.291(2)	C11–O6	1.295(10)		
C5–C6	1.39(14)	C11–C12	1.49(10)		
O7–C1–O1	124.0(5)	C11–C10–C9	121.0(5)	O1–Si–O3	89.0(6)
O7–C1–C2	125.0(2)	O6–C11–C10	123.5(3)	O6–Si–O3	90.0(6)
O1–C1–C2	111.0(3)	O6–C11–C12	115.0(5)	O2–Si–O5	93.0(6)
O2–C2–C1	109.25(15)	C10–C11–C12	122.0(5)	O1–Si–O5	88.0(6)
O3–C4–C5	123.0(3)	C1–O1–Si	114.0(6)	O6–Si–O5	93.0(6)
O3–C4–C3	114.7(17)	C2–O2–Si	113.0(3)	O3–Si–O5	85.0(7)
C5–C4–C3	122.0(5)	C4–O3–Si	129.0(2)	O2–Si–O4	90.0(6)
C4–C5–C6	121.0(5)	C6–O4–Si	129.0(5)	O1–Si–O4	91.0(6)
O4–C6–C5	123.1(9)	C9–O5–Si	127.8(12)	O6–Si–O4	87.0(6)
O4–C6–C7	116.0(5)	C11–O6–Si	128.0(6)	O3–Si–O4	92.0(6)
C5–C6–C7	121.0(6)	O2–Si–O1	91.0(6)	O5–Si–O4	176.68(7)
O5–C9–C10	123.0(4)	O2–Si–O6	91.0(6)		
O5–C9–C8	115.2(8)	O1–Si–O6	177.34(14)		
C10–C9–C8	122.0(5)	O2–Si–O3	177.25(9)		

Silicon(IV) complex **36**

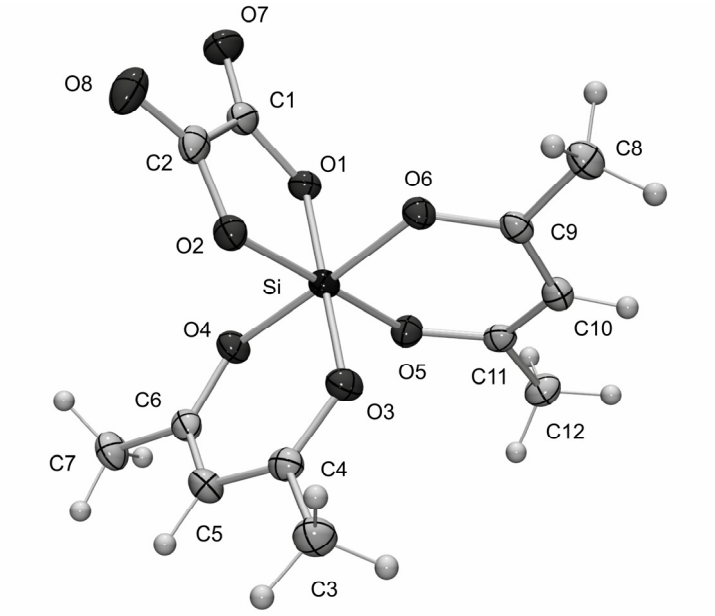

Figure A4: Molecular structure of the silicon(IV) complex **36** in the crystal showing the atomic numbering scheme (probability level of displacement ellipsoids 50%).

Table A14. Atomic coordinates ($\times 10^4$) and equivalent isotropic displacement parameters ($Å^2 \times 10^3$) for **36**. U_{eq} is defined as one third of the trace of the orthogonalized U_{ij} tensor.

	x	y	z	U_{eq}
C1	2761(1)	4127(2)	2732(1)	24(1)
C2	2247(1)	5676(2)	2147(1)	24(1)
C3	1159(1)	10890(2)	4180(1)	29(1)
C4	1183(1)	9051(2)	4073(1)	22(1)
C5	205(1)	8097(2)	3893(1)	25(1)
C6	235(1)	6380(2)	3823(1)	21(1)
C7	–808(1)	5348(2)	3686(1)	28(1)
C8	5736(1)	8279(2)	4523(1)	26(1)
C9	4707(1)	7543(2)	4706(1)	20(1)
C10	4663(1)	7283(2)	5630(1)	23(1)
C11	3799(1)	6361(2)	5810(1)	20(1)
C12	3842(1)	5845(2)	6794(1)	26(1)
Ol	2893(1)	4374(1)	3640(1)	22(1)
O2	2066(1)	6845(1)	2704(1)	22(1)
O3	2179(1)	8424(1)	4170(1)	23(1)
O4	1153(1)	5566(1)	3882(1)	22(1)
O5	2929(1)	5828(1)	5145(1)	22(1)
O6	3897(1)	7126(1)	3966(1)	21(1)
O7	3004(1)	2874(1)	2386(1)	34(1)
O8	2037(1)	5761(1)	1292(1)	35(1)
Si	2518(1)	6376(1)	3935(1)	18(1)

Table A15. Bond lengths [Å] and angles [°] for **36**.

Si−O1	1.7654(9)	C9−C8	1.4906(16)	C2−C1	1.5437(19)
Si−O2	1.7728(9)	C11−O5	1.2968(15)	C2−O2	1.3076(16)
Si−O3	1.7608(10)	C11−C10	1.3827(17)	C1−O7	1.2055(17)
Si−O4	1.7823(9)	C11−C12	1.4897(17)	C1−O1	1.3116(15)
Si−O5	1.7577(9)	C6−O4	1.2865(15)	C4−O3	1.2937(15)
Si−O6	1.7884(9)	C6−C5	1.3885(19)	C4−C5	1.3874(18)
O6−C9	1.2902(15)	C6−C7	1.4929(17)	C4−C3	1.4913(18)
C9−C10	1.3892(17)	C2−O8	1.2080(16)		
O1−Si−O2	88.39(4)	O5−Si−O6	93.74(4)	O2−C2−C1	110.55(10)
O1−Si−O3	176.25(4)	C9−O6−Si	127.26(8)	O7−C1−O1	125.62(13)
O1−Si−O4	87.92(4)	O6−C9−C10	123.13(11)	O7−C1−C2	123.67(12)
O1−Si−O5	89.94(4)	O6−C9−C8	116.15(11)	O1−C1−C2	110.71(11)
O1−Si−O6	90.14(4)	C10−C9−C8	120.68(11)	O3−C4−C5	123.05(12)
O2−Si−O3	88.69(5)	O5−C11−C10	123.20(11)	O3−C4−C3	115.04(11)
O2−Si−O4	91.03(4)	O5−C11−C12	115.37(11)	C5−C4−C3	121.90(12)
O2−Si−O5	177.37(5)	C10−C11−C12	121.36(11)	C4−O3−Si	127.93(8)
O2−Si−O6	88.30(4)	O4−C6−C5	122.95(11)	C1−O1−Si	115.07(8)
O3−Si−O4	94.49(4)	O4−C6−C7	115.35(11)	C6−O4−Si	127.86(8)
O3−Si−O5	93.06(4)	C5−C6−C7	121.69(12)	C11−O5−Si	127.76(8)
O3−Si−O6	87.42(4)	C11−C10−C9	121.01(12)	C2−O2−Si	115.09(8)
O4−Si−O5	86.87(4)	O8−C2−O2	125.77(13)	C4−C5−C6	121.78(12)
O4−Si−O6	177.96(4)	O8−C2−C1	123.68(13)		

Silicon(IV) complex **38**

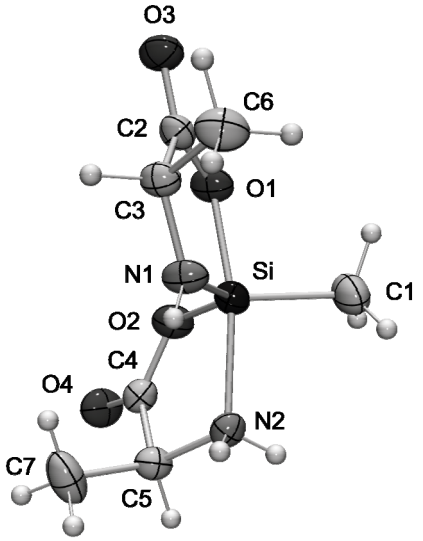

Figure A5: Molecular structure of the silicon(IV) complex **38** in the crystal showing the atomic numbering scheme (probability level of displacement ellipsoids 50%).

Table A16. Atomic coordinates ($\times 10^4$) and equivalent isotropic displacement parameters ($Å^2 \times 10^3$) for **38**. U_{eq} is defined as one third of the trace of the orthogonalized U_{ij} tensor.

	x	y	z	U_{eq}
C1	3237(2)	2863(2)	2744(1)	43(1)
C2	−1518(2)	2831(1)	3017(1)	30(1)
C3	−1443(2)	1458(1)	3110(1)	29(1)
C4	1563(2)	2351(1)	−119(1)	29(1)
C5	2301(2)	1086(1)	29(1)	31(1)
C6	−1342(3)	1100(2)	4289(1)	42(1)
C7	927(3)	154(2)	−280(2)	51(1)
N1	61(2)	1092(1)	2491(1)	31(1)
N2	2784(2)	1003(1)	1182(1)	27(1)
O1	−192(2)	3290(1)	2503(1)	33(1)
O2	1104(2)	2884(1)	780(1)	33(1)
O3	−2663(2)	3448(1)	3411(1)	39(1)
O4	1336(2)	2816(1)	−982(1)	42(1)
Si	1371(1)	2209(1)	2011(1)	26(1)

Table A17. Bond lengths [Å] and angles [°] for **38**.

Si–O1	1.7910(13)	O2–C4	1.3093(19)	C4–C5	1.506(2)
Si–O2	1.7118(11)	O3–C2	1.2099(19)	C5–N2	1.4844(19)
Si–N1	1.6901(14)	O4–C4	1.2015(19)	C5–C7	1.514(3)
Si–N2	1.9932(14)	C2–C3	1.507(2)	N1–H1N	0.91(2)
Si–C1	1.8401(18)	C3–N1	1.442(2)	N2–H2N2	0.88(2)
O1–C2	1.301(2)	C3–C6	1.520(2)	N2–H2N1	0.90(2)
O1–Si–O2	86.63(6)	C2–O1–Si	115.76(10)	N2–C5–C7	112.20(14)
O1–Si–N1	87.69(6)	C5–N2–Si	108.90(10)	N2–C5–C4	105.54(12)
O1–Si–N2	167.64(6)	H2N1–N2–Si	115.0(14)	O2–C4–C5	113.93(12)
O1–Si–C1	95.29(8)	H2N2–N2–Si	110.6(13)	O4–C4–C5	123.58(14)

O2–Si–N1	123.85(7)	H2N1–N2–C5	107.1(13)	O4–C4–O2	122.41(14)
O2–Si–N2	83.57(6)	H2N2–N2–C5	105.2(13)	C2–C3–C6	109.44(13)
O2–Si–C1	111.63(8)	H2N2–N2–H2N1	109(2)	N1–C3–C6	113.79(15)
N1–Si–N2	91.52(6)	C3–N1–Si	117.52(10)	N1–C3–C2	105.43(13)
N1–Si–C1	124.52(9)	H1N–N1–Si	127.9(14)	O1–C2–C3	113.14(14)
N2–Si–C1	95.31(8)	H1N–N1–C3	114.5(14)	O3–C2–C3	123.54(15)
C4–O2–Si	122.66(10)	C4–C5–C7	109.06(15)	O3–C2–O1	123.28(15)

Silicon(IV) complex **39**

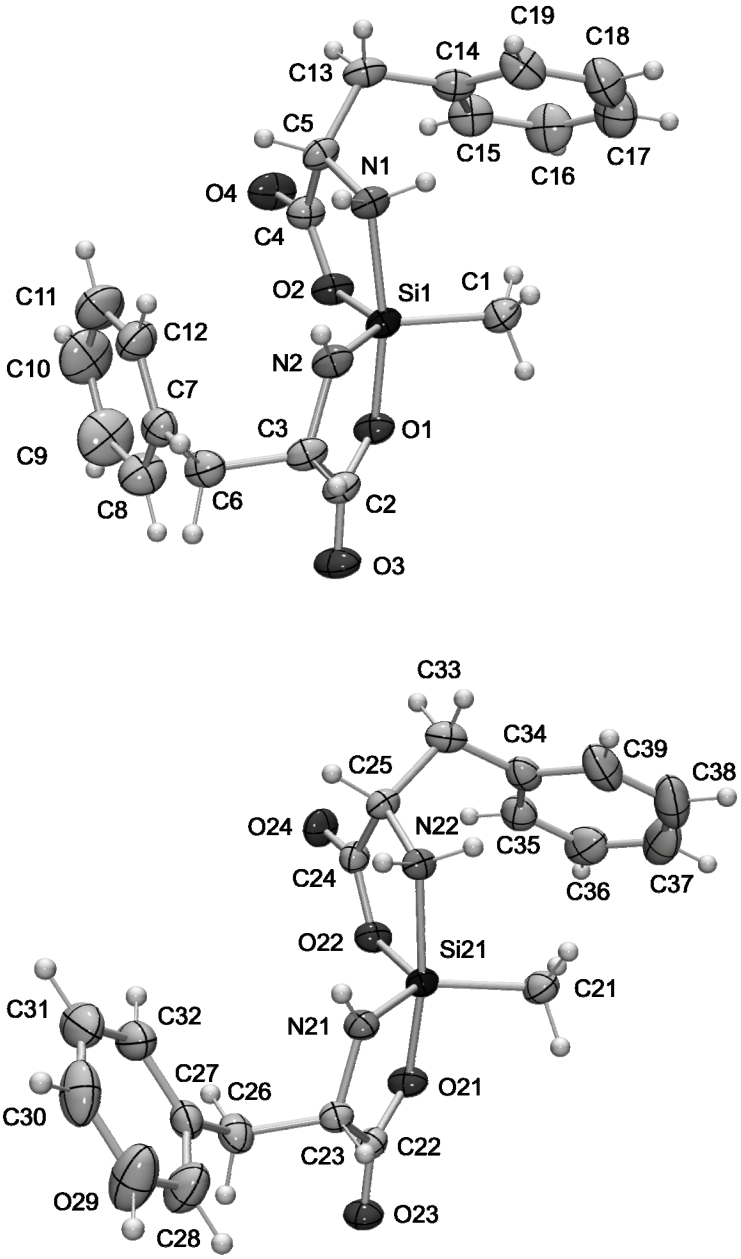

Figure A6: Molecular structures of the two crystallographically independent molecules (top molecule **I**; bottom molecule **II**) of the silicon(IV) complex **39** in the crystal showing the atomic numbering scheme (probability level of displacement ellipsoids 50%).

Table A18. Atomic coordinates ($\times 10^4$) and equivalent isotropic displacement parameters ($Å^2 \times 10^3$) for **39**. U_{eq} is defined as one third of the trace of the orthogonalized U_{ij} tensor.

	x	y	z	U_{eq}
Si1	9451(1)	1631(1)	7503(1)	26(1)
O1	12085(2)	1567(1)	7310(1)	32(1)
O2	9635(2)	2352(1)	7368(1)	33(1)
O3	14241(2)	1054(1)	6809(1)	41(1)
O4	8117(2)	3198(1)	7253(1)	46(1)
N1	8966(2)	1118(1)	7025(1)	30(1)
N2	6514(2)	1779(1)	7581(1)	28(1)
C1	9826(3)	1469(1)	8242(1)	37(1)
C2	12505(2)	1176(1)	6949(1)	30(1)
C3	10640(2)	885(1)	6716(1)	30(1)
C4	8015(2)	2692(1)	7352(1)	33(1)
C5	6017(2)	2384(1)	7454(1)	30(1)
C6	10488(3)	1000(1)	6097(1)	35(1)
C7	10445(3)	1626(1)	5957(1)	35(1)
C8	12208(3)	1913(1)	5818(1)	50(1)
C9	12177(4)	2494(1)	5699(1)	73(1)
C10	10422(5)	2798(1)	5725(1)	73(1)
C11	8658(4)	2524(1)	5859(1)	64(1)
C12	8652(3)	1941(1)	5973(1)	45(1)
C13	4730(2)	2676(1)	7900(1)	35(1)
C14	5594(3)	2612(1)	8466(1)	35(1)
C15	7147(3)	2967(1)	8653(1)	45(1)
C16	7960(4)	2891(1)	9170(1)	56(1)
C17	7257(4)	2464(1)	9510(1)	58(1)
C18	5729(4)	2110(1)	9332(1)	55(1)
C19	4897(3)	2185(1)	8818(1)	45(1)
Si21	3484(1)	4356(1)	7346(1)	23(1)
O21	856(1)	4436(1)	7533(1)	30(1)
O22	3417(2)	5057(1)	7129(1)	29(1)
O23	−1344(2)	4282(1)	8201(1)	33(1)
O24	5071(2)	5825(1)	6820(1)	35(1)
N21	3960(2)	4195(1)	8015(1)	25(1)
N22	6431(2)	4398(1)	7184(1)	25(1)
C21	2946(2)	3808(1)	6815(1)	34(1)
C22	401(2)	4289(1)	8029(1)	26(1)
C23	2240(2)	4143(1)	8378(1)	25(1)
C24	5068(2)	5330(1)	6961(1)	26(1)
C25	6967(2)	4961(1)	6941(1)	26(1)
C26	2275(2)	4552(1)	8867(1)	35(1)
C27	3876(2)	4417(1)	9286(1)	32(1)
C28	3598(3)	3984(1)	9666(1)	52(1)
C29	5042(4)	3874(1)	10063(1)	65(1)
C30	6799(3)	4197(1)	10081(1)	54(1)
C31	7093(3)	4629(1)	9709(1)	51(1)
C32	5642(3)	4736(1)	9311(1)	43(1)
C33	7766(2)	4923(1)	6356(1)	35(1)
C34	6298(3)	4653(1)	5959(1)	34(1)
C35	4531(3)	4934(1)	5788(1)	38(1)
C36	3182(3)	4671(1)	5436(1)	51(1)
C37	3583(4)	4123(1)	5241(1)	62(1)
C38	5337(5)	3846(1)	5397(1)	63(1)
C39	6678(4)	4106(1)	5753(1)	52(1)

Table A19. Bond lengths [Å] and angles [°] for **39**.

Si1–O1	1.8038(11)	C5–C13	1.541(2)	C24–O22	1.3243(18)
Si1–O2	1.7207(12)	C6–C7	1.502(2)	C24–C25	1.518(2)
Si1–N1	1.7052(15)	C7–C8	1.383(3)	C25–N22	1.486(2)
Si1–N2	1.9731(13)	C7–C12	1.390(3)	C25–C33	1.533(2)
Si1–C1	1.8654(18)	C8–C9	1.387(3)	C26–C27	1.506(2)
Si21–O21	1.7995(10)	C9–C10	1.357(4)	C27–C32	1.382(2)
Si21–O22	1.7220(12)	C10–C11	1.366(4)	C27–C28	1.385(3)
Si21–N21	1.7114(13)	C11–C12	1.389(3)	C28–C29	1.386(3)
Si21–N22	1.9823(12)	C13–C14	1.508(3)	C29–C30	1.382(3)
Si21–C21	1.8581(17)	C14–C15	1.393(3)	C30–C31	1.374(3)
N2–H2N	0.92(2)	C14–C19	1.395(3)	C31–C32	1.389(3)
N2–C5	1.4833(19)	C15–C16	1.387(3)	C33–C34	1.508(3)
N1–H1N	0.79(2)	C16–C17	1.380(3)	C34–C39	1.396(3)
N1–C3	1.445(2)	C17–C18	1.372(3)	C34–C35	1.399(3)
O1–C2	1.301(2)	C18–C19	1.387(3)	C35–C36	1.381(3)
O2–C4	1.3293(19)	C22–O23	1.2239(17)	C36–C37	1.391(3)
O3–C2	1.2263(19)	C22–O21	1.3007(19)	C37–C38	1.377(4)
O4–C4	1.206(2)	C22–C23	1.5205(19)	C38–C39	1.382(4)
C2–C3	1.515(2)	C23–N21	1.4456(18)	N22–H22N	0.95(2)
C3–C6	1.544(2)	C23–C26	1.534(2)	N21–H21N	0.85(2)
C4–C5	1.520(2)	C24–O24	1.2073(19)		
O1–Si1–O2	87.85(6)	C7–C8–C9	120.8(2)	N22–C25–C24	107.02(12)
O1–Si1–N1	86.63(6)	C10–C9–C8	120.9(2)	N22–C25–C33	113.92(13)
O1–Si1–N2	169.01(6)	C9–C10–C11	119.3(2)	C24–C25–C33	110.23(13)
O1–Si1–C1	96.42(7)	C10–C11–C12	120.7(2)	C27–C26–C23	114.45(14)
O2–Si1–N1	124.53(7)	C11–C12–C7	120.6(2)	C32–C27–C28	118.30(16)
O2–Si1–N2	85.19(5)	C14−C13−C5	113.69(13)	C32–C27–C26	120.40(17)
O2–Si1–C1	112.11(7)	C15−C14−C19	117.53(18)	C28–C27–C26	121.27(16)
N1–Si1–N2	90.32(6)	C15−C14−C13	121.42(17)	C27–C28–C29	121.2(2)
N1–Si1–C1	123.36(8)	C19−C14−C13	121.03(16)	C30–C29–C28	119.6(2)
H2N–N2–C5	109.2(13)	C16−C15−C14	120.6(2)	C31–C30–C29	119.81(18)
N2–Si1–C1	94.07(7)	C17−C16−C15	121.0(2)	C30–C31–C32	120.20(19)
H2N–N2–Si1	110.3(13)	C18−C17−C16	119.3(2)	C27–C32–C31	120.81(19)
C5–N2–Si1	111.26(9)	C17−C18−C19	120.2(2)	C34–C33–C25	114.10(13)
H1N–N1–C3	114.2(16)	C18–C19–C14	121.50(19)	C39–C34–C35	117.89(18)
H1N–N1–Si1	126.9(16)	O21–Si21–O22	87.38(5)	C39–C34–C33	120.06(18)
C3–N1–Si1	118.83(10)	O21–Si21–N21	87.39(5)	C35–C34–C33	122.05(16)
C2–O1–Si1	116.20(9)	O21–Si21–C21	93.88(7)	C36–C35–C34	120.94(19)
C4–O2–Si1	122.23(10)	O22–Si21–N21	120.56(6)	C35–C36–C37	120.1(2)
O3–C2–O1	123.39(14)	O22–Si21–C21	115.63(7)	C38–C37–C36	119.6(2)
O3–C2–C3	123.12(15)	N21–Si21–C21	123.80(7)	C37–C38–C39	120.4(2)
O1–C2–C3	113.49(12)	N21–Si21–N22	91.34(5)	C38–C39–C34	121.1(2)
N1–C3–C2	104.57(12)	O22–Si21–N22	85.21(5)	H22N–N22–C25	108.7(12)
N1–C3–C6	113.66(13)	O21–Si21–N22	170.55(6)	H22N–N22–Si21	109.5(11)
C2–C3–C6	110.23(14)	C21–Si21–N22	94.61(7)	C25–N22–Si21	110.86(9)
O4–C4–O2	123.02(14)	O23–C22–O21	122.84(13)	H21N–N21–C23	119.2(13)
O4–C4–C5	122.95(14)	O23–C22–C23	123.41(14)	H21N–N21–Si21	122.8(13)
O2–C4–C5	114.01(13)	O21–C22–C23	113.72(12)	C22–O21–Si21	115.62(9)
N2–C5–C4	107.11(11)	N21–C23–C22	104.95(11)	C24–O22–Si21	122.07(10)
N2–C5–C13	113.13(13)	N21–C23–C26	114.66(13)		
C4–C5–C13	112.61(14)	C22–C23–C26	108.19(12)		
C7–C6–C3	113.30(13)	O24–C24–O22	123.38(14)		
C8–C7–C12	117.61(18)	O24–C24–C25	122.11(14)		
C8–C7–C6	120.81(17)	O22–C24–C25	114.47(13)		
C12–C7–C6	121.57(16)				

Silicon(IV) complex **43**·CH_3CN

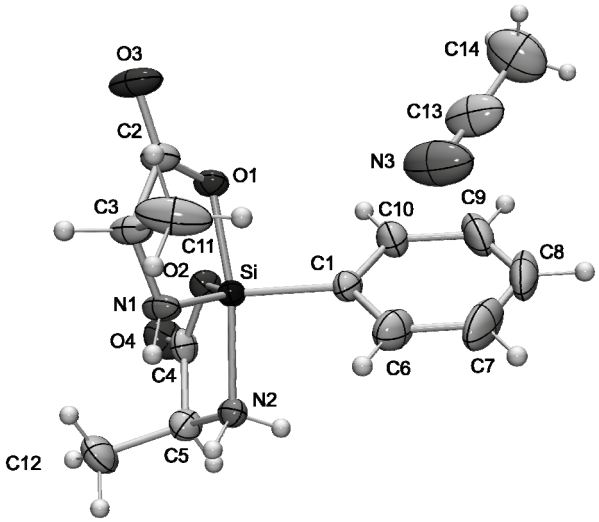

Figure A7: Molecular structure of the silicon(IV) complex **43** in the crystal of **43**·CH_3CN showing the atomic numbering scheme (probability level of displacement ellipsoids 50%).

Table A20. Atomic coordinates ($\times 10^4$) and equivalent isotropic displacement parameters ($Å^2 \times 10^3$) for **43**·CH_3CN. U_{eq} is defined as one third of the trace of the orthogonalized U_{ij} tensor.

	x	y	z	U_{eq}
C1	3066(2)	7065(2)	8170(1)	28(1)
C2	−331(3)	6685(2)	6914(1)	30(1)
C3	−401(3)	8038(2)	6869(1)	33(1)
C4	−450(2)	7044(2)	9528(1)	29(1)
C5	−26(3)	8348(2)	9621(1)	31(1)
C6	4152(3)	7938(2)	7970(1)	43(1)
C7	5741(3)	7683(4)	7947(2)	64(1)
C8	6267(3)	6552(4)	8130(2)	63(1)
C9	5224(3)	5684(3)	8330(2)	51(1)
C10	3624(3)	5928(2)	8347(1)	37(1)
C11	676(5)	8466(2)	6235(1)	62(1)
C12	−1485(3)	9123(2)	9551(2)	46(1)
C13	4434(5)	2302(3)	9165(2)	75(1)
C14	5103(7)	1168(4)	8993(3)	98(1)
Nl	75(2)	8441(2)	7617(1)	28(1)
N2	1137(2)	8614(1)	9016(1)	24(1)
N3	3854(7)	3181(3)	9308(2)	110(2)
O1	355(2)	6289(1)	7524(1)	26(1)
O2	7(2)	6577(1)	8876(1)	26(1)
O3	−866(3)	6032(1)	6424(1)	47(1)
O4	−1158(2)	6470(2)	9996(1)	47(1)
Si	935(1)	7417(1)	8195(1)	20(1)

Table A21. Bond lengths [Å] and angles [°] for **43**·CH_3CN.

O1−Si	1.7871(14)	C2−C3	1.507(3)	C7−C8	1.372(5)
O2−Si	1.7082(14)	C3−N1	1.441(3)	C8−C9	1.356(5)
N1−Si	1.6885(17)	C3−C11	1.516(4)	C9−C10	1.387(3)
N2−Si	1.9658(17)	C4−O2	1.313(3)	N1–H1N	0.81(3)
C1−Si	1.854(2)	C4–O4	1.200(3)	N2–H2N1	0.85(3)
C1−C6	1.384(3)	C4–C5	1.502(3)	N2–H2N2	0.91(3)
C1−C10	1.385(3)	C5–N2	1.478(3)	N3–C13	1.123(5)
C2−O1	1.294(3)	C5–C12	1.515(3)	C13–C14	1.415(6)
C2–O3	1.212(3)	C6–C7	1.381(4)		
C6−C1−C10	117.9(2)	C4−C5−C12	110.11(18)	C5−N2−Si	109.30(12)
C6−C1−Si	120.63(17)	C7−C6−C1	121.0(3)	C2−O1−Si	115.33(12)
C10−C1−Si	121.47(16)	C8−C7−C6	120.1(3)	C4−O2−Si	121.83(13)
O3−C2−O1	123.30(18)	C9−C8−C7	119.9(2)	N1−Si−O2	125.90(9)
O3−C2−C3	123.1(2)	C8−C9−C10	120.6(3)	N1−Si−O1	87.68(7)
O1−C2−C3	113.60(18)	C1−C10−C9	120.6(2)	O2–Si–O1	86.98(7)
N1−C3−C2	104.54(17)	H1N−N1−C3	115.6(19)	N1–Si–C1	123.49(10)
N1−C3−C11	113.5(2)	H1N–N1–Si	124.8(19)	O2–Si–C1	110.61(9)
C2−C3−C11	109.1(2)	C3–N1–Si	117.19(13)	O1–Si–C1	96.12(8)
O4−C4−O2	122.1(2)	H2N1–N2–H2N2	108(2)	N1–Si–N2	91.18(8)
O4−C4−C5	124.0(2)	H2N1–N2–C5	103.9(16)	O2–Si–N2	84.22(7)
O2−C4−C5	113.87(18)	H2N2–N2–C5	107.7(15)	O1–Si–N2	168.25(7)
N2–C5–C4	106.00(16)	H2N1–N2–Si	110.5(16)	C1−Si−N2	94.27(8)
N2–C5–C12	112.10(19)	H2N2−N2−Si	116.9(15)	N3−C13−C14	177.5(6)

Silicon(IV) complex **44**

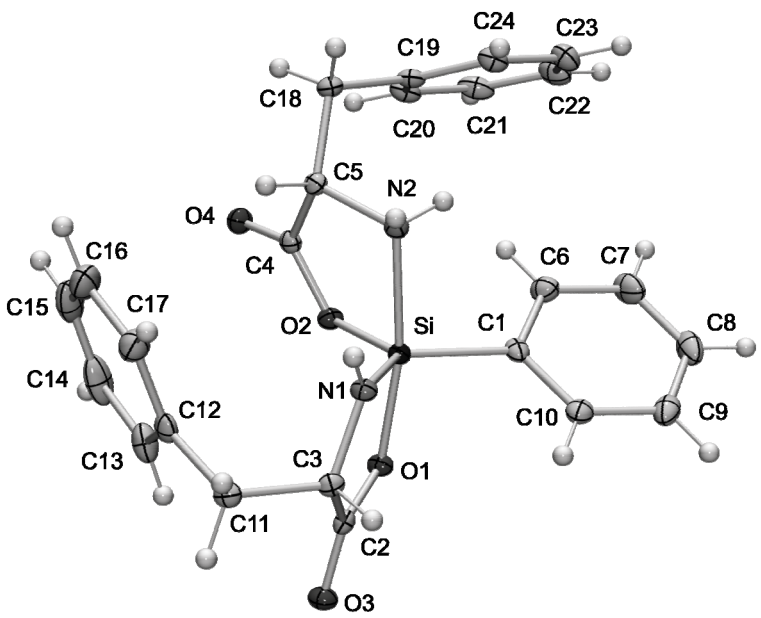

Figure A8: Molecular structure of the silicon(IV) complex **44** in the crystal showing the atomic numbering scheme (probability level of displacement ellipsoids 50%).

Table A22. Atomic coordinates ($\times 10^4$) and equivalent isotropic displacement parameters ($Å^2 \times 10^3$) for **44**. U_{eq} is defined as one third of the trace of the orthogonalized U_{ij} tensor.

	x	y	z	U_{eq}
C1	6414(2)	8483(1)	5510(1)	14(1)
C2	4512(2)	7732(1)	8084(1)	13(1)
C3	6543(2)	7223(1)	8588(1)	13(1)
C4	8534(2)	10395(1)	7901(1)	13(1)
C5	10558(2)	9901(1)	7869(1)	13(1)
C6	6657(2)	9237(1)	4757(1)	20(1)
C7	6088(2)	9103(1)	3573(1)	27(1)
C8	5265(2)	8213(1)	3124(1)	26(1)
C9	5007(2)	7457(1)	3849(1)	22(1)
C10	5585(2)	7592(1)	5034(1)	17(1)
C11	7120(2)	7283(1)	9913(1)	15(1)
C12	7771(2)	8304(1)	10334(1)	17(1)
C13	9850(2)	8520(1)	10734(1)	24(1)
C14	10485(3)	9480(1)	11047(1)	34(1)
C15	9070(3)	10221(1)	10953(2)	36(1)
C16	7013(3)	10016(1)	10583(1)	35(1)
C17	6356(3)	9059(1)	10280(1)	25(1)
C18	12040(2)	10603(1)	7456(1)	15(1)
C19	11303(2)	10841(1)	6194(1)	15(1)
C20	11895(2)	10252(1)	5375(1)	17(1)
C21	11127(2)	10427(1)	4210(1)	22(1)
C22	9787(2)	11201(1)	3855(1)	23(1)
C23	9232(2)	11811(1)	4664(1)	22(1)
C24	9976(2)	11630(1)	5827(1)	18(1)
Nl	7995(2)	7694(1)	8042(1)	13(1)
N2	10019(2)	9006(1)	7150(1)	13(1)
O1	4626(1)	8393(1)	7311(1)	13(1)
O2	6907(1)	9825(1)	7501(1)	13(1)
O3	2914(1)	7536(1)	8364(1)	16(1)
O4	8403(2)	11212(1)	8265(1)	17(1)
Si	7159(1)	8631(1)	7100(1)	11(1)

Table A23. Bond lengths [Å] and angles [°] for **44**.

O1–Si	1.8004(9)	C2–O1	1.3005(15)	C13–C14	1.388(2)
O2–Si	1.7042(10)	C2–O3	1.2220(16)	C14–C15	1.365(3)
N1–Si	1.6991(12)	C2–C3	1.5165(17)	C15–C16	1.372(3)
N2–Si	1.9677(11)	C3–N1	1.4402(16)	C16–C17	1.387(2)
C1–Si	1.8583(13)	C3–C11	1.5413(17)	C18–C19	1.5066(18)
C1–C6	1.3937(19)	C6–C7	1.388(2)	C19–C20	1.389(2)
C1–C10	1.3905(19)	C7–C8	1.379(2)	C19–C24	1.3925(19)
C4–O2	1.3280(16)	C8–C9	1.377(2)	C20–C21	1.386(2)
C4–O4	1.1977(17)	C9–C10	1.3896(19)	C21–C22	1.379(2)
C4–C5	1.5187(18)	C11–C12	1.4986(19)	C22–C23	1.386(2)
C5–N2	1.4796(17)	C12–C17	1.384(2)	C23–C24	1.383(2)
C5–C18	1.5354(18)	C12–C13	1.393(2)		
C10–C1–C6	117.78(12)	C9–C10–C1	121.29(14)	C3–N1–Si	118.49(9)
C10–C1–Si	119.78(10)	C12–C11–C3	112.08(10)	C5–N2–Si	109.39(8)
C6–C1–Si	122.44(10)	C17–C12–C13	118.59(14)	C4–O2–Si	121.58(9)
O4–C4–O2	122.80(12)	C17–C12–C11	121.47(13)	C2–O1–Si	115.82(8)
O4–C4–C5	123.75(12)	C13–C12–C11	119.86(13)	N1–Si–O2	123.98(5)

O2–C4–C5	113.44(11)	C14–C13–C12	120.47(16)	N1–Si–O1	87.11(5)
N2–C5–C4	106.03(10)	C15–C14–C13	120.07(17)	O2–Si–O1	88.35(5)
N2–C5–C18	114.02(10)	C14–C15–C16	120.16(16)	N1–Si–C1	124.37(6)
C4–C5–C18	112.57(11)	C15–C16–C17	120.37(16)	O2–Si–C1	111.65(5)
O3–C2–O1	122.94(12)	C12–C17–C16	120.29(16)	O1–Si–C1	95.04(5)
O3–C2–C3	123.61(12)	C19–C18–C5	111.63(10)	N1–Si–N2	90.24(5)
O1–C2–C3	113.44(11)	C20–C19–C24	118.89(13)	O2–Si–N2	84.66(5)
N1–C3–C2	104.88(10)	C20–C19–C18	120.14(12)	O1–Si–N2	169.43(5)
N1–C3–C11	114.14(10)	C24–C19–C18	120.94(12)	C1–Si–N2	94.90(5)
C7–C6–C1	121.06(14)	C21–C20–C19	120.63(13)		
C2–C3–C11	111.69(10)	C22–C21–C20	120.02(14)		
C8–C7–C6	120.01(14)	C21–C22–C23	119.87(13)		
C9–C8–C7	120.04(13)	C24–C23–C22	120.21(14)		
C8–C9–C10	119.83(14)	C23–C24–C19	120.34(13)		

Silicon(IV) complex **46**·C_5H_{12}·1/2CH_3CN

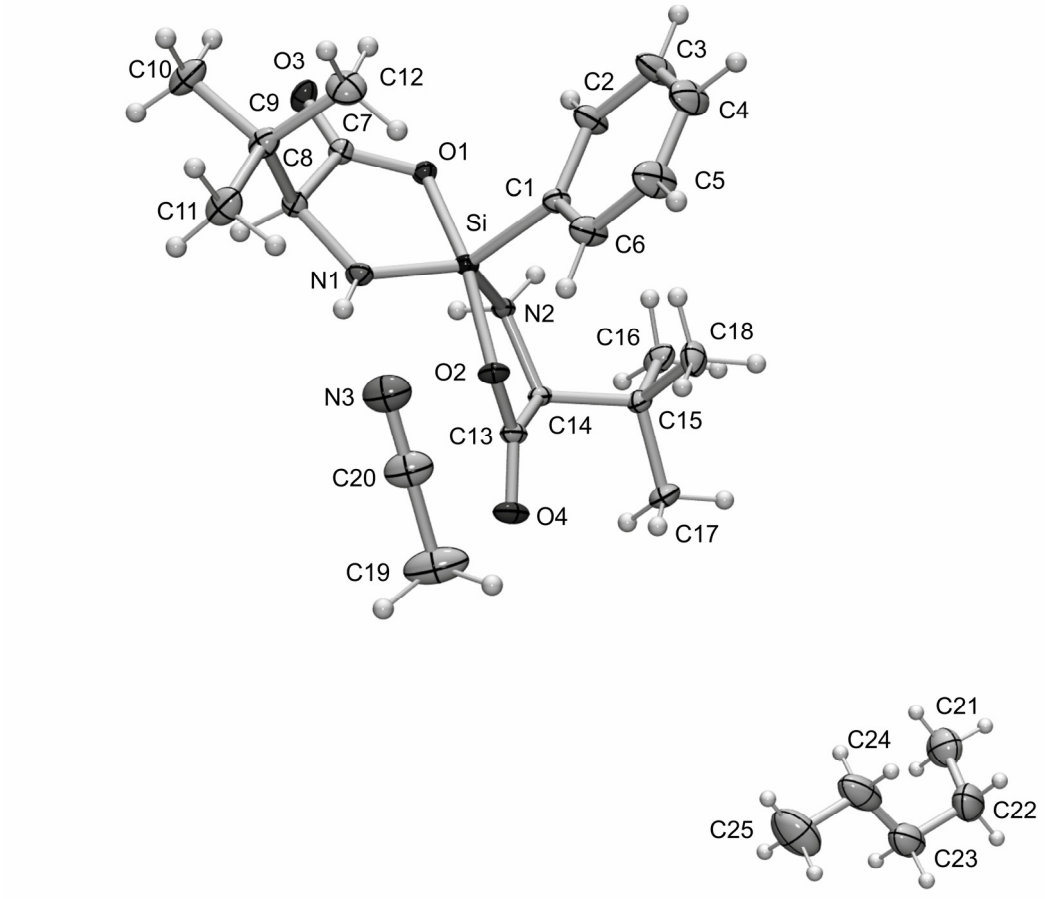

Figure A9: Molecular structure of the silicon(IV) complex **46** in the crystal of **46**·C_5H_{12}·1/2CH_3CN showing the atomic numbering scheme (probability level of displacement ellipsoids 50%).

Table A24. Atomic coordinates (× 10^4) and equivalent isotropic displacement parameters (Å^2 × 10^3) for **46**·C_5H_{12}·1/2CH_3CN. U_{eq} is defined as one third of the trace of the orthogonalized U_{ij} tensor.

	x	y	z	U_{eq}
C1	7614(1)	4940(1)	9159(1)	16(1)
C2	7041(1)	4992(1)	9739(1)	25(1)
C3	6849(1)	5670(1)	10095(1)	34(1)
C4	7234(1)	6309(1)	9884(1)	34(1)
C5	7813(1)	6270(1)	9324(1)	32(1)
C6	7996(1)	5593(1)	8958(1)	25(1)
C7	8075(1)	3068(1)	9948(1)	15(1)
C8	8871(1)	3236(1)	9695(1)	16(1)
C9	9324(1)	3614(1)	10401(1)	20(1)
C10	9443(1)	3063(1)	11112(1)	30(1)
C11	10087(1)	3834(1)	10052(1)	27(1)
C12	8928(1)	4306(1)	10722(1)	29(1)
C13	8031(1)	4141(1)	7071(1)	16(1)
C14	7272(1)	3772(1)	7153(1)	15(1)
C15	6629(1)	4273(1)	6832(1)	17(1)
C16	5881(1)	3893(1)	6997(1)	26(1)
C17	6720(1)	4357(1)	5893(1)	28(1)
C18	6636(1)	5038(1)	7243(1)	27(1)
C19	10000	5000	6607(2)	47(1)
C20	10000	5000	7513(1)	32(1)
C21	530(1)	1218(1)	108(2)	55(1)
C22	996(2)	1772(1)	–342(2)	64(1)
C23	1806(1)	1538(1)	–431(2)	54(1)
C24	2241(1)	1472(1)	385(2)	63(1)
C25	3053(2)	1233(2)	277(3)	80(1)
Nl	8789(1)	3682(1)	8955(1)	16(1)
N2	7223(1)	3566(1)	8048(1)	13(1)
N3	10000	5000	8218(1)	35(1)
O1	7575(1)	3448(1)	9537(1)	15(1)
O2	8296(1)	4393(1)	7766(1)	17(1)
O3	7910(1)	2612(1)	10482(1)	21(1)
O4	8353(1)	4200(1)	6412(1)	22(1)
Si	7938(1)	4038(1)	8718(1)	13(1)

Table A25. Bond lengths [Å] and angles [°] for **46**·C_5H_{12}·1/2CH_3CN.

O1–Si	1.8199(8)	C7–O1	1.3122(12)	C14–N2	1.4970(13)
O2–Si	1.7876(8)	C7–O3	1.2287(12)	C14–C15	1.5560(15)
N1–Si	1.7040(9)	C7–C8	1.5193(14)	C15–C18	1.5281(16)
N2–Si	1.8842(9)	C8–N1	1.4491(13)	C15–C16	1.5326(17)
C1–Si	1.8659(11)	C8–C9	1.5599(15)	C15–C17	1.5374(16)
C1–C2	1.3978(15)	C9–C12	1.5261(19)	C19–C20	1.466(3)
C1–C6	1.4000(15)	C9–C10	1.5339(17)	C20–N3	1.142(3)
C2–C3	1.3924(17)	C9–C11	1.5355(17)	C21–C22	1.492(3)
C3–C4	1.387(2)	C13–O4	1.2190(13)	C22–C23	1.523(3)
C4–C5	1.382(2)	C13–O2	1.3039(13)	C23–C24	1.540(4)
C5–C6	1.3945(17)	C13–C14	1.5247(14)	C24–C25	1.532(4)
C2–C1–Si	123.04(8)	O4–C13–O2	123.47(10)	N1–Si–O2	90.28(4)
C6–C1–Si	119.20(8)	O4–C13–C14	122.78(10)	N1–Si–O1	86.48(4)
C2–C1–C6	117.55(10)	O2–C13–C14	113.75(9)	O2–Si–O1	164.88(4)
C3–C2–C1	121.27(11)	N2–C14–C13	104.17(8)	N1–Si–C1	121.45(5)

C4–C3–C2	120.08(12)	N2–C14–C15	115.01(8)	O2–Si–C1	97.59(4)
C5–C4–C3	119.76(12)	C13–C14–C15	112.60(8)	O1–Si–C1	96.70(4)
C4–C5–C6	120.06(12)	C18–C15–C16	109.48(10)	N1–Si–N2	124.96(4)
C5–C6–C1	121.25(11)	C18–C15–C17	109.97(10)	O2–Si–N2	84.86(4)
O3–C7–O1	122.63(9)	C16–C15–C17	108.04(10)	O1–Si–N2	84.91(4)
O3–C7–C8	123.40(9)	C18–C15–C14	111.72(9)	C1–Si–N2	113.53(4)
O1–C7–C8	113.96(8)	C16–C15–C14	109.64(9)		
N1–C8–C7	103.70(8)	C17–C15–C14	107.90(9)		
N1–C8–C9	114.75(8)	N3–C20–C19	180.000(1)		
C7–C8–C9	112.49(8)	C21–C22–C23	113.54(18)		
C12–C9–C10	109.67(11)	C22–C23–C24	115.3(2)		
C12–C9–C11	109.45(10)	C25–C24–C23	114.1(2)		
C10–C9–C11	108.58(10)	C8–N1–Si	119.08(7)		
C12–C9–C8	111.11(9)	C14–N2–Si	113.94(6)		
C10–C9–C8	109.94(9)	C7–O1–Si	115.30(6)		
C11–C9–C8	108.04(10)	C13–O2–Si	119.24(7)		

Silicon(IV) complex **50**

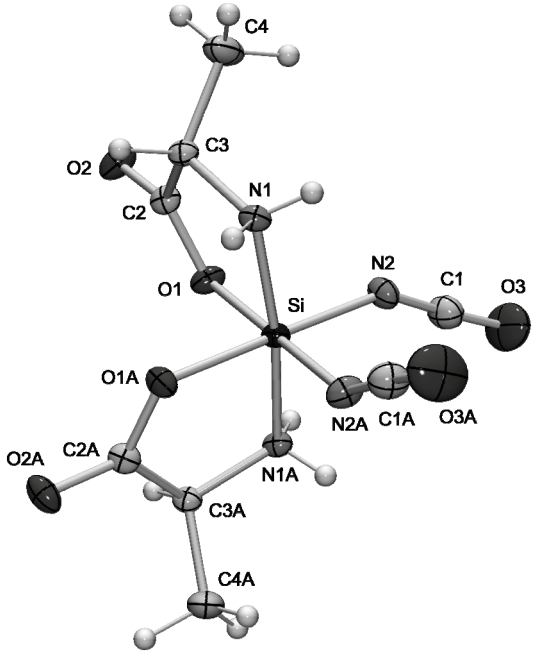

Figure A10: Molecular structure of the silicon(IV) complex **50** in the crystal showing the atomic numbering scheme (probability level of displacement ellipsoids 50%).

Table A26. Atomic coordinates ($\times 10^4$) and equivalent isotropic displacement parameters ($Å^2 \times 10^3$) for **50**. U_{eq} is defined as one third of the trace of the orthogonalized U_{ij} tensor.

	x	y	z	U_{eq}
Si	6431(1)	6431(1)	10000	13(1)
N1	7986(2)	5117(1)	10521(1)	15(1)
C3	9836(2)	5400(2)	10320(1)	15(1)
C4	10771(2)	3694(2)	10209(1)	31(1)
O1A	8276(1)	6961(1)	9489(1)	18(1)
O2A	11153(1)	6854(2)	9394(1)	22(1)
C2A	9816(2)	6488(2)	9691(1)	17(1)

N2A	5905(2)	4663(2)	9449(1)	20(1)
O3A	4157(2)	3611(2)	8568(1)	47(1)
C1A	5017(2)	4176(2)	9005(1)	26(1)

Table A27. Bond lengths [Å] and angles [°] for **50**.

Si–O1	1.7996(10)	C3–C4	1.513(2)
Si–O1A	1.7996(10)	C3–C2	1.5173(18)
Si–N2	1.8014(12)	O1–C2	1.3041(15)
Si–N2A	1.8014(12)	O2–C2	1.2217(16)
Si–N1A	1.8848(11)	N2–C1	1.1843(19)
Si–N1	1.8849(11)	O3–C1	1.183(2)
N1–C3	1.4953(17)		
O1–Si–O1A	88.27(7)	N1A–Si–N1	172.06(8)
O1–Si–N2	89.78(5)	C3–N1–Si	111.98(8)
O1A–Si–N2	176.83(5)	N1–C3–C4	111.43(11)
O1–Si–N2A	176.83(5)	N1–C3–C2	107.31(10)
O1A–Si–N2A	89.78(5)	C4–C3–C2	111.11(12)
N2–Si–N2A	92.28(8)	C2–O1–Si	118.34(8)
O1–Si–N1	87.77(5)	O2–C2–O1	123.23(12)
O1A–Si–N1A	86.53(5)	O2–C2–C3	121.74(12)
N2–Si–N1A	90.90(5)	O1–C2–C3	115.01(11)
N2A–Si–N1A	94.61(5)	C1–N2–Si	146.35(13)
O1–Si–N1	86.53(5)	O3–C1–N2	176.86(19)
O1A–Si–N1	87.77(5)		
N2–Si–N1	94.61(5)		
N2A–Si–N1	90.89(5)		

Silicon(IV) complex **54**

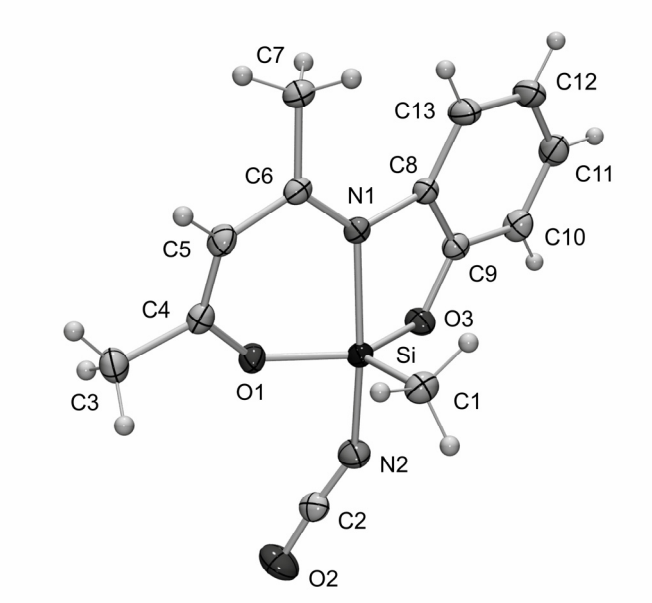

Figure A11: Molecular structure of the silicon(IV) complex **54** in the crystal showing the atomic numbering scheme (probability level of displacement ellipsoids 50%).

Table A28. Atomic coordinates ($\times 10^4$) and equivalent isotropic displacement parameters ($Å^2 \times 10^3$) for **54**. U_{eq} is defined as one third of the trace of the orthogonalized U_{ij} tensor.

	x	y	z	U_{eq}
C1	9808(2)	4764(2)	1384(1)	26(1)
C2	7633(2)	7211(2)	−77(1)	24(1)
C3	7584(2)	1907(2)	−462(1)	28(1)
C4	7231(2)	2358(2)	192(1)	22(1)
C5	7114(2)	1325(2)	670(1)	23(1)
C6	6497(2)	1736(2)	1258(1)	20(1)
C7	5876(2)	429(2)	1642(1)	24(1)
C8	5648(2)	3851(2)	1933(1)	20(1)
C9	5411(2)	5460(2)	1844(1)	21(1)
C10	4673(2)	6385(2)	2279(1)	26(1)
C11	4191(2)	5688(2)	2825(1)	30(1)
C12	4462(3)	4100(2)	2927(1)	34(1)
C13	5180(3)	3171(2)	2487(1)	31(1)
N1	6422(2)	3222(2)	1412(1)	20(1)
N2	7659(2)	6665(2)	439(1)	29(1)
O1	6974(2)	3894(1)	252(1)	25(1)
O2	7652(2)	7835(2)	−578(1)	40(1)
O3	5985(2)	6080(1)	1315(1)	24(1)
Si	7399(1)	4980(1)	937(1)	19(1)

Table A29. Bond lengths [Å] and angles [°] for **54**.

O1–Si	1.6875(12)	C3–C4	1.481(2)	C8–C9	1.392(2)
O3–Si	1.6839(12)	C4–O1	1.333(2)	C8–N1	1.4122(19)
N1–Si	1.9947(14)	C4–C5	1.345(2)	C9–O3	1.3534(19)
N2–Si	1.8033(15)	C5–C6	1.421(2)	C9–C10	1.380(2)
C1–Si	1.8466(17)	C6–N1	1.312(2)	C10–C11	1.381(2)
C2–O2	1.175(2)	C6–C7	1.489(2)	C11–C12	1.381(3)
C2–N2	1.170(2)	C8–C13	1.387(2)	C12–C13	1.382(2)
O1–C4–C3	113.01(14)	O3–C9–C10	121.45(15)	C9–O3–Si	117.49(10)
O1–C4–C5	123.22(14)	O3–C9–C8	116.50(13)	O3–Si–O1	131.69(6)
N2–C2–O2	176.15(19)	C10–C9–C8	122.03(14)	O3–Si–N2	87.54(6)
C5–C4–C3	123.73(15)	C9–C10–C11	118.52(16)	O1–Si–N2	88.42(6)
C4–C5–C6	123.20(15)	C12–C11–C10	120.06(15)	O3–Si–C1	114.85(7)
N1–C6–C5	118.89(14)	C11–C12–C13	121.38(15)	O1–Si–C1	113.19(7)
N1–C6–C7	124.32(14)	C12–C13–C8	119.22(16)	N2–Si–C1	100.80(7)
C5–C6–C7	116.71(14)	C6–N1–C8	126.49(13)	O3–Si–N1	83.65(6)
C13–C8–C9	118.77(14)	C6–N1–Si	124.92(10)	O1–Si–N1	88.77(6)
C13–C8–N1	132.00(15)	C8–N1–Si	108.59(10)	N2–Si–N1	165.40(7)
C9–C8–N1	109.20(13)	C2–N2–Si	149.40(14)		
C1–Si–N1	93.47(7)	C4–O1–Si	127.71(10)		

Silicon(IV) complex **55**

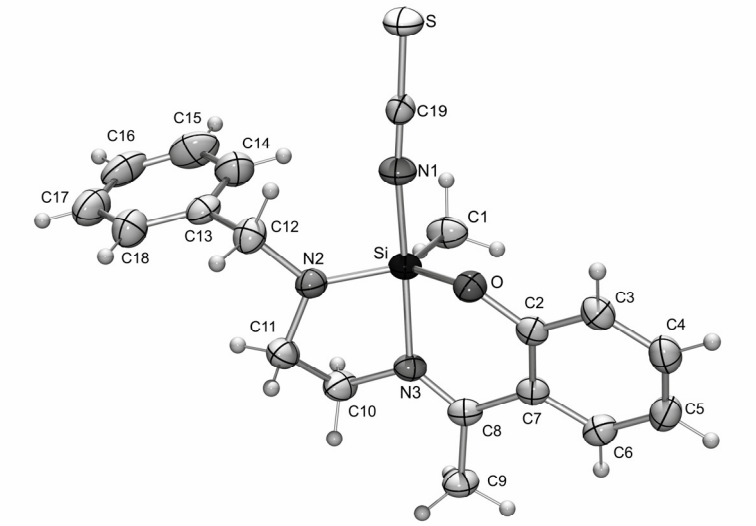

Figure A12: Molecular structure of the silicon(IV) complex **55** in the crystal showing the atomic numbering scheme (probability level of displacement ellipsoids 50%).

Table A30. Atomic coordinates ($\times 10^4$) and equivalent isotropic displacement parameters ($Å^2 \times 10^3$) for **55**. U_{eq} is defined as one third of the trace of the orthogonalized U_{ij} tensor.

	x	y	z	U_{eq}
C1	972(2)	2830(2)	4005(1)	46(1)
C2	2310(2)	437(2)	4563(1)	31(1)
C3	1718(2)	−188(2)	4863(1)	37(1)
C4	2219(2)	−10(2)	5219(1)	42(1)
C5	3322(2)	781(2)	5280(1)	42(1)
C6	3938(2)	1376(2)	4983(1)	38(1)
C7	3454(2)	1219(2)	4616(1)	31(1)
C8	4159(2)	1781(2)	4296(1)	32(1)
C9	5564(2)	2340(2)	4337(1)	40(1)
C10	4199(2)	2193(2)	3635(1)	41(1)
C11	3720(2)	1256(2)	3348(1)	43(1)
C12	1629(2)	381(2)	3107(1)	40(1)
C13	1387(2)	1358(2)	2805(1)	38(1)
C14	571(2)	2402(2)	2871(1)	55(1)
C15	380(3)	3315(3)	2597(1)	70(1)
C16	1017(3)	3189(3)	2256(1)	63(1)
C17	1809(2)	2165(3)	2188(1)	59(1)
C18	1992(2)	1249(2)	2459(1)	50(1)
C19	−1173(2)	225(2)	3723(1)	32(1)
Nl	−54(2)	564(2)	3758(1)	39(1)
N2	2306(2)	918(2)	3433(1)	35(1)
N3	3546(1)	1763(2)	3979(1)	32(1)
O	1735(1)	223(1)	4226(1)	34(1)
S	−2711(1)	−283(1)	3670(1)	50(1)
Si	1666(1)	1250(1)	3867(1)	30(1)

Table A31. Bond lengths [Å] and angles [°] for **55**.

O–Si	1.6908(13)	C5–C6	1.380(3)	C13–C14	1.380(3)
N1–Si	1.8735(16)	C6–C7	1.413(2)	C13–C18	1.383(3)
N2–Si	1.7199(15)	C7–C8	1.469(2)	C14–C15	1.394(3)
N3–Si	1.9601(15)	C8–N3	1.291(2)	C15–C16	1.384(4)
C1–Si	1.867(2)	C8–C9	1.502(2)	C16–C17	1.352(4)
C2–O	1.355(2)	C10–N3	1.469(2)	C17–C18	1.387(3)
C2–C3	1.395(2)	C10–C11	1.505(3)	N1–C19	1.159(2)
C2–C7	1.404(3)	C11–N2	1.462(2)	C19–S	1.6084(18)
C3–C4	1.385(3)	C12–N2	1.465(2)		
C4–C5	1.382(3)	C12–C13	1.518(3)		
O–C2–C3	116.39(16)	N2–C12–C13	112.63(16)	C10–N3–Si	108.55(11)
O–C2–C7	123.54(15)	C14–C13–C18	118.08(19)	C2–O–Si	126.59(11)
C3–C2–C7	120.06(16)	C14–C13–C12	120.40(18)	N1–C19–S	178.40(19)
C4–C3–C2	120.59(18)	C18–C13–C12	121.51(19)	O–Si–N2	123.55(7)
C5–C4–C3	120.38(18)	C13–C14–C15	120.3(2)	O–Si–C1	112.44(9)
C6–C5–C4	119.44(17)	C16–C15–C14	120.3(2)	N2–Si–C1	123.77(9)
C5–C6–C7	121.78(18)	C17–C16–C15	119.8(2)	O–Si–N1	87.10(7)
C2–C7–C6	117.71(16)	C16–C17–C18	120.0(2)	N2–Si–N1	93.31(7)
C2–C7–C8	120.18(15)	C13–C18–C17	121.5(2)	C1–Si–N1	94.19(8)
C6–C7–C8	122.01(16)	C19–N1–Si	172.29(16)	O–Si–N3	88.90(6)
N3–C8–C7	118.15(15)	C11–N2–C12	110.67(14)	N2–Si–N3	84.44(7)
N3–C8–C9	121.09(16)	C11–N2–Si	119.06(12)	C1–Si–N3	92.29(8)
C7–C8–C9	120.75(15)	C12–N2–Si	130.19(12)	N1–Si–N3	173.32(8)
N3–C10–C11	104.08(15)	C8–N3–C10	122.88(15)		
N2–C11–C10	108.07(15)	C8–N3–Si	128.55(12)		

Silicon(IV) complex **56**

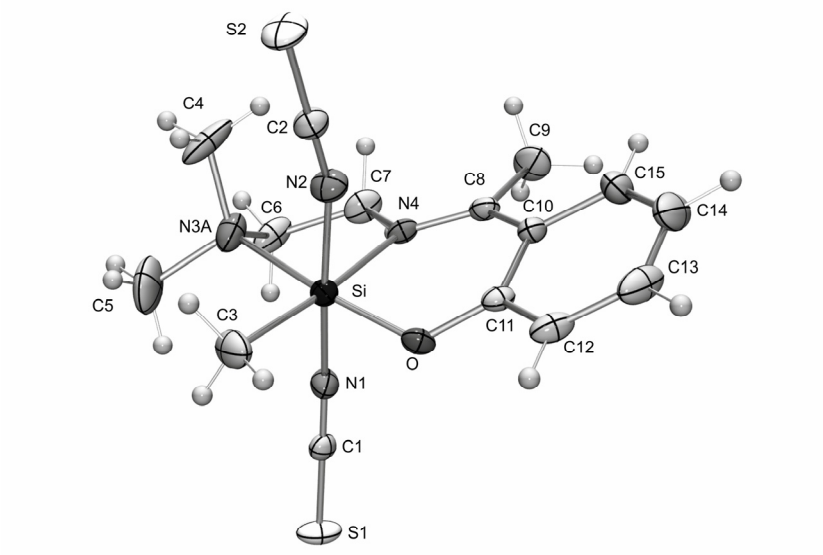

Figure A13: Molecular structure of the silicon(IV) complex **56** in the crystal showing the atomic numbering scheme (probability level of displacement ellipsoids 50%).

Table A32. Atomic coordinates ($\times 10^4$) and equivalent isotropic displacement parameters ($Å^2 \times 10^3$) for **56**. U_{eq} is defined as one third of the trace of the orthogonalized U_{ij} tensor.

	x	y	z	U_{eq}
C1	7796(2)	4616(1)	1418(1)	20(1)
C2	2168(2)	4954(1)	3041(1)	24(1)
C3	3765(2)	3940(2)	1495(1)	37(1)
C4A	3075(3)	6832(2)	1995(2)	48(1)
C4B	2626(9)	6628(7)	1499(5)	31(2)
C5A	4013(3)	6154(2)	859(1)	59(1)
C5B	5065(8)	6642(7)	1006(4)	28(2)
C6A	5866(2)	6971(2)	1916(1)	33(1)
C6B	5046(8)	7309(6)	2336(4)	26(2)
C7A	6586(2)	6882(1)	2775(1)	29(1)
C7B	6586(2)	6882(1)	2775(1)	29(1)
C8	6792(2)	5539(1)	3793(1)	21(1)
C9	7712(2)	6381(1)	4335(1)	36(1)
C10	6494(2)	4460(1)	4108(1)	22(1)
C11	6065(1)	3561(1)	3605(1)	19(1)
C12	5907(2)	2515(1)	3917(1)	27(1)
C13	6125(2)	2364(1)	4716(1)	39(1)
C14	6487(2)	3249(2)	5221(1)	47(1)
Cl5	6678(2)	4278(1)	4922(1)	38(1)
S1	9168(1)	4388(1)	917(1)	32(1)
S2	453(1)	5023(1)	3295(1)	37(1)
O	5865(1)	3663(1)	2827(1)	20(1)
N1	6802(1)	4793(1)	1777(1)	24(1)
N2	3412(1)	4920(1)	2860(1)	27(1)
N3A	4424(1)	6294(1)	1733(1)	32(1)
N3B	4424(1)	6294(1)	1733(1)	32(1)
Si	5059(1)	4785(1)	2285(1)	19(1)

Table A33. Bond lengths [Å] and angles [°] for **56**.

Si–O	1.7239(10)	N1–C1	1.1633(17)	C12–C13	1.374(2)
Si–N1	1.8666(11)	N2–C2	1.1631(18)	C13–C14	1.383(3)
Si–N2	1.8762(12)	N4–C8	1.3011(16)	C15–C14	1.374(2)
Si–N3A	2.0899(13)	N4–C7A	1.4752(16)	C7A–C6A	1.505(2)
Si–N4	1.9460(11)	C10–C11	1.4019(18)	N3A–C6A	1.465(2)
Si–C3	1.8936(15)	C10–C15	1.4085(19)	N3A–C4A	1.467(2)
S1–C1	1.6060(13)	C10–C8	1.4586(18)	N3A–C5A	1.501(3)
S2–C2	1.6086(13)	C11–C12	1.3965(18)		
O–C11	1.3325(15)	C8–C9	1.5059(18)		
O–Si–N1	89.36(5)	C1–N1–Si	168.08(12)	C13–C12–C11	120.48(14)
O–Si–N2	92.46(5)	C2–N2–Si	163.58(12)	C14–C15–C10	121.46(15)
N1–Si–N2	173.39(6)	N1–C1–S1	179.19(13)	C12–C13–C14	120.42(14)
O–Si–C3	94.98(6)	N2–C2–S2	178.95(14)	C15–C14–C13	119.68(14)
N1–Si–C3	94.02(6)	C8–N4–C7A	118.34(11)	N4–C7A–C6A	109.15(12)
N2–Si–C3	92.16(6)	C8–N4–Si	125.48(9)	C6A–N3A–C4A	111.11(16)
O–Si–N4	90.04(4)	C7A–N4–Si	116.10(8)	C6A–N3A–C5A	108.05(16)
N1–Si–N4	86.83(5)	C11–C10–C15	117.93(13)	C4A–N3A–C5A	108.22(18)
N2–Si–N4	86.81(5)	C11–C10–C8	120.62(11)	C6A–N3A–Si	104.89(9)
C3–Si–N4	174.91(7)	C15–C10–C8	121.41(13)	C4A–N3A–Si	113.59(11)
O–Si–N3A	170.04(5)	O–C11–C12	118.21(12)	C5A–N3A–Si	110.85(13)
N1–Si–N3A	86.60(5)	O–C11–C10	121.78(11)	N3A–C6A–C7A	110.21(13)

N2–Si–N3A	90.57(5)	C12–C11–C10	119.94(12)
C3–Si–N3A	94.38(7)	N4–C8–C10	120.72(11)
N4–Si–N3A	80.66(5)	N4–C8–C9	120.40(12)
C11–O–Si	125.96(8)	C10–C8–C9	118.87(12)

Silicon(IV) complex **57**

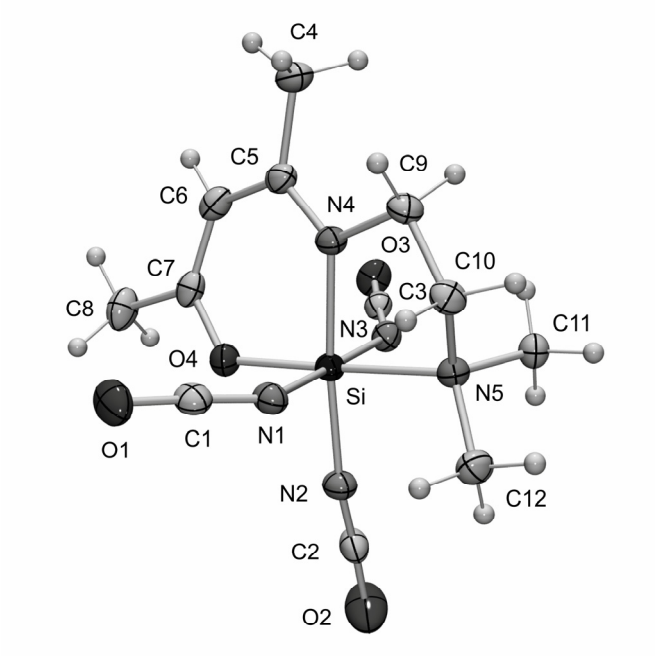

Figure A14: Molecular structure of the silicon(IV) complex **57** in the crystal showing the atomic numbering scheme (probability level of displacement ellipsoids 50%).

Table A34. Atomic coordinates ($\times 10^4$) and equivalent isotropic displacement parameters ($Å^2 \times 10^3$) for **57**. U_{eq} is defined as one third of the trace of the orthogonalized U_{ij} tensor.

	x	y	z	U_{eq}
C1	5565(1)	1284(1)	5576(1)	26(1)
C2	6042(1)	1295(1)	10769(2)	28(1)
C3	6276(1)	303(1)	9008(1)	23(1)
C4	6162(1)	209(1)	3421(2)	34(1)
C5	6001(1)	350(1)	4935(1)	25(1)
C6	5591(1)	3(1)	5749(2)	28(1)
C7	5375(1)	98(1)	6993(2)	26(1)
C8	4929(1)	−268(1)	7758(2)	34(1)
C9	6660(1)	1120(1)	4574(1)	26(1)
C10	6824(1)	1599(1)	5298(2)	26(1)
C11	7143(1)	1493(1)	7852(2)	26(1)
C12	6817(1)	2001(1)	7764(2)	29(1)
N1	5891(1)	1321(1)	6315(1)	25(1)
N2	6050(1)	1238(1)	9363(1)	26(1)
N3	6344(1)	674(1)	8578(1)	24(1)
N4	6235(1)	783(1)	5463(1)	22(1)

N5	6758(1)	1549(1)	7120(1)	23(1)
Ol	5242(1)	1263(1)	4852(1)	39(1)
O2	6025(1)	1361(1)	12183(1)	61(1)
O3	6224(1)	−62(1)	9494(1)	32(1)
Si	6110(1)	995(1)	7462(1)	20(1)

Table A35. Bond lengths [Å] and angles [°] for **57**.

O4–Si	1.7560(9)	C2–O2	1.1791(17)	C7–O4	1.3188(15)
N1–Si	1.8252(11)	C2–N2	1.1629(16)	C7–C8	1.4941(18)
N2–Si	1.8001(11)	C3–O3	1.1938(16)	C9–N4	1.4716(15)
N3–Si	1.8324(11)	C3–N3	1.1807(16)	C9–C10	1.5088(18)
N4–Si	1.8969(10)	C4–C5	1.5052(17)	C10–N5	1.4971(15)
N5–Si	2.0199(11)	C5–N4	1.3109(16)	C11–N5	1.4951(15)
C1–O1	1.1885(16)	C5–C6	1.4235(18)	C12–N5	1.4975(15)
C1–N1	1.1826(16)	C6–C7	1.3612(19)		
N1–C1–O1	177.41(15)	C11–N5–Si	114.34(7)	N1–Si–N3	178.43(5)
N2–C2–O2	177.49(16)	C10–N5–Si	105.39(7)	O4–Si–N4	94.11(4)
N3–C3–O3	176.92(13)	C12–N5–Si	113.89(7)	N2–Si–N4	174.52(5)
N4–C5–C6	121.85(11)	C5–N4–C9	118.80(10)	N1–Si–N4	90.02(5)
N4–C5–C4	119.90(12)	C5–N4–Si	124.38(9)	N3–Si–N4	88.93(5)
C6–C5–C4	118.24(11)	C9–N4–Si	116.37(8)	O4–Si–N5	176.22(4)
C7–C6–C5	123.87(11)	C1–N1–Si	143.62(10)	N2–Si–N5	91.04(5)
O4–C7–C6	123.43(11)	C2–N2–Si	159.32(11)	N1–Si–N5	86.95(5)
O4–C7–C8	113.66(12)	C3–N3–Si	145.93(9)	N3–Si–N5	91.77(4)
C6–C7–C8	122.91(12)	C7–O4–Si	126.79(8)	N4–Si–N5	83.60(4)
N4–C9–C10	107.82(9)	O4–Si–N2	91.30(5)		
N5–C10–C9	108.48(10)	O4–Si–N1	90.05(5)		
C11–N5–C10	108.88(9)	N2–Si–N1	90.80(5)		
C11–N5–C12	106.66(9)	O4–Si–N3	91.19(4)		
C10–N5–C12	107.41(10)	N2−Si−N3	90.14(5)		

Silicon(IV) complex **58**

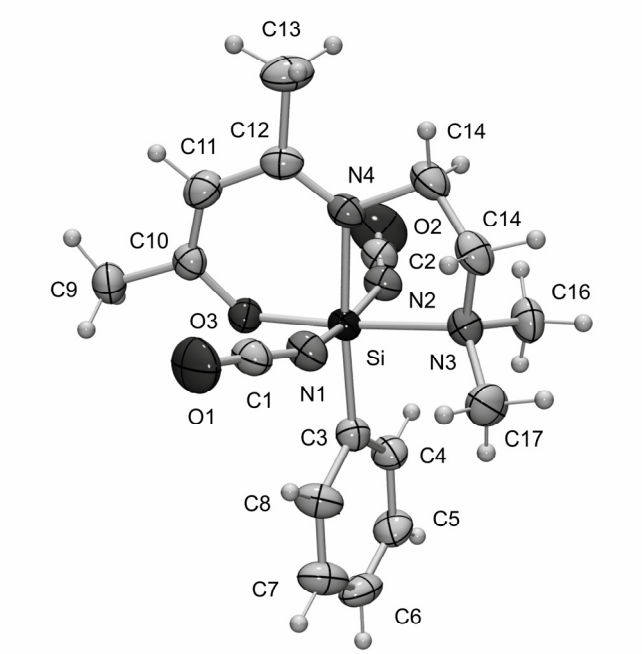

Figure A15: Molecular structure of the silicon(IV) complex **58** in the crystal showing the atomic numbering scheme (probability level of displacement ellipsoids 50%).

Table A36. Atomic coordinates ($\times 10^4$) and equivalent isotropic displacement parameters ($Å^2 \times 10^3$) for **58**. U_{eq} is defined as one third of the trace of the orthogonalized U_{ij} tensor.

	x	y	z	U_{eq}
C1	1363(1)	10178(2)	4741(1)	41(1)
C2	4279(1)	5903(2)	4056(1)	41(1)
C3	1852(1)	6555(2)	3406(1)	33(1)
C4	2110(1)	5174(2)	2961(1)	41(1)
C5	1577(1)	4489(2)	2228(1)	50(1)
C6	770(1)	5172(2)	1911(1)	51(1)
C7	489(1)	6533(2)	2329(1)	54(1)
C8	1024(1)	7208(2)	3057(1)	46(1)
C9	3529(1)	11391(2)	3061(1)	50(1)
C10	3430(1)	10330(2)	3874(1)	36(1)
C11	3751(1)	10750(2)	4741(1)	43(1)
C12	3715(1)	9755(2)	5528(1)	38(1)
C13	4184(1)	10377(2)	6415(1)	56(1)
C14	3288(1)	7362(2)	6301(1)	44(1)
C15	2356(1)	6661(2)	6277(1)	43(1)
C16	2546(1)	4314(2)	5337(1)	48(1)
C17	1122(1)	5680(2)	5238(1)	53(1)
N1	1695(1)	8915(1)	4720(1)	40(1)
N2	3577(1)	6250(1)	4277(1)	39(1)
N3	2126(1)	5936(1)	5351(1)	37(1)
N4	3299(1)	8389(1)	5483(1)	35(1)
O1	995(1)	11426(1)	4778(1)	71(1)

O2	4992(1)	5495(2)	3828(1)	86(1)
O3	3016(1)	8978(1)	3666(1)	38(1)
Si	2584(1)	7547(1)	4404(1)	30(1)

Table A37. Bond lengths [Å] and angles [°] for **58**.

O3–Si	1.7689(10)	C2–O2	1.1870(18)	C10–C11	1.360(2)
N1–Si	1.8364(12)	C3–C4	1.3972(19)	C11–C12	1.425(2)
N2–Si	1.8516(12)	C3–C8	1.3996(19)	C12–N4	1.2980(18)
N3–Si	2.0883(12)	C4–C5	1.3979(19)	C12–C13	1.5088(19)
N4–Si	1.9537(11)	C5–C6	1.370(2)	C14–N4	1.4738(18)
C3–Si	1.9281(13)	C6–C7	1.374(3)	C14–C15	1.501(2)
C1–O1	1.1829(18)	C7–C8	1.392(2)	C15–N3	1.4947(18)
C1–N1	1.1680(17)	C9–C10	1.501(2)	C16–N3	1.4953(18)
C2–N2	1.1550(18)	C10–O3	1.3102(16)	C17–N3	1.4991(19)
N1–C1–O1	177.06(19)	N4–C14–C15	106.54(12)	O3–Si–C3	92.40(5)
N2–C2–O2	177.85(19)	N3–C15–C14	108.51(11)	N1–Si–C3	95.07(6)
C4–C3–C8	114.92(12)	C1–N1–Si	152.26(13)	N2–Si–C3	94.23(5)
C4–C3–Si	123.28(10)	C2–N2–Si	157.02(12)	O3–Si–N4	92.67(5)
C8–C3–Si	121.78(10)	C15–N3–C16	108.58(11)	N1–Si–N4	85.61(5)
C3–C4–C5	122.41(14)	C15–N3–C17	107.74(12)	N2–Si–N4	84.89(5)
C6–C5–C4	120.52(15)	C16–N3–C17	106.27(12)	C3–Si–N4	174.86(5)
C5–C6–C7	119.07(13)	C15–N3–Si	106.01(8)	O3–Si–N3	175.99(5)
C6–C7–C8	120.09(15)	C16–N3–Si	114.60(9)	N1–Si–N3	87.30(5)
C7–C8–C3	122.99(15)	C17–N3–Si	113.39(9)	N2–Si–N3	89.77(5)
O3–C10–C11	123.94(13)	C12–N4–C14	120.76(11)	C3–Si–N3	91.61(5)
O3–C10–C9	113.81(12)	C12–N4–Si	125.54(10)	N4–Si–N3	83.33(5)
C11–C10–C9	122.25(13)	C14–N4–Si	113.60(9)		
C10–C11–C12	124.43(13)	C10–O3–Si	129.14(9)		
N4–C12–C11	121.68(12)	O3–Si–N1	92.14(5)		
N4–C12–C13	121.95(14)	O3–Si–N2	90.14(5)		
C11–C12–C13	116.36(13)	N1–Si–N2	170.32(6)		

Silicon(IV) complex **59**

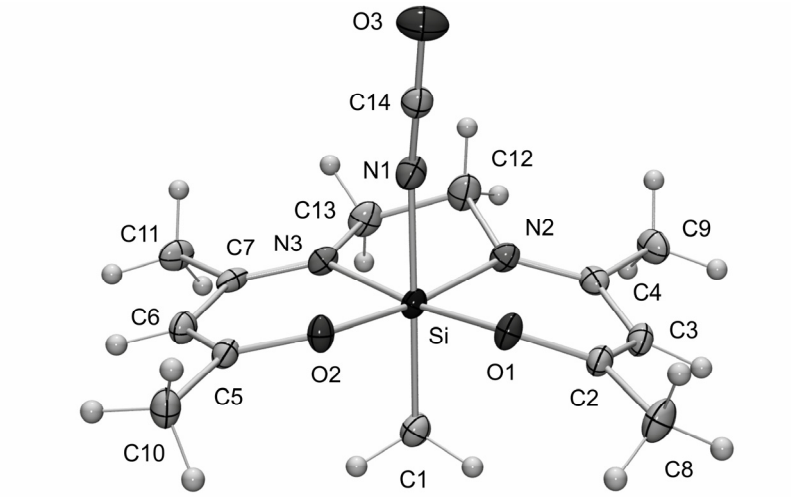

Figure A16: Molecular structure of the silicon(IV) complex **59** in the crystal showing the atomic numbering scheme (probability level of displacement ellipsoids 50%).

Table A38. Atomic coordinates ($\times 10^4$) and equivalent isotropic displacement parameters ($Å^2 \times 10^3$) for **59**. U_{eq} is defined as one third of the trace of the orthogonalized U_{ij} tensor.

	x	y	z	U_{eq}
C1	5802(2)	–551(2)	3197(1)	21(1)
C2	3821(1)	428(2)	3781(1)	18(1)
C3	4079(2)	–704(2)	4092(1)	20(1)
C4	5173(2)	–943(2)	4348(1)	19(1)
C5	6857(1)	2523(2)	2917(1)	17(1)
C6	7916(1)	1974(2)	3010(1)	19(1)
C7	8299(1)	1120(2)	3431(1)	17(1)
C8	2638(2)	734(2)	3566(1)	27(1)
C9	5271(2)	–1975(2)	4776(1)	25(1)
C10	6506(2)	3435(2)	2473(1)	22(1)
C11	9519(2)	688(2)	3498(1)	23(1)
C12	7150(2)	–351(2)	4514(1)	27(1)
C13	8045(2)	–214(2)	4166(1)	24(1)
C14	6162(1)	3544(2)	4350(1)	19(1)
N1	6283(1)	2485(2)	4136(1)	21(1)
N2	6046(1)	–255(2)	4221(1)	18(1)
N3	7619(1)	715(2)	3748(1)	17(1)
Ol	4558(1)	1358(1)	3655(1)	19(1)
O2	6060(1)	2328(1)	3204(1)	18(1)
O3	6064(1)	4625(2)	4579(1)	32(1)
Si	6021(1)	997(1)	3664(1)	15(1)

Table A39. Bond lengths [Å] and angles [°] for **59**.

O1–Si	1.7819(13)	C2–C8	1.497(2)	C7–N3	1.309(2)
O2–Si	1.7681(13)	C3–C4	1.429(3)	C7–C11	1.507(2)
N1–Si	1.8912(17)	C4–N2	1.307(2)	C12–N2	1.467(2)
N2–Si	1.9084(16)	C4–C9	1.503(3)	C12–C13	1.516(3)
N3–Si	1.9209(15)	C5–O2	1.313(2)	C13–N3	1.471(2)
C1–Si	1.921(2)	C5–C6	1.365(2)	C14–N1	1.165(2)
C2–O1	1.311(2)	C5–C10	1.495(2)	C14–O3	1.197(2)
C2–C3	1.367(3)	C6–C7	1.425(3)		
O1–C2–C3	124.17(16)	N3–C13–C12	108.89(15)	O1–Si–N2	92.99(6)
O1–C2–C8	114.09(16)	N1–C14–O3	178.1(2)	N1–Si–N2	85.74(7)
C3–C2–C8	121.71(16)	C14–N1–Si	160.26(15)	O2–Si–N3	94.16(6)
C2–C3–C4	123.42(16)	C4–N2–C12	121.74(16)	O1–Si–N3	173.34(7)
N2–C4–C3	120.85(17)	C4–N2–Si	124.73(13)	N1–Si–N3	86.26(7)
N2–C4–C9	121.67(17)	C12–N2–Si	113.50(12)	N2–Si–N3	84.13(7)
C3–C4–C9	117.45(16)	C7–N3–C13	119.45(15)	O2–Si–C1	94.14(7)
O2–C5–C6	124.14(17)	C7–N3–Si	124.74(12)	O1–Si–C1	94.24(7)
O2–C5–C10	113.70(15)	C13–N3–Si	115.14(12)	N1–Si–C1	177.89(8)
C6–C5–C10	122.15(16)	C2–O1–Si	124.25(12)	N2–Si–C1	93.04(8)
C5–C6–C7	124.46(17)	C5–O2–Si	126.79(12)	N3–Si–C1	91.91(7)
N3–C7–C6	121.52(15)	O2–Si–O1	87.94(6)		
N3–C7–C11	120.75(16)	O2–Si–N1	87.04(7)		
C6–C7–C11	117.73(16)	O1–Si–N1	87.55(7)		
N2–C12–C13	108.34(15)	O2–Si–N2	172.68(7)		

Silicon(IV) complex **60**

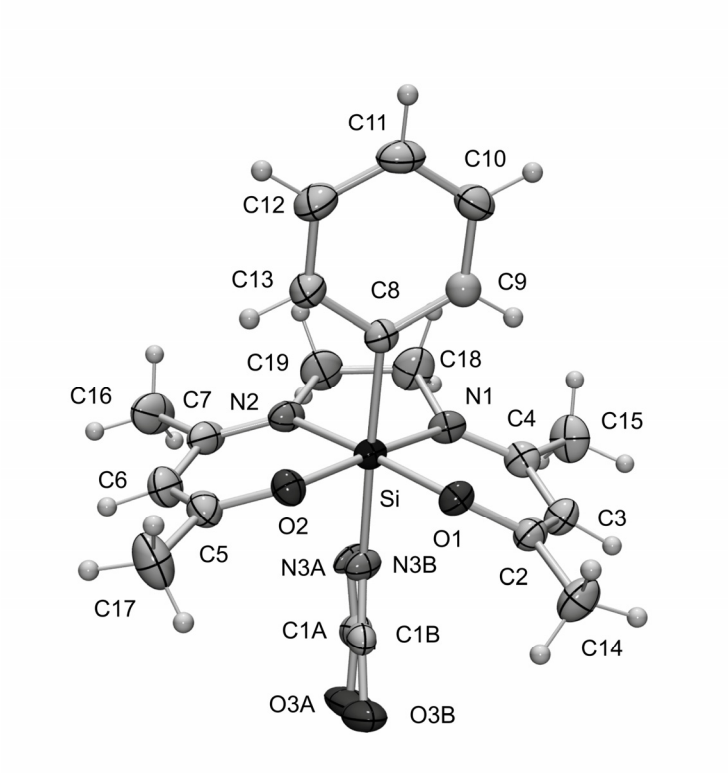

Figure A17: Molecular structure of the silicon(IV) complex **60** in the crystal showing the atomic numbering scheme (probability level of displacement ellipsoids 50%).

Table A40. Atomic coordinates ($\times 10^4$) and equivalent isotropic displacement parameters ($Å^2 \times 10^3$) for **60**. U_{eq} is defined as one third of the trace of the orthogonalized U_{ij} tensor.

	x	y	z	U_{eq}
C1A	10112(3)	1415(4)	7618(4)	29(1)
C1B	10030(9)	1394(11)	7229(12)	35(2)
C2	8601(1)	3203(1)	8333(1)	29(1)
C3	8390(1)	3765(1)	7401(1)	34(1)
C4	7630(1)	3436(1)	6380(1)	31(1)
C5	8374(1)	–574(1)	7997(1)	34(1)
C6	8118(2)	–978(1)	6979(1)	41(1)
C7	7451(1)	–456(1)	6028(1)	36(1)
C8	6061(1)	1413(1)	7450(1)	26(1)
C9	5433(1)	2332(1)	7436(1)	31(1)
C10	4353(1)	2344(1)	7615(1)	37(1)
C11	3861(1)	1429(1)	7821(1)	41(1)
C12	4450(1)	507(1)	7830(1)	43(1)
C13	5526(1)	501(1)	7641(1)	35(1)
C14	9379(2)	3599(1)	9393(1)	43(1)
C15	7325(2)	4218(1)	5476(1)	45(1)
C16	7130(2)	–1064(2)	4985(2)	54(1)
C17	9014(2)	–1190(1)	8979(2)	53(1)
Cl8	6388(2)	2174(1)	5204(1)	45(1)
C19	6442(2)	1033(1)	5051(1)	49(1)
N1	7216(1)	2487(1)	6243(1)	29(1)
N2	7127(1)	515(1)	6052(1)	30(1)
N3A	9127(4)	1433(10)	7156(9)	29(1)
N3B	9049(12)	1290(30)	7010(20)	24(2)
O1	8141(1)	2286(1)	8383(1)	27(1)
O2	8059(1)	356(1)	8206(1)	29(1)
O3A	11130(2)	1446(2)	8095(4)	58(1)
O3B	11059(6)	1368(6)	7342(18)	82(5)
Si	7605(1)	1407(1)	7286(1)	24(1)

Table A41. Bond lengths [Å] and angles [°] for **60**.

O1–Si	1.7674(10)	C5–O2	1.3022(17)	C18–N1	1.4588(18)
O2–Si	1.7647(10)	C5–C6	1.357(2)	C18–C19	1.477(2)
N1–Si	1.8856(12)	C5–C17	1.489(2)	C19–N2	1.461(2)
N2–Si	1.8992(12)	C6–C7	1.411(2)	N3A–C1A	1.148(6)
N3A–Si	1.887(5)	C7–N2	1.3042(19)	C1A–O3A	1.187(4)
C8–Si	1.9291(14)	C7–C16	1.500(2)	N3B–C1B	1.131(12)
C2–O1	1.3072(16)	C8–C13	1.3898(19)	C1B–O3B	1.199(11)
C2–C3	1.357(2)	C8–C9	1.3932(19)		
C2–C14	1.488(2)	C9–C10	1.385(2)		
C3–C4	1.416(2)	C10–C11	1.373(2)		
C4–N1	1.3021(18)	C11–C12	1.374(2)		
C4–C15	1.4956(19)	C12–C13	1.386(2)		
O1–C2–C3	123.59(12)	C11–C12–C13	120.55(14)	O2–Si–N2	93.38(5)
O1–C2–C14	114.45(12)	C12–C13–C8	122.26(14)	O1–Si–N2	174.86(5)
C3–C2–C14	121.95(13)	N1–C18–C19	110.44(13)	N1–Si–N2	84.02(6)
C2–C3–C4	124.03(13)	N2–C19–C18	111.42(12)	N3A–Si–N2	89.1(3)
N1–C4–C3	120.82(12)	C4–N1–C18	120.25(12)	O2–Si–C8	92.10(5)
N1–C4–C15	121.71(13)	C4–N1–Si	125.86(10)	O1–Si–C8	91.92(5)
C3–C4–C15	117.47(13)	C18–N1–Si	113.89(10)	N1–Si–C8	92.37(6)

O2–C5–C6	123.75(14)	C7–N2–C19	120.07(12)	N3A–Si–C8	178.3(3)
O2–C5–C17	114.38(13)	C7–N2–Si	125.21(10)	N2–Si–C8	92.50(6)
C6–C5–C17	121.84(14)	C19–N2–Si	114.42(10)	N3B–C1B–O3B	169.0(19)
C5–C6–C7	124.17(14)	C2–O1–Si	125.85(8)		
N2–C7–C6	121.57(13)	C5–O2–Si	127.24(9)		
N2–C7–C16	121.29(15)	C1A–N3A–Si	145.3(9)		
C6–C7–C16	117.15(14)	N3A–C1A–O3A	176.9(8)		
C13–C8–C9	115.58(13)	O2–Si–O1	89.07(5)		
C13–C8–Si	121.89(10)	O2–Si–N1	174.93(5)		
C9–C8–Si	122.46(10)	O1–Si–N1	93.18(5)		
C10–C9–C8	122.54(13)	O2–Si–N3A	88.2(4)		
C11–C10–C9	120.23(14)	O1–Si–N3A	86.4(3)		
C10–C11–C12	118.81(14)	N1–Si–N3A	87.5(4)		

Silicon(IV) complex **62**

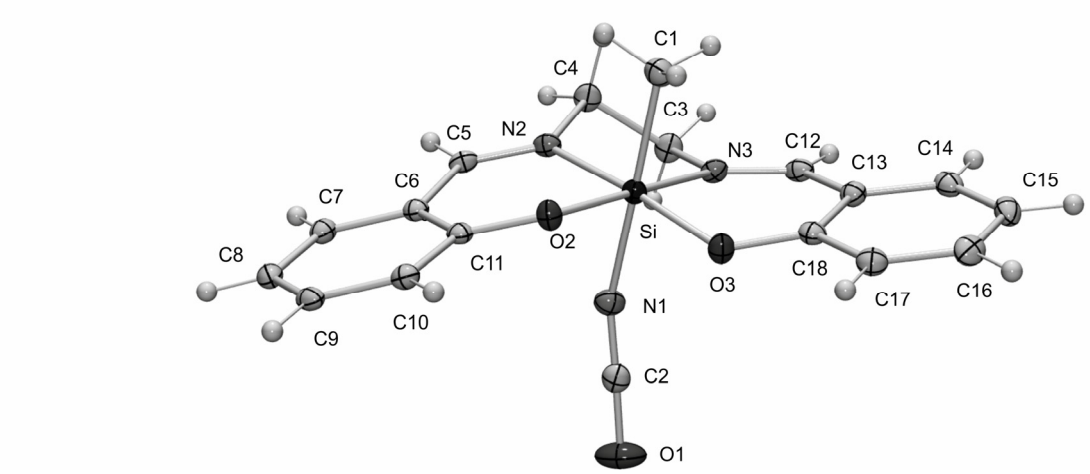

Figure A18: Molecular structure of the silicon(IV) complex **62** in the crystal showing the atomic numbering scheme (probability level of displacement ellipsoids 50%).

Table A42. Atomic coordinates ($\times 10^4$) and equivalent isotropic displacement parameters ($Å^2 \times 10^3$) for **62**. U_{eq} is defined as one third of the trace of the orthogonalized U_{ij} tensor.

	x	y	z	U_{eq}
C1	5952(1)	272(2)	6850(1)	20(1)
C2	4539(1)	3071(2)	9666(1)	19(1)
C3	5312(1)	–2328(2)	9129(1)	19(1)
C4	4904(1)	–2791(2)	8150(1)	18(1)
C5	3987(1)	–659(2)	7452(1)	15(1)
C6	3699(1)	1190(2)	7056(1)	14(1)
C7	2953(1)	1313(2)	6805(1)	17(1)
C8	2661(1)	3011(2)	6375(1)	17(1)

C9	3126(1)	4607(2)	6167(1)	17(1)
C10	3865(1)	4517(2)	6395(1)	16(1)
C11	4164(1)	2829(2)	6869(1)	14(1)
C12	6409(1)	–413(2)	9288(1)	17(1)
C13	6882(1)	1275(2)	9118(1)	16(1)
C14	7600(1)	1233(2)	9503(1)	18(1)
C15	8059(1)	2848(2)	9401(1)	20(1)
C16	7804(1)	4542(2)	8900(1)	20(1)
C17	7102(1)	4625(2)	8515(1)	18(1)
Cl8	6623(1)	3003(2)	8617(1)	16(1)
N1	4734(1)	2079(2)	8992(1)	20(1)
N2	4644(1)	–866(2)	7763(1)	15(1)
N3	5767(1)	–568(2)	8907(1)	16(1)
O1	4324(1)	4078(2)	10350(1)	39(1)
O2	4869(1)	2822(1)	7084(1)	16(1)
O3	5946(1)	3191(2)	8268(1)	18(1)
Si	5346(1)	1283(1)	7917(1)	14(1)

Table A43. Bond lengths [Å] and angles [°] for **62**.

O2–Si	1.7409(11)	C4–N2	1.4703(17)	C12–N3	1.2801(19)
O3–Si	1.7510(11)	C5–N2	1.2773(18)	C12–C13	1.446(2)
N1–Si	1.8791(14)	C5–C6	1.4470(19)	C13–C14	1.4076(19)
N2–Si	1.9445(12)	C6–C7	1.4068(19)	C13–C18	1.418(2)
N3–Si	1.9584(14)	C6–C11	1.4137(19)	C14–C15	1.379(2)
C1–Si	1.9107(16)	C7–C8	1.381(2)	C15–C16	1.396(2)
C2–O1	1.191(2)	C8–C9	1.396(2)	C16–C17	1.381(2)
C2–N1	1.165(2)	C9–C10	1.3854(19)	C17–C18	1.406(2)
C3–N3	1.4765(18)	C10–C11	1.4056(19)	C18–O3	1.3264(17)
C3–C4	1.520(2)	C11–O2	1.3206(16)		
N1–C2–O1	178.53(18)	C15–C14–C13	121.13(14)	O2–Si–N1	90.22(6)
N3–C3–C4	105.91(12)	C14–C15–C16	119.02(14)	O3–Si–N1	88.07(6)
N2–C4–C3	105.72(12)	C17–C16–C15	121.08(14)	O2–Si–C1	92.43(6)
N2–C5–C6	123.44(13)	C16–C17–C18	120.92(14)	O3–Si–C1	95.17(6)
C7–C6–C11	119.79(12)	O3–C18–C17	118.42(13)	N1–Si–C1	175.72(7)
C7–C6–C5	119.18(12)	O3–C18–C13	123.42(13)	O2–Si–N2	92.63(5)
C11–C6–C5	120.94(12)	C17–C18–C13	118.13(13)	O3–Si–N2	170.59(6)
C8–C7–C6	121.27(13)	C2–N1–Si	156.45(12)	N1–Si–N2	84.04(6)
C7–C8–C9	118.72(13)	C5–N2–C4	120.76(12)	C1–Si–N2	92.48(6)
C10–C9–C8	121.21(13)	C5–N2–Si	125.01(10)	O2–Si–N3	173.07(5)
C9–C10–C11	120.68(13)	C4–N2–Si	113.90(9)	O3–Si–N3	92.53(5)
O2–C11–C10	118.51(12)	C12–N3–C3	120.30(13)	N1–Si–N3	85.20(6)
O2–C11–C6	123.20(12)	C12–N3–Si	124.66(10)	C1–Si–N3	91.85(6)
C10–C11–C6	118.24(12)	C3–N3–Si	114.80(9)	N2–Si–N3	81.73(5)
N3–C12–C13	123.57(14)	C11–O2–Si	128.76(9)		
C14–C13–C18	119.72(13)	C18–O3–Si	127.36(10)		
C14–C13–C12	119.20(13)	O2–Si–O3	92.51(5)		
C18–C13–C12	121.00(13)				

Silicon(IV) complex **63**

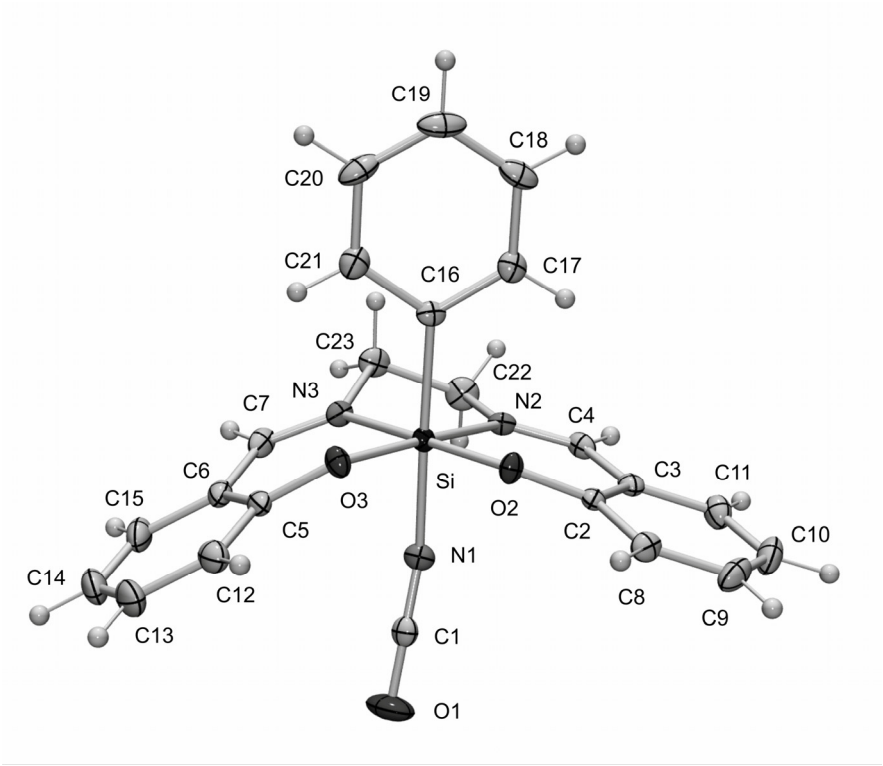

Figure A19: Molecular structure of the silicon(IV) complex **63** in the crystal showing the atomic numbering scheme (probability level of displacement ellipsoids 50%).

Table A44. Atomic coordinates ($\times 10^4$) and equivalent isotropic displacement parameters ($Å^2 \times 10^3$) for **63**. U_{eq} is defined as one third of the trace of the orthogonalized U_{ij} tensor.

	x	y	z	U_{eq}
C1	6252(4)	6656(1)	4393(2)	19(1)
C2	1546(3)	7170(1)	3057(2)	15(1)
C3	2131(4)	7828(1)	2726(2)	17(1)
C4	3604(4)	7861(1)	2188(2)	18(1)
C5	5882(4)	5127(1)	3289(2)	19(1)
C6	7651(4)	5258(1)	3061(2)	21(1)
C7	7874(4)	5780(1)	2356(2)	21(1)
C8	198(4)	7182(1)	3632(2)	20(1)
C9	–573(4)	7822(2)	3844(2)	28(1)
C10	–41(4)	8465(2)	3495(2)	29(1)
C11	1301(4)	8469(1)	2946(2)	23(1)
C12	5732(4)	4610(1)	3968(2)	27(1)
C13	7299(5)	4238(2)	4411(2)	37(1)
C14	9040(5)	4365(2)	4191(2)	36(1)
C15	9215(4)	4868(2)	3514(2)	30(1)
C16	2914(3)	6078(1)	1175(2)	15(1)
C17	1564(4)	6519(1)	639(2)	20(1)
C18	613(4)	6335(2)	–262(2)	26(1)
C19	991(4)	5694(2)	–659(2)	31(1)
C20	2320(4)	5240(2)	–149(2)	29(1)
C21	3248(4)	5429(1)	748(2)	23(1)
C22	6129(4)	7447(1)	1518(2)	24(1)
C23	6860(4)	6731(1)	1264(2)	22(1)

Nl	5599(3)	6656(1)	3589(1)	20(1)
N2	4546(3)	7319(1)	2002(1)	15(1)
N3	6590(3)	6228(1)	2008(1)	16(1)
O1	6971(4)	6676(1)	5209(1)	44(1)
O2	2167(2)	6539(1)	2814(1)	17(1)
O3	4333(2)	5466(1)	2852(1)	18(1)
Si	4229(1)	6339(1)	2422(1)	13(1)

Table A45. Bond lengths [Å] and angles [°] for **63**.

O2–Si	1.7352(17)	C3–C4	1.433(3)	C13–C14	1.379(5)
O3–Si	1.7302(17)	C4–N2	1.273(3)	C14–C15	1.370(4)
N1–Si	1.867(2)	C5–O3	1.335(3)	C16–C17	1.389(4)
N2–Si	1.943(2)	C5–C12	1.386(4)	C16–C21	1.394(3)
N3–Si	1.928(2)	C5–C6	1.404(4)	C17–C18	1.384(4)
C16–Si	1.918(2)	C6–C15	1.396(4)	C18–C19	1.369(4)
C1–O1	1.184(3)	C6–C7	1.430(4)	C19–C20	1.379(4)
C1–N1	1.158(3)	C7–N3	1.278(3)	C20–C21	1.377(4)
C2–O2	1.326(3)	C8–C9	1.372(4)	C22–N2	1.470(3)
C2–C8	1.394(3)	C9–C10	1.379(4)	C22–C23	1.501(4)
C2–C3	1.405(3)	C10–C11	1.363(4)	C23–N3	1.456(3)
C3–C11	1.397(3)	C12–C13	1.377(4)		
N1−C1−O1	177.4(3)	C15−C14−C13	119.4(3)	O3−Si−O2	93.84(8)
O2−C2−C8	118.7(2)	C14−C15−C6	120.3(3)	O3−Si−N1	89.86(9)
O2−C2−C3	122.8(2)	C17−C16−C21	115.5(2)	O2−Si−N1	89.32(9)
C8−C2−C3	118.4(2)	C17−C16−Si	122.52(18)	O3−Si−C16	94.24(9)
C11−C3−C2	119.6(2)	C21−C16−Si	121.95(19)	O2−Si−C16	92.79(10)
C11−C3−C4	118.9(2)	C18−C17−C16	122.8(2)	N1−Si−C16	175.25(10)
C2−C3−C4	121.5(2)	C19−C18−C17	119.9(3)	O3–Si–N3	91.62(9)
N2−C4−C3	124.4(2)	C18–C19–C20	119.1(2)	O2–Si–N3	173.68(9)
O3−C5−C12	118.9(2)	C21–C20–C19	120.4(3)	N1–Si–N3	87.51(9)
O3−C5−C6	122.3(2)	C20–C21–C16	122.3(3)	C16–Si–N3	89.98(9)
C12−C5−C6	118.7(2)	N2–C22–C23	108.3(2)	O3–Si–N2	170.84(9)
C15−C6−C5	120.0(2)	N3–C23–C22	106.76(19)	O2–Si–N2	93.48(8)
C15–C6–C7	119.2(3)	C1–N1–Si	159.4(2)	N1−Si−N2	84.71(9)
C5–C6–C7	120.8(2)	C4–N2–C22	118.0(2)	C16−Si−N2	90.91(9)
N3–C7–C6	123.0(2)	C4–N2–Si	125.11(16)	N3−Si−N2	80.79(9)
C9–C8–C2	120.4(2)	C22–N2–Si	116.56(16)		
C8–C9–C10	121.0(2)	C7–N3–C23	120.9(2)		
C11–C10–C9	119.6(2)	C7–N3–Si	125.02(17)		
C10–C11–C3	120.8(2)	C23–N3–Si	114.07(16)		
C13–C12–C5	120.1(3)	C2–O2–Si	129.07(15)		
C12–C13–C14	121.4(3)	C5−O3−Si	125.73(16)		

Silicon(IV) complex **64**

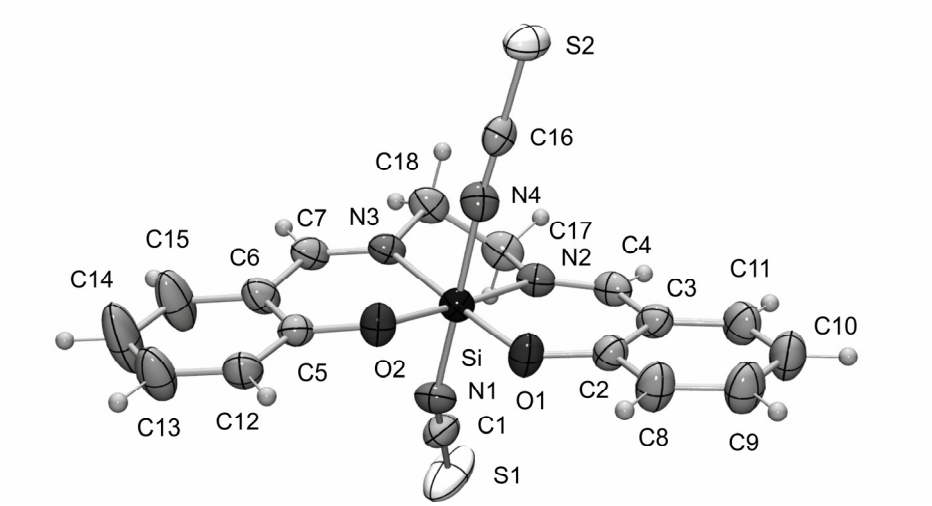

Figure A20: Molecular structure of the silicon(IV) complex **64** in the crystal showing the atomic numbering scheme (probability level of displacement ellipsoids 50%).

Table A46. Atomic coordinates ($\times 10^4$) and equivalent isotropic displacement parameters ($Å^2 \times 10^3$) for **64**. U_{eq} is defined as one third of the trace of the orthogonalized U_{ij} tensor.

	x	y	z	U_{eq}
C1	8580(1)	437(1)	2023(3)	46(1)
C2	8130(1)	1283(1)	4236(3)	36(1)
C3	7724(1)	1030(1)	3382(3)	37(1)
C4	7543(1)	550(1)	3072(3)	37(1)
C5	8905(1)	495(1)	6623(3)	33(1)
C6	8727(1)	23(1)	6384(3)	41(1)
C7	8280(1)	–257(1)	5734(3)	38(1)
C8	8294(1)	1747(1)	4504(4)	50(1)
C9	8061(1)	1955(1)	3928(4)	56(1)
C10	7663(1)	1711(1)	3073(4)	58(1)
C11	7495(1)	1251(1)	2797(4)	49(1)
C12	9332(1)	751(1)	7336(3)	42(1)
C13	9574(1)	543(1)	7806(5)	68(1)
C14	9400(1)	79(1)	7587(7)	98(2)
C15	8982(1)	–179(1)	6874(6)	75(1)
C16	7558(1)	406(1)	7583(3)	34(1)
C17	7512(1)	–173(1)	3183(3)	42(1)
Cl8	7575(1)	–414(1)	4572(3)	41(1)
N1	8569(1)	554(1)	3295(3)	42(1)
N2	7713(1)	313(1)	3630(2)	34(1)
N3	8033(1)	–98(1)	5199(2)	32(1)
N4	7825(1)	454(1)	6630(2)	38(1)
O1	8371(1)	1097(1)	4780(2)	42(1)
O2	8673(1)	704(1)	6260(2)	38(1)
S1	8590(1)	271(1)	291(1)	87(1)
S2	7188(1)	338(1)	8902(1)	48(1)
Si	8225(1)	538(1)	5004(1)	31(1)

Table A47. Bond lengths [Å] and angles [°] for **64**.

O1–Si	1.7055(17)	C3–C11	1.408(4)	C10–C11	1.381(4)
O2–Si	1.7078(17)	C3–C4	1.441(3)	C12–C13	1.377(4)
N1–Si	1.857(2)	C4–N2	1.287(3)	C13–C14	1.385(5)
N2–Si	1.909(2)	C5–O2	1.330(3)	C14–C15	1.378(5)
N3–Si	1.9175(19)	C5–C12	1.396(3)	C16–N4	1.166(3)
N4–Si	1.863(2)	C5–C6	1.407(3)	C16–S2	1.614(2)
C1–N1	1.167(3)	C6–C15	1.403(4)	C17–N2	1.479(3)
C1–S1	1.596(3)	C6–C7	1.435(3)	C17–C18	1.515(4)
C2–O1	1.336(3)	C7–N3	1.279(3)	C18–N3	1.474(3)
C2–C8	1.394(3)	C8–C9	1.384(4)		
C2–C3	1.407(3)	C9–C10	1.385(4)		
N1–C1–S1	179.2(3)	C10–C11–C3	120.7(2)	O1–Si–O2	89.44(8)
O1–C2–C8	118.5(2)	C13–C12–C5	120.2(2)	O1–Si–N1	92.80(10)
O1–C2–C3	122.2(2)	C12–C13–C14	120.9(3)	O2–Si–N1	92.87(10)
C8–C2–C3	119.3(2)	C15–C14–C13	119.7(3)	O1–Si–N4	92.29(9)
C2–C3–C11	119.3(2)	C14–C15–C6	120.6(3)	O2–Si–N4	91.86(9)
C2–C3–C4	121.1(2)	N4–C16–S2	179.9(2)	N1–Si–N4	173.08(10)
C11–C3–C4	119.7(2)	N2–C17–C18	106.27(19)	O1–Si–N2	94.31(8)
N2–C4–C3	124.1(2)	N3–C18–C17	106.21(19)	O2–Si–N2	176.24(9)
O2–C5–C12	118.3(2)	C1–N1–Si	148.7(2)	N1–Si–N2	87.25(9)
O2–C5–C6	122.3(2)	C4–N2–C17	119.6(2)	N4–Si–N2	87.70(9)
C12–C5–C6	119.4(2)	C4–N2–Si	125.23(16)	O1–Si–N3	177.18(9)
C15–C6–C5	119.1(2)	C17–N2–Si	115.12(16)	O2–Si–N3	93.35(8)
C15–C6–C7	119.6(2)	C7–N3–C18	119.82(19)	N1–Si–N3	87.43(9)
C5–C6–C7	121.2(2)	C7–N3–Si	125.18(15)	N4–Si–N3	87.26(8)
N3–C7–C6	123.6(2)	C18–N3–Si	114.87(15)	N2–Si–N3	82.90(8)
C9–C8–C2	120.3(2)	C16–N4–Si	175.8(2)		
C8–C9–C10	121.2(3)	C2–O1–Si	130.73(15)		
C11–C10–C9	119.3(3)	C5–O2–Si	129.53(15)		

Silicon(IV) complex **65**·2CH_3CN

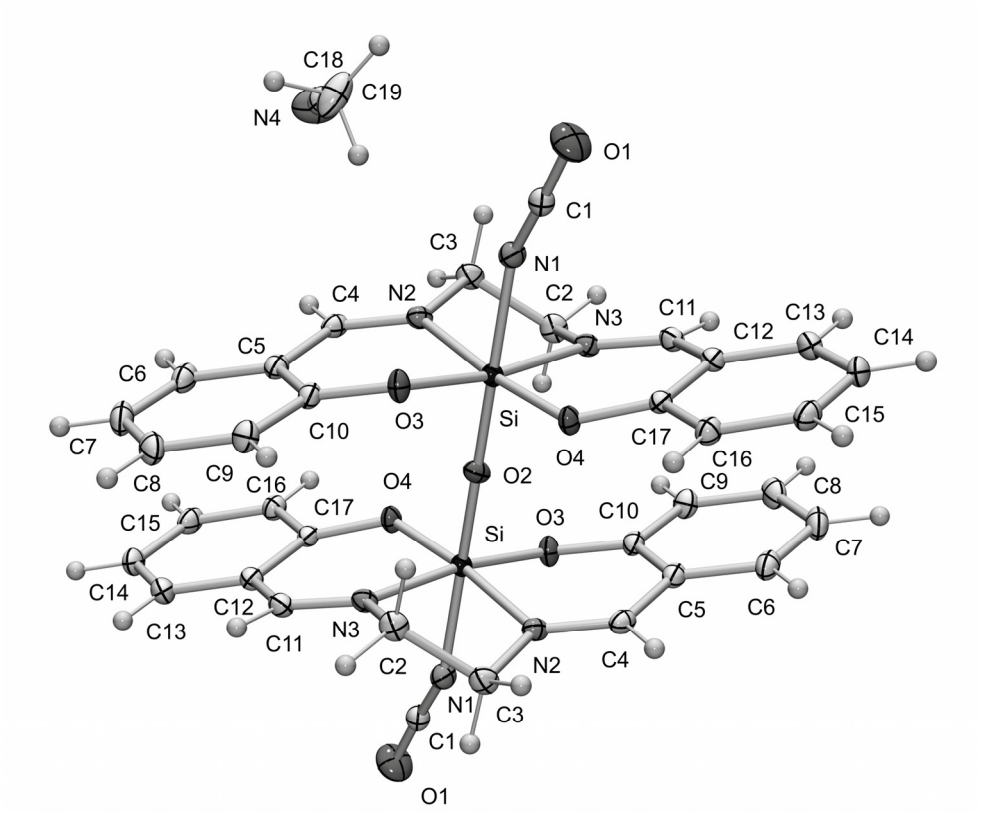

Figure A21: Molecular structure of the silicon(IV) complex **65** in the crystal of **65**·2CH_3CN showing the atomic numbering scheme (probability level of displacement ellipsoids 50%).

Table A48. Atomic coordinates ($\times 10^4$) and equivalent isotropic displacement parameters ($Å^2 \times 10^3$) for **65**·2CH_3CN. U_{eq} is defined as one third of the trace of the orthogonalized U_{ij} tensor.

	x	y	z	U_{eq}
C1	1494(1)	1642(1)	492(1)	17(1)
C2	3117(1)	–927(1)	1264(1)	18(1)
C3	3582(1)	–373(1)	2371(1)	19(1)
C4	5421(1)	557(1)	2711(1)	16(1)
C5	6231(1)	1215(1)	2405(1)	16(1)
C6	7430(1)	1419(1)	3235(1)	20(1)
C7	8241(1)	2044(1)	2988(1)	23(1)
C8	7846(1)	2487(1)	1899(1)	22(1)
C9	6661(1)	2309(1)	1075(1)	20(1)
C10	5840(1)	1664(1)	1306(1)	15(1)
C11	1614(1)	–516(1)	–589(1)	16(1)
C12	1162(1)	–2(1)	–1649(1)	15(1)
C13	–54(1)	–193(1)	–2462(1)	19(1)
C14	–480(1)	239(1)	–3534(1)	21(1)
C15	323(1)	873(1)	–3818(1)	20(1)
C16	1525(1)	1070(1)	–3040(1)	17(1)
C17	1966(1)	641(1)	–1937(1)	14(1)
Cl8	3385(1)	1419(1)	4351(1)	25(1)
C19	2972(2)	2123(1)	3551(1)	33(1)
N1	2397(1)	1181(1)	721(1)	17(1)
N2	4356(1)	296(1)	1983(1)	15(1)
N3	2673(1)	–361(1)	231(1)	14(1)

N4	3708(1)	860(1)	4959(1)	39(1)
O1	565(1)	2106(1)	316(1)	32(1)
O2	5000	0	0	15(1)
O3	4716(1)	1511(1)	487(1)	17(1)
O4	3146(1)	839(1)	–1239(1)	15(1)
Si	3805(1)	590(1)	280(1)	12(1)

Table A49. Bond lengths [Å] and angles [°] for **65**·2CH_3CN.

O2–Si	1.6475(3)	C3–N2	1.4697(13)	C11–C12	1.4425(15)
O3–Si	1.7449(8)	C4–N2	1.2832(14)	C12–C13	1.4085(14)
O4–Si	1.7395(8)	C4–C5	1.4427(15)	C12–C17	1.4130(14)
O2–Si#1	1.6475(3)	C5–C6	1.4085(14)	C13–C14	1.3783(16)
N1–Si	1.9002(9)	C5–C10	1.4134(15)	C14–C15	1.3997(16)
N2–Si	1.9340(9)	C6–C7	1.3806(17)	C15–C16	1.3823(15)
N3–Si	1.9228(9)	C7–C8	1.3990(18)	C16–C17	1.4058(14)
C1–O1	1.1972(14)	C8–C9	1.3852(15)	C17–O4	1.3288(12)
C1–N1	1.1740(14)	C9–C10	1.4057(15)	C18–N4	1.1356(18)
C2–N3	1.4684(13)	C10–O3	1.3304(12)	C18–C19	1.4530(17)
C2–C3	1.5213(16)	C11–N3	1.2843(14)		
N1–C1–O1	176.71(13)	C16–C15–C14	121.09(10)	O4–Si–N1	89.66(4)
N3–C2–C3	105.57(9)	C15–C16–C17	120.62(10)	O3–Si–N1	87.74(4)
N2–C3–C2	106.07(8)	O4–C17–C16	118.21(9)	O2–Si–N3	90.64(3)
N2–C4–C5	123.19(10)	O4–C17–C12	123.20(9)	O4–Si–N3	93.37(4)
C6–C5–C10	119.55(10)	C16–C17–C12	118.53(9)	O3–Si–N3	171.53(4)
C6–C5–C4	118.88(10)	N4–C18–C19	178.78(14)	N1–Si–N3	84.85(4)
C10–C5–C4	121.56(9)	C1–N1–Si	151.35(9)	O2–Si–N2	89.26(3)
C7–C6–C5	121.26(11)	C4–N2–C3	119.72(9)	O4–Si–N2	174.27(4)
C6–C7–C8	118.83(10)	C4–N2–Si	124.65(8)	O3–Si–N2	92.87(4)
C9–C8–C7	121.22(11)	C3–N2–Si	114.89(7)	N1–Si–N2	85.99(4)
C8–C9–C10	120.43(11)	C11–N3–C2	120.60(9)	N3–Si–N2	82.54(4)
O3–C10–C9	118.49(10)	C11–N3–Si	126.00(7)		
O3–C10–C5	122.81(9)	C2–N3–Si	113.40(7)		
C9–C10–C5	118.69(10)	Si–O2–Si#1	180.0		
N3–C11–C12	122.98(9)	C10–O3–Si	127.51(7)		
C13–C12–C17	119.62(10)	C17–O4–Si	128.74(7)		
C13–C12–C11	118.92(10)	O2–Si–O4	94.82(3)		
C17–C12–C11	121.23(9)	O2–Si–O3	96.43(3)		
C14–C13–C12	121.19(10)	O4–Si–O3	90.68(4)		
C13–C14–C15	118.94(10)	O2–Si–N1	173.83(3)		

Appendix B: Formula Index

$Si(NCX)_4$

1: X = O
2: X = S

$HMeSi(NCS)_2$

3

$RSi(NCO)_3$

4: R = Me
5: R = Ph

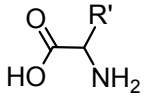

6: R' = H
7: R' = Me
8: R' = Bn
9: R' = *i*-Pr
10: R' = *t*-Bu

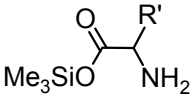

11: R' = H
12: R' = Me
13: R' = Bn
14: R' = *i*-Pr
15: R' = *t*-Bu

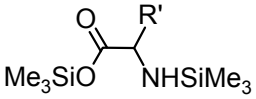

16: R' = H
17: R' = Me
18: R' = Bn
19: R' = *i*-Pr
20: R' = *t*-Bu

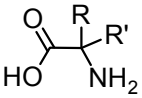

21: R = Me, R' = CH_2SiMe_3

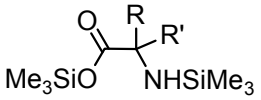

22: R = Me, R' = CH_2SiMe_3

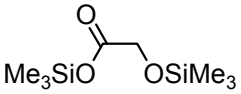

23

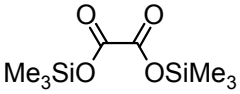

24

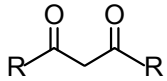

25: R = Me
26: R = Ph

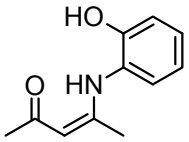

27

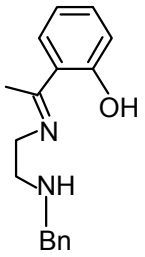

28

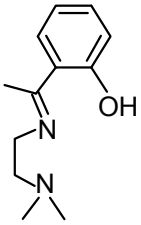

29

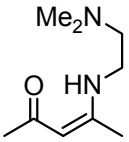

30

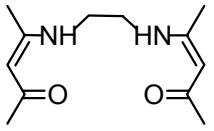

31

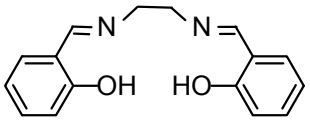

32

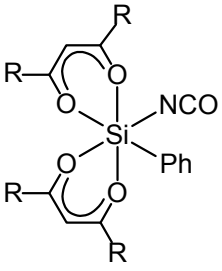

33: R = Me
34: R = Ph

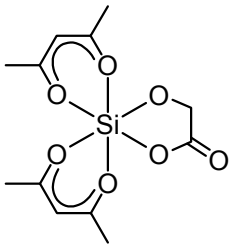

35

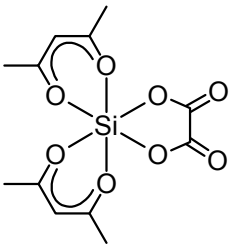

36

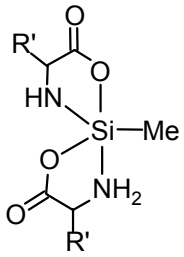

37: R' = H
38: R' = Me
39: R' = Bn
40: R' =*i*-Pr
41: R' =*t*-Bu

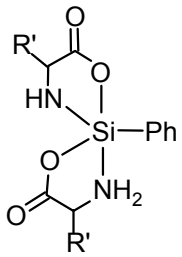

42: R' = H
43: R' = Me
44: R' = Bn
45: R' = *i*-Pr
46: R' = *t*-Bu

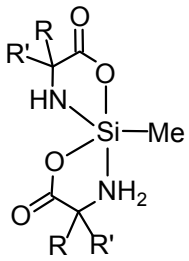

47: R = Me, R' = CH_2SiMe_3

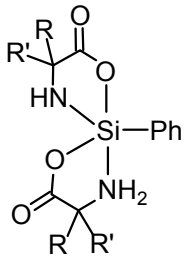

48: R = Me, R' = CH_2SiMe_3

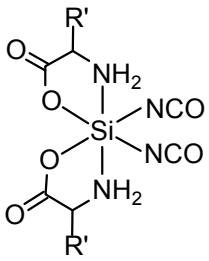

49: R' = H
50: R' = Me
51: R' = Bn
52: R' = *i*-Pr
53: R' = *t*-Bu

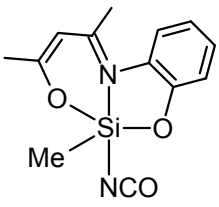

54

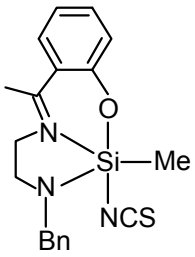

55

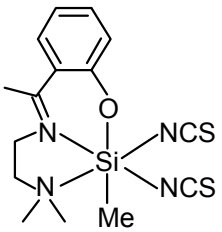

56

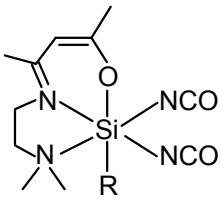

57: R = NCO
58: R = Ph

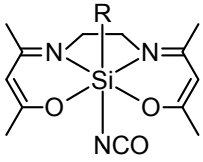

59: R = Me
60: R = Ph

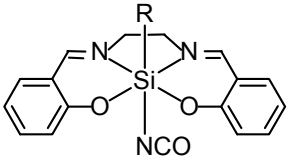

61: R = NCO
62: R = Me
63: R = Ph

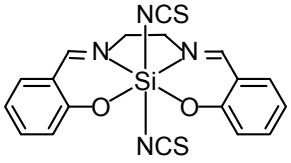

64

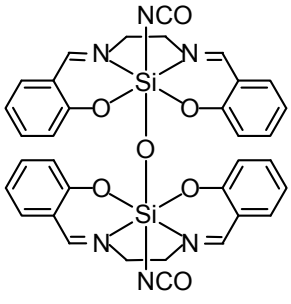

65

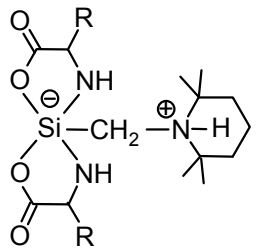

66: R = H
67: R = Me
68: R = *i*-Pr
69: R = *t*-Bu
70: R = Bn

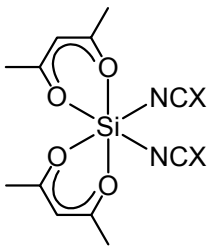

71: X = O
72: X = S

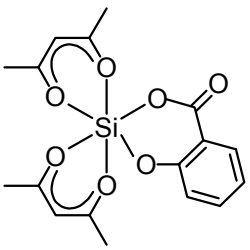

73

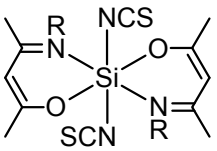

74: R = Ph
75: R = *i*-Pr

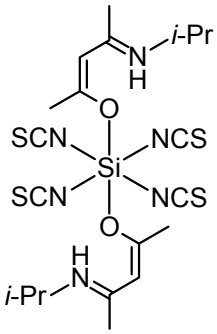

76

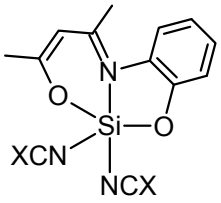

77: X = O
78: X = S

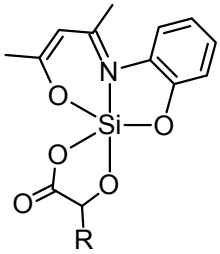

79: R = H
80: R = Me

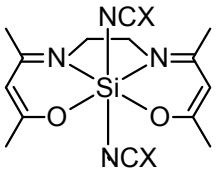

81: X = O
82: X = S

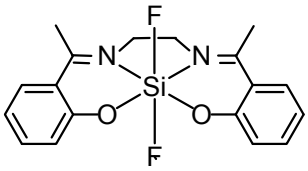

83

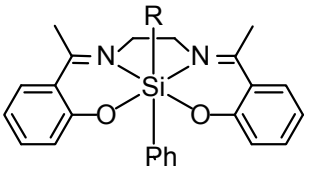

84: R = benzoate
85: R = picrate
86: R = 8-oxychinolinate

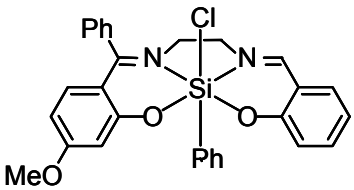

87

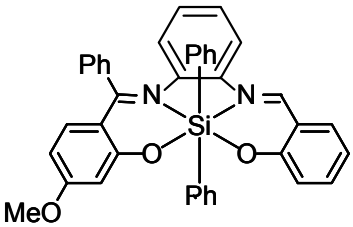

88

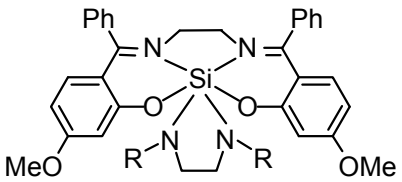

89: R = Ph
90: R = $SiMe_3$

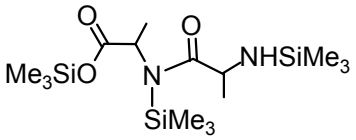

91

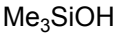

92

93

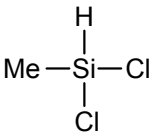

94

Danksagung

Ich danke Herrn Prof. Dr. R. Tacke für die interessante Themenstellung und die Möglichkeit, diese Arbeit in seinem Arbeitskreis durchzuführen, und für die Freiheit, meinem forscherischen Drang nachzugehen. Ich möchte mich ebenso herzlich für die Einladungen zu verschiedenen Tagungen bedanken.

Herrn Dr. R. Bertermann, Frau M.-L. Schäfer und Herrn W. P. Lippert danke ich für die Aufnahme der NMR-Spektren. Ein besonderer Dank gilt Herrn Dr. R. Bertermann für die Einarbeitung in die NMR-Programme und für die Unterstützung bei der Analyse der NMR-Spektren.

Herrn Dr. C. Burschka danke ich für die Durchführung der Kristallstrukturanalysen.

Bei Herrn Dr. S. Wagner möchte ich mich für die GC/MS-Messungen bedanken.

Frau L. Tietze, Frau I. Pross und Frau C. Walter danke ich für die Hilfe bei organisatorischen Problemen aller Art.

Für die Durchführung der Elementaranalysen danke ich Frau L. Michels und Frau S. Timmroth. Bei Herrn B. Fertig bedanke ich mich für die Reparatur kaputter Glasgeräte. Ein weiterer Dank gilt den Angestellten der Werkstatt sowie Herrn A. Schertzer für die Hilfe bei technischen Problemen. Frau M. Kromm danke ich für ihre Hilfe im Praktikum.

Für die gute Arbeitsatmosphäre und Zusammenarbeit möchte ich meinen Kollegen danken. Ein spezieller Dank geht an meine F-Praktikanten A. Voskobojnik, M. Beyer, C. Graßmann, D. Lang und B. Foster, deren Ergebnisse Teil dieser Arbeit sind, und an G. González-Garcia. Für die langjährige Unterstützung und ein immer offenes Ohr möchte ich mich herzlich bei A. Jahnke bedanken.

Besonderer Dank gilt A. Jahnke, S. Metz und J. Gluyas für das Korrekturlesen dieser Arbeit.

Für die freundliche Aufnahme einer fremden Seele aus einem fernen Land möchte ich mich auch sehr herzlich bei allen Studienkollegen aus Würzburg bedanken.

ERKLÄRUNG

Hiermit erkläre ich an Eides statt, daß ich die Dissertation

Contributions to the Chemistry of Higher-Coordinate Silicon:
Synthesis, Structure, and Stereodynamics of New Penta- and Hexacoordinate Silicon(IV) Complexes

selbstständig angefertigt und keine anderen als die von mir angegebenen Quellen und Hilfsmittel benutzt habe.

Ich erkläre außerdem, daß diese Dissertation weder in gleicher oder anderer Form bereits in einem anderen Prüfungsverfahren vorgelegen hat.

Ich habe früher außer den mit dem Zulassungsgesuch urkundlich vorgelegten Graden keine weiteren akademischen Grade erworben oder zu erwerben versucht.

Würzburg, den _____

_____

(Smaranda Cota)